The Migration of Radioactive Caesium and Strontium Through a Bentonite-like Clay

By

Stephen James Pendleton

Doctoral Thesis

Submitted in partial fulfilment of the requirements for the award of Doctor of Philosophy of Loughborough University

23rd June 2014

Acknowledgements

Firstly, I would like to thank my supervisor Dr Nick Evans for all the help I have received from him over these past few years. I appreciate the guidance and support you have given me throughout my time here, going all the way back to my undergraduate days, and for giving me the opportunity to carry out this research. Thank you also to Prof. David Read who has encouraged and supported me throughout this project.

I'd also like to give my thanks to the radiochemistry group here at Loughborough University, Dr Monica Felipe-Sotelo, Dr Ricky Hallam, Mr Oliver Preedy, Dr Sneh Jain, Dr Anumaija Leskinen, Dr Amy Young, Dr Mei Chew and especially the soon-to-be Drs James Holt, Larry Anjolaiya and John Hinchliff, who not only gave me advice and help, but were fantastic company in the lab making the most tedious of tasks that little bit more bearable! Thanks should also go to Ms Julie Turner, Ms Joan Sutherland and the late Mr David Wilson for all their help during my time here at Loughborough University. A special thank you to Dr Caroline Kirk whose knowledge on XRD was invaluable.

Thank you to my parents. I know I haven't outwardly shown my full appreciation for all the support you have given me the past 27 years but it truly has been appreciated. I should also thank you for putting up with me living at home these past few months whilst I finished writing this thing, it really has helped!

A final thanks is saved for Rachel Norman. Thank you for looking after me! It hasn't been the easiest couple of years but your encouragement and positivity has helped me finally see the light at the end of the tunnel. I'm not sure I would have gotten through this so successfully if I had been on my own.

Abstract

A number of leaks of radioactive liquors to ground are known to have occurred from several plant buildings, vaults and disposal trenches within and around the Separation area at the Sellafield nuclear site over the past 50 years[1]. The most significant of these leaks have occurred from the Magnox Silo, the Caesium Extraction Plant, the Magnox Reprocessing Pump House, the Sludge Storage Tanks, the Burial Pits and the Medium Active Evaporation and Thermal Denitration Plant[1]. The radioactive contamination will be accompanied by other components of spent fuel reprocessing, including inorganic salts from neutralised acids, solvents and other organic compounds along with the typical contaminants commonly associated with large industrial activity such as heavy metals, fuel, oils, degreasing agents etc.

The research in this thesis describes the effects of common industrial contaminants on the behaviour of Cs and Sr sorption to bentonite and montmorillonite clay minerals. Batch sorption experiments of Cs and Sr uptake onto bentonite and montmorillonite in a number of complex systems were investigated as follows:

1. Initial batch sorption experiments investigating the normal behaviour of the clay minerals.
2. Introduction of anthropogenic organic ligands EDTA, NTA and picolinic acid into the system and their influence on Sr and Cs uptake.
3. Time dependent studies investigating the effect that residence time of the anthropogenic organic ligands has on the sorption properties of montmorillonite and bentonite.
4. Quaternary systems where simulant Magnox sludge equilibrated water, at a number of concentrations, was introduced to ternary systems containing anthropogenic organic ligands.
5. Time dependent studies investigating the effect of hydrocarbons TCE, toluene and naphthalene on the uptake of Cs and Sr to bentonite and montmorillonite.

The batch sorption experiments show that the presence of anthropogenic organic ligands reduces the uptake of Cs and Sr by both montmorillonite and bentonite. It is also shown that the presence of simulant Magnox sludge in quaternary systems can also reduce the uptake of Cs and Sr, with significant reductions in sorption observed for Sr sorption in EDTA quaternary systems. Further, the uptake of Cs and Sr to bentonite and montmorillonite appears to decrease with increasing anthropogenic organic ligand

residence time. This suggests that the ligands are altering the surface of the clay minerals reducing the number of available binding sites.

The influence of hydrocarbons shows a significant decrease in sorption after 3 months for Cs and Sr sorption to montmorillonite. There were no further significant changes for all other hydrocarbon systems investigated.

Contents

List of Figures

List of Tables

List of Abbreviations

AGR – Advanced Gas-Cooled Reactor

APCAs – Aminopolycarboxylic Acids

BWR – Boiling Water Reactor

CAPS – 3-(Cyclohexylamino)-1-propanesulfonic Acid

CEC – Cation Exchange Capacity

CHES – 2-(Cyclohexylamino)ethanesulfonic Acid

EBS – Engineered Barrier System

EDTA – Ethylenediaminetetraacetic Acid

HEPES – 2-[4-(2hydroxyethyl)piperazin-1-yl]ethanesulfonic Acid

HLW – High Level Waste

ICP – Inductively Coupled Plasma

ICP-OES – Inductively Coupled Plasma Optical Emission Spectroscopy

ILW – Intermediate Level Waste

IR – Infrared

LLW – Low Level Waste

MES – 2-(-N-Morpholino)ethane-sulfonic Acid

NORM – Naturally Occurring Radioactive Material

NTA – Nitrilotriacetic Acid

PA – Picolinic Acid

PWR – Pressurised Water Reactor

PXRD – Powder X-Ray Diffraction

SEM – Scanning Electron Microscope

TBP – Tributyl Phosphate

TCE – Trichloroethene

TNT – Trinitrotoluene

TOC – Total Organic Carbon

VLLW – Very Low Level Waste

XRD – X-Ray Diffraction

Chapter 1: Introduction

1.1 Introduction

Sellafield, formerly known as Windscale, is a nuclear processing and former electricity generating site near Seascale in Cumbria, England. The Sellafield site has been operational since the 1940s when it was used as a Royal Ordnance Factory supporting the war effort by producing trinitrotoluene (TNT). In 1947, the site was acquired by the government's Department of Supply as the location for the world's first commercial nuclear power station, Calder Hall. The first generation reactors at Calder Hall were in operation from 1956 to 2003[1].

Today the site comprises of a wide range of nuclear facilities including redundant facilities associated with early defence work, as well as operating facilities associated with the Magnox reprocessing programme, the Thermal Oxide Reprocessing Plant (Thorp), the Sellafield MOX plant and a range of waste treatment plants.

A number of leaks of radioactive liquors to ground are known to have occurred from several plant buildings, vaults and disposal trenches within and around the Separation area over the past 50 years[1]. The most significant of these leaks have occurred from the Magnox Silo, the Caesium Extraction Plant, the Magnox Reprocessing Pump House, the Sludge Storage Tanks, the Burial Pits and the Medium Active Evaporation and Thermal Denitration Plant[1]. The radioactive contamination will be accompanied by other components of spent fuel reprocessing, including inorganic salts from neutralised acids, solvents and other organic compounds along with the typical contaminants commonly associated with large industrial activity such as heavy metals, fuel, oils, degreasing agents etc.

This project investigates the changes in radionuclide mobility in the environment that may occur due to the presence of contaminants in the pond liquors. The limited information provided by Sellafield states that the immediate area underneath the storage ponds consists of a 'bentonite-like' clay mineral, a clay mineral with a high exchangeable capacity. The objective of this study was to investigate radionuclide interactions with bentonite-like materials and observe possible interferences by contaminants.

1.2 Nuclear Power Reactors

Nuclear reactors are designed for the production of heat, mechanical and electric power, and the production of radioactive nuclides for these processes to occur. The design of each reactor varies depending on the purpose for instance, in the case of electric power production, the design is chosen to provide the cheapest electricity whilst taking long-term reliability into consideration[2].

The nuclear power plants rely upon nuclear fission for the generation of heat. Fission is the splitting of a heavy nucleus, such as that of uranium, into two or more fragments as well as lighter particles, such as neutrons. Fission may occur spontaneously but in nuclear reactors, splitting is induced by the interaction of a neutron with a fissionable nucleus[3]. As neutrons are often released as a by-product of a fission reaction, a 'chain' reaction of fission events may be sustained under suitable conditions. The energy released from these fission reactions provides the heat in the reaction core, which will ultimately be turned into electricity.

On average, a fission event releases about 200 MeV of energy. To produce a similar amount of energy from a typical chemical reaction such as the combustion of oil or coal, would require 6000 barrels of oil or 1000 tons of coal[3].

All nuclear reactors require a fissile material for the establishment of a chain reaction. ^{235}U is a naturally occurring fissile material and is therefore used in commercial power plants. A downside of ^{235}U is that >99% of the material is in fact ^{238}U so many reactors require the uranium to be enriched in order for it to contain a higher proportion of ^{235}U.

The neutron energy is moderated by collisions with the relatively light nuclei of the moderation material. This moderating material varies depending on the type of nuclear reactor, but is commonly water or carbon. The moderating material captures a neutron therefore limiting the number of fissionable reactions in the core and thus controls the reaction in the core. Water is a very effective moderator as the hydrogen can capture a neutron, forming deuterium and releases a gamma ray, which has only a small amount of energy when compared to that released by a fission event. This means neutrons will be absorbed by the water with very little energy yield[3].

1.2.1 Uranium Fuel Cycle

The uranium fuel cycle is the series of industrial processes which involve the production of electricity from uranium in nuclear power reactors. The nuclear fuel cycle starts with the mining or uranium ores which are then converted to UF_6 ready for

enrichment. The fissile material in nuclear fuel (^{235}U) is usually only present in small quantities, <1 %, in the natural ore and needs to be enriched to between 3.5 and 5 %. Once enriched, the fuel undergoes fabrication in order to be ready to be used in a nuclear reactor. After the uranium fuel is spent, the fuel undergoes a further series of steps including temporary storage, reprocessing and recycling before the wastes are disposed[2].

Table 1 below shows the major fission products produced by a nuclear reactor at ten years[4].

Table 1. Major fission products produced by a nuclear reactor at 10 years[4]

Nuclide	Amount / Bq KgU^{-1}	Half-Life / Years
^{90}Sr, ^{90}Y	5.14×10^{11}	28.8
^{93}Zr, ^{93}Nb	1.56×10^{7}	1.5×10^{6}
^{94}Nb	1.62×10^{3}	2.0×10^{4}
^{99}Tc	1.28×10^{8}	2.1×10^{5}
^{107}Pd	1.03×10^{6}	7.0×10^{6}
^{113m}Cd	1.70×10^{8}	7.7×10^{15}
^{121m}Sn	1.27×10^{6}	76
^{126}Sn, ^{126}Sb	5.18×10^{6}	1.0×10^{5}
^{129}I	2.93×10^{5}	1.57×10^{7}
^{135}Cs	1.01×10^{6}	2.3×10^{6}
^{137}Cs, ^{137}Ba	7.66×10^{11}	30
^{151}Sm	2.25×10^{9}	90
^{152}Eu	7.22×10^{6}	12.7

1.2.2 Thermal Reactors

The large majority of nuclear power reactors are based on fission by thermal neutrons. The two most important types of thermal reactors used are pressurised water and boiling water reactors. Each reactor type is described in more detail below.

Pressurised Water Reactors

Around 60% of the world's commercial power reactors are pressurised water reactors (PWR)[5]. A pressurised water reactor consists of a compact core in the pressure vessel capable of containing ordinary water at high pressure. The water serves as both moderator and heat-transfer medium under a pressure high enough so as to prevent

boiling due to operating temperatures in excess of 300 °C. Between three and four steam generators are connected to the pressure vessel to form the primary coolant circuit. The steam generators are towers with kilometres of narrow pipes through which water from the nuclear core is pumped, transferring heat to a secondary coolant circuit in which water at a low pressure boils to drive a steam turbine.

Modern PWR cores contain up to 241 fuel assemblies which can each hold between 200 and 300 fuel rods. Each fuel rod comprises a stack of enriched uranium dioxide fuel pellets in a sealed tube of Zircaloy. Zircaloy is a slightly alloyed zirconium with tin[6]. Figure 1 shows a schematic of a pressurised water reactor.

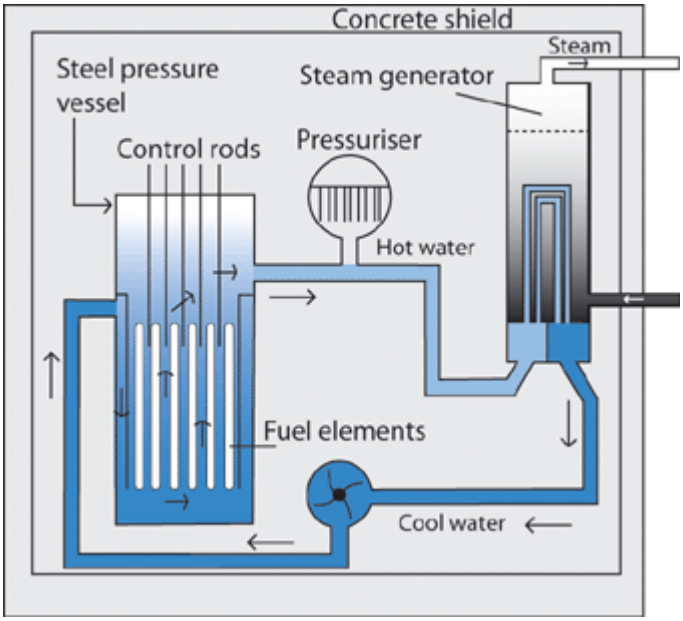

Figure 1. Schematic Diagram of a PWR[7]

Advantages of PWRs:

- PWR reactors are very stable due to their tendency to produce less power as temperatures increase; this makes the reactor easier to operate from a stability standpoint.
- PWR turbine cycle loop is separate from the primary loop, so the water in the secondary loop is not contaminated by radioactive materials.

Disadvantages of PWRs:

- Pressurised water reactors cannot be refuelled whilst operating.
- The coolant water must be highly pressurised to remain liquid at high temperatures. This requires high strength piping and a heavy pressure vessel and hence increases construction costs.

Boiling Water Reactors

Boiling water reactors (BWR) are similar to PWRs in that they both use water for moderation and cooling. The main difference between the two is that the water passing through the core in a BWR can boil as it operates at a lower pressure.

The steam passes through drier plates above the top of the core to remove water droplets and then moves directly to the steam turbines. This process means that steam generators are not required but does mean that turbines are effectively part of the reactor circuit. The coolant in any reactor is always contaminated with radionuclides so the turbine must be shielded and radiological protection is required during maintenance.

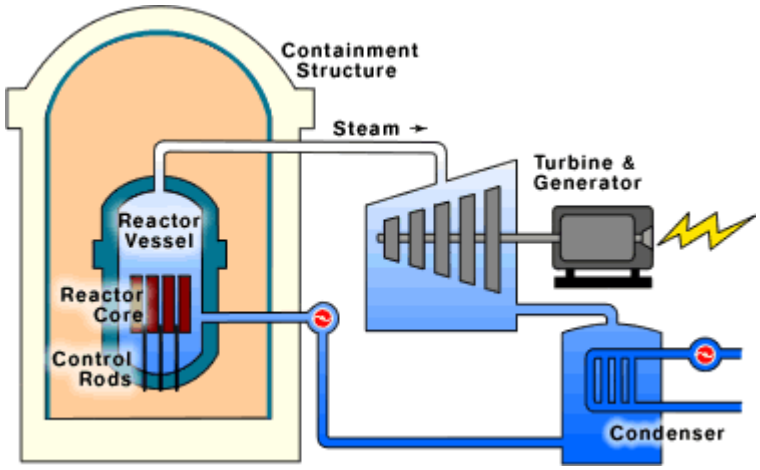

Figure 2. Schematic Diagram of a BWR[8]

As can be seen in Figure 2 above, the design of the reactor differs slightly from that of a PWR. The control rods enter from below as there is no space for them above. This arrangement makes them more effective as there is an increase in the steam fraction due to the water passing through from below.

1.2.3 Gas Reactors

Gas reactors are graphite moderated reactors cooled by pressurised carbon dioxide or helium. The first generation of these reactors uses natural uranium metal fuel in a magnesium alloy casing which absorbs very few neutrons, commonly known as Magnox.

Magnox Nuclear Power Reactor

The UK is the only country to have developed a significant programme of commercial gas-cooled reactors[5]. In 1956 the first of four Magnox reactors at Sellafield became operational. These are graphite moderated reactors cooled by pressurised carbon dioxide. Magnox is an acronym for magnesium alloy no oxide, named after the cladding used to encase the natural uranium metal fuel used in the reactor. The magnesium alloy was specifically designed for the reactor as it absorbs very few neutrons[5].

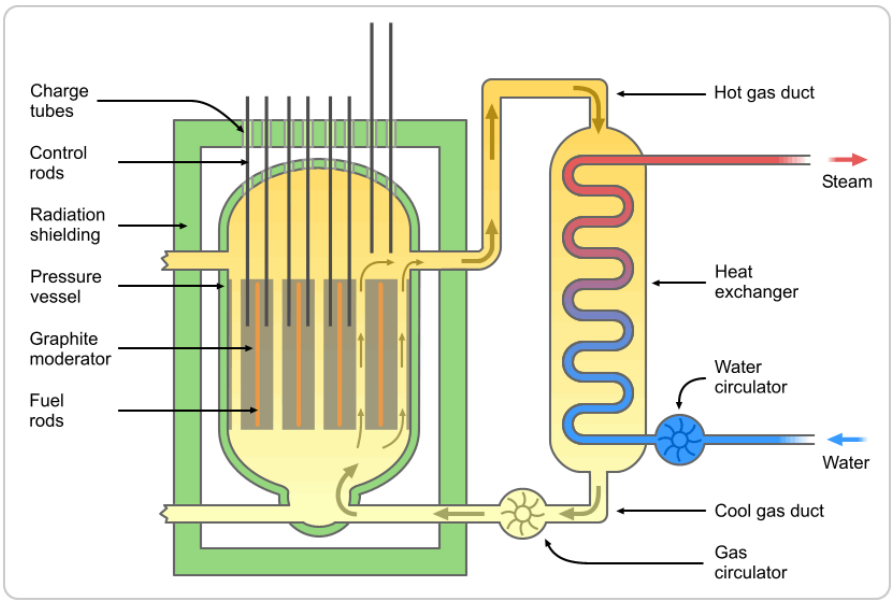

Figure 3. Schematic Diagram of a Magnox Reactor[9]

Magnox Fuel Production

Uranium metal is produced by reacting uranium tetrafluoride with magnesium metal carried out within a graphite crucible container held in a sealed stainless steel pressure

vessel under an argon atmosphere. The reaction is highly exothermic with the temperature rising to 1500 ºC within the pressure vessel.

$$UF_4 + 2Mg \rightarrow U + 2MgF_2$$

Magnesium fluoride is the by-product from the reaction which is separated from the uranium molten metal as a lighter liquid slag. After cooling, the uranium metal billets are removed from the graphite container whilst the solid magnesium fluoride is crushed and leached with acid to remove any remaining uranium before disposal[5].

The Uranium metal billets are later melted mixed with recycled metal scrap in a large, thick walled graphite crucible. Once complete melting has occurred, the molten metal is poured through a hole in the base of the crucible into a mould assembly where they are cooled to 250 ºC under argon before final cooling in air. The moulds are then disassembled and the rods extracted[5].

The rods are inserted into Magnox cladding and threaded Magnox end caps are fitted. Any space left between the fuel rod and the Magnox cladding is purged with helium and the end caps are then welded into position. The Magnox fuel is now ready to be used in the reactor. An example of finished Magnox fuel rods can be seen below in Figure 4.

Figure 4. Magnox fuel elements[10]

Advanced Gas-Cooled Reactors

The second generation gas reactor, known as the Advanced Gas-Cooled Reactor (AGR), was developed from the original Magnox reactors. Like the Magnox reactor, AGRs have a graphite moderator and use pressurised carbon dioxide as the coolant. AGRs use uranium oxide fuel in stainless steel casing as uranium oxide has a considerably higher melting point than pure uranium metal allowing higher fuel ratings, higher operating temperatures and improved thermal efficiency[11].

Large blowers drive the carbon dioxide coolant through the core from bottom to top and into the heat exchangers to produce the steam. The large size of the core makes the capital cost relatively high but there are some advantages with safety.

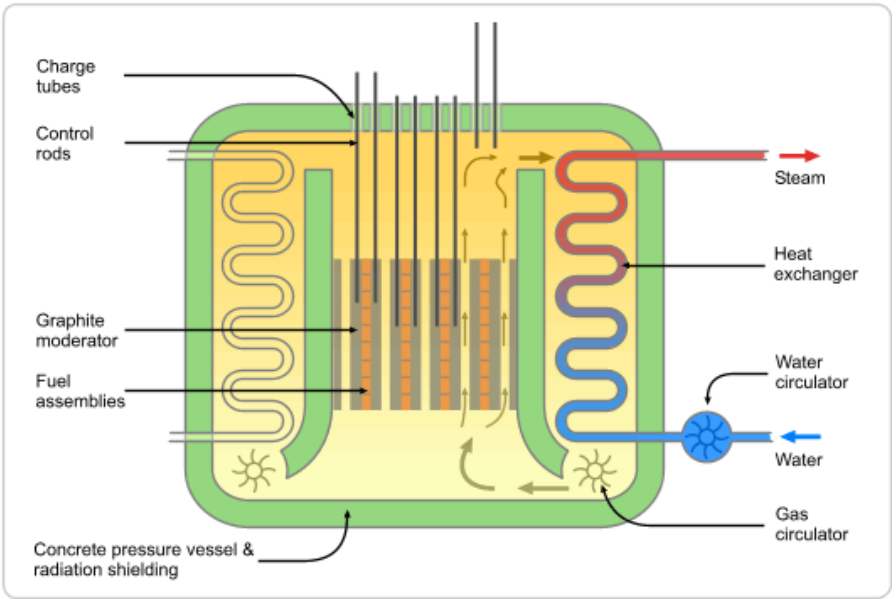

Figure 5. Schematic Diagram of an AGR[12]

1.3 Nuclear Waste

Nuclear reactors unavoidably produce radioactive by-products which can pose problems for the continued use of the reactor[4]. For instance, some of the nuclides produced will capture neutrons that are required for the continuation of the reactor process. As a result of this problem, and the gradual use of ^{235}U, the fuel becomes less efficient over time and needs to be replaced. If the fuel is not sent to be reprocessed, then it is classed as nuclear waste which will need to be disposed of effectively and efficiently to minimise the risk to the surrounding environment.

1.3.1 Nuclear Waste Classification

There are many ways that nuclear waste can be produced. Most nuclear waste occurs as a result of nuclear power generation, military defence programs, the application of radioactivity for medicinal purposes, the enhancement of naturally occurring radionuclides or from accidental arisings from incidents such as the Chernobyl disaster.

Radioactive waste is split into different categories depending on the activity of the waste. The general categorisation of waste is:

- Exempt waste
- Transition radioactive waste
- Very low level waste (VLLW)
- Low level waste (LLW)
- Intermediate level waste (ILW)
- High level waste (HLW)

1.3.2 Exempt Waste

Internationally, there are varying criteria with regards to the standards applied to the disposal of radioactive waste materials. Naturally occurring radioactive material (NORM) may be considered exempt under conditional exemption orders if it meets the guideline criteria. If the criteria are met, the NORM can be sent to landfill to be disposed of.

In the UK, exempt materials may contain anthropogenic radionuclides as well as NORM, but the activity levels of the anthropogenic radionuclides must be less than those stated in the Radioactive Substances of Low Activity (SoLA) Exemption Order 1986[13]. The requirements are:

- Solids to have activity levels <0.4 Bq g^{-1}

- Organic liquids, ^{14}C and ^{3}H to have activity levels <4 Bq ml^{-1}. All other liquids containing anthropogenic radionuclides are classed as low level waste.
- Gases must have half-lives <100 s.

1.3.3 Very Low Level Waste (VLLW)

Very low level waste is a criterion primarily intended for small volume radioactive waste. This waste can be disposed of with normal refuse waste in a dustbin. For each 0.1 m^3 of waste, the total activity must be no more than 400 kBq of β/γ and for single items of waste, the total activity must not exceed 40 kBq β/γ.

1.3.4 Low Level Waste (LLW)

Low level waste has activity levels above that of exempt waste, but does not require shielding in handling or storage. LLW may contain both natural and anthropogenic radionuclides. Anthropogenic radionuclides usually stem from the fission of uranium in nuclear reactors, for instance, the fission products themselves and the resultant decay products of these fission products. Naturally occurring radionuclides are generally uranium, thorium and their decay products.

Solid wastes are normally the only wastes acceptable for disposal as LLW. Waste considered as LLW is varied, for instance, clothing which has come into contact with radionuclides. Other items usually classified as LLW are produced from contaminated reactor building items, spent fuel storage pond and water treatment plant filters, and often wastes arriving from general operation and maintenance such as incinerator ash. These will be classed as LLW providing they are below the maximum activity levels acceptable for this classification. The acceptable levels are no greater than 4 GBq te^{-1} for α or 12 GBQ te^{-1} for β/γ.

LLW needs to be disposed of correctly and there are regulations in place to deal with this waste. The normal practice for LLW is to put the waste in containers which are placed into purpose built concrete bunkers or vaults. A system of monitored drains and break tanks are in place to allow monitoring and any leachate produced will also be monitored. The surface may be capped with soil, although capping with soil may not provide a long term solution and will need to be regularly monitored.

1.3.5 Intermediate Level Waste (ILW)

Intermediate level waste can arise from various sources; medical wastes, military wastes, fuel wastes and other industrial wastes. Medical wastes include a variety of

sealed sources such as ^{60}Co, ^{3}H and ^{14}C. This waste is either sent back to the manufacturers or sent to national disposal services. Military waste consists of waste arising from weapons manufacture, so commonly plutonium, plutonium contaminated material, filters and liquid wastes. Fuel wastes consist of many miscellaneous activated components, filters, sludges, ion exchange resins and debris.

ILW is waste that contains higher concentrations of β/γ and sometimes α emitters too. There is little heat output from this type of waste but the waste generally needs more remote handling when compared to LLW.

ILW can be sub-categorised as short lived ILW or long lived ILW. Short lived ILW are radionuclides with a half-life of less than 30 years and long lived ILW is for anything above 30 years.

1.3.6 High Level Waste (HLW)

High level wastes are wastes whose temperature may rise significantly as a result of their radioactivity. The temperature change has to be taken into account in the design, treatment and subsequent storage or disposal of these waste forms.

HLW originates from spent fuel as the spent fuel will still contain fissionable material, albeit in very small quantities. If it is economically viable, the spent fuel can be reprocessed in order to use this fissionable material, otherwise the material will need to be disposed of or stored correctly. Common HLW radionuclides are ^{235}U, ^{239}Pu and ^{241}Pu. Long lived activation products produced by neutron absorption in reactors often need to be treated as HLW.

1.4 Radioactive Waste Management

Waste disposal is the final step of the waste management chain and ideally comprises placing radioactive waste in a dedicated disposal facility. Sometimes discharging effluents into the environment is an option providing this is within any permitted limits.

All types of radioactive waste need to be carefully managed in order to keep the public safe, protect the environment and ensure security from intrusion (accidental or deliberate). Disposal of radioactive waste in a disposal facility needs to ensure that the waste is isolated from human activity and from natural processes. Any radioactive material placed in these facilities needs to be retained safely for such a period of time that any eventual release of radionuclides from the facility must be at such low concentrations that they do not pose a hazard to human health and the surrounding environment.

1.4.1 Multi-Barrier Concept

Repositories for the storage or disposal of radioactive waste generally rely on a multi-barrier system to isolate the waste from the biosphere[14]. The multi-barrier concept recognises that no barrier can be reliable forever. Thus having a sequence of barriers would improve the likelihood of containment of the radionuclides, giving radioactive decay time to remove most of the radioactivity[4]. This multi-barrier system normally comprises the natural geological barrier provided by the host rock and an engineered barrier system (EBS).

The EBS consists of a number of components such as the waste matrix, container, buffer or backfill and the repository walls and wall linings. The various barriers are engineered to initially contain the radionuclides and then to limit their release to the environment after a certain timescale.

The key functions of a repository are:

- Isolate waste from the near-surface and human activities
- Protect the biosphere
- Limit release from the progressively degrading EBS
- Dispersing and diluting the flux of long lived radionuclides

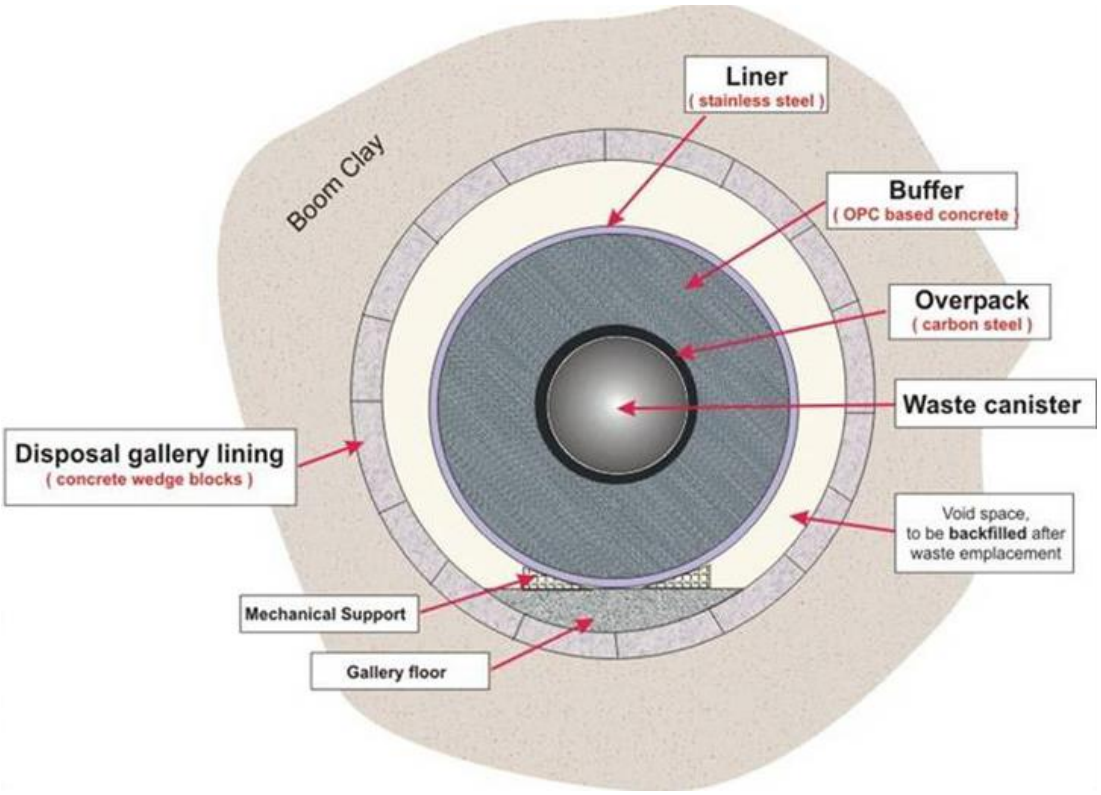

Figure 6. Diagram Detailing a Multi-Barrier System[15]

Figure 6 shows the various engineered barriers in an EBS surrounded by the host rock, in this case Boom clay.

Although the engineered barriers have an individual role in limiting the release of radionuclides to the biosphere, the engineered barriers must also function as an integrated system. There are requirements such as the need for one barrier to ensure favourable physicochemical conditions so that a neighbouring barrier can fulfil its intended function. For example, in some disposal systems the buffer has a role in minimising canister corrosion[16].

For an EBS to be effective it has to be tailored to the specific environment in which it will be functioning. Consideration must be given to factors such as the heat that will be produced by the waste, interactions between the different materials in the waste and the EBS, the ground water chemistry (e.g. pH and redox conditions) and flux, the mechanical behaviour of the host rock, and the evolution of the EBS[16].

1.4.2 Alternative Disposal Options for Long Lived Wastes

Although geological disposal of radioactive wastes is generally favoured, a number of other options have been studied and proposed for long lived wastes. The alternatives for long lived wastes include:

- Space disposal
- Ice sheet disposal
- Disposal beneath the seabed
- Rock melting
- Nuclear incineration

Space Disposal

Space disposal is attractive because it would remove the waste from the biosphere for all time. Studies by NASA have shown that the launch of nuclear payloads into a solar orbit halfway between Earth and Venus is feasible. The main problems associated with space disposal are the extremely high cost and the risk of launch failure. The current estimated rocket failure rate is 6% which all but eliminates this disposal route from further consideration. If a launch failure were to occur, it would cause widespread pollution to almost any region in the world[17].

Ice Sheet Disposal

Ice sheet disposal is another popular option for waste disposal. Apart from the remoteness of the polar ice caps and the reduced impact on human life, the idea that heat-emitting wastes would be self-sinking in the ice is appealing. The problems with ice disposal are the very high transport and handling costs, uncertainties in the evolution of these areas over the time spans for which containment must be considered, and legal constraints. Disposal in the Antarctic is forbidden by international law, whilst other sites proposed, such as Greenland, are controlled by Denmark[17].

Seabed Disposal

Disposal of high level wastes on the seabed is currently prohibited by international agreement. Considerable research has been carried out on disposal beneath the seabed instead. Advantages of disposal beneath the seabed are physical remoteness, chemical and geological stability of the sediments and rocks, and the great dilution capacity of the sea in the event of releases occurring. Disposal techniques involving self-burying containers which are allowed to free-fall from the disposal ship could be relatively inexpensive.

Some disadvantages of this proposed technique are the high cost and engineering problems associated with emplacement holes drilled in the ocean floor, or relying on self-burying containers to reach their target without incurring any problems[17].

Rock Melting

Rock melting involves emplacement of highly concentrated solid or liquid HLW into a deep borehole or cavity. The heat produced by the waste melts both the waste itself and the surrounding rock and, once cooled, the wastes are incorporated into a natural rock matrix[17].

Nuclear Incineration

Nuclear incineration is not a disposal option as such, but provides a method for destroying the long lived radionuclides which present most of the problems in other disposal systems. In nuclear incineration, long lived radionuclides are chemically extracted from the waste and emplaced in the neutron flux in a reactor core. This causes them to be activated or fissioned to form shorter lived products. This process involves handling vast quantities of very short lived and extremely active radionuclides and will expose the work force to large radiation doses[17].

1.4.3 Magnox Fuel Disposal

In the late 1950s and 1960s, the Magnox storage and decanning facility was constructed on site at Sellafield to deal primarily with spent radioactive fuel from the Magnox reactors. Once the fuel was spent, the fuel rods were transported to a large storage pond to cool before decanning of the magnesium alloy and reprocessing of the fuel rods. One of the problems from storing Magnox fuel in storage ponds is that over time the magnesium alloy will corrode. Early fuel was stored in skips in uncovered ponds resulting in chloride contamination of the pond water by chloride ions entrained in the air of the coastal environment[18]. The magnesium clad fuel was therefore even more susceptible to corrosion. As part of the planning requirement of any programme of Magnox reactors was a capacity to guarantee a smooth reprocessing cycle[19], this would reduce storage times of the fuel in the ponds.

Figure 7. Photograph of a Magnox storage pond at Sellafield

The Magnox reactors were producing comparatively large volumes of spent fuel meaning a second separation area was commissioned in 1964. At the first storage plant, the volume of radioactive waste was reduced by evaporation before being stored, but the second storage plant pre-treated the waste with tributyl phosphate (TBP) to extract ^{235}U and ^{239}Pu before storage[4]. The TBP degraded to phosphoric acid leading to substantial precipitation of solids which settled to the bottom of the tanks and created 'hot spots' where elevated rates of corrosion occurred[19]. A steam-stripping system was developed for the tanks to overcome this problem which removed phosphates and allowed the volume of waste to be reduced before storage.

Several problems, such as leakages, occurred with the new tanks leading to shut downs that lasted several months. The construction of new storage tanks couldn't keep up with the pace of waste production and in late 1972 reprocessing was suspended for 6 months whilst new storage facilities were created. Political issues in 1973, a strike at Sellafield and the 3-day-week, slowed down reprocessing and it didn't resume until 1974, over 18 months after the initial suspension.

This pause in reprocessing led to increased residence times of spent Magnox fuel in the fuel storage ponds. Reprocessing had to proceed slowly due to the condition of the fuel and a backlog of spent fuel built up in the fuel ponds[19]. By 1973 the corrosion problems that had built up led to high levels of soluble radioactive caesium and strontium being released into the ponds.

The storage and decanning buildings have handled in excess of 25,000 tons of irradiated metal clad uranium fuel[20]. The fuel that has been handled at Sellafield has

come from both the UK and overseas. The facilities ceased operations in 1986 but there was still around 1,000 tons of fuel and Magnox sludges from corrosion of the cladding, in areas of the storage pond.

A number of leaks of radioactive liquor to ground are known to have occurred from the separation areas[1]. Boreholes on site have shown the dominant radioactive species observed to be ^{90}Sr, ^{137}Cs, ^{3}H and ^{99}Tc – all highly soluble. Amongst the by-products produced, Sr^{2+} and Cs^{+} are considered the most dangerous radionuclides to human health due to their high transferability, high solubility, relatively long half-lives and easy assimilation in living organisms[21].

The environmental department at Sellafield have been monitoring the contamination and it has been noted that the movement of contamination in some areas is faster than expected given the nature of the surrounding soils. One area of significant interest is the migration of ^{137}Cs and ^{90}Sr in clay soils, with information provided by Sellafield where the observed migration is proceeding faster than the expected rate of 6 cm yr^{-1}, according to their models.

Table 2 below outlines the different characteristics associated with three of the larger storage ponds found at the Sellafield site.

Table 2. Examples of Ponds and Their Characteristics Found at the Sellafield Site

Pond Name	pH	Information
B29	8	Nominally fresh water – pH 8 due to residual Mg
B30	11	Cannot exceed 11.4 due to purge from pond 5 limiting upper pH
B38	Varied	Varies bay to bay – unpredictable due to previous treatment

There is limited released data available on the composition of the various ponds, however, there is information available about the B30 pond.

The B30 Pond at Sellafield

The B30 pond forms part of the B30 complex which provided the mainstream storage and decanning facilities for Magnox fuel at Sellafield[22]. During its 20 years of operation the corrosion of the Magnox clad fuel stored in the pond has led to the accumulation of substantial quantities of sludge on the pond floor. This sludge is predominantly

magnesium hydroxide but also contains uranium and other fuel derived constituents such as ^{137}Cs[22]. B30 pond also contains various solid items including various beta/gamma wastes, Tokai Mura end crops and skips containing a natural zeolite ion exchanger known as AW500[23]. The fuel used in the Japanese Tokai Mura Magnox reactor consists of a hollow uranium cylinder whose ends are sealed by zirconium screw plugs fusion-welded in position. The complete rod is then encased in Magnox cladding[23]. Initially the fuel was decanned and the end crops removed by cropping. These crops were stored in open mild steel bins in the B30 ponds. Under these conditions the uranium slowly corroded to an oxide, thus hydrides and soluble fission products were released to the pond water. The uranium hydride material is a pyrophoric material when dry and requires special handling minimising the exposure to air. To overcome this problem, 11.04 tonnes of uranium underwent 'in pond' cement encapsulation[23].

From 1974 end crops were removed and the fuel decanned afterwards. This end cropping process did not result in cement encapsulating as happened previously and instead they have been stored as exposed crops in bins[23].

AW500 is a natural zeolite ion exchanger which consists of cylindrical clay pellets approximately 1.5 mm in diameter and 5-10 mm in length. Skips of AW500 were loaded into the fuel storage ponds and the pond water pumped through the zeolite in order to reduce the activity loading of the pond water[23]. It has been estimated that in each skip accrued an activity loading of about 130 TBq, the bulk of this being ^{137}Cs[23]. The quantity of AW500, at the time of the Sellafield report, to be processed was 229 zeolite skips with 175 m^3 of AW500 contained in the skips.

The main elements present are aluminium, silicon, caesium, uranium and plutonium. Silicates are present too. Metals and alloys are present as the following (wt.%):

- 5 wt.% possibly as Al_2O_3
- 1 wt.% Magnox/Magnesium
- 2 wt.% Fe(2)

There are probably traces of inorganic anions too[23].

B30 is just one example of numerous ponds found at the Sellafield site and the composition of each individual pond is expected to be different.

1.5 Decommissioning and Clean-up

The term decommissioning, as used within the nuclear industry, means the actions taken when a facility has reached the end of its useful life, in order to ensure that it is managed safely in a manner that protects workers, the general public and the environment[13]. These actions can range from simply closing the facility to the complete dismantling of the facility and restoration of the site for unrestricted use.

The radioactive waste has to be categorised in order to define the types of materials that are present so that the appropriate disposal route can be undertaken, and the appropriate methods can be used for the dismantling and demolition phases. Decommissioning and dismantling involves either manual or robotic removal of all process plant and equipment and the radiological decontamination of the structure as far as possible.

Once the above has been established, standard industrial demolition techniques can be used with the land eventually being remediated for whatever future use is determined for the site.

There are three distinct stages of nuclear decommissioning, originally defined by the International Atomic Energy Association (IAEA)[24], that may be separated by periods of care and maintenance or follow directly one after the other in a continuous, systematic and progressive manner.

Stage 1: Reactors are completely defueled and the fuel shipped away from the reactor. All heat transport fluids and removable contaminated materials are taken away. For non-reactor facilities, all radioactive sources and removable equipment are taken away. The containment is maintained intact with the atmosphere inside the building and enclosures controlled. Periodic measurements and visual checks are carried out to ensure that contamination control systems continue to function correctly.

Stage 2: Contaminated areas are decontaminated to the appropriate extent, and any areas with unacceptable residual radioactivity levels are sealed to prevent unauthorised access. Contaminated parts that are easily dismantled are transported elsewhere where they are to be sealed. Some monitoring equipment will remain operational depending on specific circumstances. Surveillance around the restricted area will continue, although not as extensive as that in stage 1.

Stage 3: All materials, equipment and structures that have radioactive levels above prescribed limits are removed to an approved storage or disposal site. No further surveillance, inspection or tests are necessary.

1.5.1 Site Remediation

The ultimate end-point for decommissioning a nuclear licensed site is the termination of the license and the release of the site for unrestricted use. A site can only be delicensed if the regulator is satisfied that there is no danger from ionising radiations from anything on the site or that part of the site that is to be delicensed.

Remediation techniques for radioactively contaminated ground involve either:

- Removal of the contamination and transfer to a controlled disposal facility
- Immobilisation, solidification and stabilisation in situ to reduce the migration of the contaminants
- On-site containment of the contamination where barriers are placed adjacent to the contaminated soil to reduce migration of the contamination.

1.6 Radionuclides Investigated

The long-lived, soluble radionuclides ^{137}Cs and ^{90}Sr are of major concern principally because of their potential impacts upon human health and, as such, have been investigated throughout this report

1.6.1 Caesium

Caesium (Cs) is a soft, silvery-gold alkali metal with the atomic number 55. There are 39 known isotopes of caesium but only one of these, ^{133}Cs, is stable. There are three major radioactive caesium isotopes, ^{134}Cs, ^{135}Cs and ^{137}Cs.

^{134}Cs has a half-life of two years and is produced by neutron activation of ^{133}Cs.

^{135}Cs with a half-life of 2.3 million years is one of seven long-lived fission products. In most nuclear reactors its fission product yield is reduced because its predecessor xenon-135 is an extremely potent neutron poison and often transmuted to stable xenon-136 before it can decay to Cs-135.

^{137}Cs with a half-life of 30.17 years is one of the two principal medium-lived fission products, along with strontium-90, which are responsible for most of the radioactivity of spent nuclear fuel after several years of cooling. It constitutes most of the dose from radioactivity still left after the Chernobyl accident. ^{137}Cs decays by beta emission to ^{137m}Ba.

$$^{137}_{55}Cs \rightarrow {}^{137m}_{56}Ba + {}^{0}_{-1}\beta$$

^{137m}Ba decays by isomeric transition from the metastable excited state to the ground state with emission of a gamma particle. The half-life for this decay is relatively short, 2.55 minutes, and the γ has an energy of 662 KeV. When analysing for caesium by gamma spectroscopy, it is in fact the gamma produced by ^{137m}Ba that is measured.

Figure 8 below shows the decay scheme of ^{137}Cs.

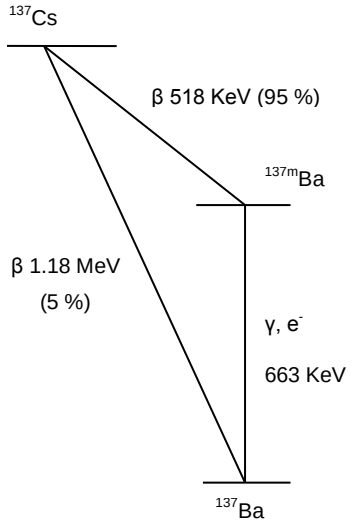

Figure 8. Decay scheme of ^{137}Cs[25]

^{137}Cs has a very low rate of neutron capture due to its small thermal neutron capture cross section (250 mb)[26], and therefore cannot be feasibly disposed of in this way so must be allowed to decay.

1.6.2 Strontium

The alkaline earth metal strontium (Sr) is a soft, silver-white, highly reactive element that has four stable, naturally occurring isotopes: ^{84}Sr (0.56%), ^{86}Sr (9.86%), ^{87}Sr (7.0%) and ^{88}Sr (82.58%).

There are three important strontium radioisotopes, ^{90}Sr, with a half-life of 28.78 years, ^{89}Sr (half-life 50.5 days) and ^{85}Sr (half-life 64.85 days). ^{90}Sr is a by-product of nuclear fission when an atom of ^{235}U splits asymmetrically. The yield of ^{90}Sr from such fission reactions is about 6%. ^{90}Sr decays fully by beta emission, with an energy of 0.20 MeV, to ^{90}Y (half-life 2.67d) which is usually in secular equilibrium with the longer lived parent isotope. ^{90}Y decays by emitting a more energetic beta particle, 0.94 MeV, and also emits a weak gamma, <0.001 MeV, at the same time to form ^{90}Zr which is stable[27]. ^{90}Sr is a hazard to humans as it substitutes for calcium in the body, preventing excretion. After entering the body, most often by ingestion with contaminated food or water, 70-80% of the dose is excreted but the remaining ^{90}Sr is deposited in bones and bone marrow. Its presence in bones can cause bone cancer, cancer of nearby tissues, and leukaemia.

^{89}Sr is used in the treatment of painful metastases associated with bone cancer[28]. Blake et al. demonstrated that ^{89}Sr follows the biochemical pathway of calcium within

bone and is preferentially taken up at sites of increased bone turnover, where it remains almost indefinitely[29].

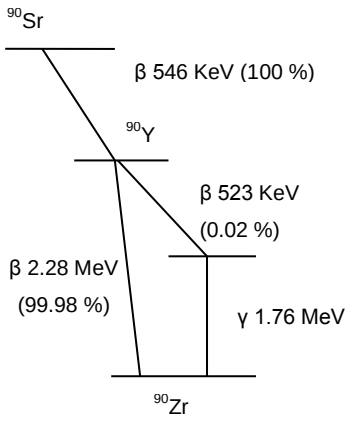

Figure 9. Decay scheme of ^{90}Sr

^{85}Sr decays to the stable ^{85}Rb by orbital electron capture followed by the emission of two gamma rays, one of energy 0.514 MeV and the second of 0.878 MeV[30,31]. The 0.878 MeV gamma ray is found to be in coincidence with the characteristic x-ray emitted by ^{85}Rb due to orbital electron capture[32].

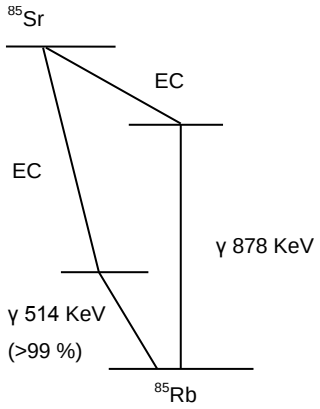

Figure 10. Decay scheme of ^{85}Sr[32]

1.7 Soils

Soil is generally made up of finely ground rock particles and can be categorised into three main groups – sands, silts and clays. The groups are classified according to particle size with sand having the largest and clay the smallest. The inorganic fraction of soils and natural sediments consist almost entirely of silica and various silicates[33].

Soil is a very good medium for the transportation of chemicals and nutrients. This can lead to problems if radionuclides and other contaminants get into the soil system as they can migrate through the soil and into the surrounding environment. Within the nuclear industry, the migration of radionuclides through the soil is a major concern due to the potential risk to human health and the environmental impact[34].

1.7.1 Silicates

Silicates are of major importance in soil chemistry due to their great abundance in the Earth's crust. Silicate minerals make up the largest form of rock types on earth covering approximately 90% of the Earth's crust. They are classed according to their structure and many different types of rocks and clays appear in each category.

The tetrahedron, SiO_4, dominates the structures of silicate minerals. The silicon atom at the centre of the tetrahedron is bonded to the four oxygen atoms via the sp^3 hybrid orbitals[35]. The SiO_4 tetrahedra are normally joined together to give chain, sheet or ring structures. The simplest silicate mineral group, the olivine group, contains separate SiO_4^{4-} anions bound to divalent cations e.g. Mg^{2+} and has a general formula Mg_2SiO_4. The olivines are readily weathered compared to the other forms of silicates as the lattice energy of the olivines is not as great[35].

Chain Silicates

Chain silicates are formed when SiO_4 tetrahedra join together in a manner where adjacent tetrahedra share a common oxygen atom. The simplest structures are continuous chains which have a repeating unit of SiO_3^{2-}, called the pyroxene chain. The pyroxenes are a group of chemically and physically related minerals which include enstatite, augite and hypersthenes. Pyroxenes are only marginally more stable than olivines.

Another repeating unit common in chain silicates is $Si_4O_{11}^{6-}$ which is known as the amphibole chain. This is slightly more complex than the pyroxene chain and includes minerals such as hornblende.

Figure 11 shows both the pyroxene chain (top structure) and the amphibole chain (bottom structure).

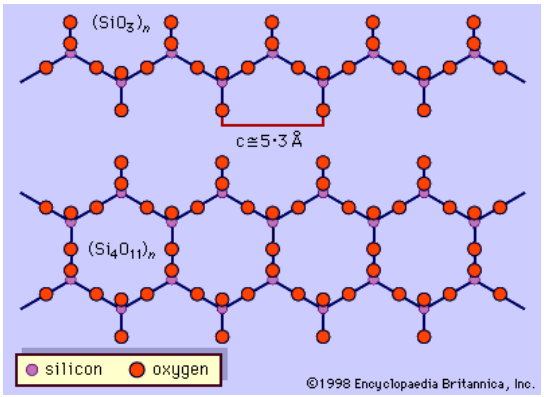

Figure 11. Comparison of the pyroxene chain and the amphibole chain[36]

Sheet Silicates

Sheet silicates consist of a network of SiO_4 tetrahedra linked to form hexagonal rings, like the amphibole structure above, which extend in two directions to form a continuous sheet. The repeating subunit is $Si_2O_5^{2-}$. The silicon atoms all lie in the same plane but there are two planes of oxygen atoms, one containing linked oxygen and the other containing unshared oxygen.

1.7.2 Octahedral Geometries

There are two main sheet structures with octahedral geometries, the gibbsite, $Al(OH)_3$, and brucite, $Mg(OH)_2$, structures. The hydroxyl groups in both structures replace the position of the oxygen in silica sheets. Each Mg or Al atom is coordinated with six hydroxyls and each hydroxyl is coordinated with two Mg or Al atoms[37].

Gibbsite is the most common Al oxide mineral and is often found in highly weathered soils. The structure of gibbsite features two planes of closely packed OH^- ions with Al^{3+} ions between these planes. Due to the ratio of hydroxyl to aluminium, the Al^{3+} ions are found in two out of the three octahedral places. This is often referred to as dioctahedral[38].

The brucite sheet resembles the gibbsite sheet in that the magnesium is octahedrally coordinated, but due to the ratio of hydroxyl to magnesium being 2:1 whereas for gibbsite it is 3:1, all of the available octahedral sites in brucite are occupied by a magnesium atom. This type of sheet is referred to as trioctahedral[35].

Many important clay minerals contain both silica and gibbsite or brucite sheets, however in some minerals the Al or Mg is replaced by other metal ions.

1.7.3 Clays and Clay Minerals

The term clay is a general term applied to materials having a particle size of less than 2 mm whereas clay minerals refers to a specific mineral that mainly occurs in the clay-sized fraction of the soil. There are many characteristics common to all clay minerals which are derived from their chemical composition, layered structure and size. All clay minerals have an affinity with water with some minerals, such as montmorillonite, swelling up to two or three times larger than their dry size.

The clay soils underneath the storage ponds at Sellafield are said to be bentonite-like in physical characteristics and structure. Bentonites consist essentially of clay minerals of the smectite group of clays. The smectite 2:1 structural units are three-layer clay minerals in which one tetrahedral sheet of one unit layer is adjacent to another tetrahedral sheet of another layer. They are classified as 2:1 phyllosilicates. A comparison of 1:1 and 2:1 layer structures is shown in Figure 12.

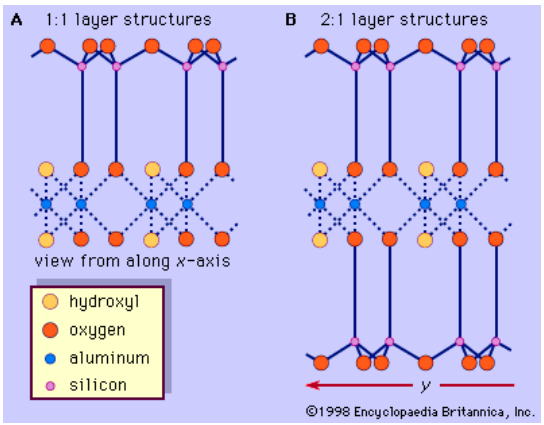

Figure 12. Comparison of 1:1 and 2:1 layer structures(3)

The oxygen atoms are opposite one another and bonding between the layers is weak. There is a high repulsive potential on the surface of the layers resulting from isomorphous substitution. This enables water to penetrate between the layers increasing the layer spacing[33]. Thus smectites have an expanding lattice, where all the layer surfaces are available for hydration and cation exchange. Interlayer surface and cation hydration between smectite structural units is a unique property of smectite clays. A particular feature of this group of minerals is the substitution of Si^{4+} and Al^{3+} in the crystal structure by lower valency cations. This leaves unsatisfied negative charges which are balanced by loosely held exchangeable cations such as Na^{+}, Ca^{2+}, Mg^{2+} and H^{+} located mainly on the interlayer crystal surfaces[39,40]. The structure, chemical composition, exchangeable ion type and small crystal size of smectite are responsible for several unique properties including a large chemically active surface

area, a high cation exchange capacity, interlayer surfaces having unusual hydration characteristics and the ability to strongly modify the flow behaviour of some liquids[40].

The smectite-saponite group includes the subgroups dioctahedral smectites and trioctahedral smectites. Common dioctahedral smectites include montmorillonite, beidellite and nontronite. The trioctahedral members of this group include saponite and hectorite. In saponite, substitution occurs in the tetrahedral sheet, but for hectorite, a lithium bearing mineral, substitution occurs in the octahedral sheet. A comparison of these clay minerals and their standard structural formulae can be seen in Table 3.

Table 3. Smectites and their Structural Formulae[41]

Dioctahedral Smectites	
Montmorillonite	$M_y^+ nH_2O\ (Al_{2y}Mg_y)\ Si_4O_{10}(OH)_2$
Beidellite	$M_x^+ nH_2O\ Al_2(Si_{4-x}\ Al_x)\ O_{10}(OH)_2$
Nontonite	$M_x^+ nH_2O\ Fe_2^{3+}(Si_{4-x}Al_x)\ O_{10}(OH)_2$
Trioctahedral Smectites	
Saponite	$(M_{x-y}^+ nH_2O)(Mg_{3-y}(AlFe)_y)\ Si_{4-x}Al_x)\ O_{10}OH_2$
Hectorite	$(M_y^+ nH_2O)(Mg_{3-y}Li_ySi_4O_{10}(OH)_2$

1.7.4 Montmorillonite

The original montmorillonite is a clay mineral from Montmorillon, France, first described by Damour and Salvetat in 1847[42] with the montmorillonite group being established by Ross and Hendricks in 1943[43] after their description of clay minerals with similar structural features to that of the original montmorillonite clay. The members of this group, however, vary widely in chemical composition. Since Ross and Hendricks described the montmorillonite group, minerals of this group are now more commonly known as smectities.

Montmorillonite clay minerals possess two kinds of electrical charges, a variable charge which is pH dependent, resulting from proton adsorption/desorption reaction of surface sites, and a structural negative charge resulting from isomorphic substitution within the clay structure[44]. It is an excellent sorbent because of high specific surface area, chemical and mechanical stability, layered structure and high cation exchange capacity[21]. The high CEC for montmorillonite is due to substantial isomorphic substitution and to the presence of fully expanded interlayers that promote the

exchange of cations[38]. The principal cations held in the exchange positions are Ca^{2+}, Mg^{2+}, Na^{+}, K^{+} and H^{+}[45].

1.7.5 Bentonite

Bentonite is part of the smectite family and is an aluminium phyllosilicate predominantly made up of montmorillonite with the remainder consisting of impurities due to cation exchange, such as Mg^{2+}, Fe^{2+}, Na^{+} and Ca^{2+} [46]. Bentonite clays have two types of charges; permanent negative charges on the basal planes originating from isomorphic substitutions and the pH-dependent charges developed on the surface hydroxyl groups at broken edges. Species having opposite charges can be adsorbed on these sites[47]. A negative charge associated with a cation replacement in the tetrahedral sheet, e.g. Al^{3+} replacing Si^{4+}, results in a localized charge distribution, whereas a diffused negative charge comes from cation exchange in the octahedral sheet, e.g. Mg^{2+} replacing Al^{3+} [48]. It is often formed from altered volcanic ash which has weathered with time[49].

Depending on the dominant exchangeable cations present, the bentonite may be referred to as either calcium bentonite or sodium bentonite, the two varieties exhibit marked differences in their properties and thus their uses differ too[39]. Studies have shown that the clay would display a higher swelling capacity if its exchangeable cations were of a lower valence, especially when it is a univalent cation[50], and thus calcium bentonite is synonymous with the term non-swelling bentonite and sodium bentonite is often termed swelling bentonite. When mixed with water, swelling bentonites exhibit greater dispersion and better rheological properties than non-swelling bentonites[39]. Particle dispersion is an important characteristic of bentonite clay minerals as it is necessary for obtaining a uniform and stable system[33]. Natural sodium bentonites are comparatively rare although the cation exchange properties of bentonite allow the more widespread calcium bentonite to be converted to the high swelling sodium bentonite with ease.

Bentonite is almost the universal choice as backfill material for sealing the emplacement tunnels in geological disposal systems. This is due to the high swelling capacity of compacted bentonite upon re-saturation, its very low transmissivity to water movement and good sorption characteristics. Bentonite is therefore a very effective near-field diffusion barrier to the movement of radionuclides[51].

Due to the physical and chemical properties of bentonite, samples vary within and between deposits because of differences in the degree of chemical substitution, amount of impurities and the nature of exchangeable cations present.

1.8 Sorption

Sorption is a general term used when the retention mechanism at the surface is unknown[38]. Adsorption, surface precipitation and polymerization are all examples of sorption.

1.8.1 Adsorption

Adsorption is defined as the accumulation of a substance or material at an interface between the solid surface and the solution and is one of the most important chemical processes in soils and clay minerals. Adsorption determines the quantity of plant nutrients, metals, pesticides and other organic chemicals retained on the soil surfaces. It is one of the primary processes that affects the transport of nutrients and contaminants in soils.

Surface functional groups play an important role in adsorption processes. Surface functional groups can be organic e.g. carboxyl, carbonyl or inorganic molecular units. The major inorganic surface functional groups in soils are the siloxane surface groups associated with the plane of oxygen atoms bound to the silica tetrahedral layer of a phyllosilicate and hydroxyl groups associated with the edges of inorganic minerals such as kaolinite.

The sorption of radionuclides on natural materials is important for the prediction of their migration rates[52]. For a sorption process to occur, a porous solid medium is required. The porous solid provides a very high surface area or high micropore volume, and it is this high surface area or micropore volume that produces a high sorptive capacity[53].

Sorption separation is based on three distinct mechanisms; steric, equilibrium and kinetic. In the steric mechanism the porous solid has a pore size that allows small molecules to enter whilst excluding larger molecules from entry. Steric adsorption commonly occurs with supercapacitors where the capacitance can be limited due to the pore size of the electrodes having a sieving effect on larger cations and anions[54]. The equilibrium mechanism is based upon the solid having different abilities to accommodate different species, i.e. the stronger sorption species will be favoured over a weaker sorption species. The kinetic mechanism is based on different rates of diffusion of different species into the pore. By controlling the time of exposure, the faster diffusing species is preferentially removed by the solid phase. These principle concepts of sorption can be applied to both liquid and gaseous phase systems.

Solutes can be adsorbed to the surface of clays as either outer-sphere or inner-sphere complexes. In inner-sphere complexation, a covalent bond is formed such that the solute is held very closely to the surface. The chemical bond with the clay surface is strong enough that the ion loses its co-ordinated H_2O molecules as it draws close to the surface and forms a bond with the solid surface. This process is often referred to as chemisorption[55].

In outer-sphere complexation, the solute draws close enough to form a co-ordinated arrangement but not close enough to lose all its co-ordinated water molecules. Figure 13 shows a schematic of the two different types of complexation mechanisms.

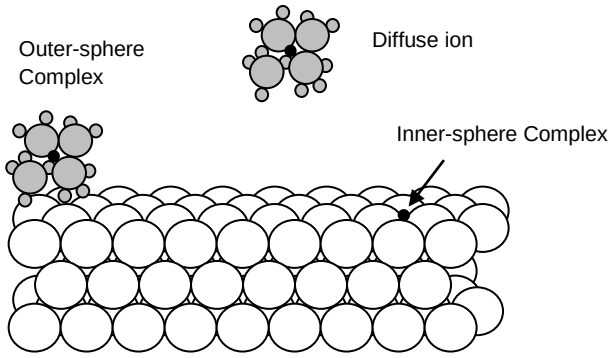

Figure 13. Diagram showing outer-sphere and inner-sphere complexation[55]

The chemistry at the surface affects its co-ordinated ions. Ligands that form strong complexes in solution tend to also form strong complexes at the surface.

Outer-sphere complexes involve electrostatic coulombic interactions and are thus weak compared to inner-sphere complexes in which the binding is covalent or ionic. Outer-sphere complexation is usually a rapid process that is reversible and adsorption occurs only on the surfaces of opposite charge to the adsorbate.

Inner-sphere complexation is usually slower than outer-sphere complexation. It is often not reversible and it can increase, reduce, neutralize or reverse the charge of the solid phase regardless of the original charge. Outer-sphere and inner-sphere complexation can, and does, occur simultaneously.

The uptake of metals to smectite clays such as montmorillonite and bentonite is interpreted in terms of two mechanisms:

1. Cation exchange
2. Surface complexation

1.8.2 Cation Exchange

Cation exchange contributes significantly to metal ion sorption if the conditions are right. Sorption by this mechanism is characterised by a strong dependency on ionic strength/solution composition and a weak dependency on pH. It is usually of the Langmuir type[51].

1.8.3 Surface Complexation

Many metal ions can be taken up on the amphoteric hydroxyl surface functional groups (≡SOH edge sites) of clay minerals and this process is probably the most important sorption process for heavy metals, transition metals, lanthanides and actinides in bentonite systems[51]. Surface complexation by metals at these edge sites is characterised by a strong dependency on pH, a weak dependency on ionic strength and a strong dependency on metal ion concentration.

1.9 Equilibrium-based Sorption Models

There are a number of equilibrium-based sorption models that are used to describe the sorption of ions to a clay mineral surface, the most widely used are Freundlich, Langmuir and double-layer models such as the diffuse double-layer and Stern models.

1.9.1 K_d Sorption Model

K_d is an empirical expression of equilibrium frequently used for the distribution between solid and aqueous phases. K_d is defined as the ratio of the concentration of adsorbate bound to the solid phase to the concentration remaining in solution at equilibrium.

K_d is given as:

$$K_d = \frac{Q}{C}$$

Where:

Q is the adsorbed concentration / mol g^{-1}

C is the concentration remaining in solution / mol dm^{-3}

K_d is the equilibrium constant / dm^3 g^{-1}

The concentration of the species retained on the solid phase, Q, can be calculated by the difference between the initial solute concentration and the solute concentration at equilibrium[56], shown in the equation below:

$$Q = \frac{V}{M}(C_{a0} - C) + Q_{a0}$$

Where:

Ca0 is the initial solute concentration

C is the solute concentration at equilibrium

V is the volume of the solution / dm^3

M is the mass of the solid phase / g

Qa0 is the concentration of the species initially retained by the solid phase at time = 0 / mol g^{-1}

Q is the concentration of the species retained on the solid phase / mol g^{-1}

The lower the value for K_d, the lower the sorption or retention of the species and thus the faster the species migrates through the subsurface. For a non-adsorbing species the value of K_d would be zero[38].

1.9.2 Freundlich Equation

The Freundlich equation is an empirical adsorption model that has been widely used in environmental soil chemistry and can be expressed as:

$$q = K_f C^{1/n}$$

Where:

q is the amount of adsorption / mol g^{-1}

C is the equilibrium concentration of the species in solution / mol dm^{-3}

K_f is the equilibrium constant / dm^3 g^{-1}

n is the adsorption intensity and is dimensionless

The linearised form of the Freundlich equation can be expressed as:

$$\log q = \log K_f + \frac{1}{n} \log C$$

If data conforms to the Freundlich model, a plot of log C versus log q should yield a straight line with slope 1/n intercepting the y axis at log K_f[57]. The value for 1/n ranges between zero and one; the more heterogeneous the surface, the closer the 1/n value is to zero[58]. If the value of n lies between one and ten, the sorption process is deemed to be a favourable process[59].

The Freundlich model is used when more than monolayer coverage of the surface is expected and the sites are heterogeneous. An unlimited supply of unreacted sites is assumed to be available and the activity coefficient of the surface species is assumed to be equal to 1.0.

A disadvantage of the Freundlich model is that it does not predict an adsorption maximum. The single K_f term in the Freundlich equation implies that the energy of adsorption on a homogeneous surface is independent of surface coverage. Plots of the Freundlich equation cannot be used for delineating adsorption mechanisms at soil surfaces[38].

1.9.3 Langmuir Equation

The Langmuir equation was developed to describe the adsorption of gas molecules on a planar surface[60]. Since being derived, it has successfully been used to describe sorption on soils and is a widely used model for soil sorption like the Freundlich equation.

The Langmuir equation is best used for describing sorption at low sorptive concentrations and relies on four major assumptions:

1. Adsorption occurs on planar surfaces that have a fixed number of sites which are identical and can only hold one molecule. Monolayer coverage is only permitted.
2. Adsorption is reversible.
3. There is no lateral movement of molecules on the surface.
4. The adsorption energy is the same for all sites and independent of surface coverage. There is no interaction between adsorbate molecules.

Most of these assumptions are not valid for heterogeneous surfaces found in clay minerals and therefore, the Langmuir equation should only be used for qualitative and descriptive purposes.

The original Langmuir equation has been adjusted by soil scientists to investigate solute sorption. By replacing the original gas pressure term with the term C for solution concentration, isotherms can be constructed for solutions in equilibrium with a known amount of solid providing sorption determinations[57]. The equation for Langmuir adsorption for solid-liquid phases is given by:

$$q = KbC / (1+KC)$$

Where:

q is the amount adsorbed to the solid phase / mol g^{-1}

C is the concentration in the aqueous phase at equilibrium / mol dm^{-3}

K is a constant related to the binding strength of the solute to the solid phase / dm^3 meq^{-1}

b is the maximum adsorption capacity of the solid phase / mol g^{-1}

The linearised form of this equation is given by:

$$\frac{C}{q} = \frac{1}{Kb} + \frac{C}{b}$$

The Langmuir isotherm is constructed by a plot of C/q versus C and if a straight line is yielded, the Langmuir model can be considered appropriate. Using least squares regression, the terms b and K can be calculated.

Chapter 2: Characterisation of Materials

2.1 Characterisation of Clay Minerals and Simulant Magnox Sludge

To understand the behaviour of the clay minerals and simulant Magnox sludge better, it is necessary to fully characterise these materials. The peculiar characteristics of bentonite clays, thixotropic, swelling and absorption properties have accounted for their demand for various industrial uses[50]. Grim, 1939, noted that the physical properties of clays may be ascribed to two factors, the character of the exchangeable cation and the composition of the clay mineral[61]. The amount of swelling of a bentonite is directly related to the amount of montmorillonite present in the bentonite. The larger the fraction of montmorillonite present, the greater the swelling capacity of the bentonite[62]. It has also been reported that octahedral substitution of aluminium by iron and magnesium would cause a decrease in the swelling properties of bentonites[63]. Wyoming bentonite is the most commonly available commercial bentonite used for drilling fluid applications. It is principally composed of sodium montmorillonite which accounts for its high swelling capacity and viscosity compared to other bentonites[50]. Most bentonite deposits contain a significant quantity of non-clay mineral particles which constitute impurities which often adversely affect their properties and quality for eventual application.

It has been found that a cationic balance of 60% Na, 20% Ca and 20% Mg is necessary to impart superior industrial properties to a bentonite. It was found that the closer a bentonite conforms to this balance, the better the rheological properties of the clay and the higher its resistance was to contamination[64]. This isn't the only factor that influences the behaviour of bentonites and it has also been found that the percentage of non-clay materials, percentage of particle size less than 0.2 μm, the amount of weathering of the sample, the presence of other clays, oxidation state of clay and the distribution of layer charge all will have an effect on the properties of the clay. For these reasons, it is important to fully characterise the clay minerals used and the simulant Magnox sludge, so that the behaviour observed in subsequent experiments can be explained.

To characterise the materials, several techniques were used including powder X-ray diffraction, elemental analysis using ICP-OES, IR, cation exchange capacity and particle size determination, all of which will be detailed further in this chapter.

2.2 Elemental Analysis of Simulant Magnox Sludge and Clay Minerals

The chemical composition of the clay minerals and simulant Magnox sludge was determined by ICP-OES. Prior to analysis, samples have to be dissolved with the use of acids, something that can be problematic for clay minerals due to the presence of strong Si-O bonds. Table 4 outlines the uses of common acids used in sample preparation techniques.

Table 4. Common acids used in sample preparation for ICP analysis[65]

Acid	Boiling Point / °C	Comments
Hydrochloric (HCl)	110	A very weak reducing agent; not generally used to dissolve organic matter. Useful for salts of carbonates, phosphates, some oxides and some sulfides.
Sulfuric (H_2SO_4)	338	Useful for releasing a volatile product. Has good oxidising properties for ores, metals, alloys, oxides and hydroxides. Often used in combination with HNO_3. Must never be used in PTFE vessels.
Nitric (HNO_3)	122	Oxidizing attack on many samples not dissolved by HCl. Liberates trace elements as the soluble nitrate salt. Useful for the dissolution of metals, alloys and biological samples.
Perchloric ($HClO_4$)	203	Strong oxidizing agent for organic matter. Care is needed as violent, explosive reactions can occur. Pre-treatment of samples with HNO_3 before use of $HClO_4$ is common.
Hydrofluoric (HF)	112	Particularly useful for digestion of silica material. Very hazardous and should not be used in glass containers, only plastic vessels.
Aqua Regia (HNO_3/HCl)	-	1:3 vol/vol mixture of HNO_3:HCl is classed as aqua regia. Used for metals, alloys, sulfides and other ores. Known for its ability to dissolve Au, Pd and Pt.

2.2.1 Elemental Analysis of Simulant Magnox Sludge

The simulant Magnox sludge was provided by Sellafield Ltd but there was no accompanying information detailing the primary constituents of the simulant sludge. The sludge was originally developed at Sellafield to mimic the physical behaviour of the sludge in the storage ponds. This meant it was possible that there might be some constituents of the simulant sludge that would not be expected to be present in the actual storage ponds. Dissolution of this sludge and subsequent elemental analysis was imperative in order to gain a better understanding of the composition of this simulant sludge.

Experimental Method

The simulant Magnox sludge was first dried out in an oven at 80 °C and then ground with a pestle and mortar to ensure a homogeneous particle size. Approximately 1 g of this dried sludge was then weighed into glass vials in triplicate. To these vials 15 cm^3 of concentrated HCl acid (37 %) was added and the samples were shaken on an orbital shaker for one hour. After an hour, the samples were filtered with a Whatman 42 ashless filter paper, and diluted with deionised water for analysis by ICP-OES. The instrumentation used was an ICP-OES Thermo Scientific, iCPA 6000 Series ICP spectrometer, operating at RF power of 1150 W, pump rate of 50 rpm, with auxiliary and nebulizer gas flow of 0.5 dm^3 min^{-1}, coolant gas flow at 12 dm^3 and normal purge gas flow. The operation conditions were a flush time of 30 s with 3 repeats for each measurement. Wavelength selection was done automatically using wavelengths recommended by the instrument software, while checking for the degree of interference from other elements that could be present in the sample.

Results

Table 5 shows the elemental composition determined by ICP-OES analysis of the simulant Magnox sludge. The majority of the sludge sample (49.98 %) consists of magnesium but some other metals (Al, Ca, Fe and Si) are present in very small quantities. The problem with acid digestion and ICP-OES analysis is that it is useful only for metal analysis meaning this method cannot be used to determine in what form the cations are present in the sample. It is suspected that the magnesium exists predominantly as $Mg(OH)_2$, but there is likely to be other phases present such as $MgCO_3$ as the sludge is a wet sample.

Table 5. Elemental analysis of simulant Magnox sludge

Element	% of Original Weight	% Expected for Pure Mg(OH)2*
Aluminium	0.55	-
Calcium	0.73	-
Iron	1.14	-
Magnesium	49.98	41.68
Silicon	0.13	-

*From Fisher Scientific – Mg 41.68 %, O 54.86 % and H 3.46 %

2.2.2 Elemental Analysis of Montmorillonite and Bentonite Clays

As there are numerous variations in elemental composition reported for bentonite and montmorillonite clays, it is important to determine the dominant cations found in the clays used throughout this report.

Experimental Method

A hotplate aqua regia digestion method by Chen and Ma[66] was used to accurately determine the elemental concentrations in the montmorillonite and bentonite clays. In a 250 cm^3 glass beaker covered with a watch glass, 0.5 g of clay was digested in 12 cm^3 of aqua regia on a hotplate for three hours at 110 °C. After evaporation to near dryness, the sample was diluted with 20 cm^3 of 2% nitric acid and filtered through Whatman no. 42 ashless filter paper into a volumetric flask. The method further dilutes the solution with deionised water to 100 cm^3 however this was not initially done as the majority of elements except calcium, magnesium and aluminium would have been below the limit of quantification. For all but these three elements the only dilution carried out was the initial nitric acid dilution. The analysis of magnesium, aluminium and calcium required a further 100 fold dilution with deionised water after the initial nitric acid dilution.

Results

The results for the elemental analysis of montmorillonite and bentonite clays can be found in Table 6 below. The dominant cation found for montmorillonite was aluminium, although large quantities of magnesium, iron and calcium were also found. The calcium content of the montmorillonite is five times that of the sodium content meaning this type of montmorillonite would be classed as a calcium-montmorillonite and therefore a non-swelling montmorillonite. The bentonite contains significantly larger amounts of calcium, iron and magnesium when compared with the montmorillonite. It

also contains a large amount of aluminium too. Like the montmorillonite, bentonite contains considerably more calcium than sodium (approximately 30 times more) and is therefore classed as a calcium-bentonite and therefore non-swelling.

What is surprising is that both montmorillonite and bentonite contain small quantities of silicon according to the ICP-OES results. This is most likely due to the digestion method using aqua-regia as the acid, as total dissolution of the samples was not achieved. Silicates are very difficult dissolve and the use of HF, either with or without aqua-regia, would need to be used for a more complete dissolution of these silicates. XRD of the remaining solid minerals was carried out to determine what phases remained undissolved and these results can be found in Figure 14 and Figure 15.

Table 6. Elemental analysis of montmorillonite and bentonite clays

Element	Montmorillonite / mg g^{-1}	Bentonite / mg g^{-1}
Aluminium	263.68	249.51
Calcium	20.04	194.84
Iron	59.18	178.53
Potassium	10.22	19.06
Magnesium	59.42	237.26
Manganese	-	3.84
Sodium	5.04	6.40
Silicon	6.45	1.64
Zinc	0.07	0.55

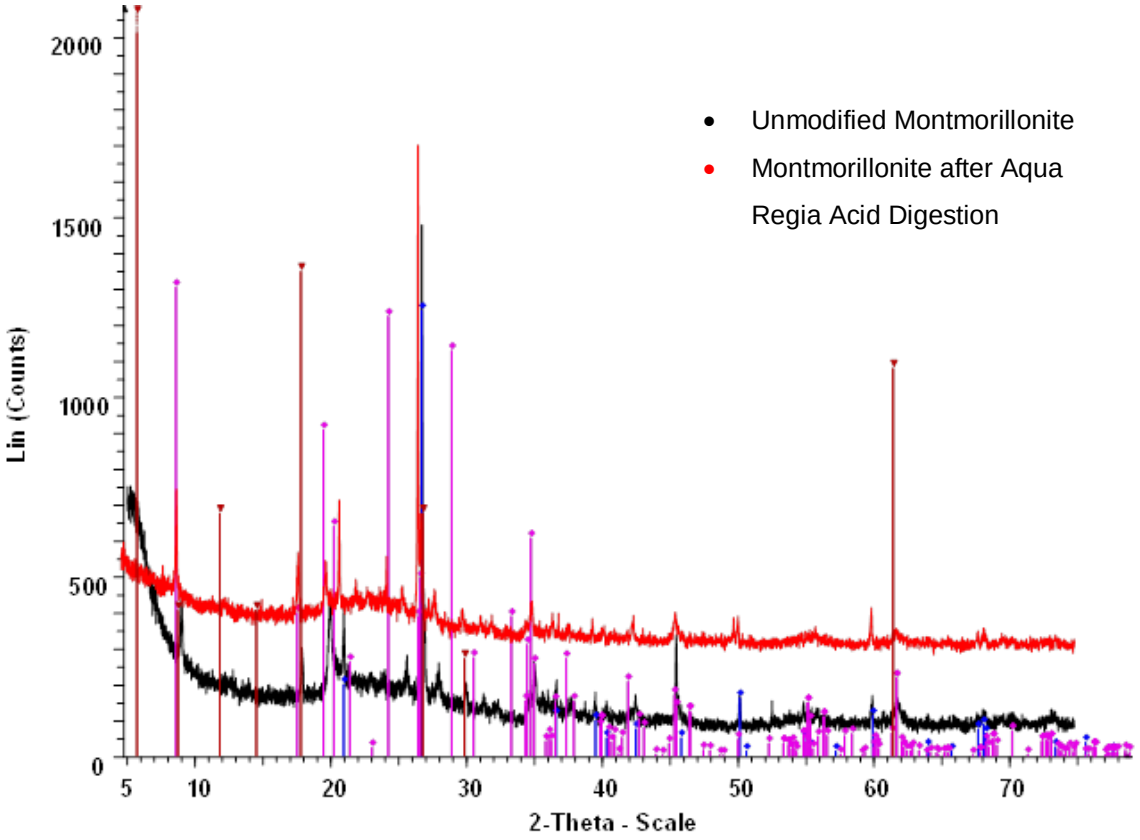

Figure 14. PXRD patterns comparing the unmodified montmorillonite with a montmorillonite sample after aqua regia acid digestion, using Cu K_{a1} radiation between 5 ° and 75 ° with a step size of 0.014 ° and a step time of 1.6 s

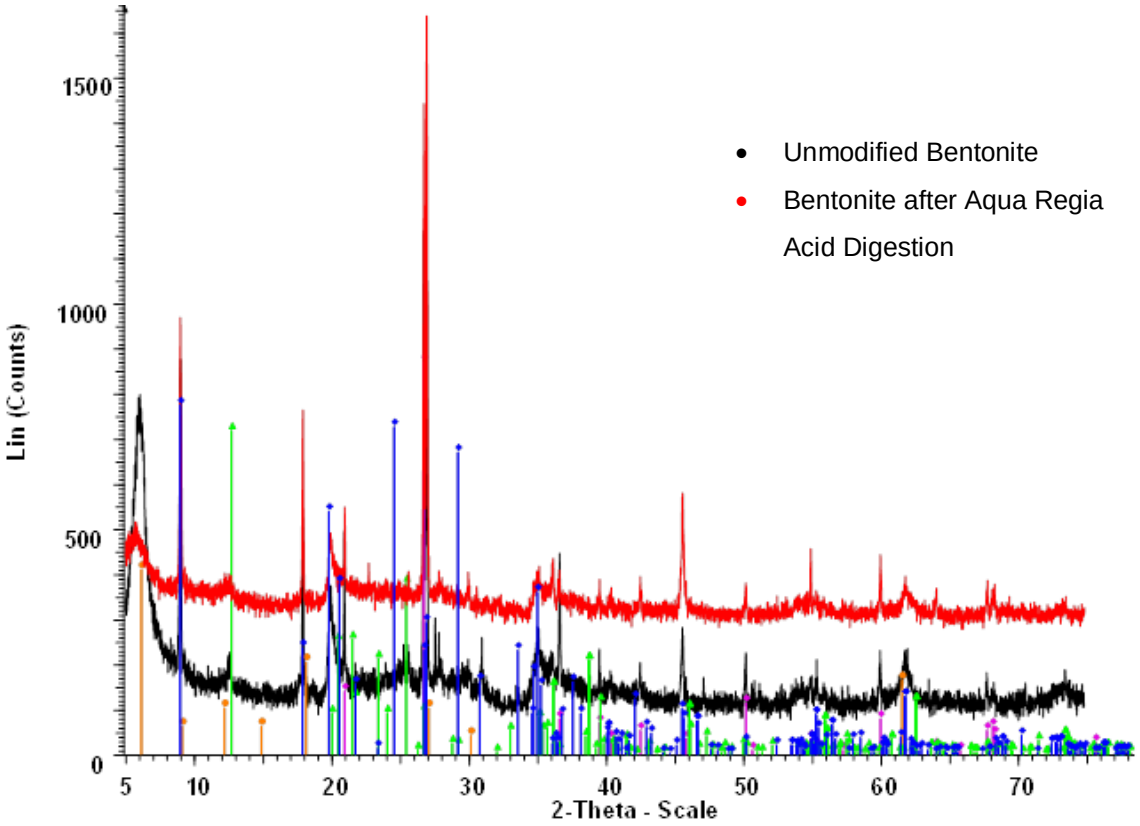

Figure 15. PXRD patterns comparing the unmodified bentonite with a bentonite sample after aqua regia acid digestion , using Cu K_{a1} radiation between 5 ° and 75 ° with a step size of 0.014 ° and a step time of 1.6 s

2.3 Powder X-Ray Diffraction

X-ray diffraction (XRD) is a technique for the determination of solid crystalline structures and it is able to determine the precise atomic positions of molecules within a single crystal[67]. XRD has been used in this instance to identify any impurities present in the clay minerals or simulant sludge.

2.3.1 Principle

X-rays are electromagnetic radiation of wavelength ~1 Å. X-rays are produced when high energy charged particles e.g. electrons, collide with matter. The electrons are slowed down or stopped by the collision and some of their lost energy is converted into electromagnetic radiation. X-rays that are used in almost all diffraction experiments are produced by a different process which leads to monochromatic X-rays. A beam of electrons, again accelerated, strike a metal target, often copper[68]. The incident electrons have sufficient energy to ionize some of the copper's K shell electrons. An electron in an outer orbital immediately drops down to occupy the vacant K shell and the energy released in the transition appears as X-rays.

For diffraction to take place, the wavelength of the incident light has to be the same order of magnitude as the spacings of the grating. Because of the periodic nature of the internal structure, it is possible for crystals to act as a three dimensional diffraction grating to light of a suitable wavelength. For the reflected beams to emerge as a single beam of reasonable intensity, they must arrive in phase with one another. This is known as constructive interference and for constructive interference to take place, the path lengths of the interfering beams must differ by an integral number of wavelengths[67].

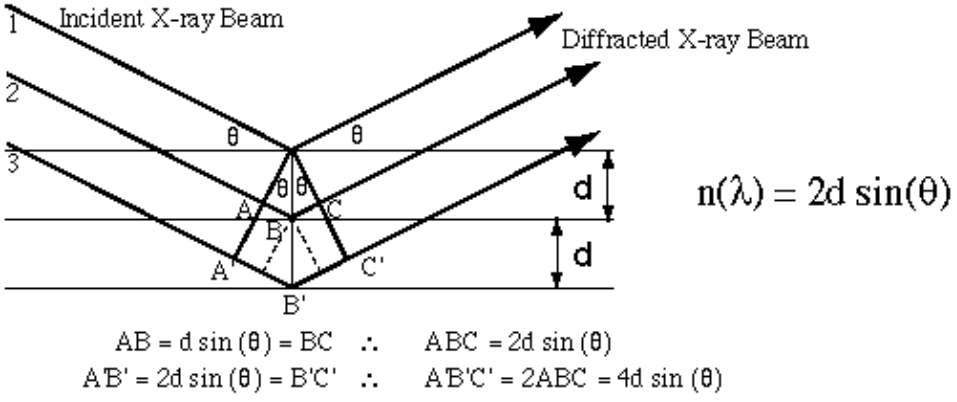

Figure 16. Diagram demonstrating the Bragg equation[69]

The difference in the path lengths is given by the equation:

$$\text{Difference in path length} = 2d_{hkl} \sin\theta$$

This must be equal to an integral number, *n*, of wavelengths. If the wavelength of the X-rays is λ, then:

$$n\lambda = 2d_{hkl} \sin\theta$$

This equation is known as the Bragg equation and it relates to the spacing between the crystal planes, d_{hkl}, to the particular Bragg angle, θ, at which reflections from these planes are observed.

In powder diffraction, a monochromatic beam of X-rays strikes a finely powdered sample that will have crystals randomly arranged in every possible orientation. In such a powder sample, the various lattice planes are also present in every possible orientation. This means that for each set of planes some crystals must be oriented at the Bragg angle, θ, to the incident beam, therefore, diffraction occurs for these crystals and planes[68]. The diffracted beams can be detected by surrounding the sample with photographic film or by using a moveable detector connected to a chart recorder.

The most important use of the powder method is in the qualitative identification of crystalline phases or compounds. Each crystalline phase has a characteristic powder pattern which can be used as a fingerprint for identification purposes. Common uses of the powder method are outlined in the table below, Table 7.

Table 7. Common uses of X-ray powder diffraction[68]

Characterisation of materials by X-ray fingerprints
Qualitative phase analysis
Quantitative phase analysis
Refinement of unit cell parameters
Study of solid solution formation
Determination of crystal size
Study of crystal distortion by stress
Study of phase transformations
Crystal structure determination
Study of the reactions of solids

Soil mineral quantification is 'semi-quantitative' at best. Accurate mineral quantification by XRD can only be achieved under ideal conditions that include the following:

- Mineral phases are discrete and well crystalline, which rarely applies for soils,
- The degree of preferred orientation for each phase can be controlled or accounted for,
- Relatively few phases are present[70]

Several methods can be used for the quantification of soils such as:

The Rietveld method: The Rietveld quantitative XRD method provides a standard-less approach to quantitative XRD, relying only on crystal structure information for the minerals analysed. Rietveld parameters, or variables causing intensity aberrations in XRD data, are adjusted theoretically to fit a synthetic profile to the measured pattern. The whole calculated pattern is adjusted by least-squares fitting to obtain the best profile match with the experimental pattern[71].

Peak area ratio and peak height ratio: These methods involve the comparison of peak widths or heights at a particular reflection for the sample. Calibration curves can be generated by plotting the ratio of the maximum peak height or maximum peak areas against a known value such as the weight fraction of the sample[72].

Internal standard method: This involves spiking a sample with a known amount of a particular compound. Optimally, the chosen standard should have a strong diffraction peak near to but not interfering with that of the analyte, nor with that of any other powder component[73].

2.4 Powder X-Ray Diffraction of Montmorillonite

In these studies, montmorillonite and bentonite samples were analysed with a Bruker D8 Advance diffractometer, fitted with a germanium double single crystal monochromator producing $CuK\alpha_1$ radiation at $\lambda = 1.5406$Å. Perspex deep well sample holders were used to mount the samples.

Phase identification was performed using a continuous scan between the 2θ range of 5-75° with a step size of 0.014° over a period of 2 hours 20 minutes. Figure 17 shows the powder x-ray diffraction pattern obtained for montmorillonite. With help from the results obtained from the elemental analysis of the montmorillonite clay, the phases present were determined to be quartz, montmorillonite and muscovite magnesian.

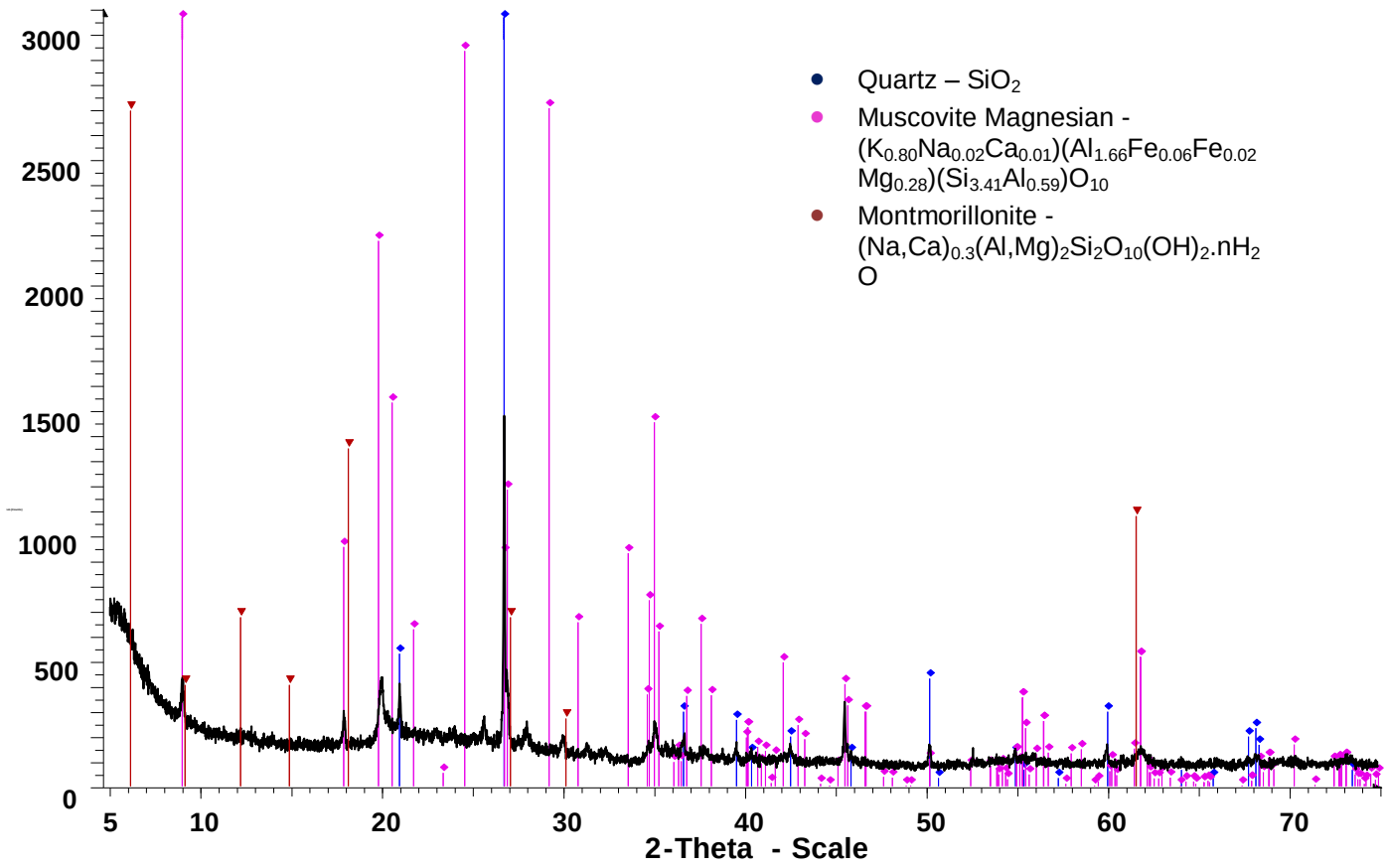

Figure 17. PXRD pattern of montmorillonite, using Cu K_{a1} radiation between 5° and 75° with a step size of 0.014° and a step time of 1.6 s

2.5 Powder X-Ray Diffraction of Bentonite

Bentonite was analysed in the same manner as montmorillonite, mounted in a Perspex deep well sample holder and phases identified by a continuous scan between the 2θ range of 5-75° with a step size of 0.014° over a period of 2 hours 20 minutes. Four dominant phases were found to be present in the bentonite, with the kaolinite phase being the only identified difference between the montmorillonite and bentonite clay samples.

From the diffraction pattern, Figure 18, at 2θ 27-30°, there appears to be reflections that have not been identified. The problem with x-ray diffraction analysis of natural samples, particularly clay minerals like bentonite, is that there can be numerous contaminants present in quantities observed by XRD analysis, but in small enough quantities that some peaks are lost behind the more dominant phases. This makes determination of all phases problematic.

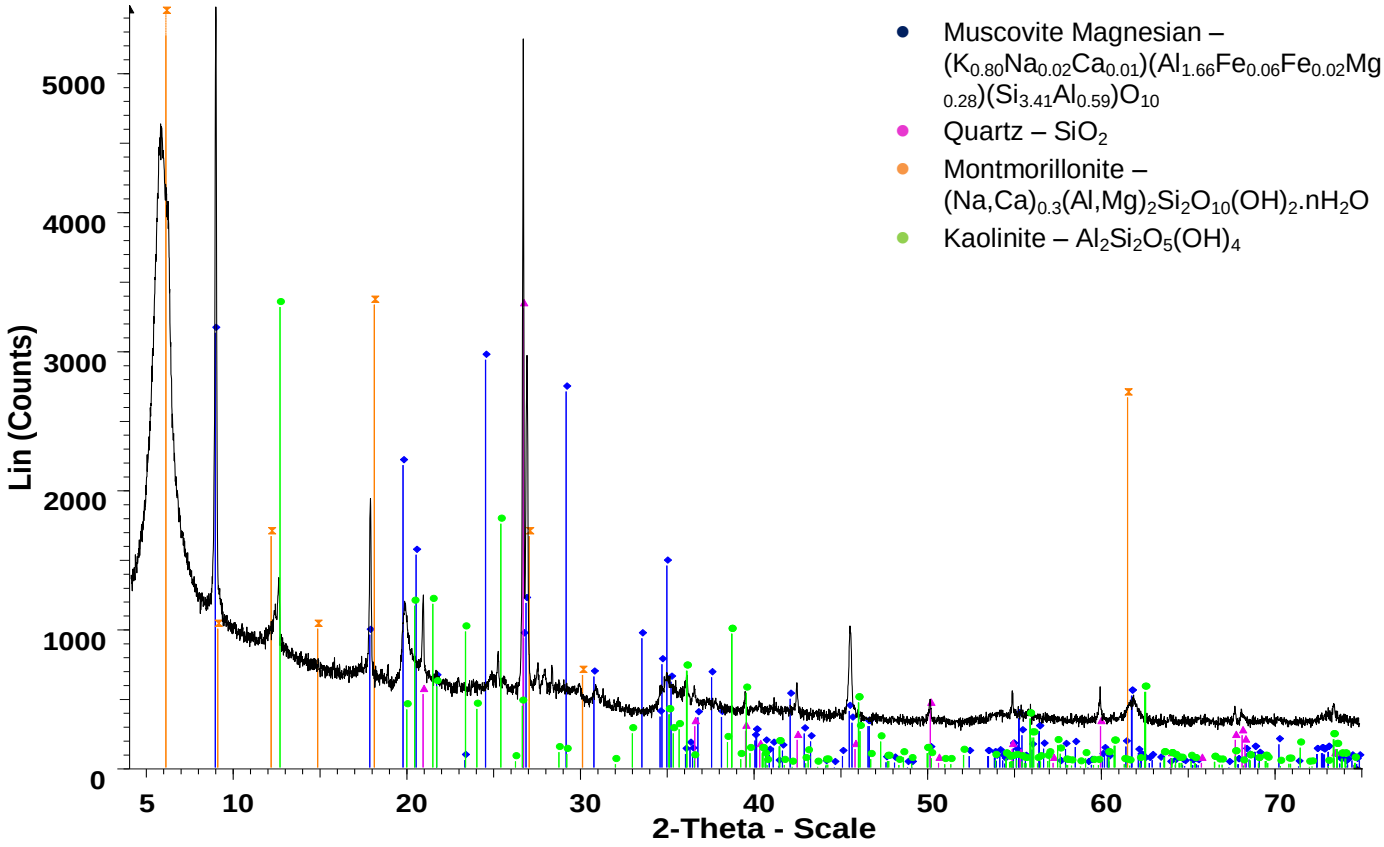

Figure 18. PXRD pattern of bentonite, using Cu K_{a1} radiation between 5° and 75° with a step size of 0.014° and a step time of 1.6 s

2.6 Powder X-Ray Diffraction of Simulant Magnox Sludge

For the analysis of simulant Magnox sludge a different diffractometer was used, a Bruker D8 Discover Diffractometer in transmission geometry, Co $K\alpha_1$ radiation, selected from a Ge 111 single crystal monochromator, with a Braun linear position sensitive detector. The samples were ground to a fine powder in an agate pestle and mortar and a small amount mounted between two pieces of 'Scotch Magic Tape'. The diffraction pattern for the scotch tape exhibits two small peaks at ~26.45 and ~ 29.50°, shown in Figure 19. For phase identification, data were collected over the 2θ range 5 - 80˚ 2θ with a step size of 0.014˚ and a step time of 10s. The XRD pattern was collected over 15 hours to reduce any background interference.

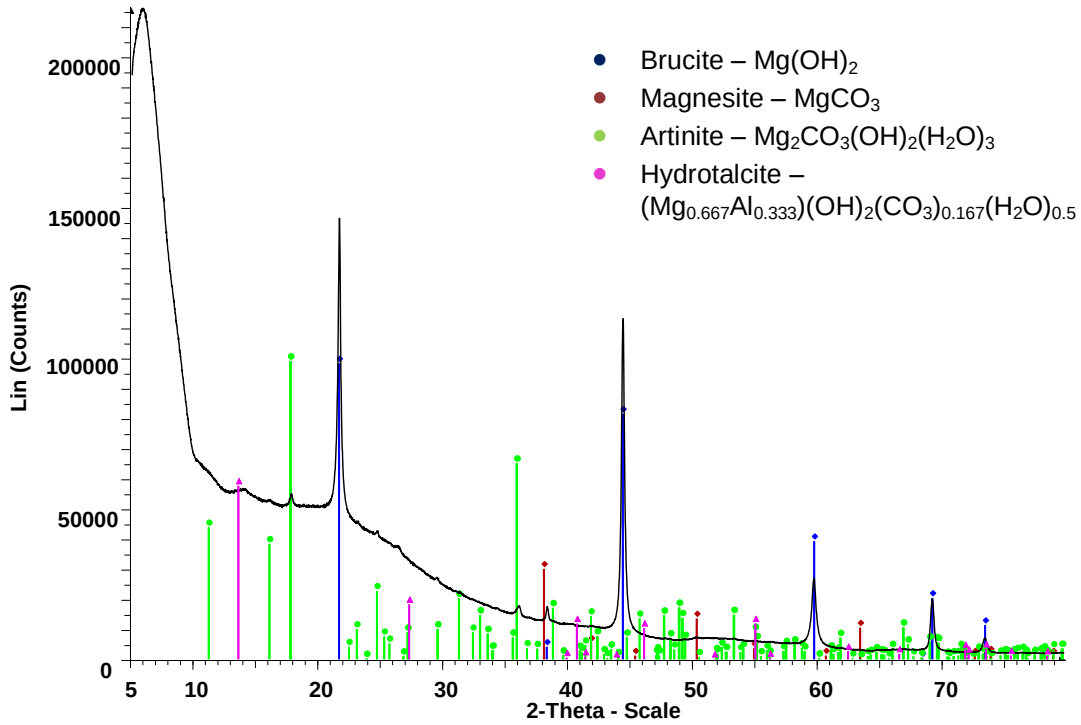

Figure 19. PXRD pattern of simulant Magnox sludge, using Co K_{a1} radiation between 5° and 80° with a step size of 0.014° and a step time of 10 s

Previous powder-X-ray Diffraction and electron microscopic studies of simulated sludge, corroded from unirradiated Magnox alloy in the laboratory under conditions representative of the Sellafield legacy ponds, also led to the identification of brucite and artinite ($Mg_2CO_3(OH)_2.3H_2O$) phases as the main constituents of the sludge[74]. Mg-hydroxycarbonate phases are also expected to be present in sludge phases[75].

2.7 SEM Analysis of Simulant Magnox Sludge

The principle of the scanning electron microscope (SEM) involves a beam of electrons from an electron gun being focused on a spot as small as possible on the surface of a specimen[76]. The incident beam knocks electrons out of the surface of the specimen which are collected by a detector and the current is converted electrically into a voltage signal. As the electron beam explores the surface of the specimen a picture of the surface is built up on the screen because the current received from any point is determined by the characteristics of the surface[76].

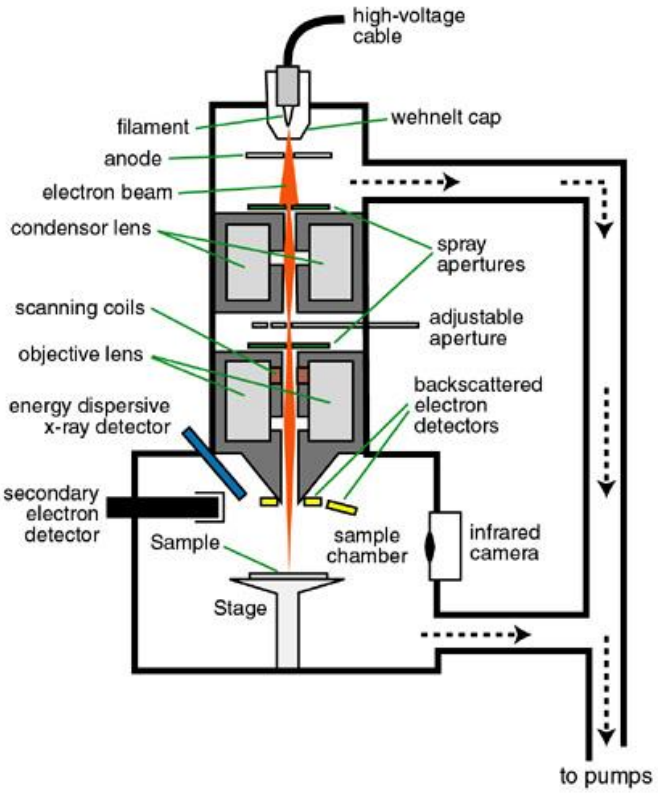

Figure 20: Schematic Diagram of a Scanning Electron Microscope[77]

The electrons are emitted by an electron gun of the type used in electron microscopes with a heated tungsten filament, wehnelt cap (used for the focussing and control of an electron beam) and anode. Such a gun produces a crossover about 100 µm in diameter when a reasonable size for the final size on a sample is around 3 nm. The crossover is reduced by the use of three electron lenses and sometimes magnetic lenses are used too. On their own, the lenses would form a stationary probe on the axis so the specimen is scanned by deflecting the beam with the aid of coils which are placed between the second and third lenses.

The electrons in the probe knock slow-moving secondary electrons out of the surface of the sample which are attracted to a scintillator by a metal gauze. The scintillator

emits light when electrons strike it and this light is conveyed to a photocathode which converts the light back into an electronic signal, which is then amplified.

The signals that derive from interactions between the electrons and the sample reveal information about the sample including:

- External morphology (texture)
- Chemical Composition
- Crystalline structure and orientation of materials that make up the sample.

2.7.1 Advantages and Disadvantages of SEM

Advantages: SEM is a relatively simple technique and the machinery is easy to operate. Samples require minimal preparation for analysis and data acquisition is rapid (less than 5 minutes per image).

Disadvantages: Samples must be solid and fit into the microscope chamber. Maximum sample size is usually around 10 cm wide and 40 mm high[78].

2.7.2 Results

As can be seen in Figure 21 two morphological types appeared to be present in the simulant Magnox sludge sample. The platelet morphology (present in both left and right images) is synonymous with brucite ($Mg(OH)_2$) whilst the needles/rods (right image only) are synonymous with artinite (hydrated magnesium carbonate, $Mg_2(CO_3)(OH)_2.3H_2O$) phases[75].

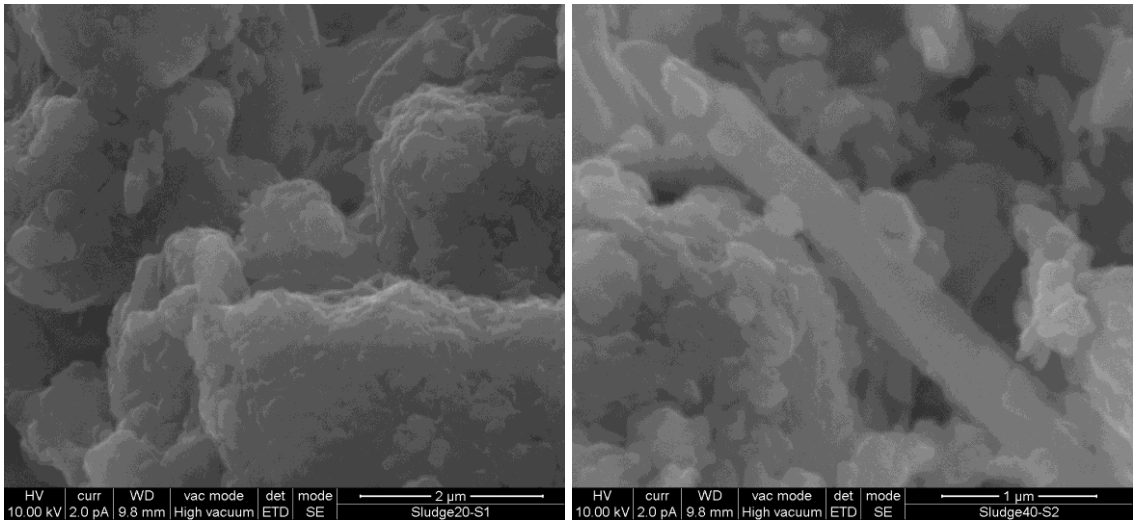

Figure 21. SEM image showing platelet morphology (l) and needles/rod morphology (r) found in simulant Magnox sludge

2.8 Simulant Magnox Sludge Dry Matter Fraction

The dry matter content of simulant Magnox sludge was calculated. Wet sludge samples were weighed in to glass beakers and placed in an oven at 80 °C until fully dry. Once fully dry, the beakers were reweighed and the dry matter content was calculated as a percentage of the original wet weight. The average dry matter fraction was found to be 48.7 ± 0.8 %, the error being standard deviation. Table 8 shows the calculated values. For experimental ease, the dry matter content was taken to be 50 %.

Table 8. Dry Matter Content of Simulant Magnox Sludge

Sample Number	Mass of Wet Sludge / g	Mass of Dried Sludge / g	Dry Weight / %
1	5.91	2.83	47.9
2	5.72	2.76	48.3
3	5.24	2.61	49.8

2.9 Simulant Magnox Sludge Particle Size Analysis

To calculate the particle size of the simulant Magnox sludge, approximately 70 g of wet sludge was weighed into a beaker and left to dry at 80 °C in an oven. Sieves with varying aperture sizes were each weighed to establish the mass of each sieve without dry sludge. The sieves were then stacked on top of each other with the largest aperture size, 1400 µm, at the top and the rest stacked in descending aperture size order. Once the sludge was dry, the sludge was placed in the top sieve and the sieve stack was then placed on a shaking table for an hour. After an hour, each sieve and dried sludge fraction was weighed and the mass of dry sludge at each aperture size was calculated. Figure 22 shows the % composition of dried sludge at each aperture size.

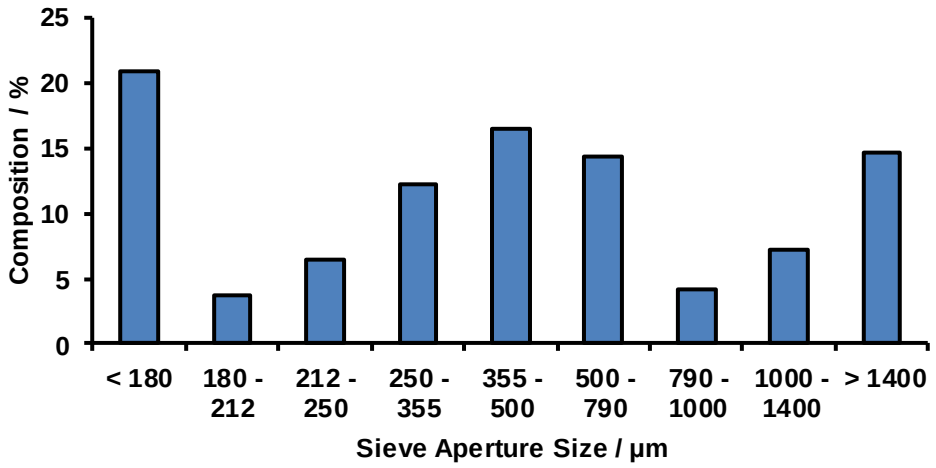

Figure 22. Composition of particle size for simulant Magnox sludge

2.10 IR Spectroscopy of Clay Minerals and Simulant Magnox Sludge

Isomorphous substitution in the tetrahedral and octahedral layers results in a reduction of crystalline order and structural imperfections arise[79]. Further characterisation using infrared spectroscopy was carried out to check for structural imperfections and scans were performed in the mid-infrared range of 400 – 4000 cm^{-1}. Sample preparation was as a KBr disc pressed to ~10 t using a 13 mm die.

2.10.1 IR Spectroscopy of Montmorillonite

The peak of Al-Al-OH stretching vibration at 3602 cm^{-1} is typical for smectites with high amount of aluminium in the octahedral layer[80]. The peaks at 3457 cm^{-1} and 1621 cm^{-1} are the H-O-H stretching and bending vibrations of adsorbed water. OH bending vibrations in dioctahedral 2:1 layer silicates were assigned for Mg-Fe-OH at 787 cm^{-1} and a possible Al-Al-OH vibration at 907 cm^{-1} [80]. Table 9 shows the assigned functional groups for the montmorillonite clay.

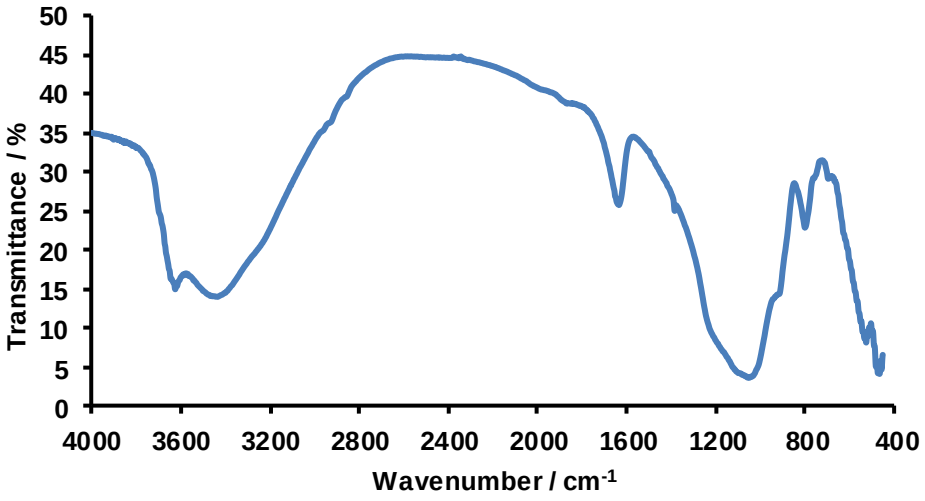

Figure 23. IR spectrum of montmorillonite clay

Table 9. Assigned functional groups for montmorillonite derived from IR spectroscopy

Wavenumber / cm-1	Assigned Functional Group
3602	OH stretching of structural hydroxyl groups[81]
3457	OH stretching of water[81]
1621	OH stretching of water[80]
907	OH stretching of structural hydroxyl groups[80]
787	OH stretching of structural hydroxyl groups[80]

2.10.2 IR Spectroscopy of Bentonite

The peak of Al-Al-OH stretching vibration at 3638 cm^{-1} is typical for smectites with high amount of aluminium in the octahedral layer. The peaks at 3456 cm^{-1} and 1649 cm^{-1} are the H-O-H stretching and bending vibrations of adsorbed water. CO stretching was assigned for the broad peak at 1489 cm-1. OH deformation band of Al-Fe-OH groups attributed to the peak at 897 cm^{-1} and a possible Al-O-Si deformation peak at 520 cm^{-1} [80]. A comparison between the montmorillonite and bentonite IR spectra shows a number of similarities which can be associated to the presence of montmorillonite in the bentonite sample. Table 10 shows the assigned functional groups for the bentonite clay.

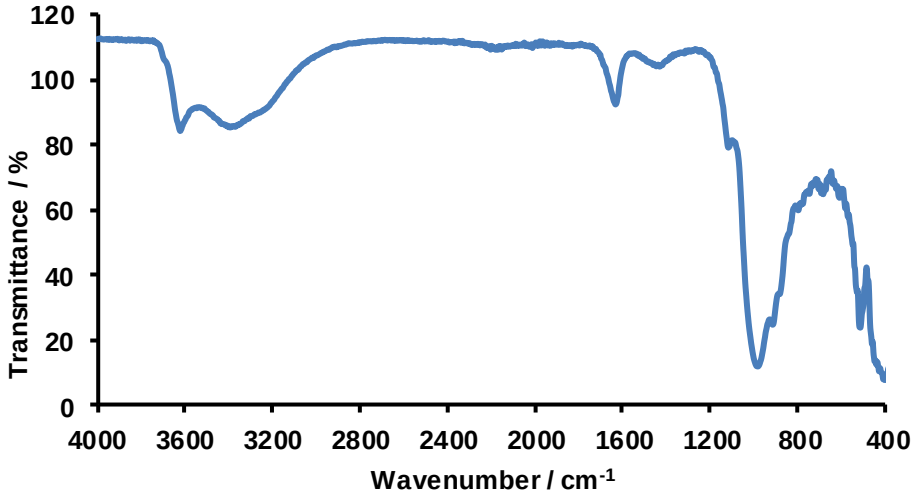

Figure 24. IR spectrum of bentonite clay

Table 10. Assigned functional groups for bentonite derived from IR spectroscopy

Wavenumber / cm-1	Assigned Functional Group
3638	OH stretching of structural hydroxyl groups[81]
3456	OH stretching of water[81]
1649	OH stretching of water[80]
1489	CO stretching[82]
1125	Si-O stretching, longitudinal mode[81]
1000	Attributed to Si-O[83]
897	OH deformation band of $AlFe^{3+}OH$ groupings[79]
856	Small response could be associated with a CO bend[82]
520	Al-O-Si deformation[81]

2.10.3 IR Spectroscopy of Simulant Magnox Sludge

The IR spectrum for simulant Magnox sludge is shown in Figure 25, alongside that of magnesium carbonate and magnesium hydroxide. From the spectra, it can be seen that the simulant Magnox sludge shares peaks with both the magnesium carbonate and magnesium hydroxide data. The peak at 3699 cm^{-1} is associated with the stretching frequency of OH species in brucite[84] and the bands at 1485 and 1420 cm^{-1} are CO_3^{2-} adsorption bands[85] commonly associated with magnesium hydroxide.

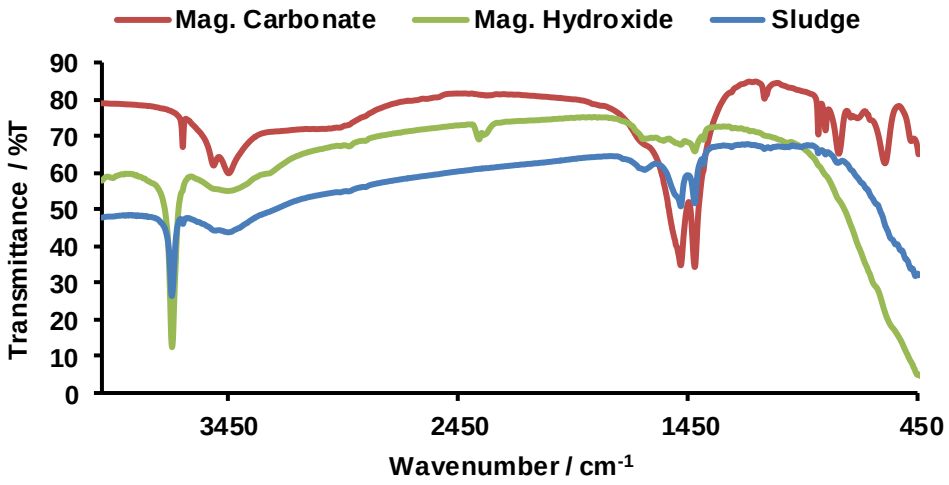

Figure 25. IR spectrum of simulant Magnox sludge

2.11 Swelling Capacity of Clays

Smectite clays are known for their swelling behaviour and as such the swelling behaviour of these clay minerals has been studied extensively[86,87]. Bentonite is often used as a buffer material where its function is to create an impermeable zone around the containers keeping radioactive material separate from the surrounding environment. In Sellafield's case, the bentonite is found immediately beneath the concrete pond structure providing an impermeable layer between the concrete pond and the surrounding geosphere.

In a disposal facility the bentonite is expected to swell and thereby fill the space surrounding the waste. Therefore it is necessary to choose the right form of bentonite with swelling capacities of sealing the waste[88].

The swelling capacities of the montmorillonite and bentonite clays used in the following experiments were calculated using a method reported by the British Geological Survey[39]. This test involves sprinkling a small amount of clay into a graduated measuring cylinder, leaving the sample for 24 hours and recording the volume of the swollen material. A moderately swelling bentonite will give a result of 15-20 cm^3, a good quality bentonite around 25 cm^3 and an excellent grade will produce a result of 30 cm^3 or more per 10 g of clay.

2.11.1 Experimental Method

A 10 cm^3 measuring cylinder was filled to the mark with deionised water. To this 1 g of bentonite or montmorillonite clay was roughly divided into eight equal portions and one portion was added to the measuring cylinder every five minutes. After each addition, the measuring cylinder was lightly tapped so that the final surface of the clay was level. Once all additions had been added, the samples were left for 24 hours and the volume of the clay was measured to the nearest 0.1 cm^3. This value was then multiplied by 10 to give the final swelling volume of the clay.

2.11.2 Results

The swelling capacities of montmorillonite and bentonite have been calculated and can be found in Table 11. The swelling behaviour for both montmorillonite and bentonite is very similar, 21 and 22 cm^3 / 10 g respectively, and both can be classified as having a moderate swelling behaviour.

Table 11. Swelling capacities of studied clays

Clay Mineral	Swelling Capacity / cm^3 10 g^{-1}
Montmorillonite	21
Bentonite	22

2.12 Cation Exchange Capacity of Montmorillonite and Bentonite

One of the most important properties of smectite clays is the cation exchange capacity (CEC) resulting from both the structural permanent charge and the pH dependent variable charge[89]. CEC is a physicochemical characteristic of coils and clays that gives an insight into the ability of a soil or clay to bind cations and release them in soil solution at the soil pH. This cation holding capacity is related to the amount of colloids present with negative charges[90]. CEC is defined as the equivalent amount of exchangeable cations in one kilogram of clay mineral, $cmol^{+}\ kg^{-1}$.

With regards to nuclear waste disposal, the CEC of a clay buffer or backfill is of great importance. Clay materials are used within the nuclear industry as an adsorbent material to retard the movement of radionuclides and have been proposed for the backfill material in a closed repository for this purpose[91]. Clay minerals with high isomorphic substitution have a higher CEC than those where the degree of isomorphic substitution is small. A clay material with a high CEC will be able to exchange with the radioactive cations and thus retard their movement through a repository or the environment. Table 12 shows some common clay minerals and their corresponding CEC.

Table 12. Cation exchange capacities of some clay minerals[38]

Clay Mineral	Cation Exchange Capacity / cmol^{+} kg^{-1}	Structural Formula
Talc	<1	$Mg_3Si_4O_{10}(OH)_2$
Kaolinite	2-15	$Al_2Si_2O_5(OH)_4$
Allophane	5-350	$Al_2O_3{\cdot}(SiO_2)_{1.3\text{-}2}{\cdot}(2.5\text{-}3)H_2O$
Halloysite	10-40	$Al_2Si_2O_5(OH)_4$
Muscovite	10-40	$KAl_2(AlSi_3O_{10})(F,OH)_2$
Biotite	10-40	$K(Mg,Fe)_3(AlSi_3O_{10})(F,OH)_2$
Chlorite	10-40	$(Mg,Fe)_3(Si,Al)_4O_{10}(OH)_2{\cdot}(Mg,Fe)_3(OH)_6$
Dioctahedral Vermiculite	10-150	$(Mg_{0.5}4H_2O)(Mg,Fe^{+2})_3Si_3AlO_{10}(OH)_2$
Montmorillonite	80-150	$(Na,Ca)_{0.33}(Al,Mg)_2(Si_4O_{10})(OH)_2{\cdot}nH_2O$
Tetrahedral Vermiculite	100-200	$(Mg_{0.5}4H_2O)(Mg,Fe^{+2})_3Si_3AlO_{10}(OH)_2$

2.12.1 Experimental Method

For the determination of the CEC of montmorillonite and bentonite, the cobalt hexamine method[90] was used. 2 g of clay was placed in contact with 40 cm^3 of 0.0167 M hexamminecobalt(III) chloride ($[Co(NH_3)_6]Cl_3$) solution and shaken continuously for one hour on an orbital shaker. The samples were centrifuged for ten minutes and the supernatant filtered through 0.22 µm syringe filters.

As hexamminecobalt(III) chloride solution is coloured and absorbs at 472 nm, the CEC can be determined simply by measuring the absorbance of the filtered solutions at 472 nm using UV/Vis Spectrometry.

CEC was calculated from the absorbance of the original solution and of the extractive solution using the following equation:

$$CEC_{A472} = \left[\frac{(A_{orig} - A_{sample})}{A_{orig}}\right] \times 50 \times \frac{V}{m} \times 100$$

Where:

A_{orig} is the absorbance of the original solution at 472 nm

A_{sample} is the absorbance of the sample supernatant at 472 nm

V is the volume of the original solution / dm^3

And m is the dry mass of the sample / g

The results for CEC are expressed as $cmol^+ kg^{-1}$.

Samples were also prepared for analysis of exchangeable cations present by ICP-OES. Each sample was diluted 15 fold with deionised water and acidified with ultrapure nitric acid so that the final solutions contained 1 % nitric acid.

2.12.2 Results

Table 13 shows the averaged values obtained for CEC of montmorillonite and bentonite using the cobalt hexamine chloride method. The pH of the stock hexamminecobalt(III) chloride solution was 4.69.

Table 13. CECs for montmorillonite and bentonite clays using the hexamminecobalt(III) chloride method

Sample	CEC / $cmol^+ kg^{-1}$	pH
Montmorillonite	19.99 ± 0.47	2.81
Bentonite	58.04 ± 0.27	6.95

The experimental results show that bentonite has a CEC which is nearly three times higher than that found for montmorillonite. The higher CEC of bentonite means there are more readily exchangeable cations present with the difference in the values between bentonite and montmorillonite being associated with the impurities found in bentonite clays. The CEC allows us to predict differences in behaviour between the two clays for instance, a higher CEC for bentonite could mean that it possesses a higher sorption capacity than that of the montmorillonite clay.

The experimental montmorillonite value observed is considerably less than the literature reported range of 70-100 $cmol^+ kg^{-1}$ [45]. Variation in CEC depends upon the amount of impurities present in the clay and the pH at which the CEC is measured. It has previously been reported that a higher pH can lead to a higher CEC[92]. The literature value was observed at pH 7 whereas the experimental value is observed at pH 2.8 which could explain the difference between these values.

Faust and Murata, 1953, reported stevensite (a type of montmorillonite) to have an exchange capacity of 36 $cmol^+ kg^{-1}$, which can be explained by the lack of substitution

in the tetrahedral unit[93]. The montmorillonite clay used therefore may have a low CEC due to a lack of substitution in the tetrahedral unit.

ICP-OES analysis was carried out on each sample and the concentration of exchangeable cations present are shown in Table 14. The errors for each cation were calculated as standard deviation. The dominant exchangeable cations released from montmorillonite were found to be aluminium (57.8 ± 1.2 mg dm^{-3}) and calcium (43.1 ± 1.7 mg dm^{-3}), whereas the dominant cations released from bentonite were found to be calcium (426.7 ± 4.5 mg dm^{-3}) and magnesium (144.5 ± 1.9 mg dm^{-3}). Almost ten times as much calcium is released from bentonite compared to montmorillonite and the overall concentration of cations released from bentonite is over five times greater.

Table 14. Concentrations of released cations from montmorillonite and bentonite clays

Cation	Montmorillonite Concentration / mg dm^{-3}	Bentonite Concentration / mg dm^{-3}
Al^{3+}	57.8 ± 1.2	-
Ca^{2+}	43.1 ± 1.7	426.7 ± 4.5
K^{+}	-	7.3 ± 0.7
Mg^{2+}	1.8 ± 0.3	144.5 ± 1.9
Si^{4+}	4.6 ± 0.2	1.4 ± 0.5

2.13 Investigations into the Sorption Capacity of Montmorillonite and Bentonite with Cs and Sr

Clays have received wide attention for use as adsorbents of metal ions from aqueous media because of their easy availability and comparatively lower cost[94]. Montmorillonite and bentonite are known for their high sorption capacity, in particular their adsorption and retardation of the uranium fission and activation products such as ^{137}Cs, ^{90}Sr, ^{99}Tc, ^{147}Pm, ^{155}Eu, ^{129}I $^{239,240}Pu$ and ^{241}Am, all known for their high migration ability[95].

Sorption of cations from solution by clay minerals is usually considered a simple ion exchange process. In non-selective sorption, the amount of cations sorbed is proportional to their relative concentrations in solution. However, certain cations are sorbed more selectively than others and are held more tightly against replacement by other cations. Large monovalent cations are sometimes held so strongly that they are said to be fixed[96]. The low hydration energy of cations is considered to be the major factor in their fixation and selectivity[97] and data have shown greater sorption and fixation of Cs^+ ions than that of K^+ ions, with Cs having the smaller hydration energy[98].

Cations with a low hydration energy, such as Cs, produce interlayer dehydration and layer collapse becoming fixed in interlayer positions. Conversely cations with high hydration energy, such as Sr, produce expanded interlayers and are therefore not fixed[96].

As the clay immediately beneath the storage ponds at Sellafield is believed to be bentonite-like in behaviour, the migration of radioactive leaks from these ponds should be strongly retarded by this clay layer. The following experiments investigate the sorption capacity of montmorillonite and bentonite clay minerals.

2.13.1 Experimental Method

Solutions of $CsNO_3$ or $Sr(NO_3)_2$ with concentrations of 1×10^{-4} to 1×10^{-8} mol dm^{-3} were prepared and 20 cm^3 of these solutions were added to 0.1 g of montmorillonite or bentonite clay in a 50 cm^3 centrifuge vial, establishing a liquid to solid ratio of 200:1 - an internal laboratory standard ratio used for all future sorption experiments. Samples were carried out in triplicate. Each vial was then spiked with 100 µl of ^{137}Cs or ^{85}Sr establishing a final total activity of ~3 kBq per vial. The samples were thoroughly mixed with a whirlimixer and then placed on an orbital shaker for 1 week at 100 rpm. After a week, the samples were centrifuged at 6000 rpm for 20 minutes and the

supernatant then decanted. 2 cm^3 of supernatant was filtered through a 0.45 µm syringe filter and the gamma radiation counted with a Packard Cobra II Auto Gamma counter. pH of the remaining supernatant was recorded.

2.13.2 Results

Sorption of Cs to Montmorillonite

A log plot of free caesium concentration against bound caesium concentration can be seen in Figure 26. At low concentrations the curve is linear but it appears to bend at about 5.3 x 10^{-5} mol g^{-1} indicating the beginning of the saturation of available sorption sites occurs above this concentration of caesium, though it is not yet completely saturated.

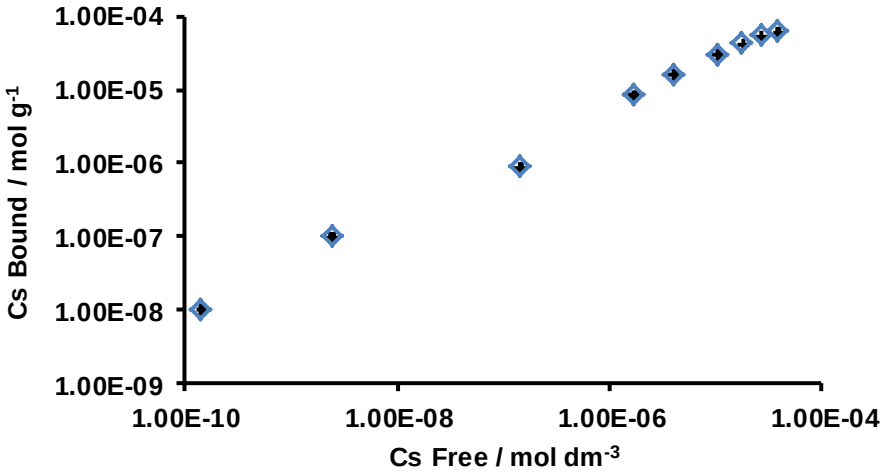

Figure 26. Log-Log plot of Cs bound and free in solution showing Cs distribution for montmorillonite with a solid:liquid ratio of 1:200 at room temperature, equilibrating for 7 days. pH *ca* 4.6

Saturation of sorption sites is evident with the decrease in R_d as the concentration of Cs increases, Figure 27. The R_d appears to decrease rapidly above 1 x 10^{-8} mol dm^{-3} showing a relatively weak capacity for Cs sorption.

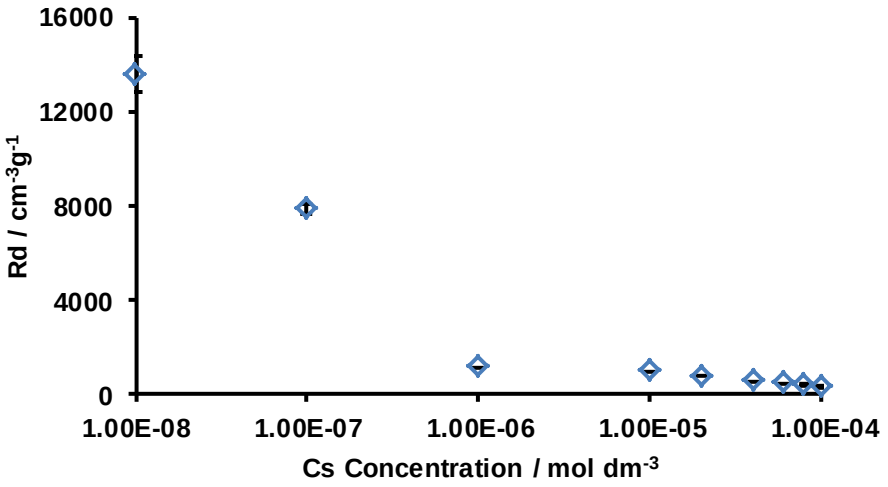

Figure 27. Plot showing R_d versus log Cs ion concentration for montmorillonite with a solid:liquid ratio of 1:200 at room temperature, equilibrating for 7 days. pH *ca* 4.6

The equilibrium adsorption isotherm is of fundamental importance in understanding the adsorption behaviour of systems[99]. From the experimental data, the Freundlich isotherm seems to adequately represent the adsorption process for Cs sorption to montmorillonite. There is a high correlation coefficient with an R^2 value calculated to be 0.9959. The Freundlich constants n and K_f were calculated from the linear regression equation and found to be 1.43 and 0.08 $dm^3\ g^{-1}$ respectively, where n is a dimensionless parameter which describes the heterogeneity of the sorption sites and K_f is the distribution constant.

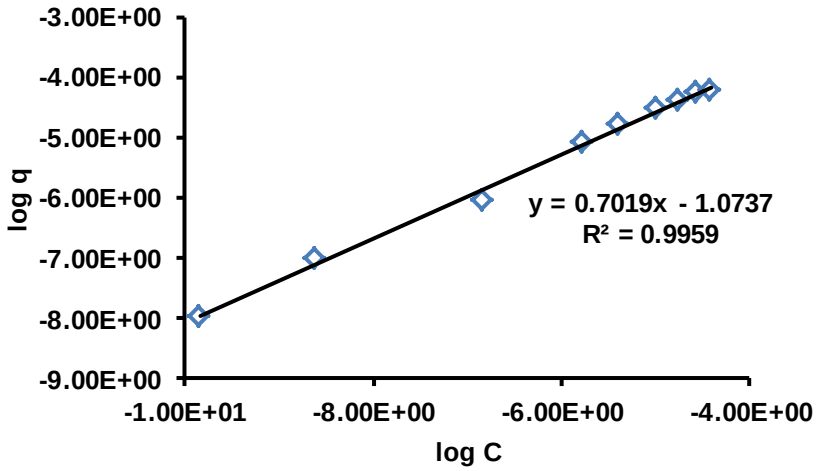

Figure 28. Freundlich isotherm for Cs sorption to montmorillonite

The Langmuir isotherm was also plotted from the experimental results for Cs sorption to montmorillonite, Figure 29. The correlation coefficient is highly significant, R^2 = 0.9837 although this is less significant than that found with the Freundlich isotherm (R^2

= 0.9959). From the linear equation, the maximum absorption capacity of the montmorillonite, b, was calculated to be 8.42 x 10^{-5} mol g^{-1} and the constant K was found to be 5.99 x 10^{4} dm^{3} meq^{-1}.

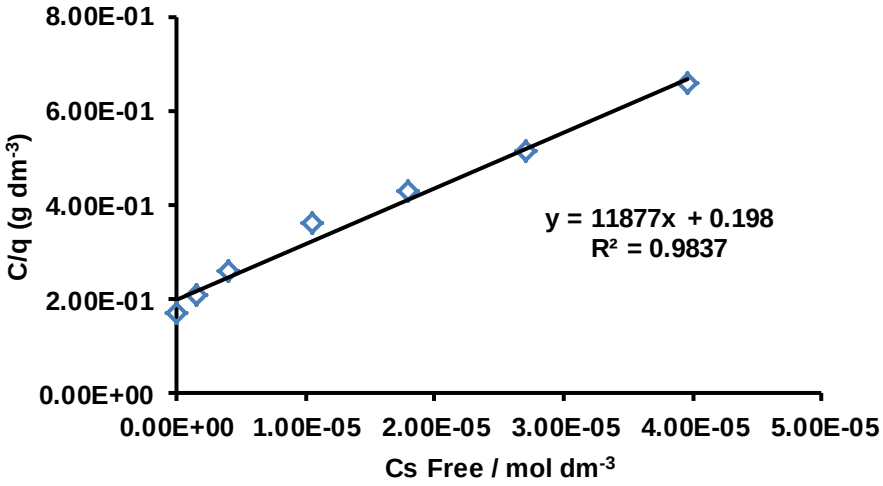

Figure 29. Langmuir isotherm for Cs sorption to montmorillonite

Sorption of Sr to Montmorillonite

A log plot of free strontium concentration against bound strontium concentration can be seen in Figure 30. At low concentrations the curve is linear but it appears to bend at 3.47 x 10^{-5} mol g^{-1} indicating saturation of available sorption sites occurs above this concentration of strontium.

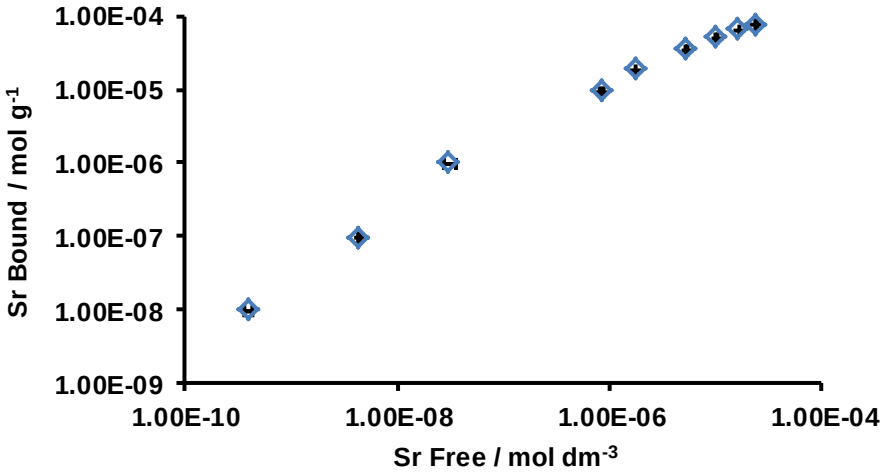

Figure 30. Log-Log plot of Sr bound and free in solution showing Sr distribution for montmorillonite with a solid:liquid ratio of 1:200 at room temperature, equilibrating for 7 days. pH *ca* 4.7

Saturation of sorption sites is evident from the decrease in R_d with metal loading above 1 x 10^{-6} mol dm^{-3}, Figure 31. At very low Sr concentration the sorption isotherm is linear with constant R_d but this decreases above a Sr concentration of 1 x 10^{-6} mol dm^{-3}.

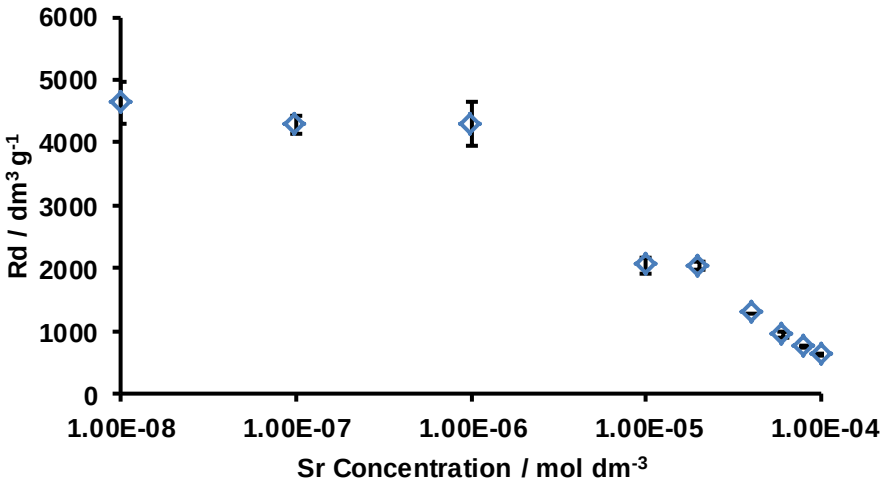

Figure 31. Plot showing R_d versus log Sr ion concentration for montmorillonite with a solid:liquid ratio of 1:200 at room temperature, equilibrating for 7 days. pH *ca* 4.7

As with Cs sorption to montmorillonite, it was found that the Freundlich isotherm best represented the sorption process for Sr sorption to montmorillonite. The correlation coefficient was found to be 0.9881, a slightly weaker correlation than that calculated for Cs sorption to montmorillonite. From the linear regression line, the constants n and K_f were calculated to be 1.24 and 0.58 dm^3 g^{-1} respectively.

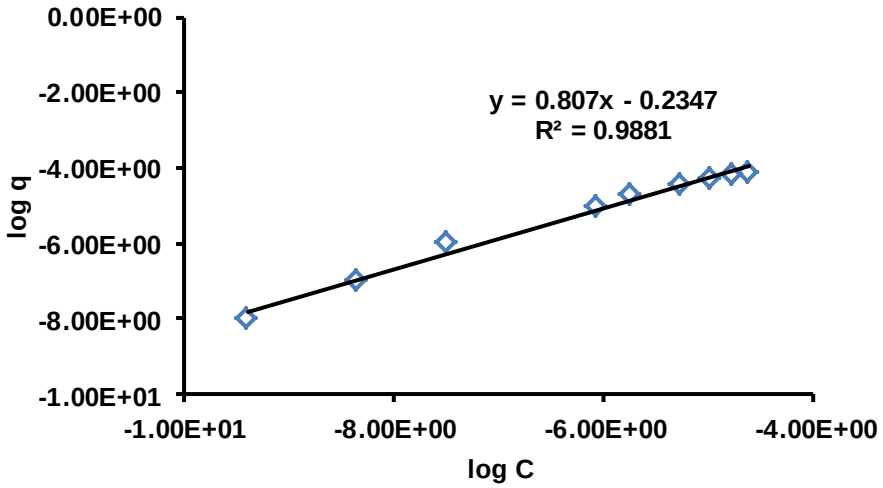

Figure 32. Freundlich isotherm for Sr sorption to montmorillonite

The Langmuir isotherm was also plotted from the experimental results for Sr sorption to montmorillonite, Figure 33. The correlation coefficient is highly significant, $R^2 = 0.9469$ although this is less significant than that found with the Freundlich isotherm ($R^2 = 0.9881$). From the linear equation, the maximum absorption capacity of the montmorillonite, b, was calculated to be 8.69 x 10^{-5} mol g^{-1} and the constant K was found to be 1.82 x 10^5 dm^3 meq^{-1}.

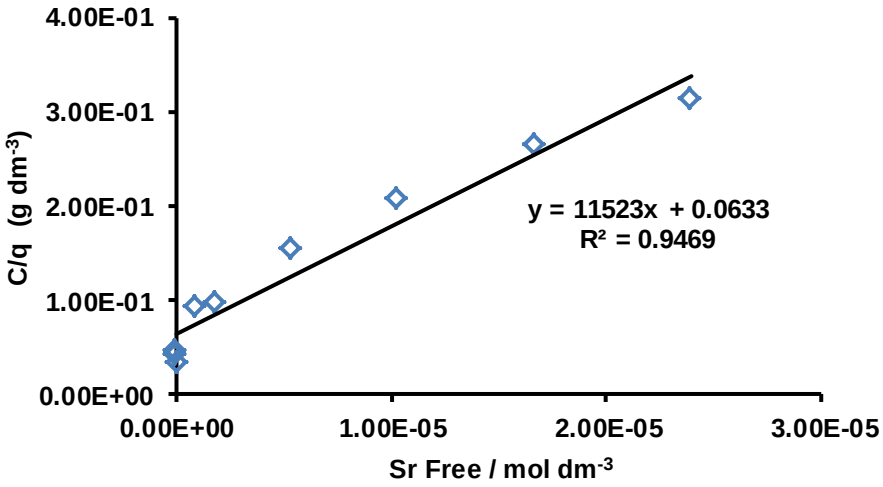

Figure 33. Langmuir isotherm for Sr sorption to montmorillonite

Sorption of Cs to Bentonite

A log plot of free caesium concentration against bound caesium concentration can be seen in Figure 34. At low concentrations the curve is linear but it appears to bend at 7.95 x 10^{-5} mol g^{-1} indicating saturation of available sorption sites occurs above this concentration of caesium.

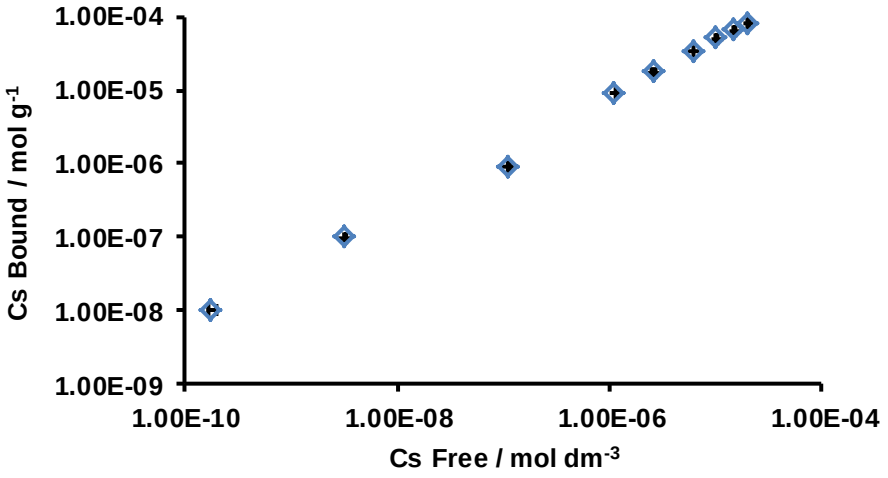

Figure 34. Log-Log plot of Cs bound and free in solution showing Cs distribution to bentonite with a solid:liquid ratio of 1:200 at room temperature, equilibrating for 7 days. pH *ca* 7.8

R_d follows a similar pattern of that found for Cs sorption to montmorillonite, with saturation of sorption sites occurring at low Cs concentration, Figure 35. R_d continues to decrease as metal ion concentration increases.

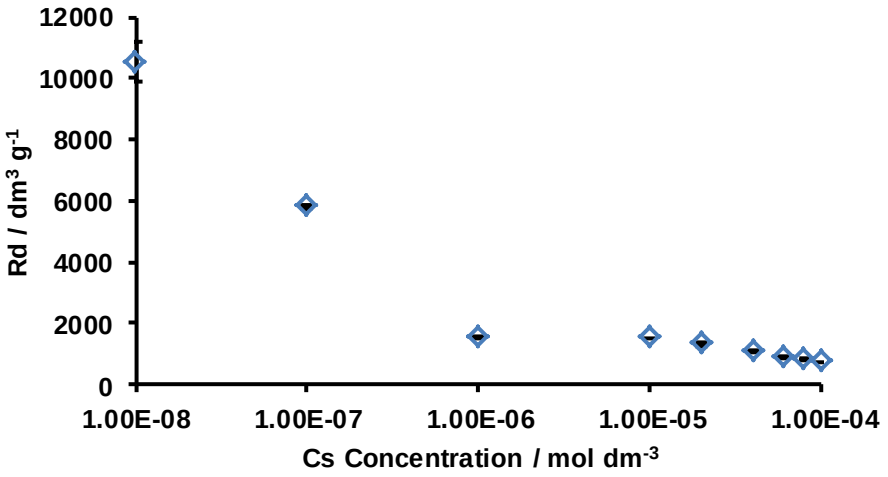

Figure 35. Plot showing R_d versus log Cs ion concentration for bentonite with a solid:liquid ratio of 1:200 at room temperature, equilibrating for 7 days. pH *ca* 7.8

The Freundlich isotherm was found to fit the data best for Cs sorption to bentonite, as can be seen in Figure 36, with a high correlation coefficient value of $R^2 = 0.9972$. From the linear regression line, the Freundlich constants n and K_f were calculated as 1.28 and 0.37 $dm^3\ g^{-1}$ respectively.

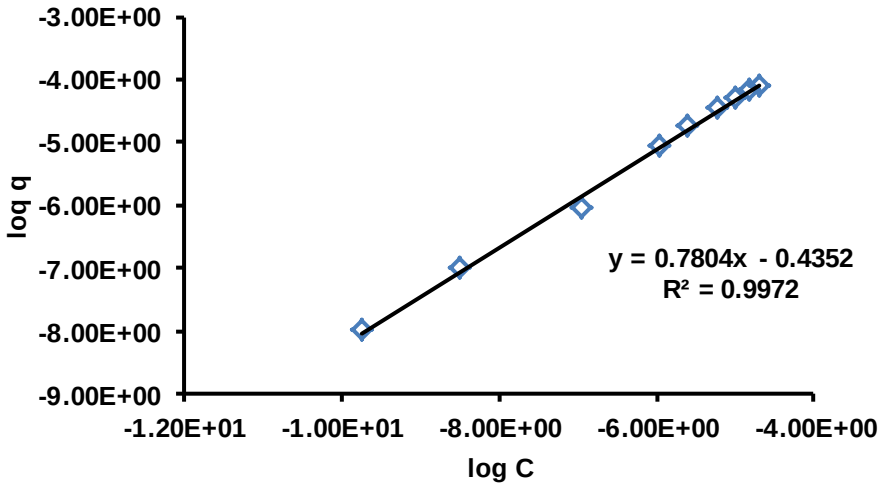

Figure 36. Freundlich isotherm for Cs sorption to bentonite

The Langmuir isotherm was also plotted from the experimental results for Cs sorption to bentonite, Figure 37. The correlation coefficient is highly significant, R^2 = 0.9733 although this is less significant than that found with the Freundlich isotherm (R^2 = 0.9972). From the linear equation, the maximum absorption capacity of the bentonite, b, was calculated to be 1.49 x 10^{-4} mol g^{-1} and the constant K was found to be 5.13 x 10^4 dm^3 meq^{-1}.

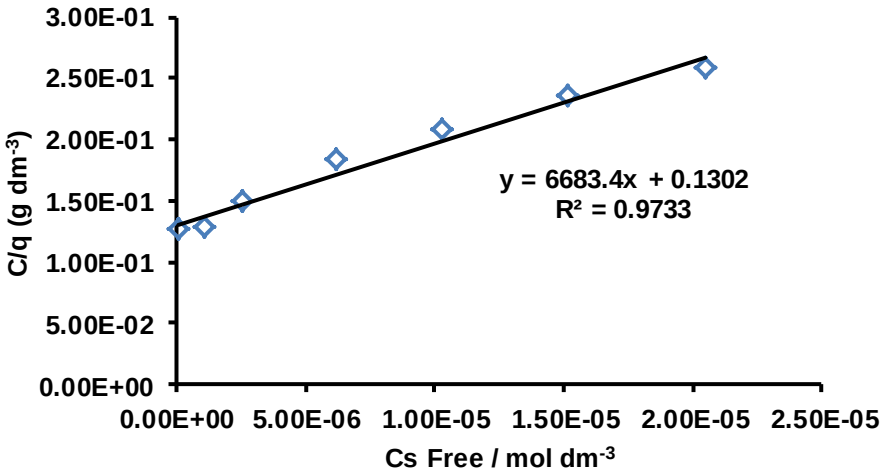

Figure 37. Langmuir isotherm for Cs sorption to bentonite

Sorption of Sr to Bentonite

A log plot of free strontium concentration against bound strontium concentration can be seen in Figure 38. At low concentrations the curve is linear but it appears to bend at

7.04 x 10^{-5} mol g^{-1} indicating saturation of available sorption sites occurs above this concentration of strontium.

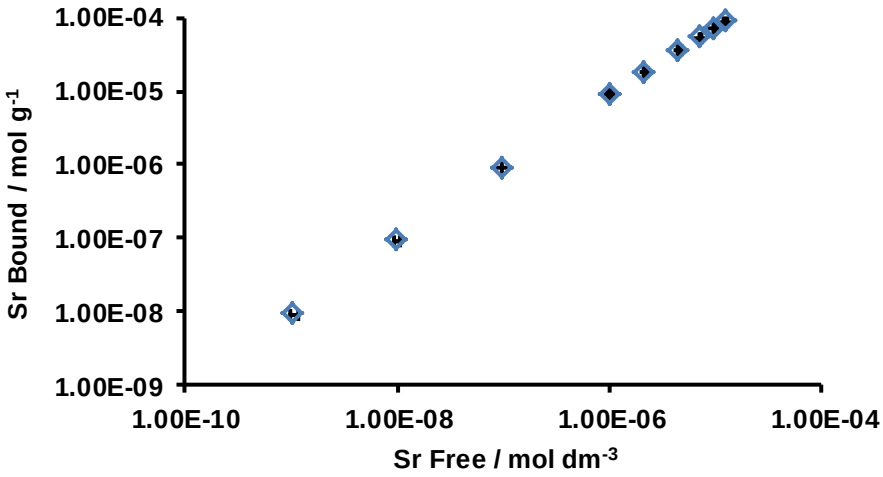

Figure 38. Log-Log plot of Sr bound and free in solution showing Sr distribution to bentonite with a solid:liquid ratio of 1:200 at room temperature, equilibrating for 7 days. pH *ca* 7.9

Saturation of sorption sites is evident from the decrease in R_d with metal loading above 1 x 10^{-5} mol dm^{-3}, Figure 39, compared to Sr sorption with montmorillonite where saturation appears to occur above 1 x10^{-6} mol dm^{-3}. At low metal ion concentration the sorption isotherm is linear with constant R_d, decreasing as concentration increases above 1 x 10^{-5} mol dm^{-3}.

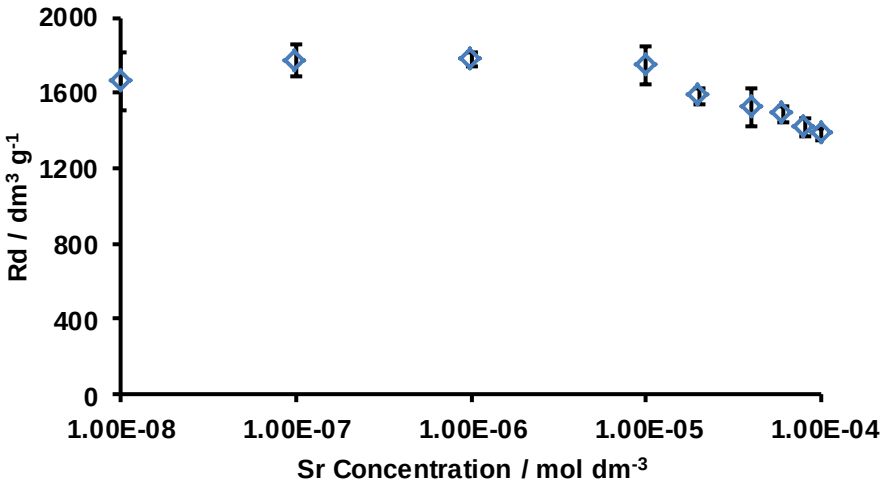

Figure 39. Plot showing R_d versus log Sr ion concentration for bentonite with a solid:liquid ratio of 1:200 at room temperature, equilibrating for 7 days. pH *ca* 7.9

Figure 40 shows that the Freundlich isotherm was found to fit the data very well for Sr sorption to bentonite with correlation coefficient value of R^2 = 0.9995, a slightly stronger

correlation compared to Cs sorption to bentonite. The Freundlich constants n and K_f were calculated to be 1.02 and 6.06 $dm^3\ g^{-1}$ respectively.

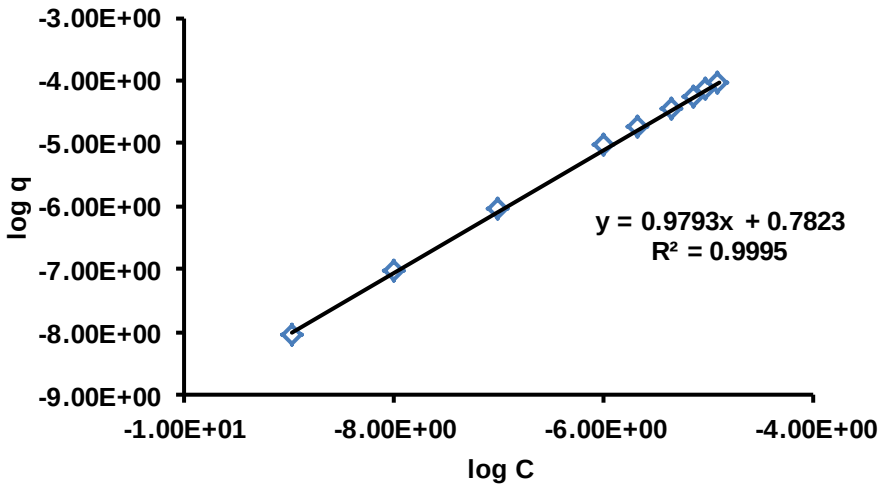

Figure 40. Freundlich isotherm for Sr sorption to bentonite

The Langmuir isotherm was also plotted from the experimental results for Sr sorption to bentonite, Figure 41. The R^2 value of 0.9011 shows strong correlation although the correlation is significantly less than that found for the Freundlich isotherm (R^2 = 0.9995). From the linear equation, the maximum absorption capacity of the bentonite, b, was calculated to be 3.96 x 10^{-4} mol g^{-1} and the constant K was found to be 2.24 x 10^4 dm^3 meq^{-1}.

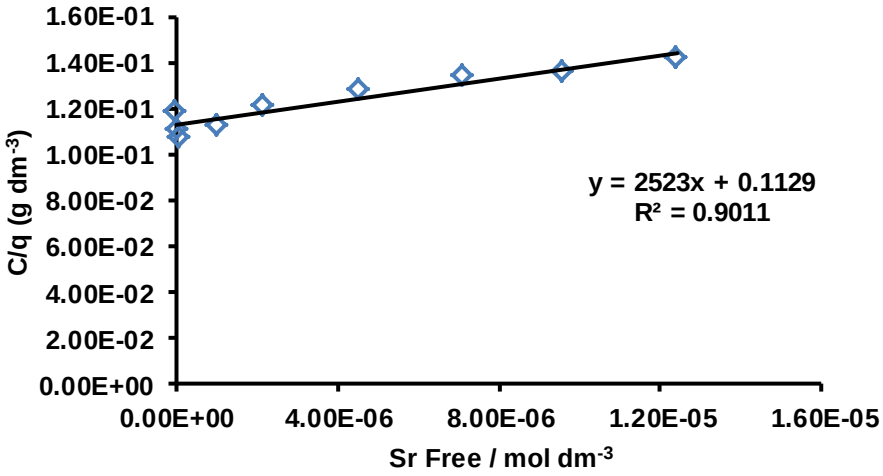

Figure 41. Langmuir isotherm for Sr sorption to bentonite

The Freundlich and Langmuir parameters calculated from the isotherms are compared in **Error! Not a valid bookmark self-reference.** on the following page. The results

fitted to the linearised Freundlich model are highly significant with R^2 values above 0.99 for Cs sorption to montmorillonite and bentonite, and Sr sorption to bentonite. Strong correlation was also seen with Sr sorption to montmorillonite with an R^2 value above 0.98. All the calculated values for n are above one meaning the sorption of both cations studied to montmorillonite and bentonite clays is deemed to be favourable.

As with the Freundlich model, most of the results conformed well to the Langmuir model with Cs sorption to montmorillonite and bentonite showing strong correlation, whereas with Sr sorption to montmorillonite and bentonite, the correlation was found to be weaker. Using linear regression the maximum sorption capacity, b, was calculated for each system. Bentonite was found to have a greater maximum sorption capacity for both Cs and Sr when compared to montmorillonite. For both clay minerals, the maximum sorption capacity was found to be greater for Sr sorption than Cs, although this difference was less significant with the montmorillonite.

The Freundlich adsorption isotherm is generally regarded as being less sensitive than the Langmuir isotherm in describing sorption phenomena[100]. This is because the Langmuir model requires more assumptions, specifically, that the solid phase is homogeneous with respect to the bonding energy of the sites and that no desorption takes place. Hence, where a soil fits the Freundlich model better than the Langmuir model as seen in all cases studied, it is supposed that these assumptions are not valid[57]. The Freundlich model assumes an unlimited supply of unreacted sites and therefore it cannot predict an adsorption maximum. Plots of the Freundlich equation cannot be used for delineating adsorption mechanisms at soil surfaces[38].

Table 15. Freundlich and Langmuir parameters for Cs and Sr sorption to montmorillonite and bentonite clays

Sorbent	Cation	Freundlich Parameters			Langmuir Parameters		
		K_f / dm^3 g^{-1}	n	R^2	b / mol g^{-1}	K / dm^3 meq^{-1}	R^2
Montmorillonite	Cs^+	0.08	1.42	0.9959	8.42×10^{-5}	5.99×10^{4}	0.9837
Montmorillonite	Sr^{2+}	0.58	1.24	0.9881	8.69×10^{-5}	1.82×10^{5}	0.9469
Bentonite	Cs^+	0.37	1.28	0.9972	1.49×10^{-4}	5.13×10^{4}	0.9733
Bentonite	Sr^{2+}	6.06	1.28	0.9995	3.96×10^{-4}	2.24×10^{4}	0.9011

2.14 Kinetics

Kinetics of soil sorption processes are generally known to be essential in understanding soil chemistry and are important with regards to equilibrium sorption. Information regarding sorption kinetics can be used in accurately predicting how rapidly reactions approach equilibrium as well as in investigating reaction mechanisms[101].

The kinetics describes the solute uptake rate on the solid phase. It is important to understand this sorption rate to predict the degree of migration of dissolved cations in the pond liquor before it is retarded by the buffering material. The following experiments were designed to investigate the rate of sorption of Cs and Sr to montmorillonite and bentonite clays.

2.14.1 Experimental Method

Solutions of $CsNO_3$ or $Sr(NO_3)_2$ with a concentration of 1×10^{-4} mol dm^{-3} were prepared and 20 cm^3 of these solutions were added to 0.1 g of montmorillonite or bentonite clay in a 50 cm^3 centrifuge vial. Each vial was then spiked with 100 µl of ^{137}Cs or ^{85}Sr establishing a final total activity of ~3 kBq per vial. Samples were carried out in triplicate. The samples were thoroughly mixed with a whirlimixer and then placed on an orbital shaker for 1 week at 100 rpm. The samples were left on the orbital shaker for the required length of time which ranged from one hour to 14 days. The samples were then centrifuged at 6000 rpm for 20 minutes and the supernatant decanted. 2 cm^3 of supernatant was filtered through a 0.45 µm syringe filter and the gamma radiation counted with a Packard Cobra II Auto Gamma counter. The pH of the remaining supernatant was recorded.

2.14.2 Results

Kinetic Studies into Cs Sorption to Montmorillonite

The sorption of Cs to montmorillonite was studied as a function of shaking time at an aqueous Cs concentration of 1×10^{-4} mol dm^{-3}. Figure 42 shows the variation of Cs bound concentration (mol g^{-1}) with shaking time (hours). The results show that the rate of Cs sorption on bentonite is fast with equilibrium occurring in less than 96 hours. No significant change was observed above 96 hours.

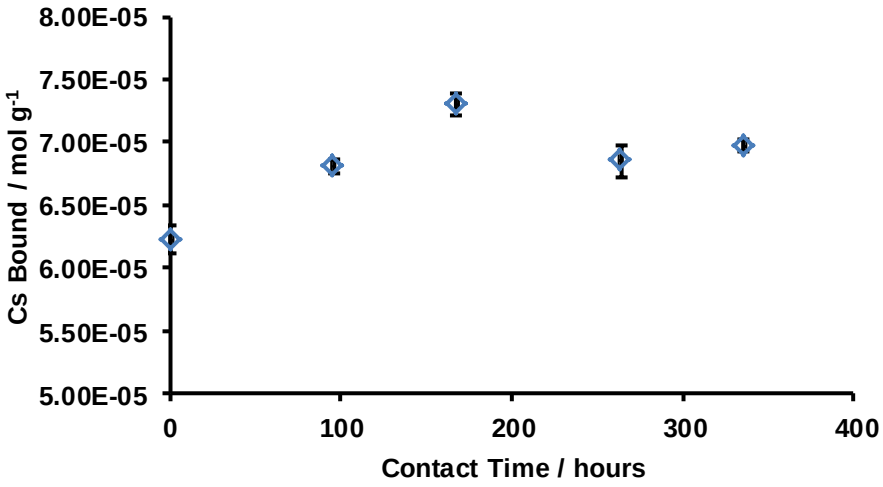

Figure 42. Kinetic studies of Cs (1 x 10^{-4} mol dm^{-3}) sorption to montmorillonite with a solid:liquid ratio of 1:200 at room temperature

Kinetic Studies into Sr Sorption to Montmorillonite

Figure 43 shows the kinetic studies of Sr sorption to montmorillonite as a function of shaking time at an aqueous Sr concentration of 1 x 10^{-4} mol dm^{-3}. The results show that the rate of sorption of strontium to montmorillonite is rapid with equilibrium appearing to be reached instantaneously. This instantaneous uptake of strontium by montmorillonite indicates that ion exchange may be the sorption mechanism. Some of the Sr uptake could also be due to the precipitation of Sr^{2+} as carbonate on the adsorbent surface[52].

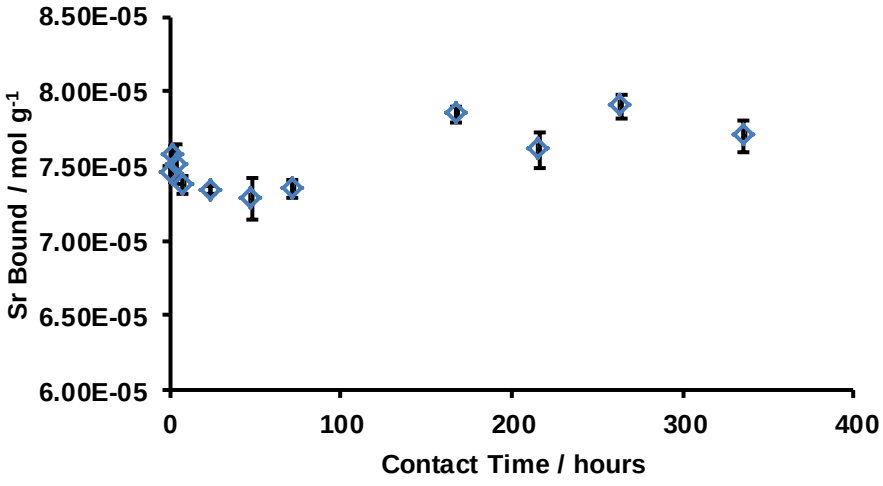

Figure 43. Kinetic studies of Sr (1 x 10^{-4} mol dm^{-3}) sorption to montmorillonite with a solid:liquid ratio of 1:200 at room temperature

Kinetic Studies into Cs Sorption to Bentonite

The sorption of Cs to bentonite was studied as a function of shaking time at an aqueous Cs concentration of 1 x 10^{-4} mol dm^{-3}. Figure 44 shows that the rate of Cs sorption on bentonite is instantaneous with equilibrium occurring within one hour. No significant change was observed above this time. Instantaneous sorption of Cs to bentonite suggests ion exchange as the main sorption mechanism[102].

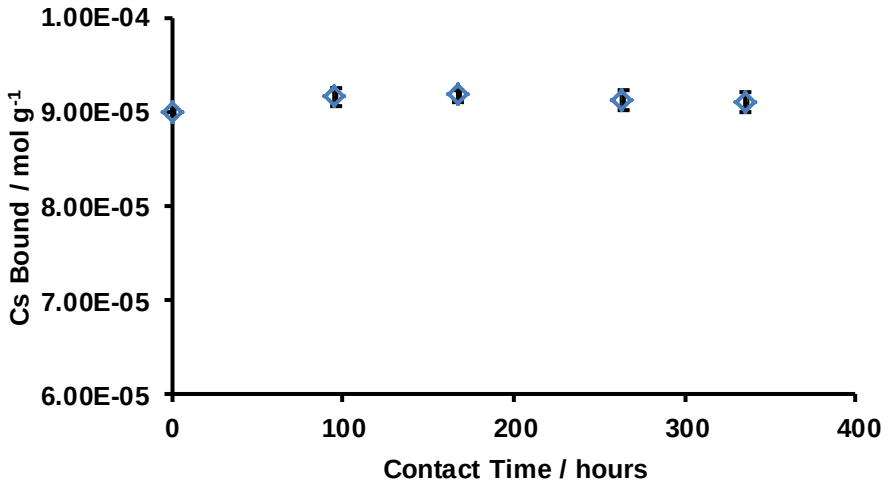

Figure 44. Kinetic studies of Cs (1 x 10^{-4} mol dm^{-3}) sorption to bentonite with a solid:liquid ratio of 1:200 at room temperature

Kinetic Studies into Sr Sorption to Bentonite

Figure 45 shows the kinetic studies of Sr sorption to bentonite as a function of shaking time with an aqueous Sr concentration of 1 x 10^{-4} mol dm^{-3}. The results show that the rate of sorption of strontium to bentonite is rapid with equilibrium appearing to be reached instantaneously. This instantaneous uptake of strontium by bentonite indicates that ion exchange may be the sorption mechanism or some of the Sr uptake could be due to the precipitation of Sr^{2+} as carbonate on the adsorbent surface.

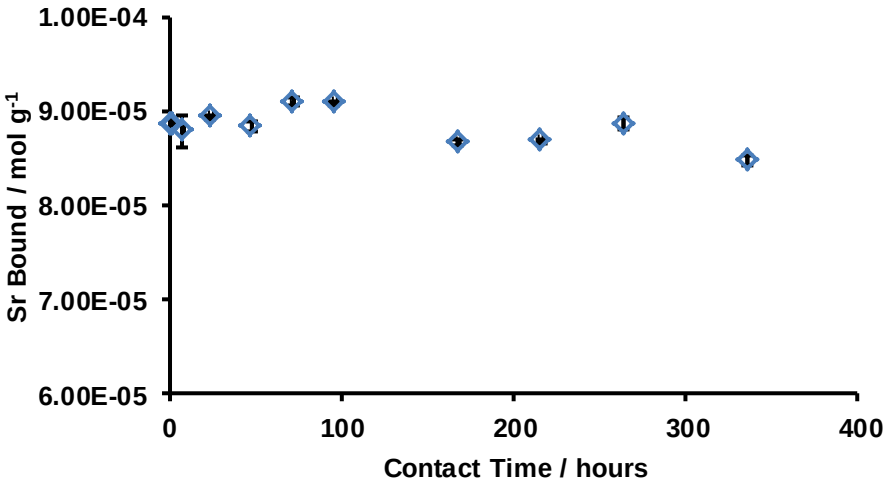

Figure 45. Kinetic studies of Sr (1 x 10^{-4} mol dm^{-3}) sorption to bentonite with a solid:liquid ratio of 1:200 at room temperature

2.15 Effect of pH on Sorption

Complexation reactions with amphoteric functional groups, such as aluminol (≡Al(OH)(H_2O)) and silanol (≡Si-OH), at the edges of the particles are strongly pH dependent[103] whilst sorption of cations is enhanced at high pH due to the number of negative sites increasing. The following experiments investigate the effect that pH has on the sorption of caesium and strontium to montmorillonite and bentonite.

2.15.1 Experimental Method

1 x 10^{-2} mol dm^{-3} buffer solutions with pHs between 6 and 11 were prepared using the buffers given in Table 16 below, and adjusted to the required pH with 1 x 10^{-2} mol dm^{-3} NaOH solution. These buffers were chosen because of their insignificant complexation with metals[104]. 20 cm^3 of buffer solution was added to 0.1 g of clay mineral in 50 cm^3 centrifuge vials and 200 µl of 1 x 10^{-2} mol dm^{-3} inactive $CsNO_3$ or $Sr(NO_3)_2$ was added to each solution, establishing a final metal ion concentration of 1 x 10^{-4} mol dm^{-3}, along with 100 µl of ^{137}Cs or ^{85}Sr, resulting in a total activity of ~3 kBq per vial. Samples were carried out in triplicate. The samples were thoroughly mixed with a whirlimixer and then placed on an orbital shaker for 1 week at 100 rpm. After a week, the samples were centrifuged at 6000 rpm for 20 minutes and the supernatant then decanted. 2 cm^3 of supernatant was filtered through a 0.45 µm syringe filter and the gamma radiation counted with a Packard Cobra II Auto Gamma counter. pH of the remaining supernatant was recorded.

Table 16. Buffers used in the sorption measurements

Buffer	pKa	Useful pH Range	Adjusted Solution pH
MES 2-(-N-Morpholino)ethane-sulfonic acid	6.15	5.5 – 6.7	6
HEPES 2-[4-(2-hydroxyethyl)piperazin-1-yl]ethanesulfonic acid	7.5	6.8 – 8.2	7 and 8
CHES 2-(Cyclohexylamino)ethanesulfonic acid	9.3	8.6 - 10	9
CAPS 3-(Cyclohexylamino)-1-propanesulfonic acid	10.4	9.7 – 11.1	10 and 11

2.15.2 Results

Effect of pH on the Sorption of Cs to Montmorillonite and Bentonite

It has been widely reported that caesium adsorption onto clays is strongly dependent on the ionic strength of the solution but not on pH, especially at low concentrations[105]. The results shown in Figure 46, show that pH does have an effect on the sorption of Cs to both bentonite and montmorillonite. The degree of sorption of Cs at pH 6 appears to be the same for both montmorillonite and bentonite but as the pH increases, the amount of Cs sorption to montmorillonite is greater compared to bentonite.

The degree of sorption of Cs to bentonite as a result of pH, does increase as pH increases from 6 to 11, however the increase in sorption is not as greatly affected by pH as it is for Cs sorption to montmorillonite. Cs sorption to montmorillonite is therefore more pH dependent than Cs sorption to bentonite.

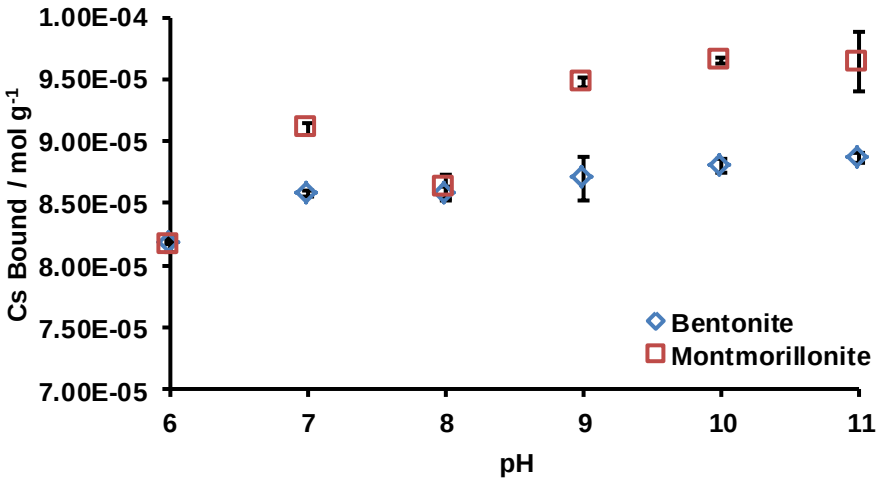

Figure 46. Effect of pH on maximum sorption of Cs (1×10^{-4} mol dm^{-3}) to bentonite and montmorillonite with a solid:liquid ratio of 1:200 at room temperature

A plot of R_d versus pH for Cs sorption to montmorillonite and bentonite is shown in Figure 47. As pH increases, the R_d for Cs sorption to montmorillonite increases before appearing to become linear above pH 10. R_d for Cs sorption to bentonite exhibits different behaviour, appearing to be linear at all pHs investigated between 6 and 11.

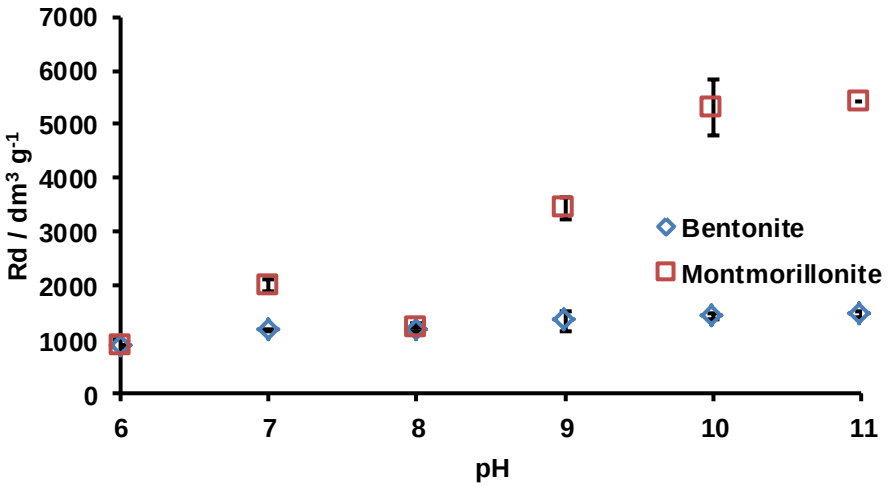

Figure 47. Effect of pH on R_d for Cs (1 x 10^{-4} mol dm^{-3}) sorption to bentonite and montmorillonite with a solid:liquid ratio of 1:200 at room temperature

Effect of pH on the Sorption of Sr to Montmorillonite and Bentonite

Studies have shown that the sorption of strontium to bentonite is independent of pH in the range of 3 to 8, sorption then increases slightly at pH > 8[106]. The experimental results shown in Figure 48, show an increase in sorption of Sr to bentonite in the pH range of 6 to 10, with sorption at pH 11 similar to that at pH 10. The different behaviour of the sorption of strontium to montmorillonite, where pH does not appear to have an effect on sorption, implies this element is only involved in ion exchange reactions[103]. Sorption of Sr to montmorillonite is higher than that of Sr to bentonite at all pH values.

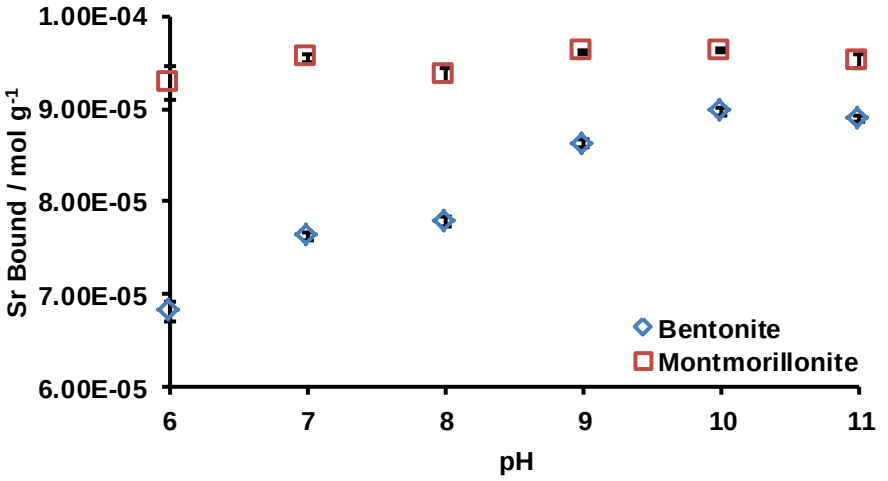

Figure 48. Effect of pH on sorption of Sr (1 x 10^{-4} mol dm^{-3}) to bentonite and montmorillonite with a solid:liquid ratio of 1:200 at room temperature

A plot of R_d versus pH for Sr sorption to montmorillonite and bentonite is shown in Figure 49. As pH increases, a plot of R_d for Sr sorption to bentonite shows linearity at

pH 6-8 before a slight increase at pH before becoming linear above pH 10. Sr sorption to montmorillonite displays different behaviour, R_d increases above pH 6, although there is a decrease observed at pH 8, before decreasing again after pH 10.

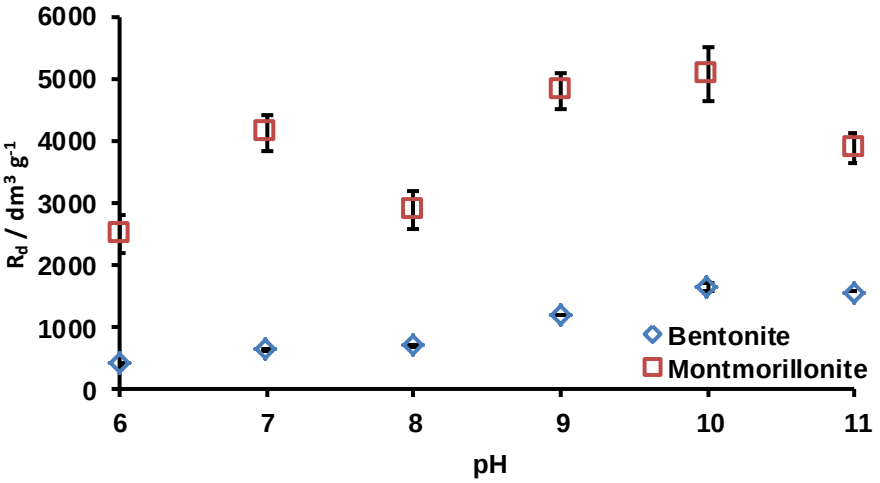

Figure 49. Effect of pH on R_d for Sr (1×10^{-4} mol dm^{-3}) sorption to bentonite and montmorillonite with a solid:liquid ratio of 1:200 at room temperature

2.16 Conclusions

XRD of the simulant Magnox sludge determined that the dominant phase present in the Magnox sample was brucite with magnesite, hydromagnesite and hydrotalcite present as minor phases.

Three dominant phases were found to be present in the montmorillonite clay sample – quartz, muscovite magnesian and montmorillonite. The predominant cations determined via ICP-OES analysis were aluminium, magnesium, iron and calcium.

With the bentonite clay sample, four dominant phases were found to be present – quartz, muscovite magnesian, montmorillonite and kaolinite. The predominant cations determined via ICP-OES analysis were aluminium, calcium, iron and magnesium. There were a significantly higher number of cations present in the bentonite sample explaining why the CEC capacity of bentonite was found to be three times higher than that of montmorillonite.

The swelling capacity of both clays was moderate, which is synonymous behaviour with calcium bentonites. This agrees with the data provided by the ICP analysis which showed calcium to be more abundant in both samples than sodium.

Both clays displayed strong Freundlich behaviour for the sorption of caesium and strontium. Saturation of strontium to montmorillonite occurred sooner than saturation of caesium. Strontium sorption to montmorillonite is said to be mononuclear, outer-sphere complexes[107,108] whereas caesium sorption to montmorillonite is said to form both inner- and outer-sphere complexes[109]. Caesium sorption increased with increasing pH for both clay minerals investigated. This behaviour also occurred with strontium sorption to bentonite but strontium sorption to montmorillonite was found to be independent of pH suggesting strontium is only involved in exchange reactions with the montmorillonite clay.

Likewise with bentonite, saturation of strontium sorption occurs sooner than that for caesium, however saturation occurs at a much higher concentration, 7.04×10^{-5} mol g^{-1} instead of 3.47×10^{-5} mol g^{-1} for strontium sorption to montmorillonite and 7.85×10^{-5} mol g^{-1} instead of 5.3×10^{-5} mol g^{-1} for caesium sorption to montmorillonite.

Sorption was found to be instantaneous for both caesium and strontium sorption to bentonite and with strontium sorption to montmorillonite, but was found to be slower for caesium sorption to montmorillonite.

Cations such as caesium and strontium are not generally competitive with specifically sorbing materials therefore these cations do not usually influence sorption by surface complexation[51].

The order of replaceability of the common divalent cations found in clay minerals has been found to be:

$$Mg^{2+} < Ca^{2+} < Sr^{2+} < Ba^{2+}$$ [45]

As the montmorillonite has been determined to be a calcium-montmorillonite, it is likely that Sr is exchanging with the Ca present in the montmorillonite sample. Ion exchange is independent of pH, this may explain why pH does not appear to have an effect on the sorption of strontium.

Chapter 3: Effect of Anthropogenic Ligands on the Sorption of Cs and Sr to Montmorillonite and Bentonite

3.1 Effect of Anthropogenic Organic Ligand Concentration on the Sorption of Cs and Sr to Bentonite and Montmorillonite

It is now well established that metal-complexing ligands in solution can fundamentally alter the ability of metal ions to bond to clay surfaces. Organic ligands in a solution facilitate metal ion release by the formation of dissolved metal ion complexes[110]. On permanent-charge clays, like smectite clays, metal-complexing molecules such as EDTA, inhibit the adsorption of metals by lowering the free metal ion activity in solution[111]. Anthropogenic organic ligands form stable aqueous complexes with many radionuclides and metals, and therefore may increase their mobility through the environment[112]. EDTA was implicated in the migration of radionuclides up to several meters from two radioactive waste burial trenches at Oak Ridge National Laboratory[113] and the mobilisation of plutonium species from trench leachates, at the Maxey Flats radioactive waste disposal site in the USA[114].

Conversely, it has been shown that some metal ligands enhance metal adsorption, presumably by forming stable surface-metal-ligand complexes[115,116]. These ligands appear capable of complexing or chelating the metal ion while allowing simultaneous coordination of the metal to the surface. The metal:ligand ratio is critical in determining whether metal adsorption at surfaces is enhanced or inhibited, because a large excess of complexing molecules in solution shifts the equilibrium in favour of soluble metal complexes[111].

Organic ligands adsorbed onto oxide surfaces facilitate metal ion release if all their ligand donor groups are utilized in ligand-surface attachment[110]. If one or more ligand donor groups remain free, organic ligands can facilitate metal ion adsorption by acting as a bridge between the surface site and the metal ion[110]. Relative amounts of surface sites, metal ions and organic ligands in the system are crucial as once the surface becomes saturated, organic ligand additions simply raise the organic ligand concentration in solution and encourage the formation of dissolved metal ion complexes[111].

The aim of the following experiments was to investigate the effects of organic ligands EDTA, picolinic acid and NTA, on the sorption of Cs or Sr to the surface of bentonite and montmorillonite as these ligands were identified by Sellafield as being present in the storage ponds in significant amounts.

3.2 Anthropogenic Organic Ligands Studied

Anthropogenic complexing agents are organic compounds used widely in the nuclear industry as solvents, decontamination and purification agents, degreasing agents and flocculating agents due to their ability to form multiple complexes with metals such as calcium, zinc and iron[117]. Complexing agents have been widely used in reactor decontamination to prevent precipitation of dissolved material[118]. Subsequently, the use of complexing agents has resulted in their co-disposal in nuclear waste streams and studies have shown them to be regularly found in radioactive contamination[119,120,121]. It is believed that some complexing agents are present in the storage ponds at Sellafield due to legacy clean-up operations, forming complexes with radionuclides and thus increasing their migration through the environment[122].

The degree to which an organic ligand will affect the sorption of a cation to a solid surface through complexation, is controlled by the stability constant, log K, of the complex. The stability constant is the equilibrium constant for the complexation reaction, and the stability of the complex compound is high if the value of log K is large[123]. Conversely, if the stability constant is low, it has been observed that the ligand readily dissociated from the metal making the metal ions available for adsorption[123]. K is defined as:

$$K = \frac{[MeL]}{[Me] \cdot [L]}$$

Where:

[Me] is the concentration of the metal ion

[L] is the concentration of the ligand

[MeL] is the concentration of the metal-ligand complex at equilibrium[124]

Aminopolycarboxylic acids (APCAs) are compounds that contain several carboxylate groups bound to one or more nitrogen atoms. The major chemical property of APCAs is their ability to form stable and water-soluble complexes with many metal ions. APCAs form one or more heteroatomic rings with the metal ion resulting in a higher stability of the metal-ligand complex in addition to the presence of secondary or tertiary amino groups and the large negative charge of APCAs[124]. The two most widely used APCAs are Ethylenediaminetetraacetic acid (EDTA) and nitrilotriacetic acid (NTA).

3.2.1 Ethylenediaminetetraacetic Acid (EDTA)

EDTA is a hexadentate ligand and forms stable complexes with a number of cations. Due to this, it is one of the most widely used complexing agents for industrial use. The chemical structure of EDTA is shown below in Figure 50.

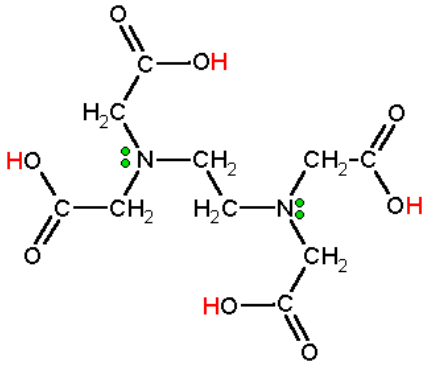

Figure 50. Structure of EDTA

The reactions of EDTA in ground water involve adsorption to iron and aluminium oxides and dissolution of iron oxides[117]. An example of EDTA forming strong complexes in the environment is the remobilization of metals in a river sediment[125]. Remobilization of metals could result in hazardous levels of toxic metals in the ground water and which could ultimately find their way into drinking water.

$$MeEDTA_{(dissolved)} + Me^*_{(adsorbed)} \longrightarrow Me^*EDTA_{(dissolved)} + Me_{(adsorbed)}$$ [125]

3.2.2 Picolinic Acid

The adsorption of picolinic acid and metal-picolinic complexes has been studied far less than EDTA[126]. Picolinic acid is a bidentate ligand and can complex metals through the carboxylate group, the nitrogen from the pyridine ring or both. The chemical structure of picolinic acid is shown below in Figure 51 and possible coordination modes for picolinic acid can be seen in Figure 52.

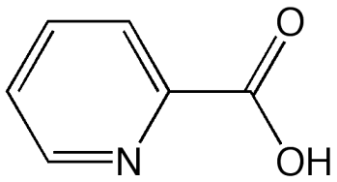

Figure 51. Structure of Picolinic Acid

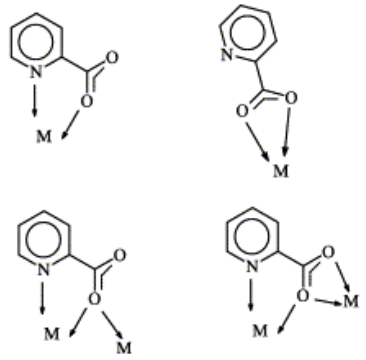

Figure 52. Possible picolinic acid coordination modes[127]

3.2.3 Nitrilotriacetic Acid (NTA)

NTA, like EDTA, is also very well known for its complexing and oxide dissolving capabilities. NTA contains four donor atoms and is known as a tetradentate ligand. The metal complexes of NTA have lower stability constants when compared to the corresponding complexes of EDTA[128]. Figure 53 shows the chemical structure of NTA.

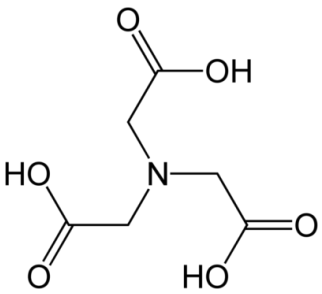

Figure 53. Structure of NTA

NTA has been investigated to see its effect at removing lead from highly polluted soils (Pb = 21%)[129]. There have also been investigations into NTA's ability to remove cadmium from sea water due to the high levels of cadmium poisoning which kills shrimp[130]. NTA was found to be an effective ligand for metal removal.

3.3 Effect of Anthropogenic Organic Ligand Concentration on Sorption of Cs and Sr to Montmorillonite and Bentonite

3.3.1 Effect of Picolinic Acid on the Sorption of Cs and Sr to Montmorillonite and Bentonite

Experimental Method

Three picolinic acid solutions were prepared with concentrations of 1 x 10^{-2} (high PA), 1 x 10^{-4} (med. PA) and 1 x 10^{-6} (low PA) mol dm^{-3}. 20 cm^3 of picolinic acid solution was added to 0.1 g of clay mineral in 50 cm^3 centrifuge vials, to which 200 µl of 1 x 10^{-2} to 1 x 10^{-6} mol dm^{-3} inactive $CsNO_3$ or $Sr(NO_3)_2$ was added, establishing final metal ion concentrations between 1 x 10^{-4} to 1 x 10^{-8} mol dm^{-3}, along with 100 µl of ^{137}Cs or ^{85}Sr, resulting in a total activity of ~3 kBq per vial. Samples were carried out in triplicate. The samples were thoroughly mixed with a whirlimixer and then placed on an orbital shaker for 1 week at 100 rpm. After a week, the samples were centrifuged at 6000 rpm for 20 minutes and the supernatant then decanted. 2 cm^3 of supernatant was filtered through a 0.45 µm syringe filter and the gamma radiation counted with a Packard Cobra II Auto Gamma counter. The pH of the remaining supernatant was.

Results

Effect of Picolinic Acid on the Sorption of Cs to Montmorillonite

A log-log plot showing the effect of picolinic acid concentration on the sorption of Cs to montmorillonite is shown in Figure 54. From the graph, it appears that with a higher picolinic acid concentration, there is more Cs bound to the montmorillonite clay. At the lowest Cs concentration, 1 x 10^{-8} mol dm^{-3}, sorption does not appear to be affected by the concentration of picolinic acid in solution. When the concentration of Cs in solution increases, sorption appears to increase with high picolinic acid concentration in solution.

The results also show that the presence of picolinic acid at low and medium concentrations has no real effect on the sorption of Cs to montmorillonite as the results appear to be similar to those calculated with no picolinic acid present in the system.

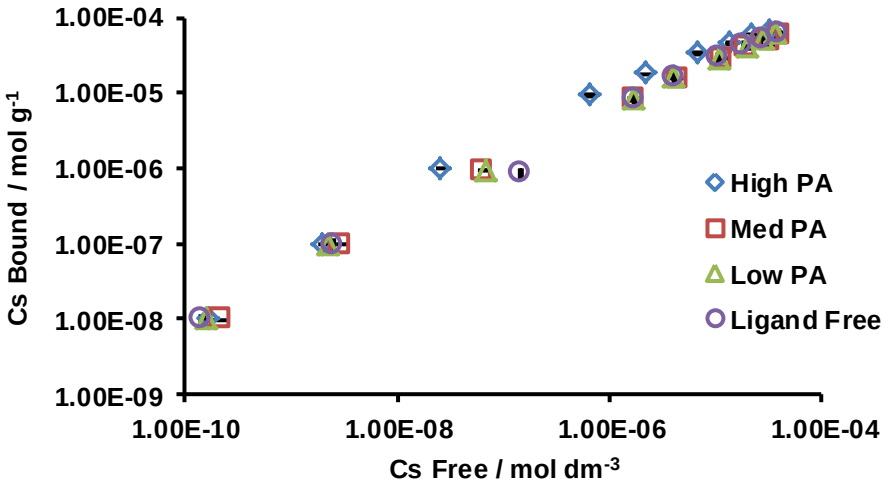

Figure 54. Log-Log plot showing the effect of picolinic acid concentration on the sorption of Cs to montmorillonite. pH *ca.* 3.7 at high PA concentration, 4.5 at medium and 4.6 at low and ligand free solutions. Experiments carried out at room temperature with a solid:liquid ratio of 1:200, equilibrating *ca.* 7 days. Three replicates per sample

Figure 55 illustrates the change in R_d for Cs sorption to montmorillonite as the concentration of Cs increases. It is evident that as metal concentration in solution increases the R_d decreases. The trend appears to be the same for all picolinic acid and ligand free solutions investigated.

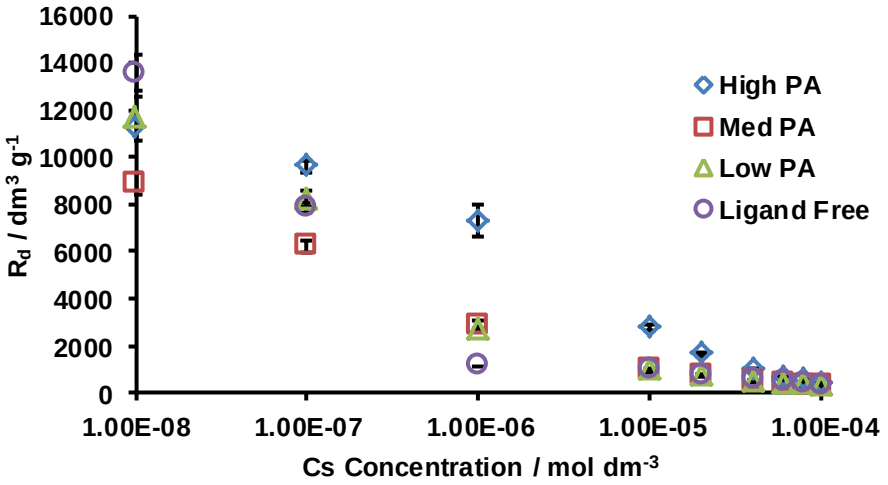

Figure 55. Plot of R_d versus Cs ion concentration at pH *ca.* 3.7 for high PA concentration, 4.5 for medium and 4.6 for low and ligand free solutions. Experiments carried out at room temperature with a solid:liquid ratio of 1:200, equilibrating *ca.* 7 days. Three replicates per sample

TOC analysis on picolinic acid, with a concentration of 1 x 10^{-2} mol dm^{-3}, in the presence of montmorillonite with varying Cs ion concentrations (1 x 10^{-4}, 1 x 10^{-6} and 1 x 10^{-8} mol dm^{-3}) was carried out with the aim to see if there was any metal-ligand-clay complexes being formed in order to explain the sorption behaviour seen in Figure 54

above. From the TOC results shown in Figure 92, 72% (7.2×10^{-5} mol dm^{-3}) of the picolinic acid in solution appears to sorb to the montmorillonite when there is no caesium present in solution. When caesium is added to the system, the amount of picolinic acid in solution decreases from 28% to approximately 24% suggesting a Cs-picolinic acid-montmorillonite complex might be occurring although this may be cause by instrument error.

Table 17 shows the experimental pH ranges for the sorption of Cs to montmorillonite in the presence of picolinic acid.

Table 17. pHs for Cs sorption to montmorillonite in the presence of picolinic acid

Picolinic Acid Concentration / mol dm^{-3}	pH Range
1×10^{-2} (High)	3.57 – 3.70
1×10^{-4} (Medium)	3.95 – 4.49
1×10^{-6} (Low)	4.13 – 4.58
Ligand Free	3.87 – 4.63

Effect of Picolinic Acid on the Sorption of Sr to Montmorillonite

Figure 56 illustrates the effect of picolinic acid concentration on the sorption of Sr to montmorillonite. At high picolinic acid concentration, sorption of Sr to montmorillonite is reduced at lower strontium concentration however, at higher Sr concentration sorption does not appear to be affected by the concentration of picolinic acid present in solution. The amount of sorption occurring is the same for Sr to montmorillonite in the presence of medium and low picolinic acid concentrations, however even at these ligand concentrations, it can be seen that the presence of picolinic acid is having some effect on the sorption of Sr to montmorillonite and retaining more of the strontium in the aqueous phase when compared to the ligand free data.

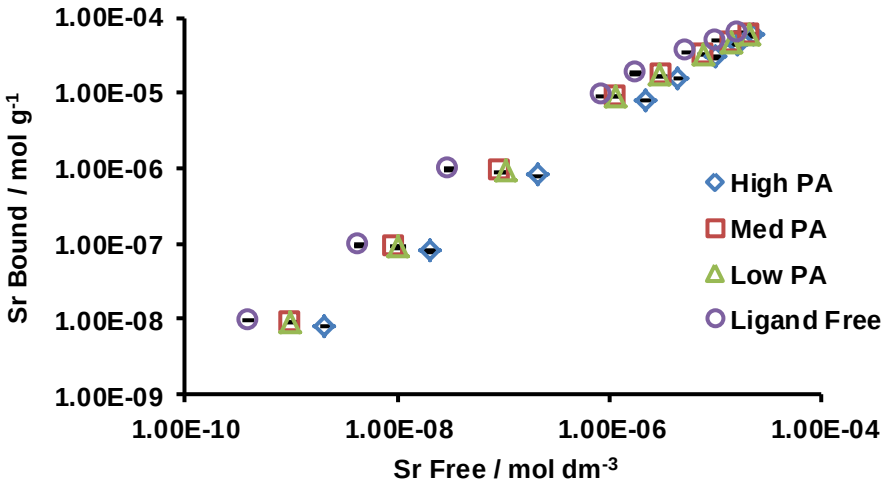

Figure 56. Log-Log plot showing the effect of picolinic acid concentration on the sorption of Sr to montmorillonite. pH *ca.* 3.7 at high PA concentration, 5.1 at medium, 5.3 at low and 4.7 for ligand free solutions. Experiments carried out at room temperature with a solid:liquid ratio of 1:200, equilibrating *ca.* 7 days. Three replicates per sample

Figure 57 illustrates the change in R_d for Sr sorption to montmorillonite as the concentration of Sr increases. It is evident that as metal concentration in solution increases the R_d decreases. The trend appears to be the same for all picolinic acid and ligand free solutions investigated.

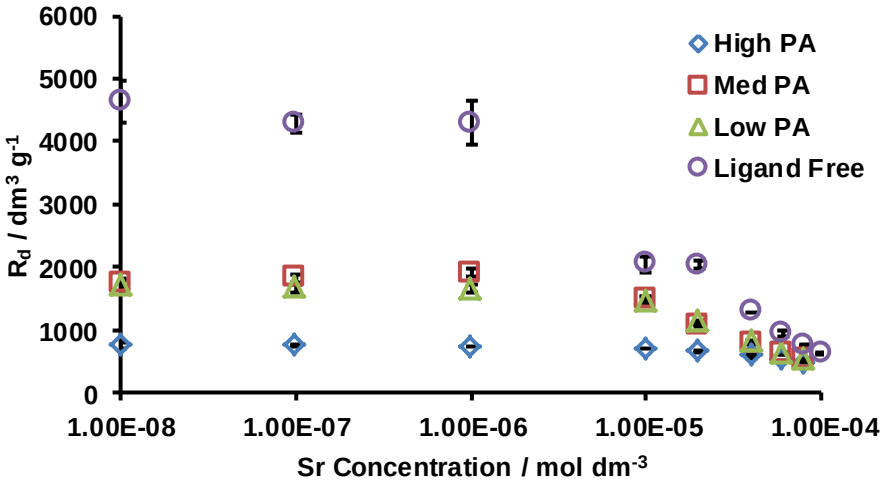

Figure 57. Plot of Rd versus Sr ion concentration at pH *ca.* 3.7 for high PA concentration, 5.1 for medium, 5.3 for low PA and 4.7 for ligand free solutions. Experiments carried out at room temperature with a solid:liquid ratio of 1:200, equilibrating *ca.* 7 days. Three replicates per sample

The pHs were recorded and can be found in Table 18. The pH is lowest at highest picolinic acid concentration although there isn't a great difference in equilibrium pH across all picolinic acid concentrations. The highest pHs recorded for medium picolinic acid (5.08) and low picolinic acid (5.30) were found at the highest Sr ion concentration.

The remainder of the Sr ion concentrations produced pHs at the low end of the recorded pH range.

Table 18. pHs for Sr sorption to montmorillonite in the presence of picolinic acid

Picolinic Acid Concentration / mol dm^{-3}	pH Range
1 x 10^{-2} (High)	3.65 – 3.71
1 x 10^{-4} (Medium)	4.03 – 5.08
1 x 10^{-6} (Low)	4.07 – 5.30
Ligand Free	4.09 – 4.67

Effect of Picolinic Acid on the Sorption of Cs to Bentonite

Figure 58 illustrates the effect that picolinic acid has on the sorption of caesium to bentonite. There is no apparent effect by the picolinic acid at medium and low concentrations on sorption when compared to the experimental results found for ligand free sorption of Cs to bentonite. There does appear to be a slight effect on the sorption of Cs to bentonite when in the presence of high picolinic acid concentration.

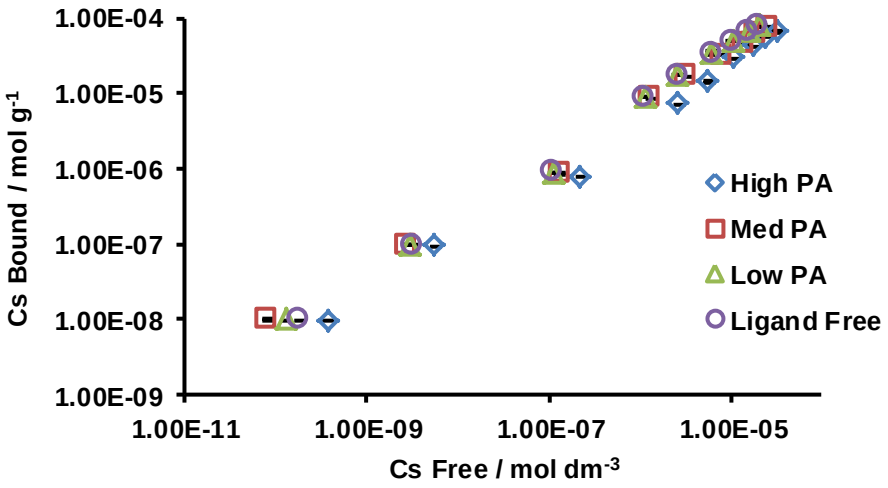

Figure 58. Log-Log plot showing the effect of picolinic acid concentration on the sorption of Cs to bentonite. pH *ca.* 4.7 at high PA concentration, 7.5 at medium and 7.7 at low PA concentration. Experiments carried out at room temperature with a solid:liquid ratio of 1:200, equilibrating *ca.* 7 days. Three replicates per sample

Figure 59 illustrates the change in R_d for Cs sorption to bentonite as the concentration of Cs increases. It is evident that as metal concentration in solution increases the R_d decreases. The trend appears to be the same for all picolinic acid and ligand free solutions investigated.

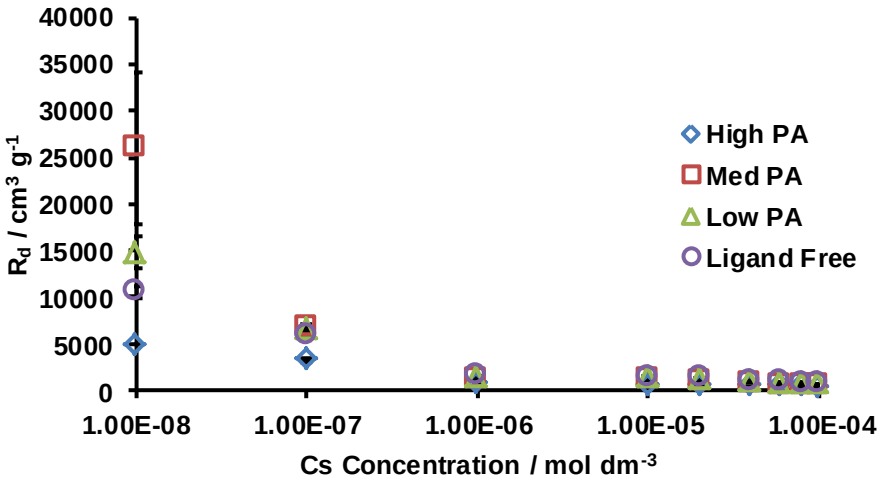

Figure 59. Plot of R_d versus Cs ion concentration at pH *ca.* 4.7 for high PA concentration, 7.5 for medium and 7.7 at low PA concentration. Experiments carried out at room temperature with a solid:liquid ratio of 1:200, equilibrating *ca.* 7 days. Three replicates per sample

The pHs for the sorption of Cs to bentonite in the presence of picolinic acid can be found in Table 19. The pH at high picolinic acid concentration is almost three pH units lower than that for medium, low and ligand free. The high concentration of picolinic acid exceeds the buffering capacity of the bentonite at this concentration, however, the sorption behaviour does not appear to change so the sorption is independent of pH.

Table 19. pHs for Cs sorption to bentonite in the presence of picolinic acid

Picolinic Acid Concentration / mol dm^{-3}	pH Range
1 x 10^{-2} (High)	4.55 – 4.65
1 x 10^{-4} (Medium)	7.40 – 7.52
1 x 10^{-6} (Low)	7.43 – 7.65
Ligand Free	7.41 – 7.76

TOC analysis investigating the amount of picolinic acid in solution after Cs was added with bentonite as the solid phase, shows a decrease in picolinic acid concentration from 93% to 85% indicating a Cs-picolinic acid-bentonite complex might be forming. It appears that 7% of picolinic acid sorbs to the bentonite when there is no metal cation present in solution.

Effect of Picolinic Acid on the Sorption of Sr to Bentonite

From Figure 60 it appears that Sr sorption to bentonite is significantly affected by the presence of a high picolinic acid concentration but not affected by medium or low concentrations of picolinic acid.

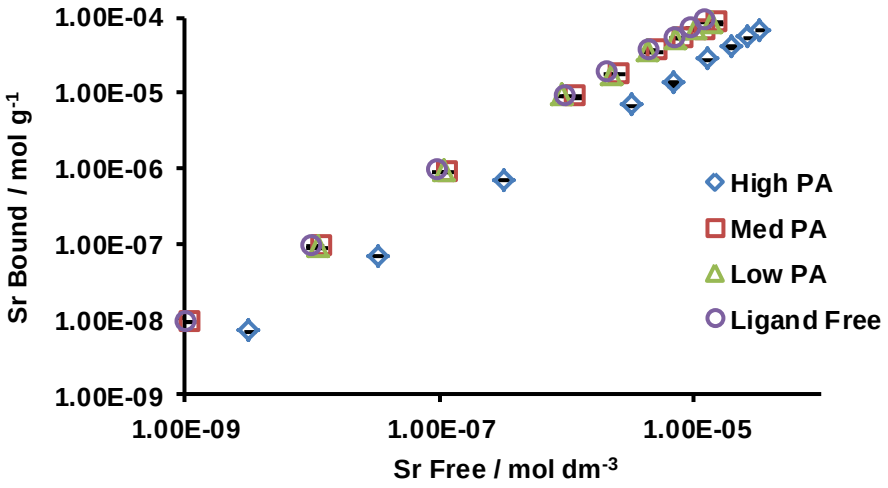

Figure 60. Log-Log plot showing the effect of picolinic acid concentration on the sorption of Sr to bentonite. pH *ca.* 4.9 at high PA concentration, 8.0 at medium and 7.9 for low and ligand free solutions. Experiments carried out at room temperature with a solid:liquid ratio of 1:200, equilibrating *ca.* 7 days. Three replicates per sample

Figure 61 illustrates the change in R_d for Sr sorption to bentonite as the concentration of Sr increases. It is evident that as metal concentration in solution increases the R_d decreases. The trend appears to be the same for all picolinic acid and ligand free solutions investigated although the decrease in R_d at high picolinic acid concentration does not appear to be dramatic.

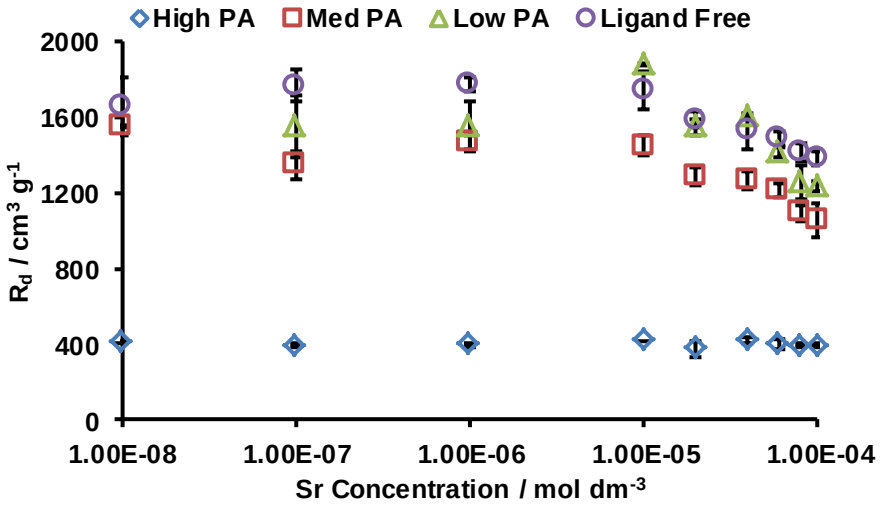

Figure 61. Plot of R_d versus Sr ion concentration at pH *ca.* 4.9 for high PA concentration, 8.0 for medium and 7.9 for low and ligand free solutions. Experiments carried out at room temperature with a solid:liquid ratio of 1:200, equilibrating *ca.* 7 days. Three replicates per sample

Table 20. pHs for Sr sorption to bentonite in the presence of picolinic acid

Picolinic Acid Concentration / mol dm^{-3}	pH Range
1 x 10^{-2} (High)	4.74 – 4.85
1 x 10^{-4} (Medium)	7.80 – 8.01
1 x 10^{-6} (Low)	7.74 – 7.93
Ligand Free	7.61 – 7.89

3.3.2 Effect of NTA on the Sorption of Cs and Sr to Montmorillonite and Bentonite

Experimental Method

Three NTA solutions were prepared with concentrations of 1 x 10^{-2} (high NTA), 1 x 10^{-4} (med. NTA) and 1 x 10^{-6} (low NTA) mol dm^{-3}. 20 cm^3 of NTA solution was added to 0.1 g of clay mineral in 50 cm^3 centrifuge vials, to which 200 µl of 1 x 10^{-2} to 1 x 10^{-6} mol dm^{-3} inactive $CsNO_3$ or $Sr(NO_3)_2$ was added, establishing final metal ion concentrations between 1 x 10^{-4} to 1 x 10^{-8} mol dm^{-3}, along with 100 µl of ^{137}Cs or ^{85}Sr, resulting in a total activity of ~3 kBq per vial. Samples were carried out in triplicate. The samples were thoroughly mixed with a whirlimixer and then placed on an orbital shaker for 1 week at 100 rpm. After a week, the samples were centrifuged at 6000 rpm for 20 minutes and the supernatant then decanted. 2 cm^3 of supernatant was filtered through

a 0.45 µm syringe filter and the gamma radiation counted with a Packard Cobra II Auto Gamma counter. The pH of the remaining supernatant was recorded.

Results

Effect of NTA Concentration on Sorption of Cs to Montmorillonite

The effect of NTA concentration on sorption of Cs to montmorillonite is shown in Figure 62. High NTA concentration appears to affect the sorption of Cs at low Cs concentration, but as Cs concentration increases, the behaviour appears to mirror that of the ligand free results. Low and Medium NTA concentrations mirror the ligand free results up until 5.3 x 10^{-5} mol dm^{-3} where saturation appears to have occurred for ligand free results, but saturation does not appear to occur with the presence of NTA.

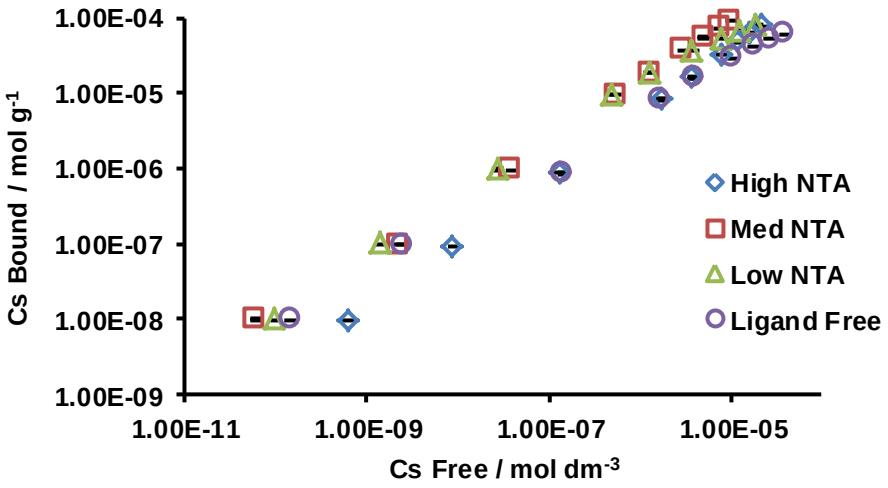

Figure 62. Log-Log plot showing the effect of NTA concentration on the sorption of Cs to montmorillonite. pH *ca.* 10.2 at high NTA concentration, 7.1 at medium, 5.8 at low NTA concentration and 4.6 for ligand free solutions. Experiments carried out at room temperature with a solid:liquid ratio of 1:200, equilibrating *ca.* 7 days. Three replicates per sample

Figure 63 illustrates the change in R_d for Cs sorption to montmorillonite as the concentration of Cs increases in the presence of varying NTA ligand concentrations. It is evident that as the metal concentration in solution increases the R_d decreases. The trend appears to be the same for all NTA and ligand free solutions investigated.

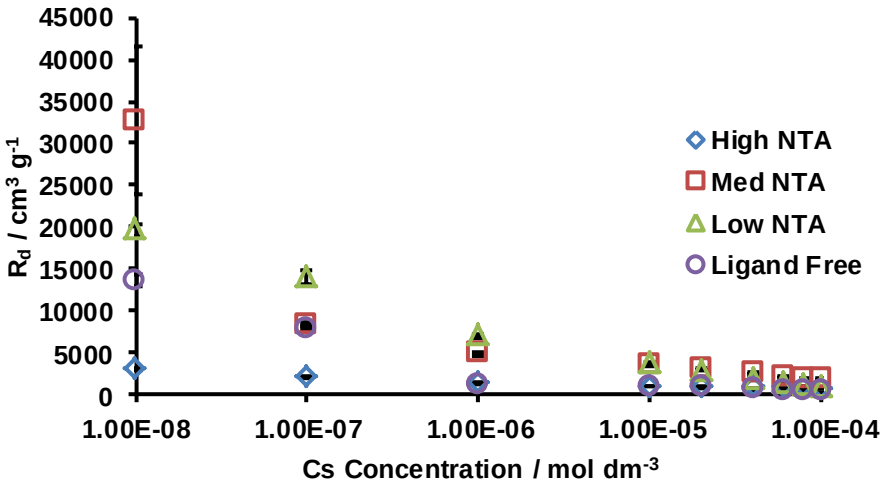

Figure 63. Plot of R_d versus Cs ion concentration at pH *ca.* 10.2 for high NTA concentration, 7.1 for medium, 5.8for low NTA concentration and 4.6 for ligand free solutions. Experiments carried out at room temperature with a solid:liquid ratio of 1:200, equilibrating *ca.* 7 days. Three replicates per sample

Table 21. pHs for Cs sorption to montmorillonite in the presence of NTA

NTA Concentration / mol dm^{-3}	pH Range
1 x 10^{-2} (High)	10.09 – 10.19
1 x 10^{-4} (Medium)	6.35 – 7.05
1 x 10^{-6} (Low)	4.84 – 5.82
Ligand Free	3.87 – 4.63

Effect of NTA Concentration on Sorption of Sr to Montmorillonite

Figure 64 illustrates the results obtained for sorption of Sr to montmorillonite in the presence NTA at different concentrations. Low and medium NTA concentrations match the experimental results for ligand free sorption below 8.5 x 10^{-7} mol dm^{-3}. Above this value, saturation of sorption sites occurs for the ligand free data above 3.5 x 10^{-5} mol g^{-1} and at 5.8 x 10^{-5} mol g^{-1} at the lowest NTA concentration. The presence of low and medium concentrations of NTA seems to enhance the sorption of Sr at higher metal concentration. At highest NTA concentration, the presence of NTA inhibits the sorption of Sr to montmorillonite across the whole range of Sr concentrations studied. Saturation of the sorption sites does not occur at high or medium NTA concentration.

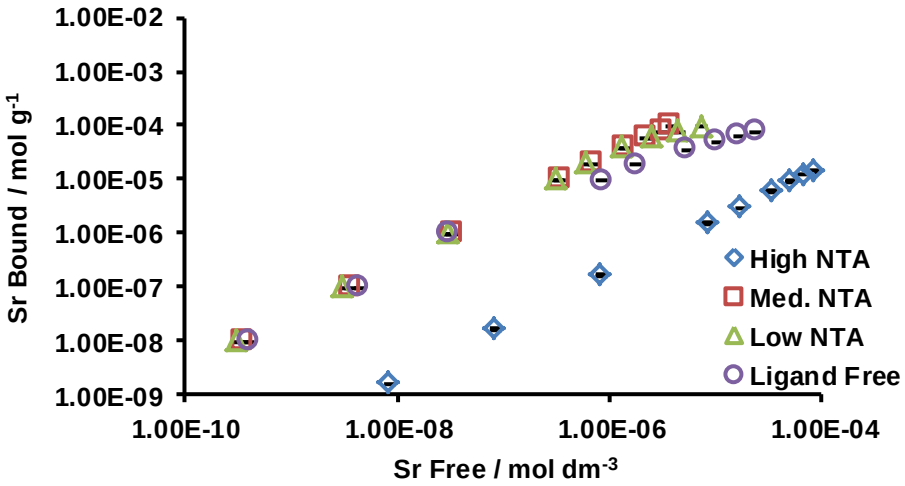

Figure 64. Log-Log plot showing the effect of NTA concentration on the sorption of Sr to montmorillonite. pH *ca.* 10.2 at high NTA concentration, 6.9 at medium, 5.5 at low NTA concentration and 4.7 for ligand free solutions. Experiments carried out at room temperature with a solid:liquid ratio of 1:200, equilibrating *ca.* 7 days. Three replicates per sample

Figure 65 illustrates the change in R_d for Sr sorption to montmorillonite as the concentration of Sr increases in the presence of varying NTA ligand concentrations. It is evident that as the metal concentration in solution increases the R_d decreases. At low NTA, deviation from linearity occurs above Sr concentration of 4×10^{-5} mol dm^{-3}, whereas deviation from linearity at medium and high NTA concentrations does not appear to occur. For a ligand free system, deviation from linearity occurs above 1×10^{-6} mol dm^{-3}.

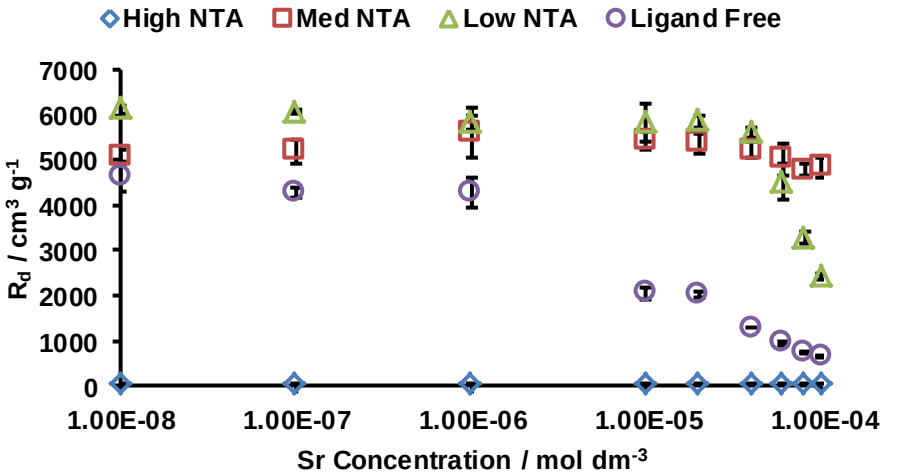

Figure 65. Plot of R_d versus Sr ion concentration at pH *ca.* 10.2 for high NTA concentration, 6.9 for medium, 5.5 for low NTA concentration and 4.7 for ligand free solutions. Experiments carried out at room temperature with a solid:liquid ratio of 1:200, equilibrating *ca.* 7 days. Three replicates per sample

Table 22. pHs for Sr sorption to montmorillonite in the presence of NTA

NTA Concentration / mol dm^{-3}	pH Range
1 x 10^{-2} (High)	10.10 – 10.18
1 x 10^{-4} (Medium)	6.36 – 6.90
1 x 10^{-6} (Low)	4.82 – 5.49
Ligand Free	4.09 – 4.67

Effect of NTA Concentration on Sorption of Cs to Bentonite

The presence of NTA does not appear to affect the sorption of Cs to bentonite regardless of the concentration of NTA in the system, as shown in Figure 66.

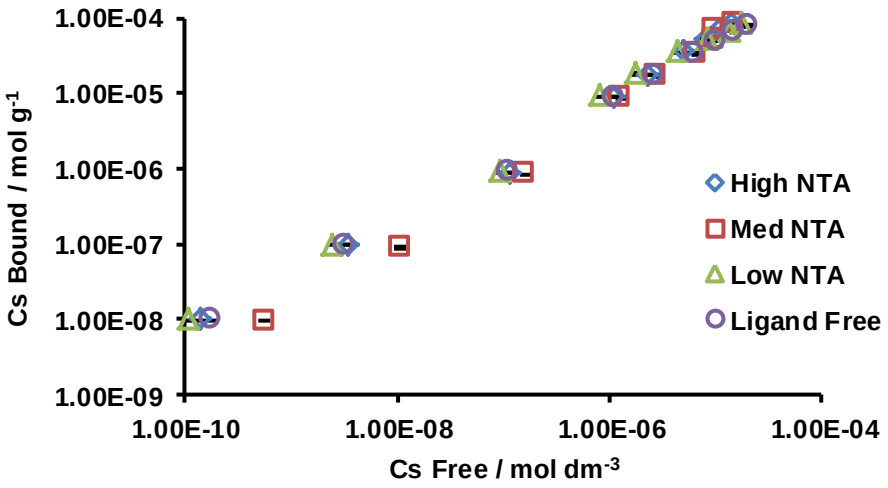

Figure 66. Log-Log plot showing the effect of NTA concentration on the sorption of Cs to bentonite. pH *ca.* 10.9 at high NTA concentration, 9.2 at medium and 7.7 at low NTA concentration. Experiments carried out at room temperature with a solid:liquid ratio of 1:200, equilibrating *ca.* 7 days. Three replicates per sample

Figure 67 illustrates the change in R_d for Cs sorption to bentonite as the concentration of Cs increases in the presence of varying NTA ligand concentrations. It is evident that as the metal concentration in solution increases the R_d decreases. The trend appears to be the same for all NTA and ligand free solutions investigated.

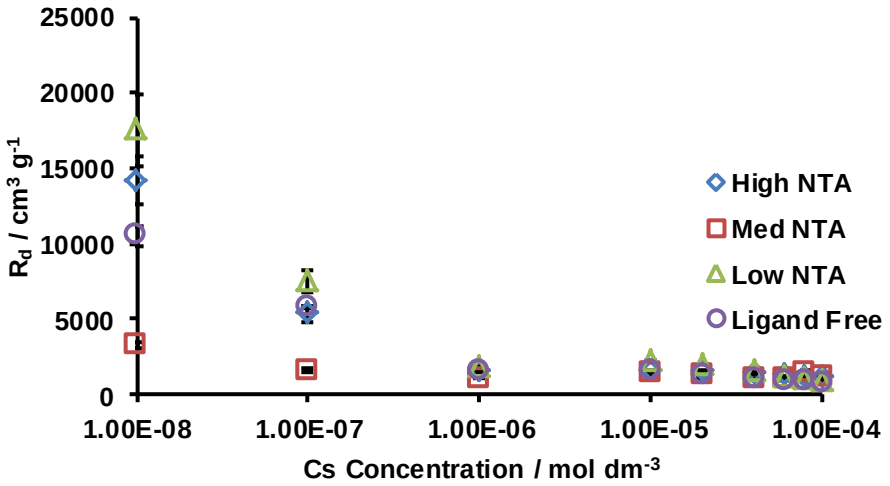

Figure 67. Plot of R_d versus Cs ion concentration at pH *ca.* 10.9 for high NTA concentration, 9.2 for medium and 7.7 for low NTA concentration. Experiments carried out at room temperature with a solid:liquid ratio of 1:200, equilibrating *ca.* 7 days. Three replicates per sample

Table 23. pHs for Cs sorption to bentonite in the presence of NTA

NTA Concentration / mol dm^{-3}	pH Range
1 x 10^{-2} (High)	10.61 – 10.88
1 x 10^{-4} (Medium)	8.04 – 9.16
1 x 10^{-6} (Low)	7.41 – 7.69
Ligand Free	7.41 – 7.76

Effect of NTA Concentration on Sorption of Sr to Bentonite

Unlike the data found for Cs sorption to bentonite in the presence of NTA, the sorption of Sr to bentonite appears to be affected by the presence of NTA at medium and high NTA concentrations. The sorption of Sr at low NTA concentration matches the data of that found for with no ligand present in the system. Figure 68 shows the experimental results of Sr sorption to bentonite in the presence of NTA.

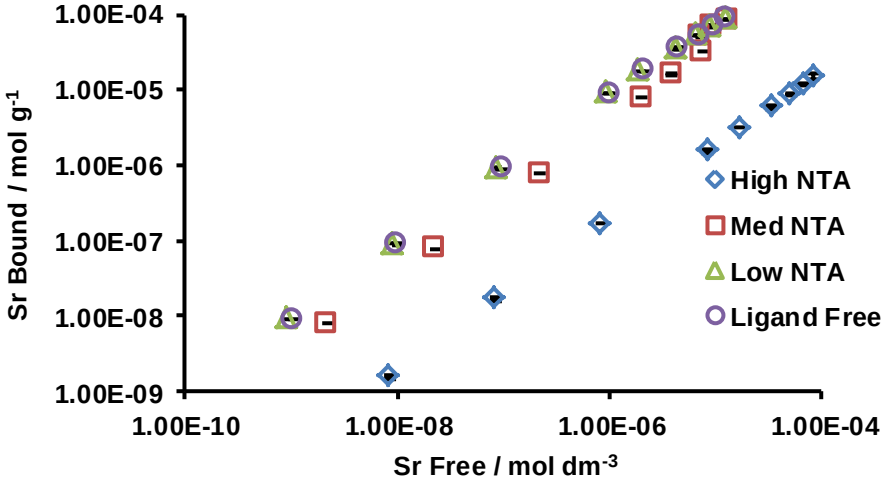

Figure 68. Log-Log plot showing the effect of NTA concentration on the sorption of Sr to bentonite. pH *ca.* 10.8 at high NTA concentration, 9.5 at medium, 7.8 at low NTA and 7.9 for ligand free solutions. Experiments carried out at room temperature with a solid:liquid ratio of 1:200, equilibrating *ca.* 7 days. Three replicates per sample

Figure 69 illustrates the change in R_d for Sr sorption to bentonite as the concentration of Sr increases in the presence of varying NTA ligand concentrations. It is evident that as the metal concentration in solution increases the R_d decreases. The trend appears to be the same for all NTA and ligand free solutions investigated apart from medium NTA concentration.

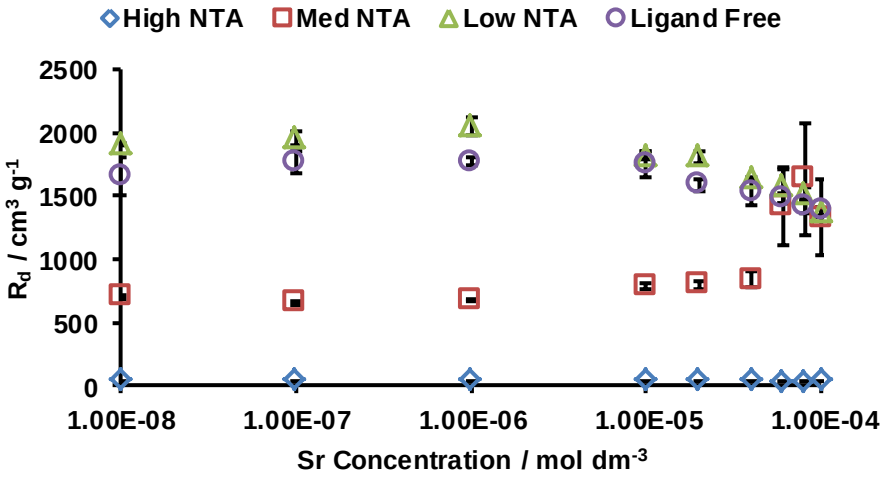

Figure 69. Plot of R_d versus Sr ion concentration at pH *ca.* 10.8 for high NTA concentration, 9.5 for medium, 7.8 for low NTA and 7.9 for ligand free solutions. Experiments carried out at room temperature with a solid:liquid ratio of 1:200, equilibrating *ca.* 7 days. Three replicates per sample

Table 24. pHs for Sr sorption to bentonite in the presence of NTA

NTA Concentration / mol dm^{-3}	pH Range
1 x 10^{-2} (High)	10.67 – 10.81
1 x 10^{-4} (Medium)	8.21 – 9.53
1 x 10^{-6} (Low)	7.46 – 7.81
Ligand Free	7.61 – 7.89

3.3.3 Effect of EDTA on the Sorption of Cs and Sr to Montmorillonite and Bentonite

Experimental Method

Three EDTA solutions were prepared with concentrations of 1 x 10^{-2} (high NTA), 1 x 10^{-4} (med. EDTA) and 1 x 10^{-6} (low EDTA) mol dm^{-3}. 20 cm^3 of EDTA solution was added to 0.1 g of clay mineral in 50 cm^3 centrifuge vials, to which 200 µl of 1 x 10^{-2} to 1 x 10^{-6} mol dm^{-3} inactive $CsNO_3$ or $Sr(NO_3)_2$ was added, establishing final metal ion concentrations between 1 x 10^{-4} to 1 x 10^{-8} mol dm^{-3}, along with 100 µl of ^{137}Cs or ^{85}Sr, resulting in a total activity of ~3 kBq per vial. Samples were carried out in triplicate. The samples were thoroughly mixed with a whirlimixer and then placed on an orbital shaker for 1 week at 100 rpm. After a week, the samples were centrifuged at 6000 rpm for 20 minutes and the supernatant then decanted. 2 cm^3 of supernatant was filtered through a 0.45 µm syringe filter and the gamma radiation counted with a Packard Cobra II Auto Gamma counter. The pH of the remaining supernatant was recorded.

Results

Effect of EDTA Concentration on Sorption of Cs to Montmorillonite

Investigations into the effect of EDTA concentration on Cs sorption to montmorillonite are shown below in Figure 70. At low Cs concentration, a high EDTA concentration reduces the degree of sorption occurring when compared with the ligand free results. As Cs concentration increases, the effect of EDTA on sorption appears to be less significant, and the results approach the values seen for ligand free sorption. There is no apparent effect on sorption of Cs to montmorillonite in the presence of low or medium EDTA concentrations.

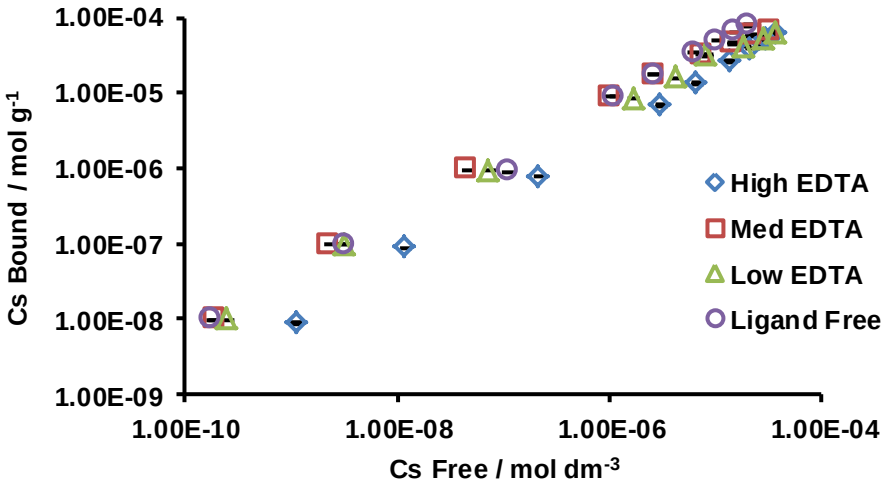

Figure 70. Log-Log plot showing the effect of EDTA concentration on the sorption of Cs to montmorillonite. pH *ca.* 4.2 at high EDTA concentration, 4.8 at medium, 4.5 at low EDTA and 4.6 for ligand free solutions. Experiments carried out at room temperature with a solid:liquid ratio of 1:200, equilibrating *ca.* 7 days. Three replicates per sample

Figure 71 illustrates the change in R_d for Cs sorption to montmorillonite as the concentration of Cs increases in the presence of varying EDTA ligand concentrations. It is evident that as the metal concentration in solution increases the R_d decreases. The trend appears to be the same for all EDTA and ligand free solutions investigated.

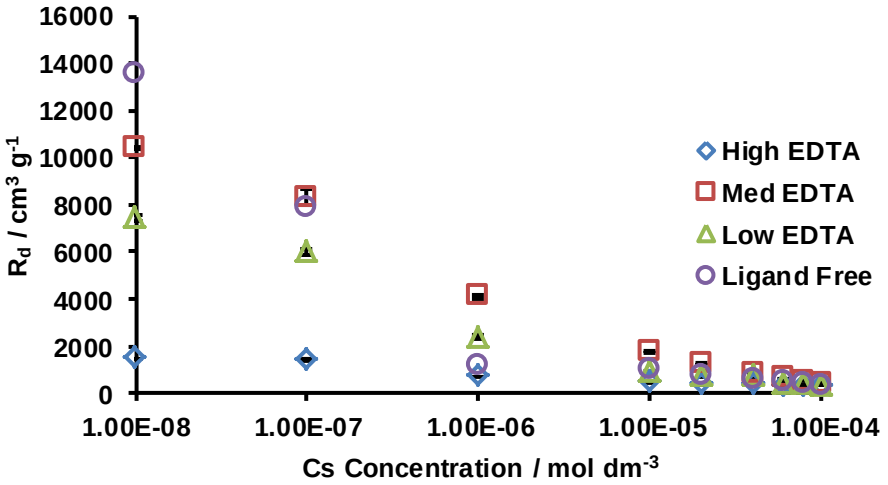

Figure 71. Plot of R_d versus Cs ion concentration at pH *ca.* 4.2 for high EDTA concentration, 4.8 for medium, 4.5 for low EDTA and 4.6 for ligand free solutions. Experiments carried out at room temperature with a solid:liquid ratio of 1:200, equilibrating *ca.* 7 days. Three replicates per sample

Table 25. pHs for Cs sorption to montmorillonite in the presence of EDTA

EDTA Concentration / mol dm^{-3}	pH Range
1 x 10^{-2} (High)	4.17 – 4.21
1 x 10^{-4} (Medium)	4.16 – 4.76
1 x 10^{-6} (Low)	4.10 – 4.47
Ligand Free	3.87 – 4.63

Effect of EDTA Concentration on Sorption of Sr to Montmorillonite

Figure 72 shows the effect of EDTA concentration on Sr sorption to montmorillonite. As with Cs sorption to montmorillonite in the presence of EDTA, the results show that sorption to montmorillonite is only affected at highest EDTA concentration and at the lower range of Sr ion concentration. At the highest Sr concentration, the sorption data shows that EDTA has little effect on the sorption to montmorillonite, producing similar results to the ligand free data. Low and medium EDTA concentrations have little or no effect on the Sr sorption to montmorillonite.

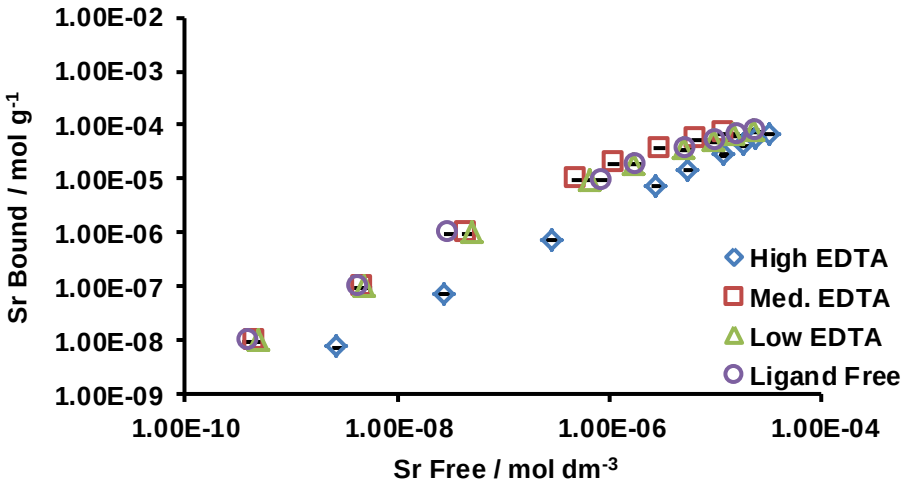

Figure 72. Log-Log plot showing the effect of EDTA concentration on the sorption of Sr to montmorillonite. pH *ca.* 4.2 at high EDTA concentration, 4.8 at medium, 4.6 at low EDTA and 4.7 for ligand free solutions. Experiments carried out at room temperature with a solid:liquid ratio of 1:200, equilibrating *ca.* 7 days. Three replicates per sample

Figure 73 illustrates the change in R_d for Sr sorption to montmorillonite as the concentration of Sr increases in the presence of varying EDTA ligand concentrations. It is evident that as the metal concentration in solution increases the R_d decreases. For low EDTA and ligand free solutions, deviation from linearity occurs above a Sr

concentration of 1 x 10^{-6} mol dm^{-3}, however, deviation from linearity occurs at higher Sr concentrations for medium and high EDTA concentrations.

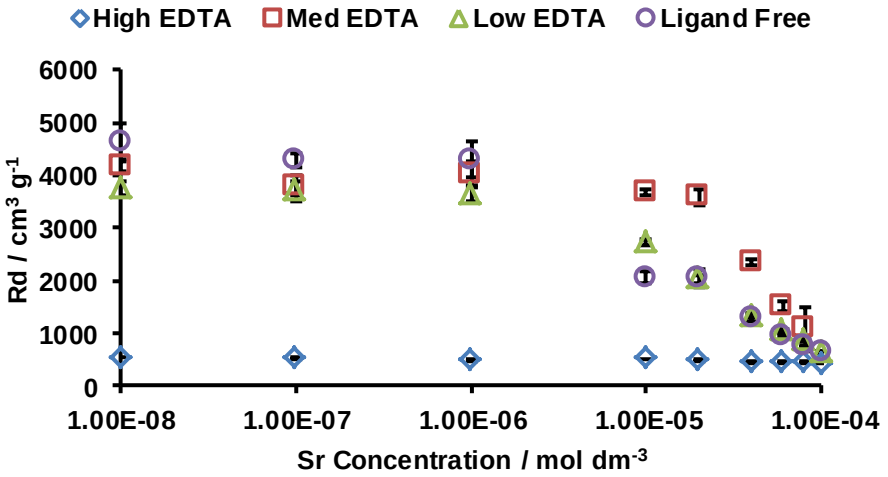

Figure 73. Plot of R_d versus Sr ion concentration at pH *ca.* 4.2 for high EDTA concentration, 4.8 for medium, 4.6 for low EDTA and 4.7 for ligand free solutions. Experiments carried out at room temperature with a solid:liquid ratio of 1:200, equilibrating *ca.* 7 days. Three replicates per sample

Table 26. pHs for Sr sorption to montmorillonite in the presence of EDTA

EDTA Concentration / mol dm^{-3}	pH Range
1 x 10^{-2} (High)	4.15 – 4.19
1 x 10^{-4} (Medium)	4.32 – 4.77
1 x 10^{-6} (Low)	4.39 – 4.57
Ligand Free	4.09 – 4.67

Effect of EDTA Concentration on Sorption of Cs to Bentonite

From the results illustrated in Figure 74 it appears that the presence of EDTA at high, medium and low concentrations has little effect on the Cs sorption to bentonite, much like the results found for Cs sorption to montmorillonite in the presence of EDTA. At the lowest Cs ion concentrations, it does appear that the low and medium EDTA concentrations may help enhance the sorption of Cs when compared to the ligand free data. This may occur through a Cs-EDTA-bentonite complex. At higher Cs ion concentration, the presence of EDTA appears to have little or no effect on sorption.

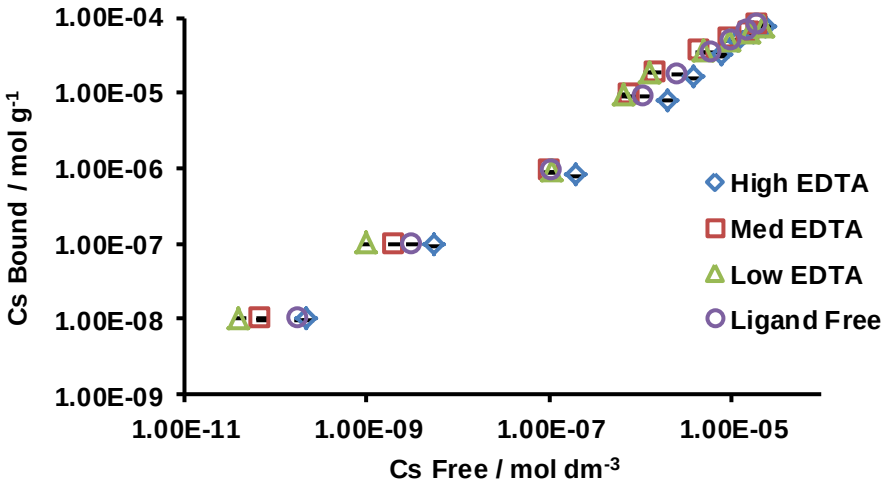

Figure 74. Log-Log plot showing the effect of EDTA concentration on the sorption of Cs to bentonite. pH *ca.* 4.6 at high EDTA concentration, 8.0 at medium and 8.3 at low EDTA concentration. Experiments carried out at room temperature with a solid:liquid ratio of 1:200, equilibrating *ca.* 7 days. Three replicates per sample

Figure 75 illustrates the change in R_d for Cs sorption to bentonite as the concentration of Cs increases in the presence of varying EDTA ligand concentrations. It is evident that as the metal concentration in solution increases the R_d decreases. The trend appears to be the same for all EDTA and ligand free solutions investigated.

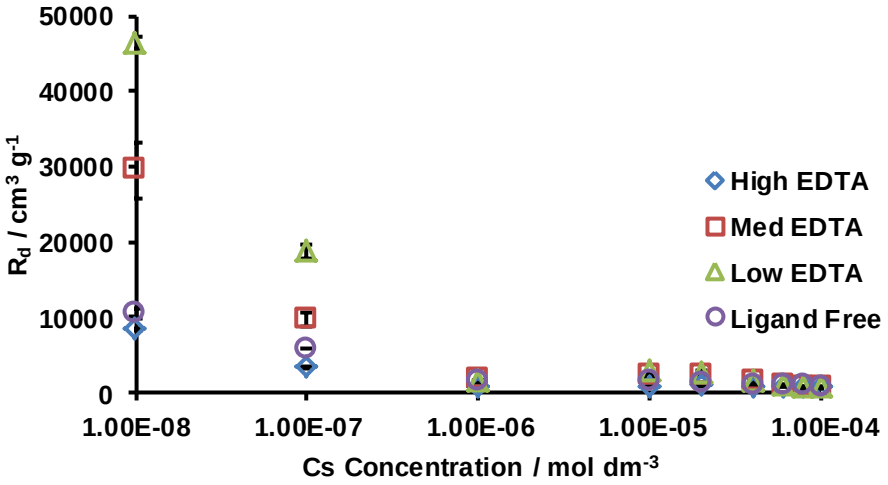

Figure 75. Plot of R_d versus Cs ion concentration at pH *ca.* 4.6 for high EDTA concentration, 8.0 for medium and 8.3 for low EDTA concentration. Experiments carried out at room temperature with a solid:liquid ratio of 1:200, equilibrating *ca.* 7 days. Three replicates per sample

Table 27. pHs for Cs sorption to bentonite in the presence of EDTA

EDTA Concentration / mol dm^{-3}	pH Range
1 x 10^{-2} (High)	4.48 – 4.57
1 x 10^{-4} (Medium)	7.78 – 8.01
1 x 10^{-6} (Low)	8.06 – 8.29
Ligand Free	7.41 – 7.76

Effect of EDTA Concentration on Sorption of Sr to Bentonite

The results for Sr sorption to bentonite in the presence of various EDTA concentrations shows that at high EDTA concentration, the sorption of Sr to bentonite reduces (Figure 76) compared to the ligand free results. The presence of low or medium EDTA concentrations in the system shows little effect on the sorption of Sr to bentonite.

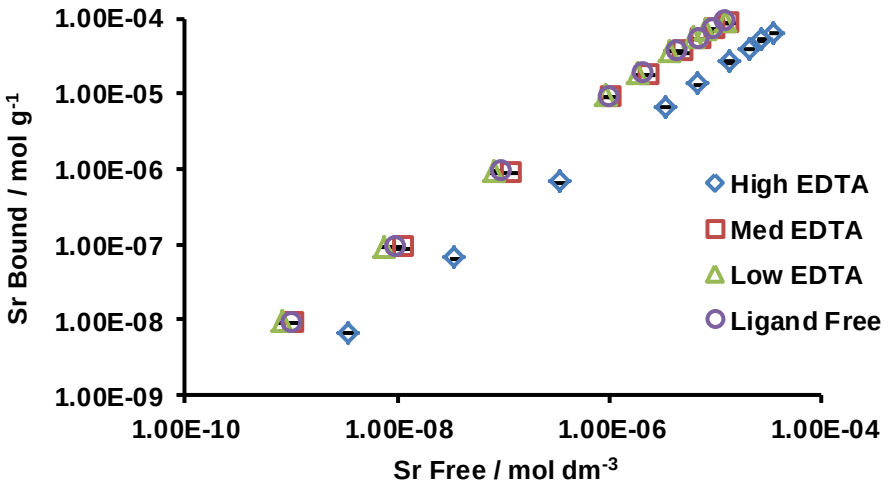

Figure 76. Log-Log plot showing the effect of EDTA concentration on the sorption of Sr to bentonite. pH *ca.* 4.6 at high EDTA concentration, 8.0 at medium, 8.8 at low EDTA and 7.9 for ligand free solutions. Experiments carried out at room temperature with a solid:liquid ratio of 1:200, equilibrating *ca.* 7 days. Three replicates per sample

Figure 77 illustrates the change in R_d for Sr sorption to bentonite as the concentration of Sr increases in the presence of varying EDTA ligand concentrations. It is evident that as the metal concentration in solution increases the R_d decreases. The trend appears to be the same for all EDTA and ligand free solutions investigated.

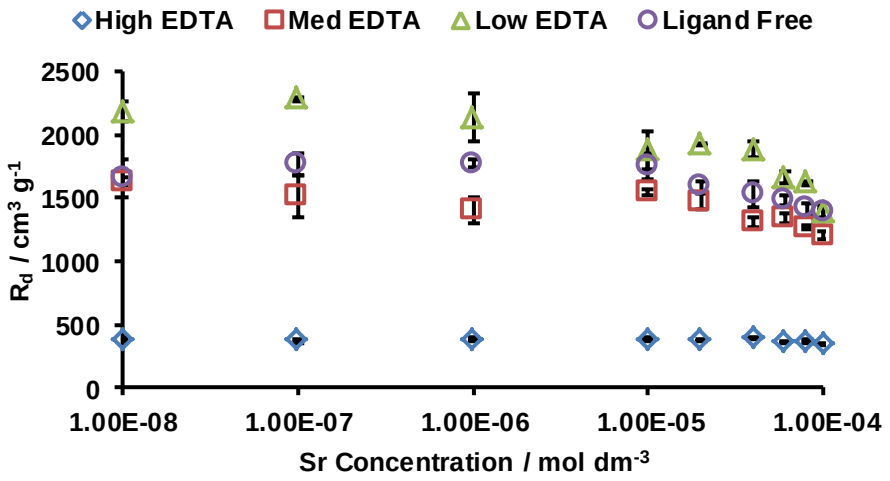

Figure 77. Plot of R_d versus Sr ion concentration at pH *ca.* 4.6 for high EDTA concentration, 8.0 for medium, 8.8 for low EDTA and 7.9 for ligand free solutions. Experiments carried out at room temperature with a solid:liquid ratio of 1:200, equilibrating *ca.* 7 days. Three replicates per sample

Table 28. pHs for Sr sorption to bentonite in the presence of EDTA

EDTA Concentration / mol dm^{-3}	pH Range
1 x 10^{-2} (High)	4.51 – 4.56
1 x 10^{-4} (Medium)	7.60 – 7.99
1 x 10^{-6} (Low)	7.81 – 8.76
Ligand Free	7.61 – 7.89

3.3.4 Comparison of Anthropogenic Organic Ligands on Sorption Effects

The results obtained previously have shown the effect that anthropogenic organic ligands have on the sorption behaviour of Cs and Sr to montmorillonite and bentonite clays. The following section compares the effect that these anthropogenic organic ligands have on sorption, allowing for the easy determination of which ligand has the greatest influence on sorption behaviour.

Comparison of Anthropogenic Organic Ligand Presence on Cs Sorption to Montmorillonite

At high ligand concentration, EDTA and NTA appear to have the greatest effect on the sorption of Cs to montmorillonite, particularly at Cs concentrations below 1 x 10^{-6} mol dm^{-3}, where there is an increase of Cs in the aqueous phase compared to the results obtained for the ligand free system (Figure 78). High picolinic acid concentration has

the least effect on the sorption of Cs to montmorillonite, mirroring the ligand free sorption results, although it does appear to enhance sorption between Cs concentrations of 1×10^{-6} and 2×10^{-5} mol dm^{-3}.

From Figure 79 and Figure 80, the EDTA and picolinic acid appear to have similar effects on the Cs sorption to montmorillonite, whereas NTA behaves differently, reducing sorption at medium ligand concentration when the Cs concentration is low (Figure 79), and apparently increasing sorption when NTA concentration is low but Cs concentration is high (Figure 80).

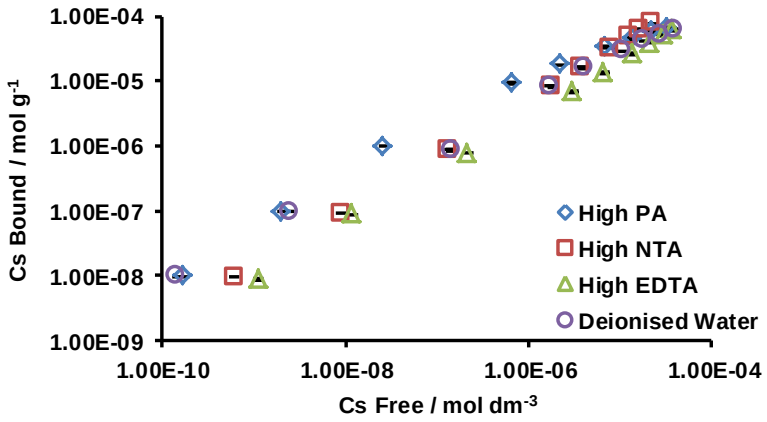

Figure 78. Comparison of anthropogenic organic ligand presence at high concentrations (1 x 10^{-2} mol dm^{-3}) on the sorption of Cs to montmorillonite. pH *ca.* 3.7 at high PA concentration, 10.2 at high NTA, 4.2 at high EDTA and 4.6 for ligand free solutions

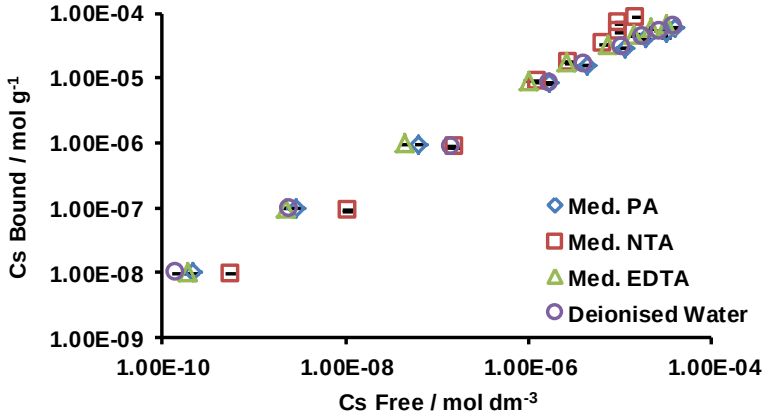

Figure 79. Comparison of anthropogenic organic ligand presence at medium concentrations (1 x 10^{-4} mol dm^{-3}) on the sorption of Cs to montmorillonite. pH *ca.* 4.5 at medium PA concentration, 7.1 at medium NTA, 4.8 at medium EDTA and 4.6 for ligand free solutions

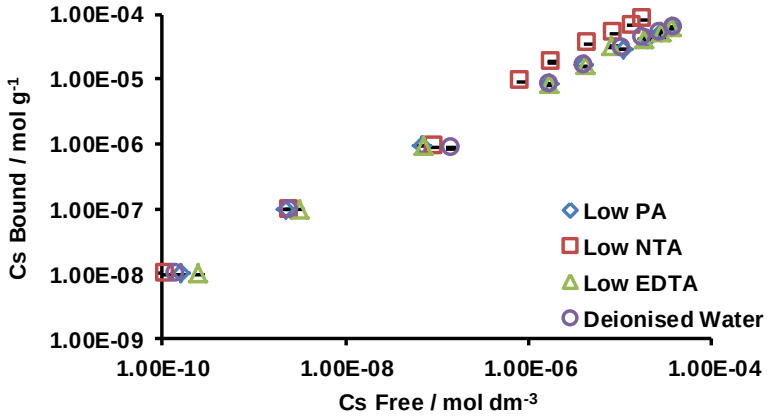

Figure 80. Comparison of anthropogenic organic ligand presence at low concentrations (1 x 10^{-6} mol dm^{-3}) on the sorption of Cs to montmorillonite. pH *ca.* 4.6 at low PA concentration, 5.8 at low NTA, 4.5 at low EDTA and 4.6 for ligand free solutions

Comparison of Anthropogenic Organic Ligand Presence on Sr Sorption to Montmorillonite

Figure 81 shows that all three anthropogenic organic ligands have some effect on Sr sorption to montmorillonite. NTA had the greatest effect, significantly greater then both EDTA and picolinic acid. EDTA and picolinic acid both affected sorption, however, this effect on sorption was less than that seen for NTA.

At medium ligand concentration (Figure 82) this behaviour is reversed with picolinic acid having the greater effect on Sr sorption and NTA having minimal effect. At higher Sr ion concentration, it appears that NTA is actually helping enhance the sorption of Sr to montmorillonite. EDTA has a similar effect to NTA on the sorption, but does not appear to enhance Sr sorption at high Sr ion concentrations.

At lowest ligand concentration, picolinic acid once again has the greatest effect on sorption, increasing the Sr ion concentration in solution at low Sr concentrations (Figure 83). As with medium NTA concentration, low NTA has the least negative effect on Sr sorption appearing to increase the sorption of Sr to montmorillonite across the entire range of Sr ion concentrations investigated. EDTA mirrors the results obtained for a ligand free system.

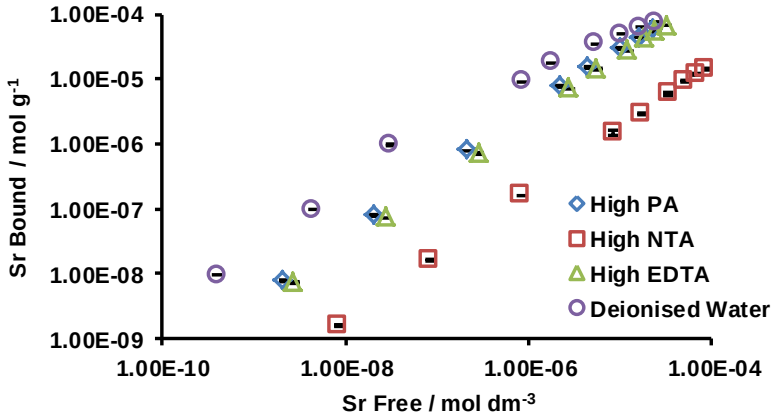

Figure 81. Comparison of anthropogenic organic ligand presence at high concentrations (1 x 10^{-2} mol dm^{-3}) on the sorption of Sr to montmorillonite. pH *ca.* 3.7 at high PA concentration, 10.2 at high NTA, 4.2 at high EDTA and 4.7 for ligand free solutions

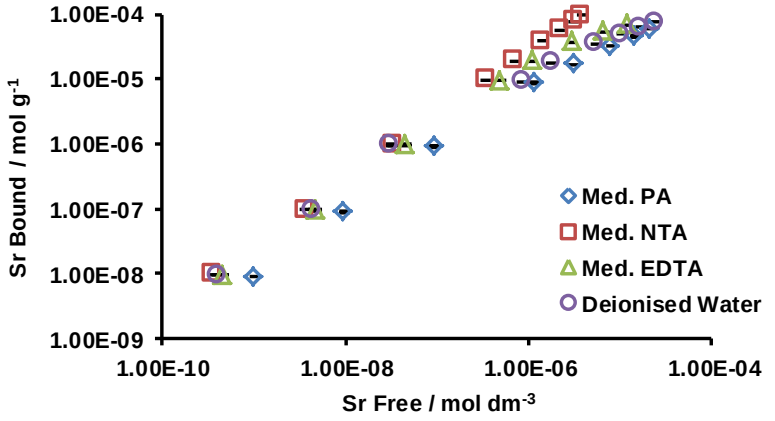

Figure 82. Comparison of anthropogenic organic ligand presence at medium concentrations (1 x 10^{-4} mol dm^{-3}) on the sorption of Sr to montmorillonite. pH *ca.* 5.1 at medium PA concentration, 6.9 at medium NTA, 4.8 at medium EDTA and 4.7 for ligand free solutions

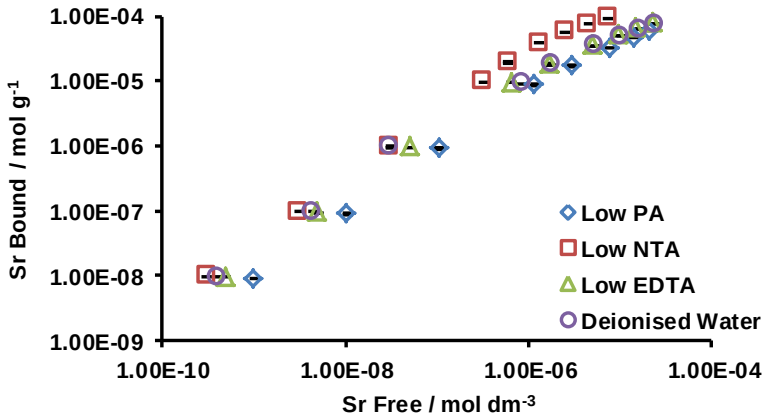

Figure 83. Comparison of anthropogenic organic ligand presence at low concentrations (1 x 10^{-6} mol dm^{-3}) on the sorption of Sr to montmorillonite. pH *ca.* 5.3 at low PA concentration, 5.5 at low NTA, 4.6 at low EDTA and 4.7 for ligand free solutions

Comparison of Anthropogenic Organic Ligand Presence on Cs Sorption to Bentonite

Figure 84 - Figure 86 show the comparisons of anthropogenic organic ligand effects on Cs sorption to bentonite. For all three ligand concentrations, it can be seen that there is little effect on the sorptive behaviour of Cs in this system. All three anthropogenic organic ligands appear to be behaving similarly in these systems, however, at medium NTA concentration with low Cs ion concentration, there does appear to be a slight reduction in sorption behaviour. At these levels it may be deduced that there is a slight preference towards the NTA complex compared with picolinic acid and EDTA.

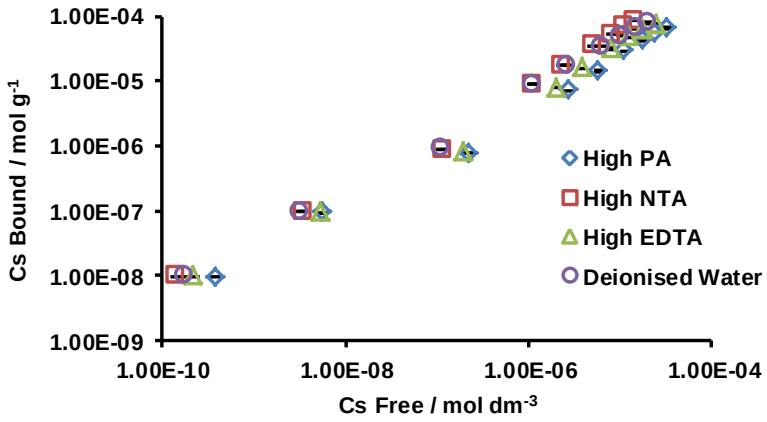

Figure 84. Comparison of anthropogenic organic ligand presence at high concentrations (1 x 10^{-2} mol dm^{-3}) on the sorption of Cs to bentonite. pH *ca.* 4.7 at high PA concentration, 10.9 at high NTA, 4.6 at high EDTA and 7.8 for ligand free solutions

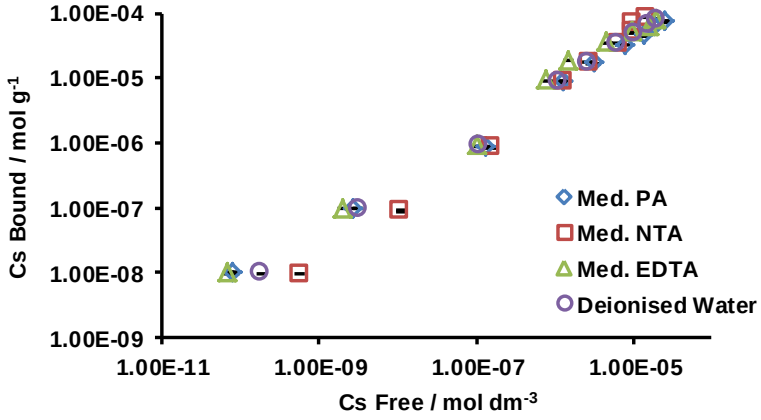

Figure 85. Comparison of anthropogenic organic ligand presence at medium concentrations (1 x 10^{-4} mol dm^{-3}) on the sorption of Cs to bentonite. pH *ca.* 7.5 at medium PA concentration, 9.2 at medium NTA, 8.0 at medium EDTA and 7.8 for ligand free solutions

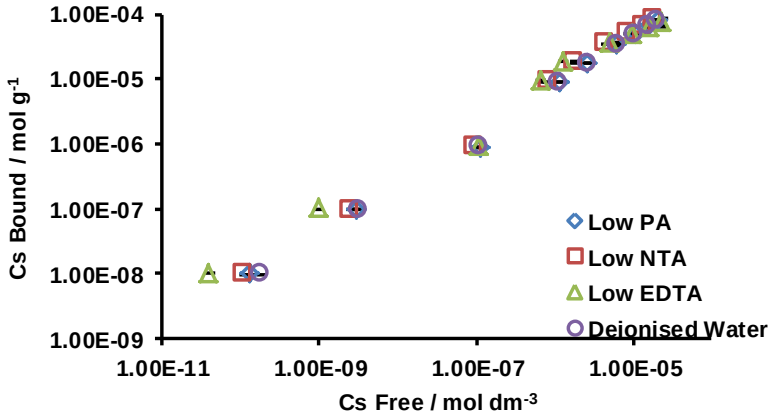

Figure 86. Comparison of anthropogenic organic ligand presence at low concentrations (1 x 10^{-6} mol dm^{-3}) on the sorption of Cs to bentonite. pH *ca.* 7.7 at low PA concentration, 7.7 at low NTA, 8.3 at low EDTA and 7.8 for ligand free solutions

Comparison of Anthropogenic Organic Ligand Presence on Sr Sorption to Bentonite

Figure 87 - Figure 89 compare the effects of anthropogenic organic ligands on Sr sorption to bentonite. At high ligand concentration, NTA has the greatest effect on sorption with a significant amount of Sr being retained in the aqueous phase across all Sr ion concentrations investigated. Once again, EDTA and picolinic appear to behave similarly on the sorption behaviour; both affecting the Sr sorption to bentonite at high ligand concentration, but not as greatly as the NTA presence.

At medium ligand concentration, only NTA appears to affect the sorption of Sr whereas EDTA and picolinic acid have no effect on sorption at this concentration. Low ligand concentrations have no effect on the Sr sorption to bentonite for all three anthropogenic organic ligands studied.

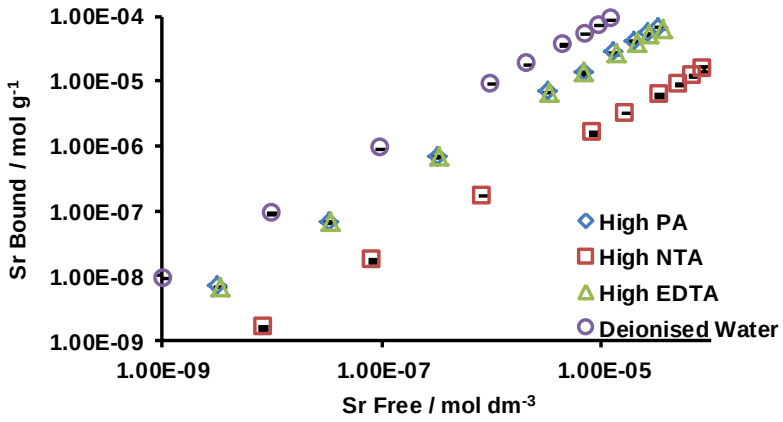

Figure 87. Comparison of anthropogenic organic ligand presence at high concentrations on the sorption of Sr to bentonite. pH *ca.* 4.9 at high PA concentration, 10.8 at high NTA, 4.6 at high EDTA and 7.9 for ligand free solutions

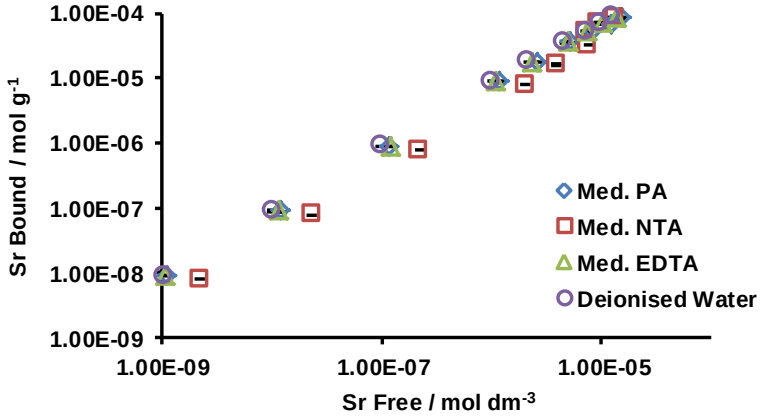

Figure 88. Comparison of anthropogenic organic ligand presence at medium concentrations on the sorption of Sr to bentonite. pH *ca.* 8.0 at medium PA concentration, 9.5 at medium NTA, 8.0 at medium EDTA and 7.9 for ligand free solutions

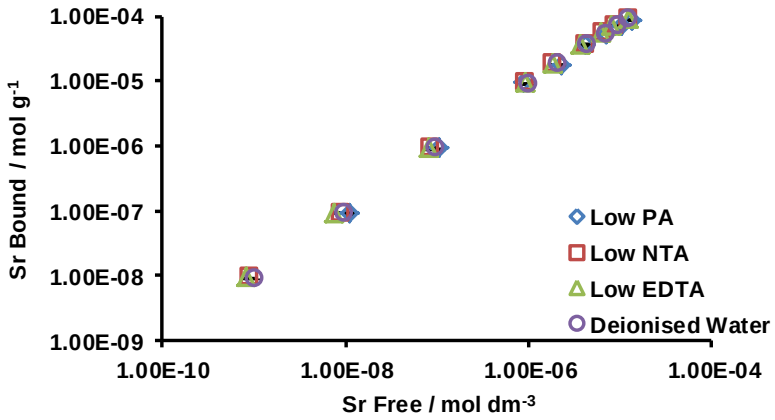

Figure 89. Comparison of anthropogenic organic ligand presence at low concentrations on the sorption of Sr to bentonite. pH *ca.* 7.9 at low PA concentration, 7.8 at low NTA, 8.8 at low EDTA and 7.9 for ligand free solutions

3.4 Analysis of Total Organic Content of Supernatants for Anthropogenic Organic Ligands after Contact with Montmorillonite and Bentonite

Analysis of the total organic carbon content of the aqueous phases allows the determination of any solid-ligand complexes forming. If these solid-ligand complexes are indeed forming, the overall carbon content in solution should decrease.

3.4.1 Experimental Method

Samples were prepared in the same way as with the basic batch sorption experiments. 20 cm^3 of anthropogenic organic ligand solution, at a concentration of 1 X 10^{-2} mol dm^{-3}, was added to 50 cm^3 centrifuge vials containing 0.1 g of clay mineral. To each solution a 100 µl spike of inactive $Sr(NO_3)_2$ or $CsNO_3$ was added so that the final metal ion concentration was 1 X 10^{-4} mol dm^{-3}. All samples were carried out in triplicate. These samples were thoroughly mixed with a whirlimixer and then shaken on an orbital shaker at 100 rpm for 1 week.

After 1 week the samples were centrifuged at 6000 rpm for 20 minutes. The supernatant was decanted with 5 cm^3 of supernatant filtered through 0.45 µm syringe filters into 40 cm^3 glass vials and analysed by a Sievers TOC.

3.4.2 Results

Figure 90 shows the concentration of NTA in solution after being in contact with montmorillonite and bentonite. No significant change in NTA concentration is observed for all systems investigated suggesting that ternary complexes are unlikely to be occurring.

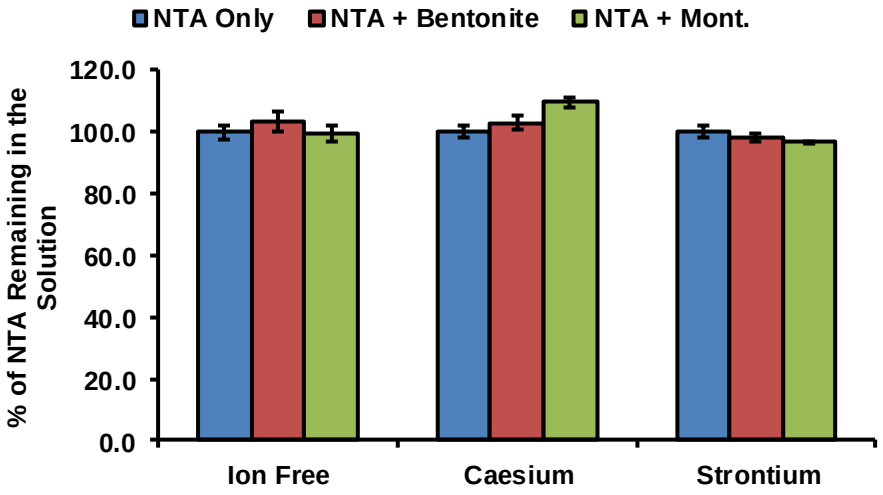

Figure 90. Studies into the effect of Cs and Sr (1 x 10^{-4} mol dm^{-3}) on the amount of NTA in solution by TOC analysis

Figure 91 illustrates the concentration of EDTA in solution in the presence of montmorillonite and bentonite, and a comparison of EDTA concentration when Cs and Sr are present in the system. The results show that EDTA does not appear to form a complex with the surface of both montmorillonite and bentonite clays when there is no metal ion present or with Cs in the system. There does appear to be a reduction of EDTA concentration when Sr is present in both montmorillonite and bentonite systems. The concentration of EDTA in solution reduces by 47 ppm for montmorillonite and 56 ppm for bentonite.

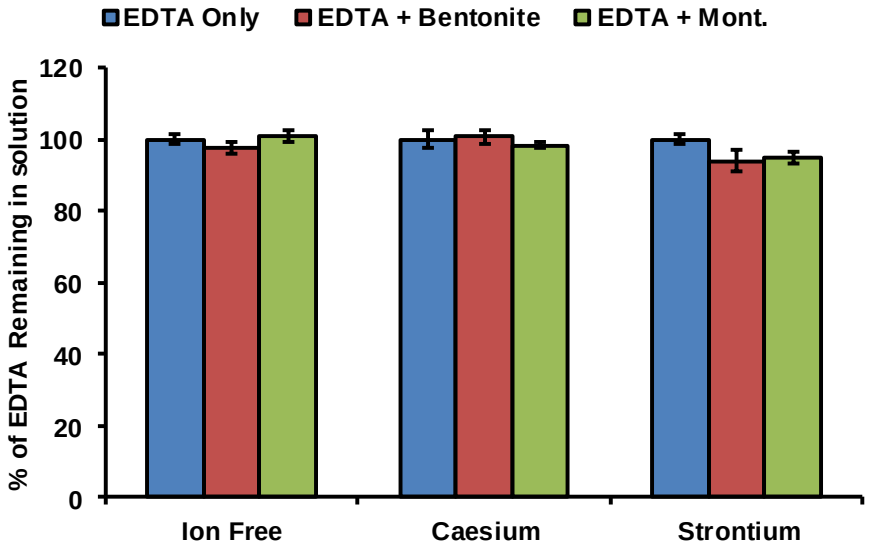

Figure 91. Studies into the effect of Cs and Sr (1 x 10^{-4} mol dm^{-3}) on the amount of EDTA in solution by TOC analysis

Figure 92 illustrates the concentration of picolinic acid in solution in the presence of montmorillonite and bentonite, and a comparison in the picolinic acid concentration when Cs and Sr are present in the system. The results show a dramatic decrease in picolinic acid concentration in solution when montmorillonite is the solid phase present suggesting a solid-ligand complex is occurring. There is a further reduction in the amount of picolinic acid present in solution when strontium is added, decreasing from 28 % to 16.8 % when compared with an ion free system whereas no real change is observed when caesium is present. This suggests a solid-metal-ligand complex may be forming with Sr but not with Cs.

Figure 92 also shows a decrease in picolinic acid concentration in solution with bentonite as the solid phase. The measured change in picolinic acid in an ion free system is found to be only 7 % compared to 72 % with montmorillonite as the solid phase. The amount of picolinic acid remaining in solution for a bentonite system decreases with the addition of strontium, decreasing from 93 % to 80 %, suggestion solid-metal-ligand complexes may be occurring.

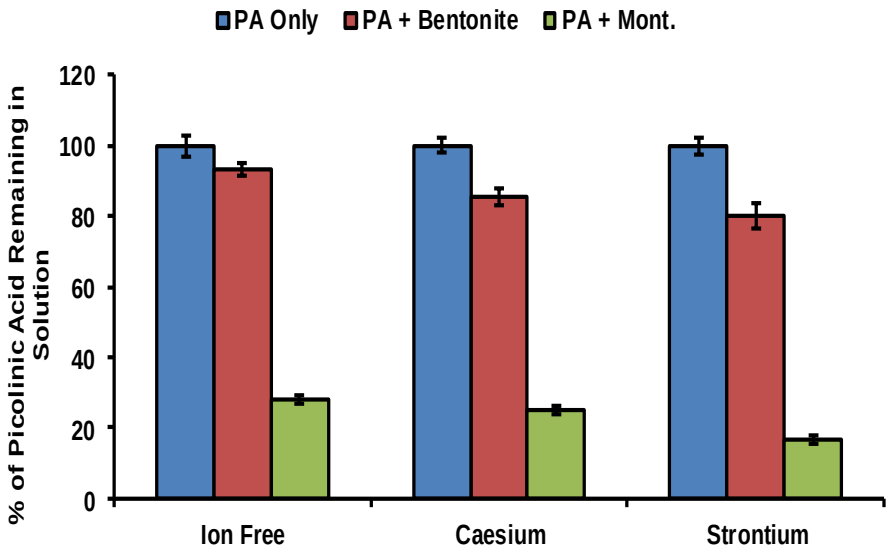

Figure 92. Studies into the effect of Cs and Sr (1×10^{-4} mol dm^{-3}) on the amount of picolinic acid in solution by TOC analysis

Due to the concentrations of Cs and Sr used in these experiments (1×10^{-4} mol dm^{-3}) and the concentrations of organic ligand (1×10^{-2} mol dm^{-3}), the maximum theoretical decrease in ligand concentration in solution due to ternary complexes is only 1×10^{-4} mol dm^{-3}, or 1 % of the total solution concentration. This would equate to roughly 12 ppm for EDTA and 7 ppm for NTA and picolinic acid. Any changes observed in ligand concentration are likely to be due other effects such as low instrument sensitivity.

3.5 Effect of pH on the Sorption of Cs and Sr to Montmorillonite and Bentonite in the Presence of Anthropogenic Organic Ligands

The sorption of picolinic acid to iron oxides has been studied and shows that adsorption is highly pH dependent, displaying ligand-like behaviour. The sorption of picolinic acid is highest at a low pH range of 4 to 5, decreasing in the pH range of 5 to 7, and is negligible at pH values higher than 8[131]. Nicholls and Evans found that the sorption of picolinic acid to soils decreased rapidly at pH values less than 5, possibly because of the dissociation of metal oxide coatings at these lower pH values[132,133].

Evidence for possible ternary complexes was found in the sorption studies of Ni onto kaolinite. At pH values lower than 5, the sorption of Ni was greater in the system with picolinic acid present than in the experiments without picolinic acid[134]. In general, it was found that the sorption of metal ions in the presence of picolinic acid is related only to the formation of aqueous species, and the formation of any adsorbed metal-picolinate complexes appears to be a minor effect, if it occurs at all[126].

3.5.1 Experimental Method

The same buffering solutions used in Chapter 2 for investigations into the effect of pH on Cs and Sr sorption to bentonite and montmorillonite, were used in the following experimental. Solutions of 1 mol dm^{-3} of picolinic acid, NTA and EDTA were prepared. Picolinic acid and NTA are readily soluble at this concentration however, the maximum solubility of disodium EDTA is 2.6 x 10^{-1} mol dm^{-3} at room temperature. A 1 mol dm^{-3} solution of EDTA was achieved by gradual addition of concentrated sodium hydroxide solution until complete solubility was achieved.

20 cm^3 of required buffer solution was added to 0.1 g of bentonite or montmorillonite in 50 cm^3 centrifuge vials. To this 200 µl of ligand (EDTA, NTA or picolinic acid), 200 µl of 1 x 10^{-2} mol dm^{-3} $CsNO_3$ or $Sr(NO_3)_2$ and 100 µl of ^{137}Cs or ^{85}Sr were added establishing a final ligand concentration of 1 x 10^{-2} mol dm^{-3} and a final metal ion concentration of 1 x 10^{-4} mol dm^{-3}. Each sample was prepared in triplicate with a final activity of 3 kBq per vial.

The samples were thoroughly mixed with a whirlimixer and then placed on an orbital shaker for 1 week at 100 rpm. After a week, the samples were centrifuged at 6000 rpm for 20 minutes and the supernatant then decanted. 2 cm^3 of supernatant was filtered through a 0.45 µm syringe filter and the gamma radiation counted with a Packard Cobra II Auto Gamma counter. The pH of the remaining supernatant was recorded.

3.5.2 Results

pH Effect on the Sorption of Cs to Montmorillonite in the Presence of Anthropogenic Organic Ligands

The sorption of Cs on montmorillonite in the presence of anthropogenic ligands as a function of pH is shown in Figure 93. Between pH range 6 to 8 the sorption profile is unaffected by the presence of organic ligands except for NTA, where at pH 7 there appears to be less Cs sorption occurring. Above pH 9, it appears that the presence of picolinic acid, EDTA and NTA inhibits sorption compared to the ligand free system. Above pH 10, there appears to be a slight decrease in sorption in the presence of EDTA and NTA suggesting that the anionic complex species with Cs is favoured over the sorption of Cs to bentonite. This decrease is however very small, 1.3 x 10^{-6} and 2.7 x 10^{-6} mol g^{-1} for EDTA and NTA respectively.

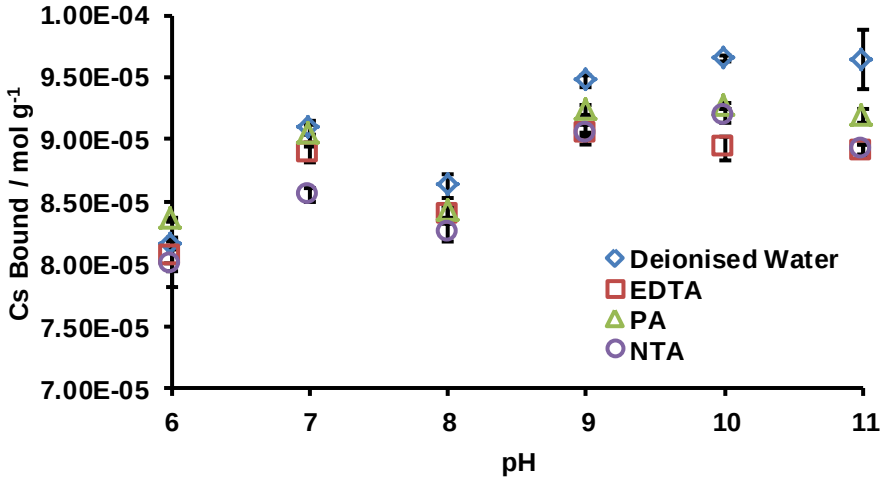

Figure 93. Effect of pH on the sorption of Cs (concentration: 1 x 10^{-4} mol dm^{-3}) to montmorillonite in the presence of anthropogenic organic ligands (concentrations: 1 x 10^{-2} mol dm^{-3}). Experiments carried out with a solid:liquid ratio of 1:200, equilibrating *ca.* 7 days at room temperature. Three replicates per sample

Figure 94 illustrates the change in R_d for Cs sorption to montmorillonite as the pH of the solution increases in the presence and absence of anthropogenic ligands. It is evident that there is no real change in R_d as pH increases when in the presence of anthropogenic ligands, unlike the increase in R_d observed in the presence of deionised water.

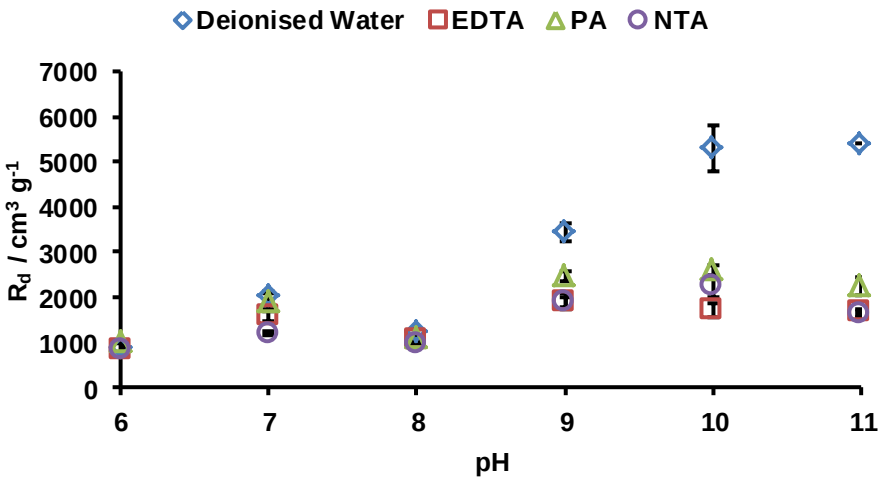

Figure 94. Plot of R_d versus pH for the sorption of Cs (concentration: 1 x 10^{-4} mol dm^{-3}) to montmorillonite in the presence of anthropogenic organic ligands (concentrations: 1 x 10^{-2} mol dm^{-3}). Experiments carried out with a solid:liquid ratio of 1:200, equilibrating *ca.* 7 days at room temperature. Three replicates per sample

pH Effect on the Sorption of Sr to Montmorillonite in the Presence of Anthropogenic Organic Ligands

Figure 95 shows the effect that pH has on the sorption of Sr to montmorillonite in the presence of anthropogenic organic ligands compared to the results obtained in the absence of these ligands. The effect of pH on the sorption of Sr to montmorillonite in the absence of anthropogenic organic ligands has been discussed previously in Chapter 2.15. The graph illustrates that the presence of picolinic acid does not have an effect on sorption across the pH range studied and the results appear to match those determined without organic ligands present.

As pH increases, the sorption of Sr decreases in the presence of both EDTA and NTA. When EDTA is present in the system, sorption decreases rapidly in the range pH 6 to 8, sorption becomes independent of pH in the range 8 to 11, although it is significantly reduced when compared to the ligand free results. Studies have shown that as pH increases the sorption of metal-EDTA species to the solid phase decreases[135,136]. The sorption of Sr-EDTA to montmorillonite exhibits typical anionic adsorption behaviour; the adsorption is strongest at low pH and decreases with increasing pH[136]. Similar sorption behaviour occurs for Sr in the presence of NTA with sorption decreasing above pH 7 suggesting anionic sorption behaviour.

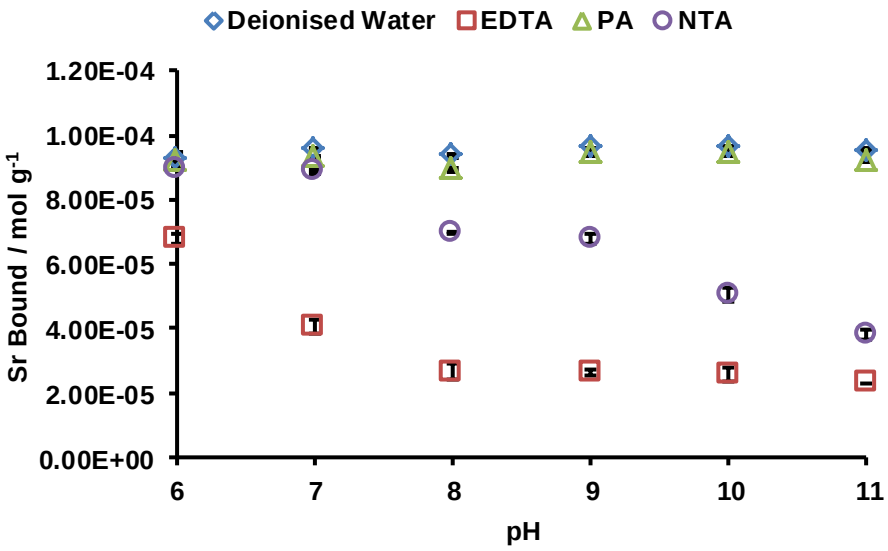

Figure 95. Effect of pH on the sorption of Sr (1 x 10^{-4} mol dm^{-3}) to montmorillonite in the presence of anthropogenic organic ligands (1 x 10^{-2} mol dm^{-3}). Experiments carried out with a solid:liquid ratio of 1:200, equilibrating *ca.* 7 days at room temperature. Three replicates per sample

Figure 96 illustrates the change in R_d for Sr sorption to montmorillonite as pH of the solution increases in the presence of anthropogenic ligands or deionised water. It is evident that R_d increases as pH increases when in the presence of deionised water and picolinic acid, but a decrease in R_d is observed in the presence of both EDTA and NTA.

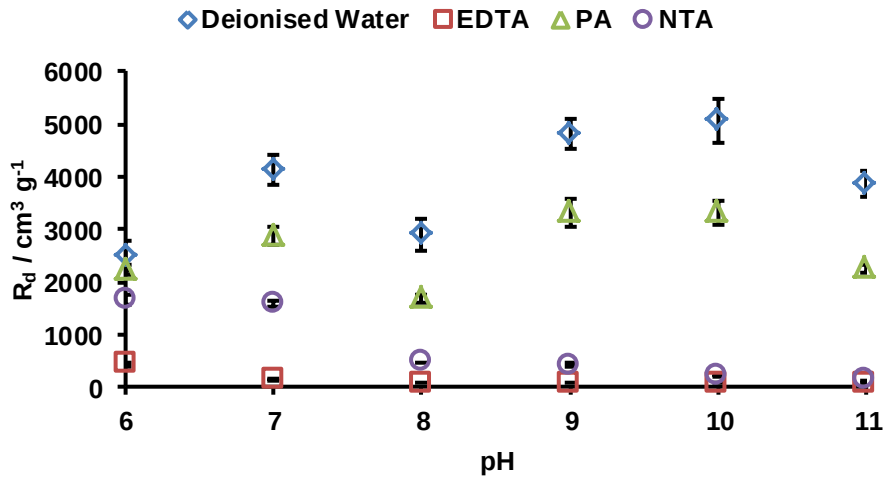

Figure 96. Plot of Rd versus pH for the sorption of Sr (1 x 10^{-4} mol dm^{-3}) to montmorillonite in the presence of anthropogenic organic ligands (1 x 10^{-2} mol dm^{-3}). Experiments carried out with a solid:liquid ratio of 1:200, equilibrating *ca.* 7 days at room temperature. Three replicates per sample

pH Effect on the Sorption of Cs to Bentonite in the Presence of Anthropogenic Organic Ligands

The effect of pH on the sorption of Cs to bentonite in the presence of anthropogenic organic ligands can be seen in Figure 97. The presence of EDTA and NTA appears to slightly increase the amount of Cs sorption to bentonite when compared to results obtained for a ligand free system, a trend which is seen across the entire pH range studied. Picolinic acid does not appear to affect the sorption of Cs across the entire studied pH range, producing results similar to those observed for a ligand free system. For all systems investigated, the amount of sorption occurring continues to increase as the pH increases from pH 6 to 11.

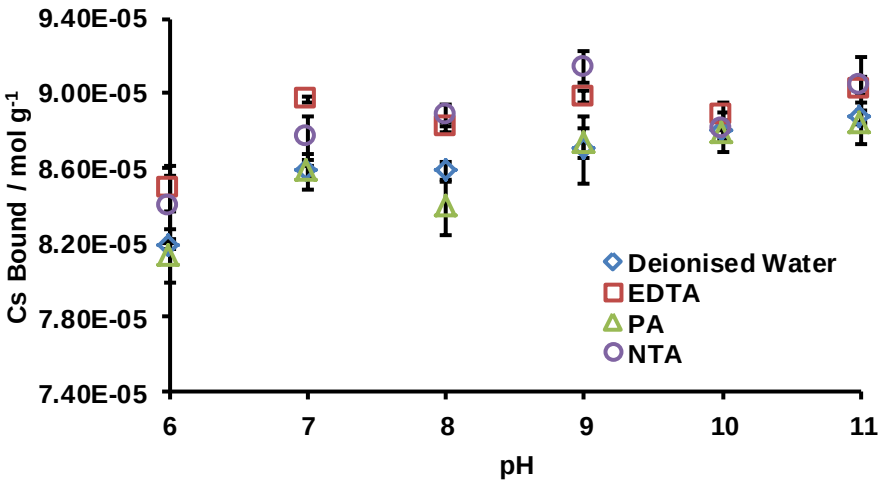

Figure 97. Effect of pH on the sorption of Cs (1×10^{-4} mol dm^{-3}) to bentonite in the presence of anthropogenic organic ligands (1×10^{-2} mol dm^{-3}). Experiments carried out with a solid:liquid ratio of 1:200, equilibrating *ca.* 7 days at room temperature. Three replicates per sample

Figure 98 illustrates the change in R_d for Cs sorption to bentonite as pH of the solution increases in the presence of anthropogenic ligands or deionised water. It is evident that there is no real change in R_d between pH 7 - 11 with a slight decrease in R_d at pH 6 for all solutions investigated.

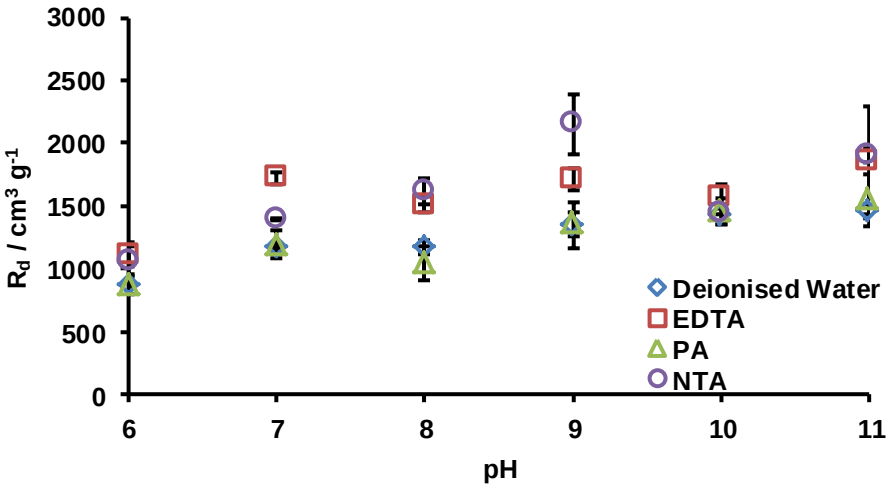

Figure 98. Plot of Rd versus pH for the sorption of Cs (1 x 10^{-4} mol dm^{-3}) to bentonite in the presence of anthropogenic organic ligands (1 x 10^{-2} mol dm^{-3}). Experiments carried out with a solid:liquid ratio of 1:200, equilibrating *ca.* 7 days at room temperature. Three replicates per sample

pH Effect on the Sorption of Sr to Bentonite in the Presence of Anthropogenic Organic Ligands

Results from investigations into the effect of Sr sorption to bentonite in the presence of anthropogenic organic ligands are shown in Figure 99. The presence of picolinic acid appears to only slightly affect Sr sorption across the pH range studied although the trend follows that determined for the absence of organic ligands. The presence of EDTA appears to enhance sorption at low pH, with a slight increase in sorption occurring from pH 6 to 7. There is no further increase, and no decrease, in sorption at pH > 7 however, above pH 10 the amount of sorption occurring is less than that occurring for a ligand free system. NTA follows a similar pattern to that found for EDTA however the degree of sorption occurring at pH 6 is 5 x 10^{-6} mol g^{-1} lower than that for EDTA. There is no real difference between NTA and EDTA values when pH > 7. The sorption behaviour displayed with picolinic acid and deionised water is cationic, lower sorption at low pH with increasing sorption as pH increases, whereas Sr sorption appears to be unaffected as pH increases above 7 for EDTA and NTA.

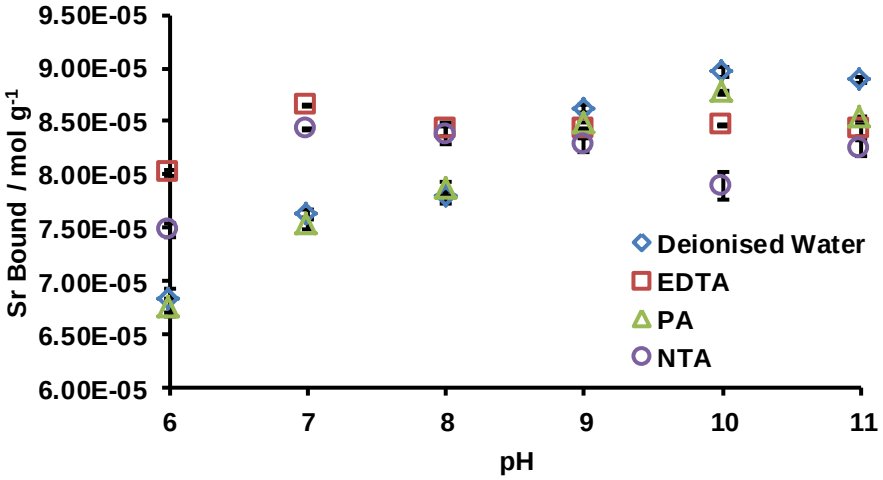

Figure 99. Effect of pH on the sorption of Sr (1×10^{-4} mol dm^{-3}) to bentonite in the presence of anthropogenic organic ligands (1×10^{-2} mol dm^{-3}). Experiments carried out with a solid:liquid ratio of 1:200, equilibrating *ca.* 7 days at room temperature. Three replicates per sample

Figure 100 illustrates the change in R_d for Sr sorption to bentonite as pH of the solution increases in the presence of anthropogenic ligands or deionised water. It can be seen that that there is no real change in R_d between pH 7 - 11 with a slight decrease in R_d at pH 6 for EDTA and NTA whereas, R_d increases between pH 6-10 for deionised water and picolinic acid with a slight decrease at pH 11 observed.

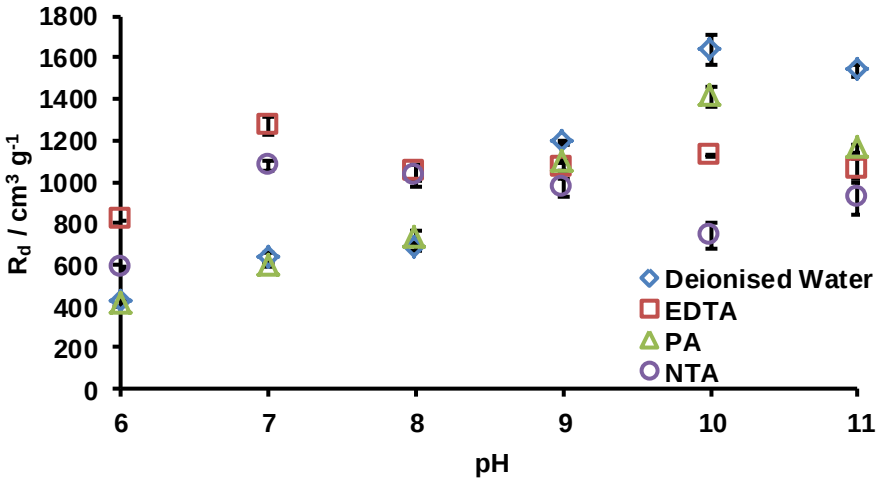

Figure 100. Plot of Rd versus pH for the sorption of Sr (1×10^{-4} mol dm^{-3}) to bentonite in the presence of anthropogenic organic ligands (1×10^{-2} mol dm^{-3}). Experiments carried out with a solid:liquid ratio of 1:200, equilibrating *ca.* 7 days at room temperature. Three replicates per sample

3.6 Kinetic Studies

Some studies have shown that the presence of anthropogenic organic ligands can increase the rate of sorption of metal cations to solid surfaces[137]. The following experiments are designed to investigate whether the presence of these anthropogenic organic ligands affect the sorption of Cs and Sr to montmorillonite and bentonite.

3.6.1 Experimental Method

Solutions of $CsNO_3$ or $Sr(NO_3)_2$ with a concentration of 1×10^{-4} mol dm^{-3} and 1 mol dm^{-2} of EDTA, NTA and picolinic acid were prepared. 20 cm^3 of the nitrate solutions were added to 0.1 g of montmorillonite or bentonite clay in a 50 cm^3 centrifuge vial. Each vial was then spiked with 200 µl of organic ligand and 100 µl of ^{137}Cs or ^{85}Sr establishing a final total activity of ~3 kBq per vial. Samples were carried out in triplicate. The samples were thoroughly mixed with a whirlimixer and then placed on an orbital shaker for 1 week at 100 rpm. The samples were left on the orbital shaker for the required length of time which ranged from one hour to 14 days. The samples were then centrifuged at 6000 rpm for 20 minutes and the supernatant decanted. 2 cm^3 of supernatant was filtered through a 0.45 µm syringe filter and the gamma radiation counted with a Packard Cobra II Auto Gamma counter. The pH of the remaining supernatant was recorded.

3.6.2 Results

Kinetic Investigations into the Sorption of Cs to Montmorillonite in the Presence of Anthropogenic Organic Ligands

The effect of anthropogenic organic ligands on kinetics of Cs sorption to montmorillonite can be seen in Figure 101. Although there is a difference in the amount of Cs remaining in solution, equilibrium still occurs before 96 hours contact time for all systems investigated, and there is no significant change in the degree of sorption after 96 hours.

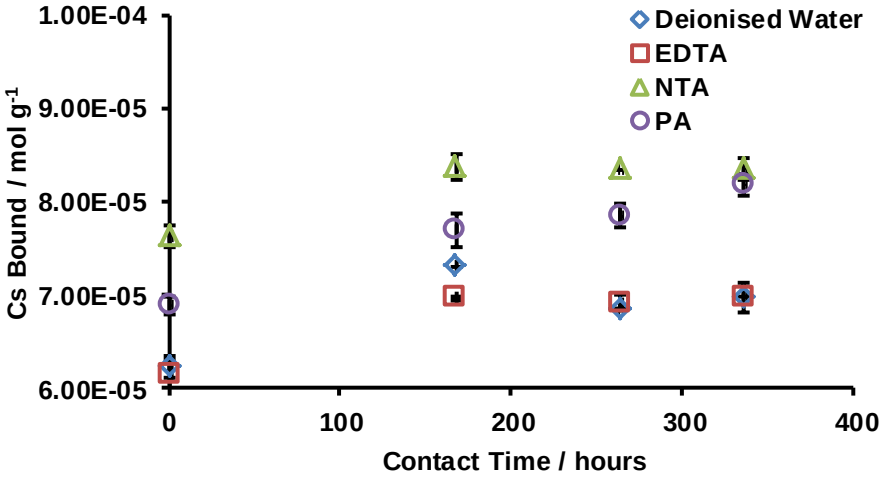

Figure 101. Kinetic studies into Cs (1×10^{-4} mol dm^{-3}) sorption to montmorillonite in the presence of anthropogenic organic ligands (1×10^{-2} mol dm^{-3}). Experiments carried out with a solid:liquid ratio of 1:200, equilibrating *ca.* 7 days at room temperature. Three replicates per sample

Kinetic Investigations into the Sorption of Sr to Montmorillonite in the Presence of Anthropogenic Organic Ligands

The effect of anthropogenic organic ligands on the kinetics of Sr sorption to montmorillonite is shown in Figure 102. Equilibrium appears to be instantaneous for all systems investigated and there is no significant change in sorption as the contact time increases.

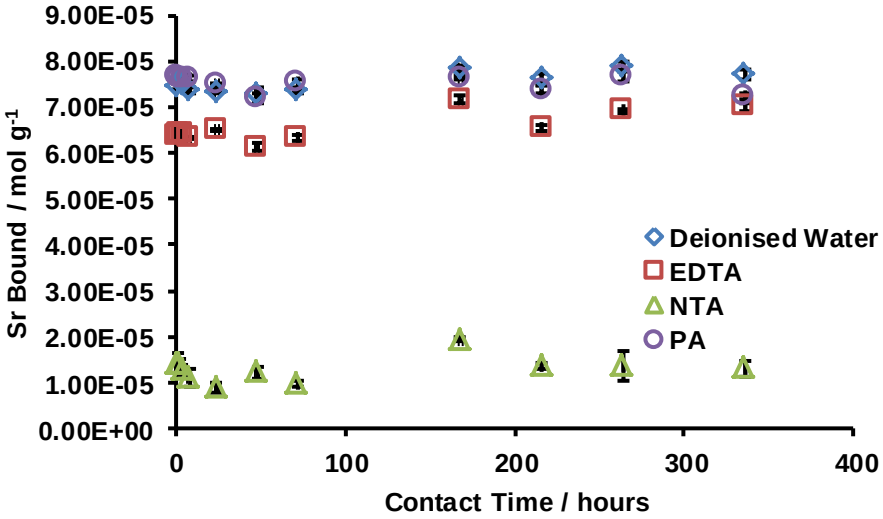

Figure 102. Kinetic studies into Sr (1×10^{-4} mol dm^{-3}) sorption to montmorillonite in the presence of anthropogenic organic ligands (1×10^{-2} mol dm^{-3}). Experiments carried out with a solid:liquid ratio of 1:200, equilibrating *ca.* 7 days at room temperature. Three replicates per sample

Kinetic Investigations into the Sorption of Cs to Bentonite in the Presence of Anthropogenic Organic Ligands

From Figure 103 it can be seen that the presence of anthropogenic organic ligands has no effect on the Cs sorption kinetics to bentonite. Sorption is instantaneous and there is no apparent change in the amount of Cs sorption occurring as the contact time increases.

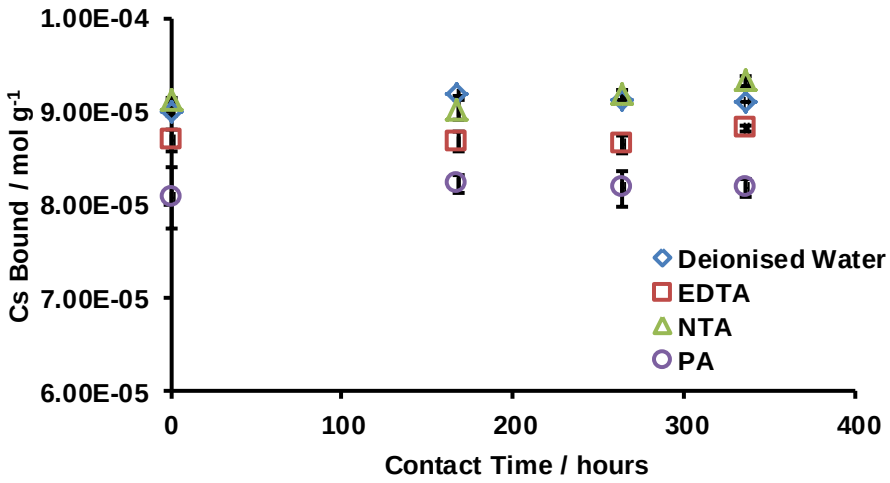

Figure 103. Kinetic studies into Cs (1×10^{-4} mol dm^{-3}) sorption to bentonite in the presence of anthropogenic organic ligands (1×10^{-2} mol dm^{-3}). Experiments carried out with a solid:liquid ratio of 1:200, equilibrating *ca.* 7 days at room temperature. Three replicates per sample

Kinetic Investigations into the Sorption of Sr to Bentonite in the Presence of Anthropogenic Organic Ligands

Investigations into Sr sorption kinetics to bentonite in the presence of anthropogenic organic ligands, shows that there is no effect on equilibrium time and equilibrium is instantaneous for all systems investigated.

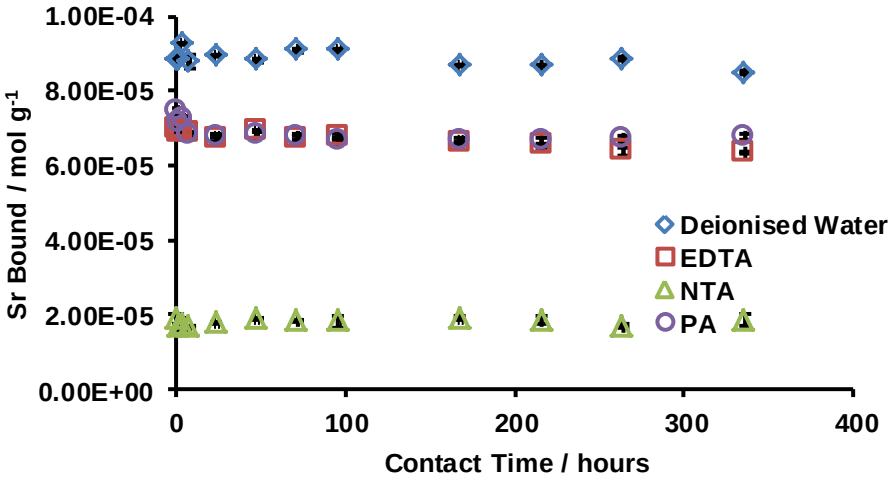

Figure 104. Kinetic studies into Sr (1×10^{-4} mol dm^{-3}) sorption to bentonite in the presence of anthropogenic organic ligands (1×10^{-2} mol dm^{-3}). Experiments carried out with a solid:liquid ratio of 1:200, equilibrating *ca.* 7 days at room temperature. Three replicates per sample

3.7 Effect of Anthropogenic Organic Ligand Residence Time on the Sorption of Cs and Sr to Bentonite and Montmorillonite

Recent studies have suggested that increasing residence time reduced desorption of metals from soils and their potential bioavailability[138]. It has been shown that sorption surfaces dynamically alter in response to chemical perturbations at the mineral-water interface with Al-bearing oxide minerals. This results in a release of Al lattice ions that co-precipitate with the sorbate, effectively directly competing with sorption reactions[138]. Structural changes over time could lead to a significant change over time with the sorption properties of the mineral.

It has been suggested recently that continuous decrease in dissolution rates of smectite minerals occurs over a long period of time during laboratory experiments. The reason for this decrease is that the edges of clay minerals dissolve faster than the basal planes[139]. Bickmore et al. discovered that nontronite, a 2:1 phyllosilicate smectite clay similar to montmorillonite, appeared to dissolve exclusively from the edges whilst the basal surfaces did not appear to significantly participate in the dissolution reactions[139]. Basal surfaces are characterised exclusively by charge-satisfied and extremely stable siloxane bonds, whereas the edge surfaces are characterised by broken bonds and a tendency to form inner-sphere complexes with cations[139]. As a result, the dissolution tends to change the clay morphology, decreasing the percentage of reactive edge sites[140].

The following experiments expose the montmorillonite and bentonite clays to anthropogenic organic ligands over a range of residence times with the aim to see if increased exposure time causes a change in the sorptive behaviour of the clay. The experimental residence times were 1 week, 1 month and 3 month contact time with anthropogenic organic ligands before Cs or Sr was added to the system.

3.7.1 Experimental Method

Solutions of 1 x 10^{-2} mol dm^{-3} of EDTA, NTA and picolinic acid were prepared and 20 cm^3 of these solutions was added to 0.1 g of montmorillonite or bentonite in 50 cm^3 centrifuge vials. The samples were thoroughly mixed with a whirlimixer and then placed on an orbital shaker at 100 rpm for 1 week, 1 month or 3 months.

After the required amount of time had passed, to each sample, 200 µl of 1 x10^{-2} mol dm^{-3} of either $CsNO_3$ or $Sr(NO_3)_2$ and 100 µl of ^{137}Cs or ^{85}Sr was added to each vial. These vials were thoroughly mixed once more with a whirlimixer, placed on an orbital

shaker and then left for 1 week. Each sample was prepared in triplicate with a final activity of 3 kBq per vial.

After 1 week, the samples were centrifuged at 6000 rpm for 20 minutes and the supernatant then decanted. 2 cm^3 of supernatant was filtered through a 0.45 µm syringe filter and the gamma radiation counted with a Packard Cobra II Auto Gamma counter. pH of the remaining supernatant was recorded.

3.7.2 Results

The Effect of Anthropogenic Organic Ligand Residence Time on Cs Sorption to Montmorillonite

Figure 105 shows how the sorption behaviour of Cs to montmorillonite changes in relation to anthropogenic organic ligand residence time. Sorption to montmorillonite in the presence of EDTA steadily decreases with increasing EDTA residence time. After one week residence time, sorption was found to be 5.91 x 10^{-5} mol g^{-1} which decreased to 5.72 x 10^{-5} mol g^{-1} after one month and to 5.08 x 10^{-5} mol g^{-1} after three months, a decrease of 14%.

The presence of NTA does not appear to change the sorption characteristics between one week and one month residence time with the concentration of bound Cs to montmorillonite calculated to be 7.41 x 10^{-5} and 7.37 x 10^{-5} mol g^{-1} respectively. After three months of NTA in contact with montmorillonite, sorption decreased significantly to 4.83 x 10^{-5} mol g^{-1}, a decrease of 35%.

Picolinic acid appears to follow a similar behaviour as to NTA with there being no apparent difference between one week and one month residence time. Bound Cs ion concentrations were calculated to be 7.16 x 10^{-5} and 7.19 x 10^{-5} mol g^{-1} for these residence times. After three months of picolinic acid being in contact with montmorillonite, the sorption of Cs bound decreases dramatically to 3.01 x 10^{-5} mol g^{-1}, a decreases in sorption of 68%. The pH of the final solution increases from 3.61 after one week to 4.42 after three months, as seen in Table 29.

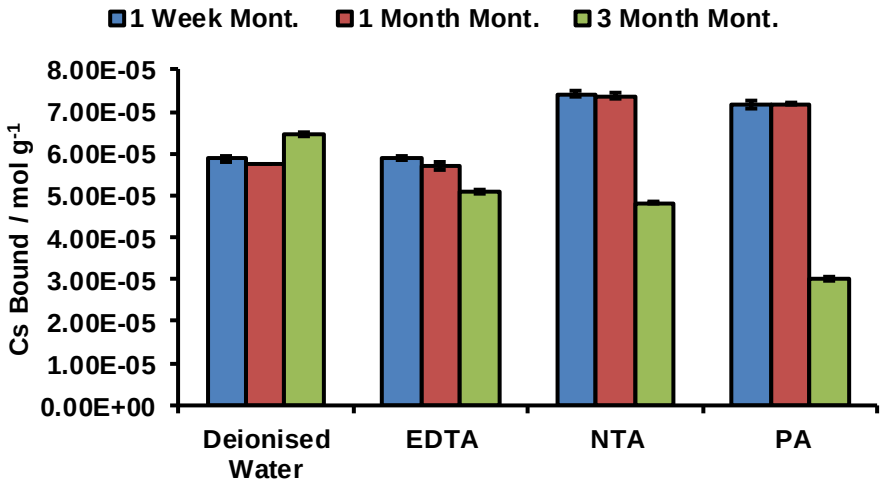

Figure 105. The effect of anthropogenic organic ligand residence time on the sorption of Cs (1 x 10^{-4} mol dm^{-3}) to montmorillonite. Experiments carried out with a solid:liquid ratio of 1:200, equilibrating *ca.* 7 days at room temperature. Three replicates per sample

Figure 106 illustrates the change in R_d for Cs sorption to montmorillonite as residence time of the anthropogenic organic ligand solution increases. It is evident that as residence time increases so does the R_d. This trend is most significant when NTA is present in solution.

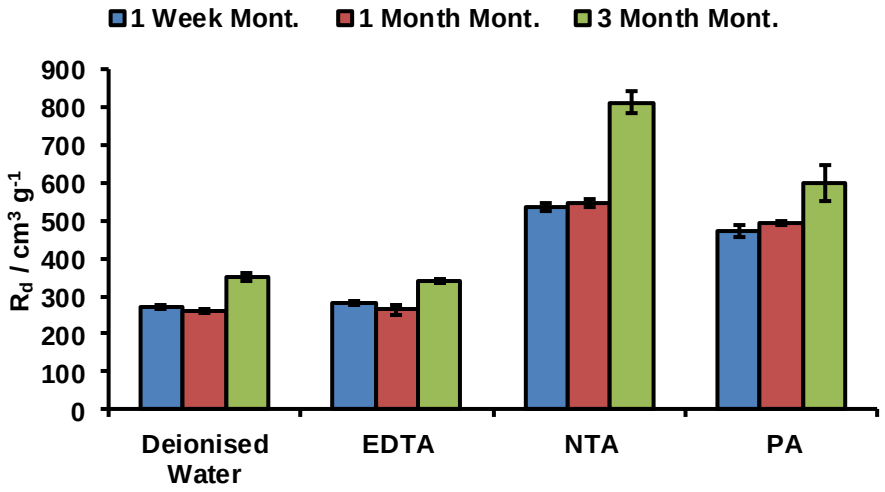

Figure 106. Effect of organic ligand residence time on R_d for Cs (1 x 10^{-4} mol dm^{-3}) sorption to montmorillonite. Experiments carried out with a solid:liquid ratio of 1:200, equilibrating *ca.* 7 days at room temperature. Three replicates per sample

Table 29. pHs of Cs sorption to montmorillonite in the presence of anthropogenic organic ligands at different residence times

Contaminant	Residence Time	pH Range
Deionised Water	1 Week	4.12 – 4.14
	1 Month	4.39 – 4.42
	3 Months	4.22 – 4.28
EDTA	1 Week	4.20 – 4.22
	1 Month	4.22 – 4.23
	3 Months	4.25 – 4.26
NTA	1 Week	10.16 – 10.19
	1 Month	10.06 – 10.13
	3 Months	10.01 – 10.03
Picolinic Acid	1 Week	3.61 – 3.67
	1 Month	3.64 – 3.71
	3 Months	4.42 – 4.47

The Effect of Anthropogenic Organic Ligand Residence Time on Sr Sorption to Montmorillonite

Figure 107 illustrates the effect that anthropogenic organic ligand residence time has on Sr sorption to montmorillonite. It can be seen that after one month of deionised water only, the amount of Sr bound to montmorillonite decreases from 9.58 x 10^{-5} to 6.96 x 10^{-5} mol g^{-1}, a decrease of 37%, with a similar decrease determined after three months residence time. From Table 30, the pH of the deionised water solutions decreases from 5.09 to 4.18 after one month, with a similar pH after three months. This decrease in pH would result in an increase in positively charged surface sites on the surface of the montmorillonite clay thus decreasing the cationic sorption of Sr to montmorillonite.

The effect of EDTA residence time does not appear to alter the sorption of Sr to montmorillonite. There is a minor decrease in sorption observed after one month, down from 6.61 x 10^{-5} mol g^{-1} after one week to 6.09 x 10^{-5} mol g^{-1} after one month, however, the amount of sorption occurring after three months was determined to be 6.54 x 10^{-5} mol g^{-1}, ultimately no real change in sorption occurs after three months.

The greatest effect of residence time on sorption was observed for picolinic acid. After one week contact with montmorillonite, the amount of Sr sorption occurring was calculated to be 8.62 x 10^{-5} mol g^{-1}. This had decreased to 6.46 x 10^{-5} mol g^{-1} after one

month and 6.79 x 10^{-5} mol g^{-1} after three months. pH decreased slightly from 3.81 to 3.62 over this range of time.

NTA produced a similar trend as to EDTA with no real change in sorption capacity after three months.

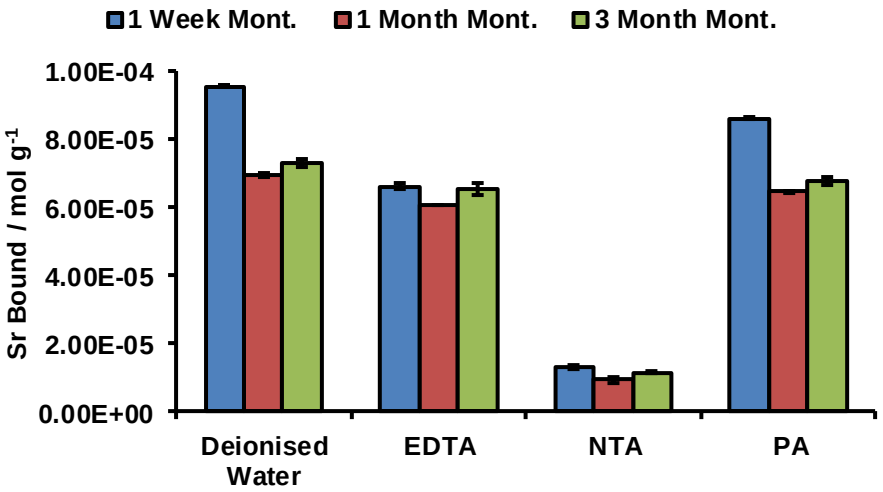

Figure 107. The effect of anthropogenic organic ligand residence time on the sorption of Sr (1 x 10^{-4} mol dm^{-3}) to montmorillonite. Experiments carried out with a solid:liquid ratio of 1:200, equilibrating *ca.* 7 days at room temperature. Three replicates per sample

Figure 108 illustrates the change in R_d for Sr sorption to montmorillonite as residence time of the anthropogenic organic ligand solution increases. It is evident that as residence time increases the R_d decreases. This trend is most significant with deionised water.

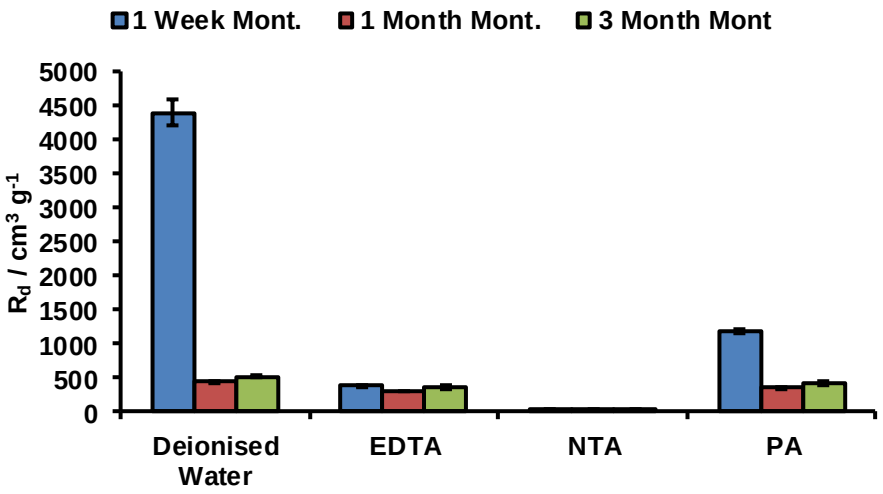

Figure 108. Effect of organic ligand residence time on R_d for Sr (1×10^{-4} mol dm^{-3}) sorption to montmorillonite. Experiments carried out with a solid:liquid ratio of 1:200, equilibrating *ca.* 7 days at room temperature. Three replicates per sample

Table 30. pHs of Sr sorption to montmorillonite in the presence of anthropogenic organic ligands at different residence times

Contaminant	Residence Time	pH Range
Deionised Water	1 Week	5.09 – 5.28
	1 Month	4.18 – 4.22
	3 Months	4.20 – 4.33
EDTA	1 Week	4.28 – 4.29
	1 Month	4.22 – 4.23
	3 Months	4.25 – 4.27
NTA	1 Week	10.17 – 10.19
	1 Month	10.07 – 10.11
	3 Months	9.98 – 10.03
Picolinic Acid	1 Week	3.81 – 3.85
	1 Month	3.63 – 3.68
	3 Months	3.62 – 3.73

The Effect of Anthropogenic Organic Ligand Residence Time on Cs Sorption to Bentonite

The effect of anthropogenic organic ligand residence time on the sorption of Cs to bentonite can be seen in Figure 109. A system with deionised water only does not alter the sorption behaviour of bentonite after three months contact time. For a system with EDTA in contact with bentonite, no change in sorption of Cs to bentonite is seen

after one month residence time, with bound Cs concentrations of 7.15 x 10^{-5} mol g^{-1} after one week and 7.12 x 10^{-5} mol g^{-1} after one month. After three months EDTA residence time, sorption of Cs to bentonite decreases to 6.17 x 10^{-5} mol g^{-1}, a decrease of 14%. This decrease was of the same magnitude as seen for the effect of EDTA residence time on Cs sorption to montmorillonite.

NTA residence time appears to significantly affect Cs sorption to bentonite after three months residence time. After one week, Cs sorption to bentonite was calculated to be 8.33 x 10^{-5} mol g^{-1} which decreases to 5.29 x 10^{-5} mol g^{-1} after three months, a decrease of 37%, compared to 35% observed for Cs sorption to montmorillonite in the presence of NTA after three months. There was no real change in sorption capacity between one week and one month residence time. The pH of the solutions decreased from 10.92 to 10.20 after three months (Table 31).

Picolinic acid also significantly decreased Cs sorption to bentonite after three months. Cs sorption after one week was calculated to be 6.30 x 10^{-5} mol g^{-1} compared to 2.84 x 10^{-5} mol g^{-1} after three months, a decrease in sorption of 55%. pH across this time range increased from 4.72 to 5.01 (Table 31).

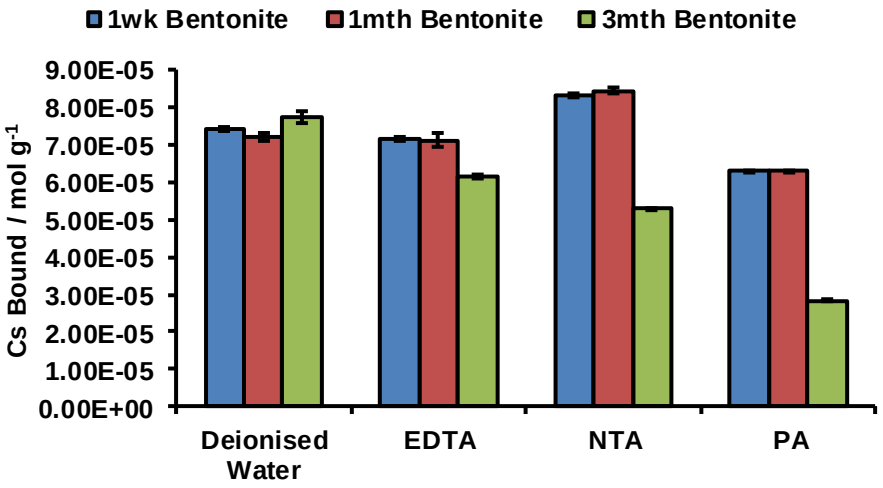

Figure 109. The effect of anthropogenic organic ligand residence time on the sorption of Cs (1 x 10^{-4} mol dm^{-3}) to bentonite. Experiments carried out with a solid:liquid ratio of 1:200, equilibrating *ca.* 7 days at room temperature. Three replicates per sample

Figure 110 illustrates the change in R_d for Cs sorption to bentonite as residence time of the anthropogenic organic ligand solution increases. It is evident that as residence time increases so does the R_d. This trend is observed for all anthropogenic ligands studied and for deionised water.

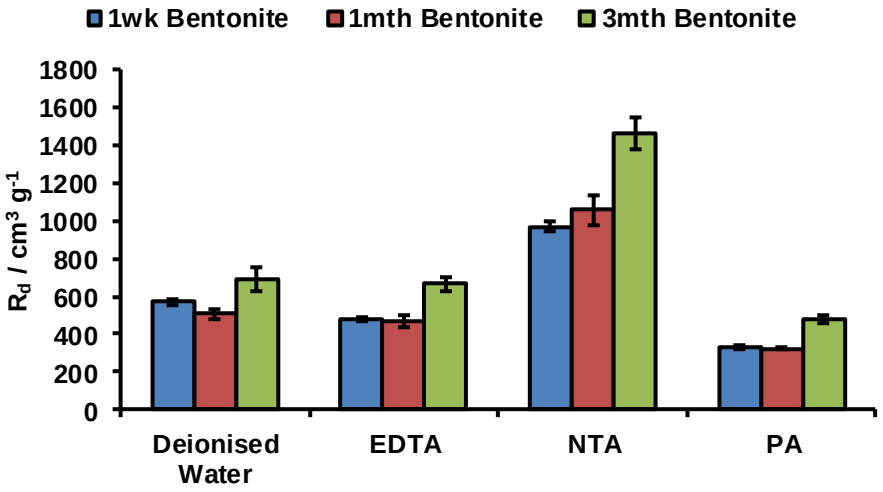

Figure 110. Effect of organic ligand residence time on R_d for Cs (1 x 10^{-4} mol dm^{-3}) sorption to bentonite. Experiments carried out with a solid:liquid ratio of 1:200, equilibrating *ca.* 7 days at room temperature. Three replicates per sample

Table 31. pHs of Cs sorption to bentonite in the presence of anthropogenic organic ligands at different residence times

Contaminant	Residence Time	pH Range
Deionised Water	1 Week	7.66 – 7.74
	1 Month	7.62 – 7.78
	3 Months	7.52 – 7.92
EDTA	1 Week	4.56
	1 Month	4.73 – 4.76
	3 Months	4.80 – 4.90
NTA	1 Week	10.92 – 10.93
	1 Month	10.77 – 10.85
	3 Months	10.20 – 10.35
Picolinic Acid	1 Week	4.72 – 4.75
	1 Month	4.88 – 4.91
	3 Months	5.01 – 5.07

The Effect of Anthropogenic Organic Ligand Residence Time on Sr Sorption to Bentonite

Figure 111 illustrates the effect of anthropogenic organic ligand residence time on the sorption of Sr to bentonite. From the graph, it can be seen that sorption is affected by the presence of all three ligands studied and deionised water over the three month period. Sr sorption decreases across the three month period in a system of deionised

water, decreasing from 8.58 x 10^{-5} to 7.43 x 10^{-5} mol g^{-1} after one month. After three months of deionised water residence, Sr sorption had decreased to 7.06 x 10^{-5} mol g^{-1}.

EDTA appears to affect the Sr sorption to bentonite after a residence time of one month in comparison to a one week residence time, decreasing from 6.03 x 10^{-5} mol g^{-1} to 5.14 x 10^{-5} mol g^{-1}. There does not appear to be any further change in sorption behaviour between one month and three month residence times of EDTA with 5.10 x 10^{-5} mol g^{-1} of Sr bound to bentonite after three months. The pH of the EDTA solutions increased slightly over the three month period from 4.61 to 4.80 as can be seen in Table 32.

NTA follows a similar trend to that of EDTA on Sr sorption to bentonite, with the amount of Sr sorption occurring decreasing after one month with no further decreases after three months. Sr sorption decreases from 1.41 x 10^{-5} mol g^{-1} to 1.14 x 10^{-5} mol g^{-1} after three months. There was a decrease in the pH over the three months from 10.89 to 10.20.

For picolinic acid, sorption of Sr also decreases as residence time increases. After one week, the amount of Sr bound to bentonite was calculated to be 6.14 x 10^{-5} mol g^{-1}, decreasing to 5.80 x 10^{-5} mol g^{-1} after one month and finally to 5.60 x 10^{-5} mol g^{-1} after three months. pH increased from 4.75 to 4.89 after three months.

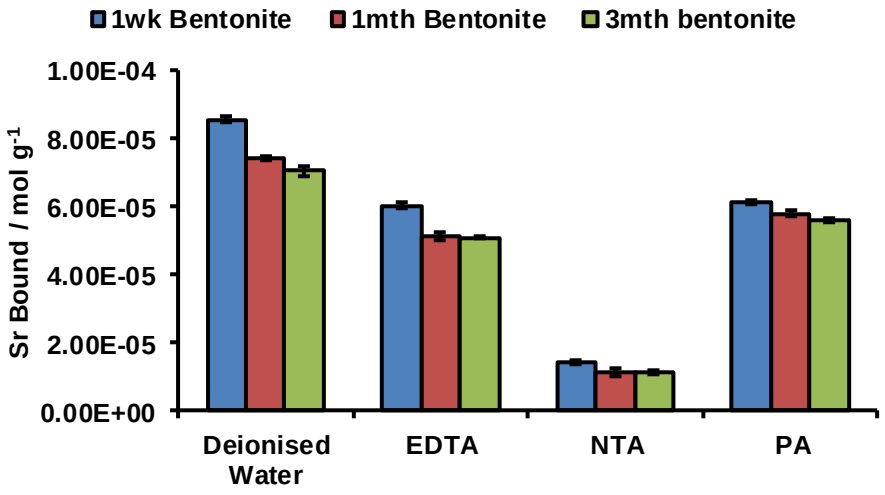

Figure 111. The effect of anthropogenic organic ligand residence time on the sorption of Sr (1 x 10^{-4} mol dm^{-3}) to bentonite. Experiments carried out with a solid:liquid ratio of 1:200, equilibrating *ca.* 7 days at room temperature. Three replicates per sample

Figure 112 illustrates the change in R_d for Sr sorption to bentonite as residence time of the anthropogenic organic ligand solution increases. It is evident that as residence

time increases the R_d decreases for all solutions investigated. This trend is most significant for deionised water.

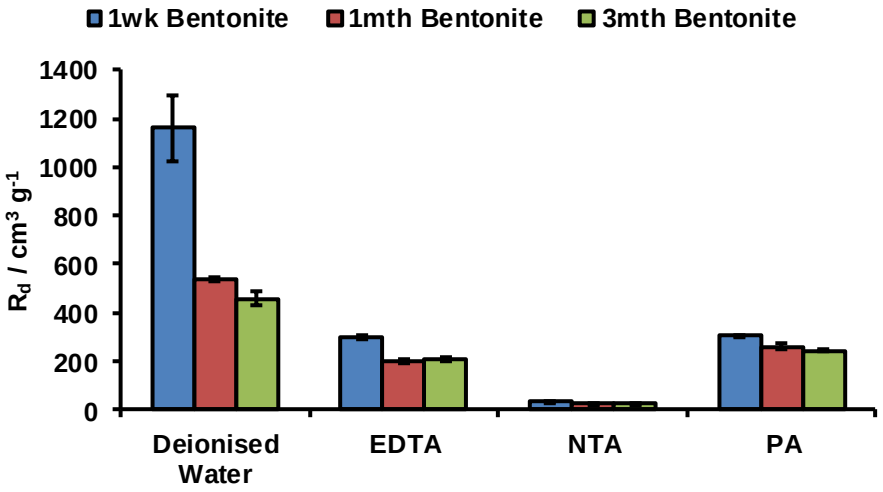

Figure 112. Effect of organic ligand residence time on R_d for Sr (1×10^{-4} mol dm^{-3}) sorption to bentonite. Experiments carried out with a solid:liquid ratio of 1:200, equilibrating *ca.* 7 days at room temperature. Three replicates per sample

Table 32. pHs of Sr sorption to bentonite in the presence of anthropogenic organic ligands at different residence times

Contaminant	Residence Time	pH Range
Deionised Water	1 Week	7.91 – 8.00
	1 Month	7.63 – 7.64
	3 Months	7.78 – 7.90
EDTA	1 Week	4.61
	1 Month	4.72 – 4.73
	3 Months	4.80 – 4.87
NTA	1 Week	10.89 – 10.90
	1 Month	10.66 – 10.78
	3 Months	10.20 – 10.33
Picolinic Acid	1 Week	4.75 – 4.76
	1 Month	4.85 – 4.89
	3 Months	4.89 – 4.95

3.8 PXRD Study of the Effect of Anthropogenic Organic Ligand Contact Time on Montmorillonite and Bentonite

The evolution of the clay mineral structure and the formation of any secondary phases were monitored by Powder XRD.

3.8.1 Experimental Method

20 cm^3 of 1 x 10^{-2} mol dm^{-3} of organic ligand or deionised water was added to 1 g of clay mineral in a 50 cm^3 centrifuge vial. Samples were thoroughly mixed with a whirlimixer and placed on an orbital shaker at 100 rpm for 1 week, 1 month or 3 months. After the required shaking time, samples were then centrifuged at 6000 rpm for 20 minutes and the supernatant decanted and kept for leachate analysis. The solid phases were air dried at room temperature in a fume cupboard ready for PXRD.

Samples were mounted in deep well Perspex holders and phase identification was performed using a continuous scan between the 2θ range of 5-75° with a step size of 0.014° over a period of 2 hours 20 minutes.

3.8.2 Results

PXRD of Deionised Water Residence Time on Montmorillonite Clay

The XRD patterns for deionised water residence time appear to be identical and very close to the initial non-reacted montmorillonite clay even after three months residence time (Figure 113).

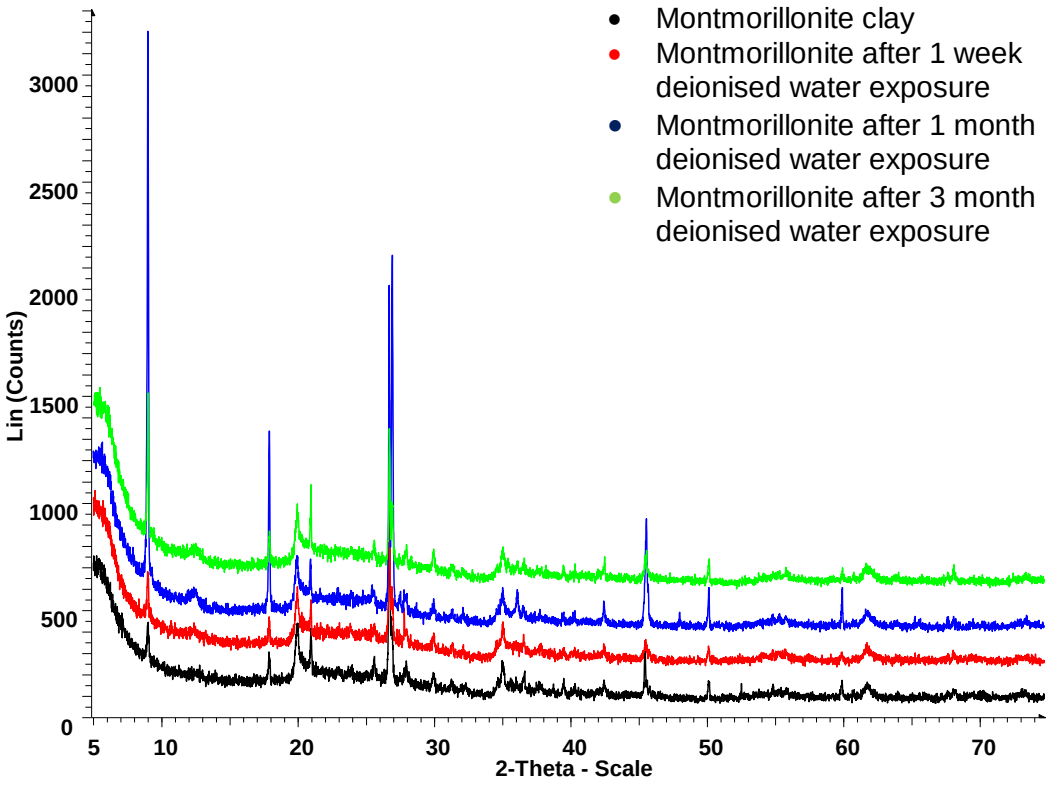

Figure 113. PXRD comparing deionised water residence time and its effect on the structure of montmorillonite clay, using Cu K_{a1} radiation between 5 ° and 75 ° with a step size of 0.014 ° and a step time of 1.6 s

PXRD of Picolinic Acid Residence Time on Montmorillonite Clay

The XRD patterns for picolinic acid residence time appear to be identical and very close to the initial non-reacted montmorillonite clay even after three months residence time (Figure 114). At 2θ 18°, the sharp reflection appears to disappear in the three month sample, although there is a minor 'bump' in the pattern. The change in the reflection could be due to preferred orientation in the crystal lattice as there does still appear to be a response from the sample at this angle.

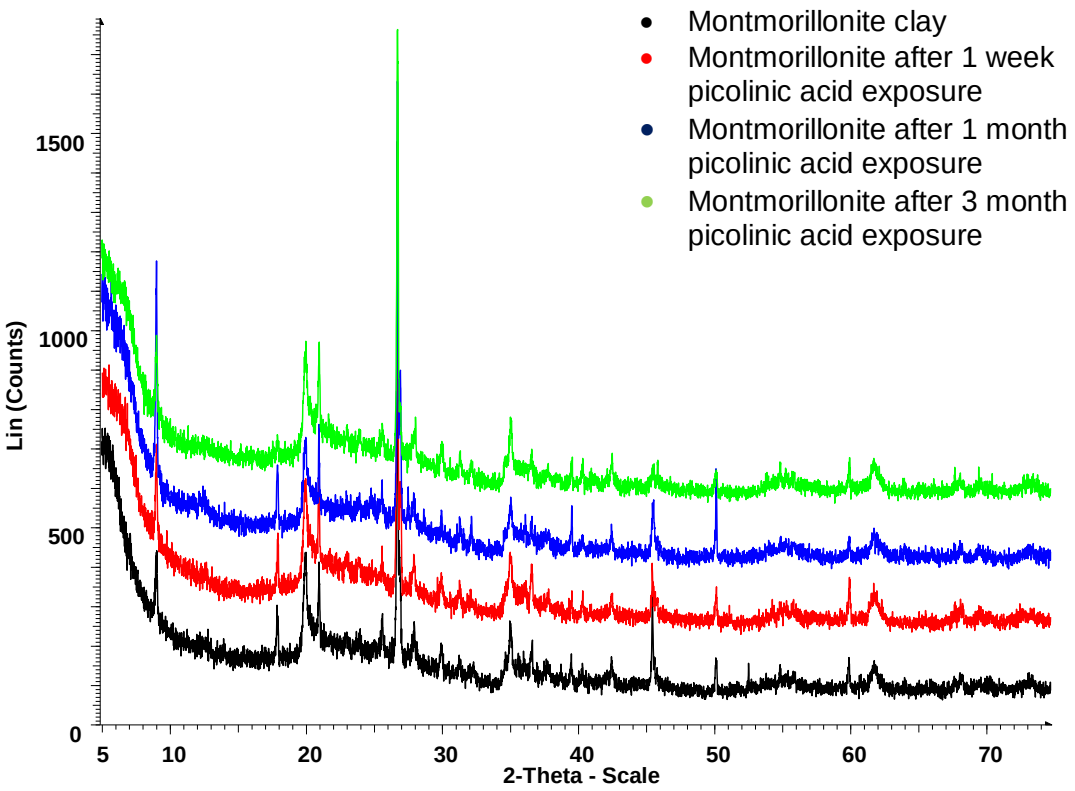

Figure 114. PXRD comparing picolinic acid residence time and its effect on the structure of montmorillonite clay, using Cu K_{a1} radiation between 5 ° and 75 ° with a step size of 0.014 ° and a step time of 1.6 s

PXRD of NTA Residence Time on Montmorillonite Clay

The XRD patterns for NTA residence time appear to be identical and very close to the initial non-reacted montmorillonite clay even after three months residence time (Figure 115).

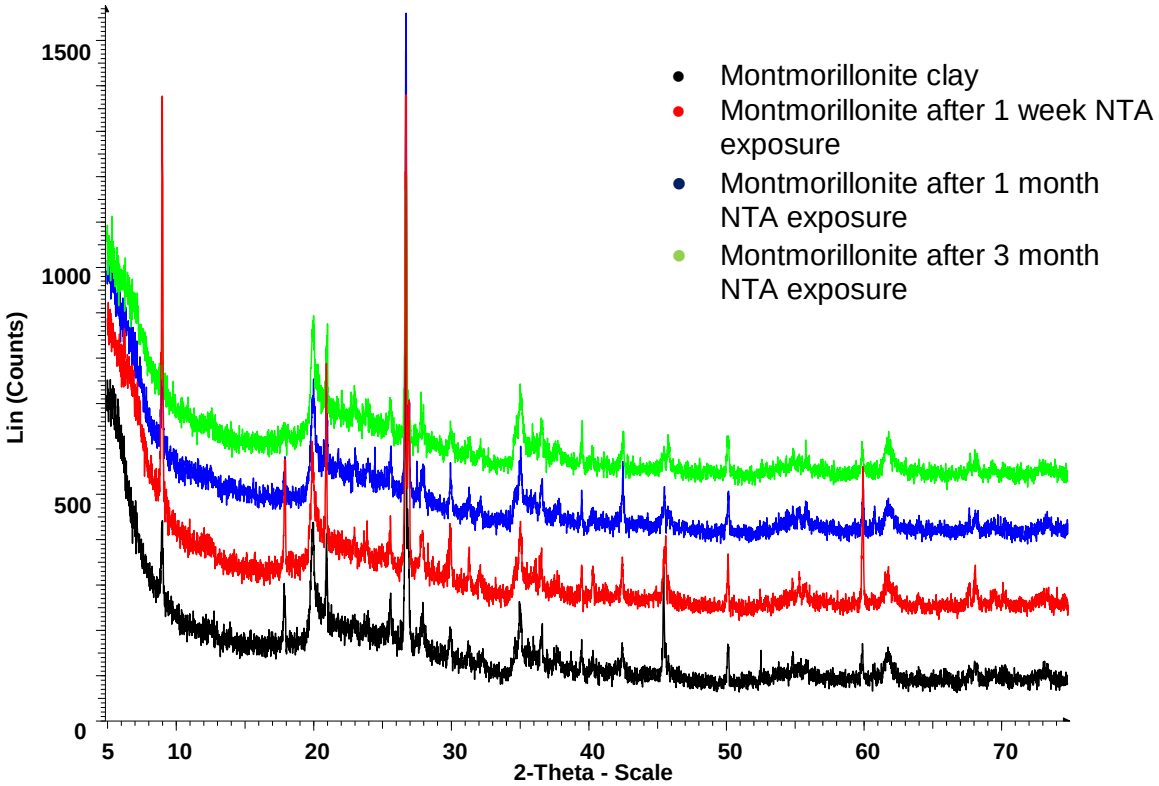

Figure 115. PXRD comparing NTA residence time and its effect on the structure of montmorillonite clay, using Cu K_{a1} radiation between 5 ° and 75 ° with a step size of 0.014 ° and a step time of 1.6 s

PXRD of EDTA Residence Time on Montmorillonite Clay

The XRD patterns for EDTA residence time appear to be identical and very close to the initial non-reacted montmorillonite clay even after three months residence time, although there are a few minor differences in the patterns (Figure 116). There appears to be a large degree of preferred orientation occurring in the three month sample and a secondary phase appears after one week of EDTA exposure at 2θ 51°, but this is not present in the one month and three month samples.

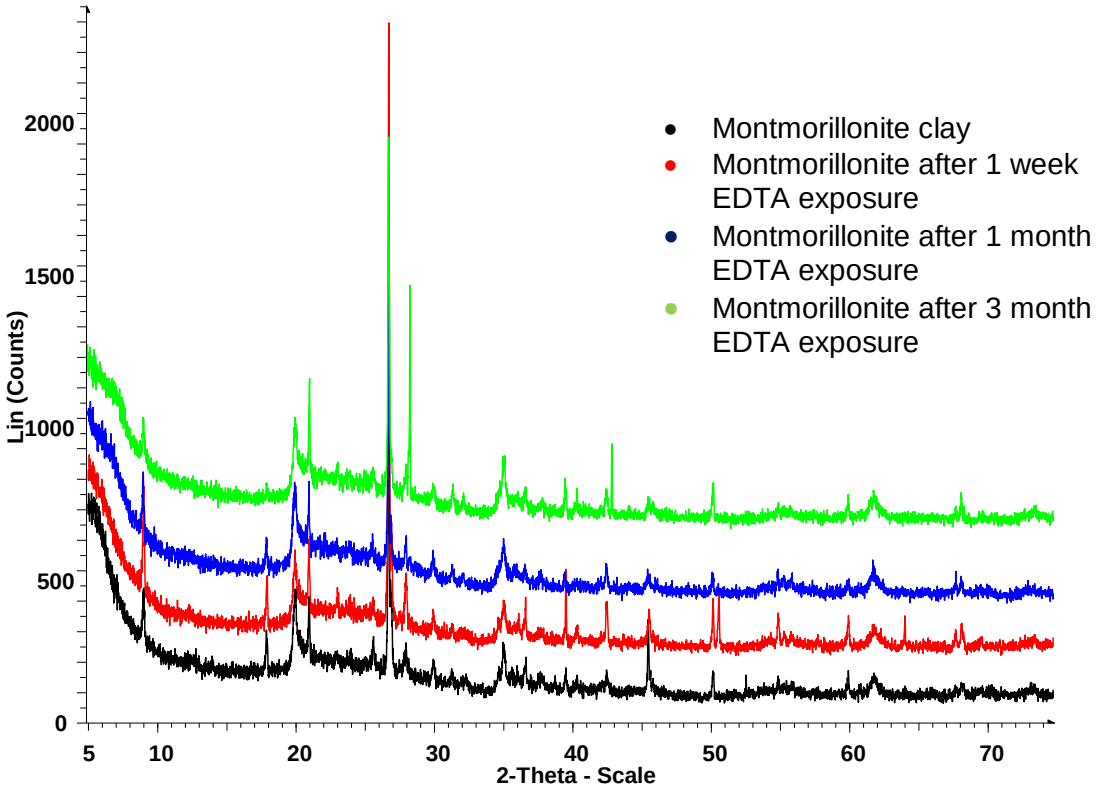

Figure 116. PXRD comparing EDTA residence time and its effect on the structure of montmorillonite clay, using Cu K_{a1} radiation between 5 ° and 75 ° with a step size of 0.014 ° and a step time of 1.6 s

PXRD of Deionised Water Residence Time on Bentonite Clay

The XRD patterns for deionised water residence time appear to be identical and very close to the initial non-reacted bentonite clay even after three months residence time (Figure 117). There appears to be preferred orientation in the three month sample at 2θ 28°, 31° and 46° which are phases associated with muscovite magnesian in the bentonite.

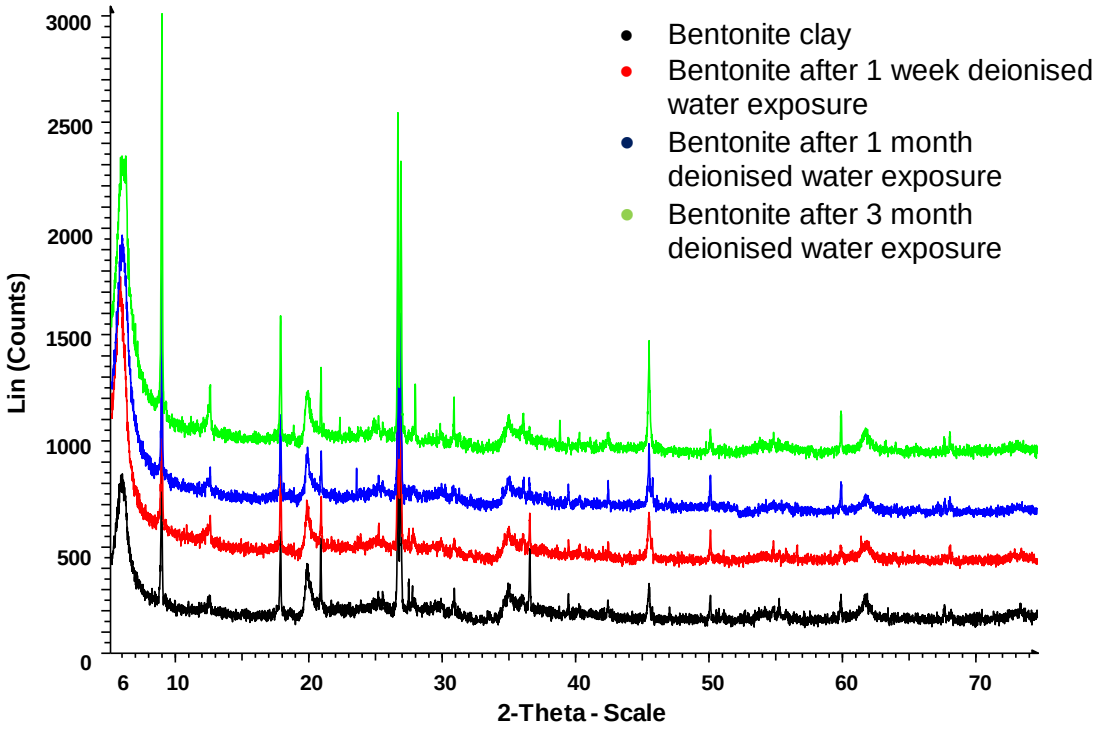

Figure 117. PXRD comparing deionised water residence time and its effect on the structure of bentonite clay, using Cu K_{a1} radiation between 5 ° and 75 ° with a step size of 0.014 ° and a step time of 1.6 s

PXRD of Picolinic Acid Residence Time on Bentonite Clay

The XRD patterns for picolinic acid residence time appear to be identical and very close to the initial non-reacted bentonite clay even after three months residence time (Figure 119). The only noticeable differences are peak intensities in the one week diffraction pattern which is most likely due to preferred orientation in the lattice structure.

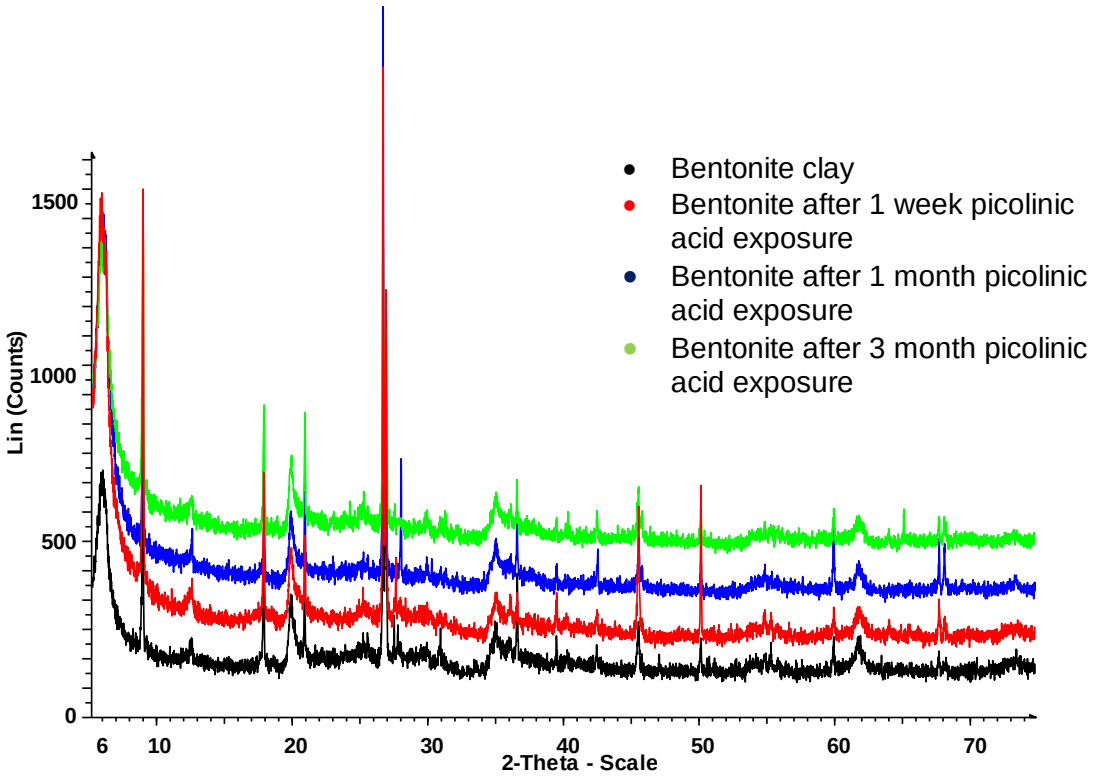

Figure 118. PXRD comparing picolinic acid residence time and its effect on the structure of bentonite clay, using Cu K_{a1} radiation between 5 ° and 75 ° with a step size of 0.014 ° and a step time of 1.6 s

PXRD of NTA Residence Time on Bentonite Clay

The XRD patterns for NTA residence time appear to be identical and very close to the initial non-reacted bentonite clay even after three months residence time (Figure 119). There does appear to be a shift in the montmorillonite peak around 2θ 6° for the one week and one month samples which could be due to substitution of sodium for calcium[141], however, this shift is not visible after three months.

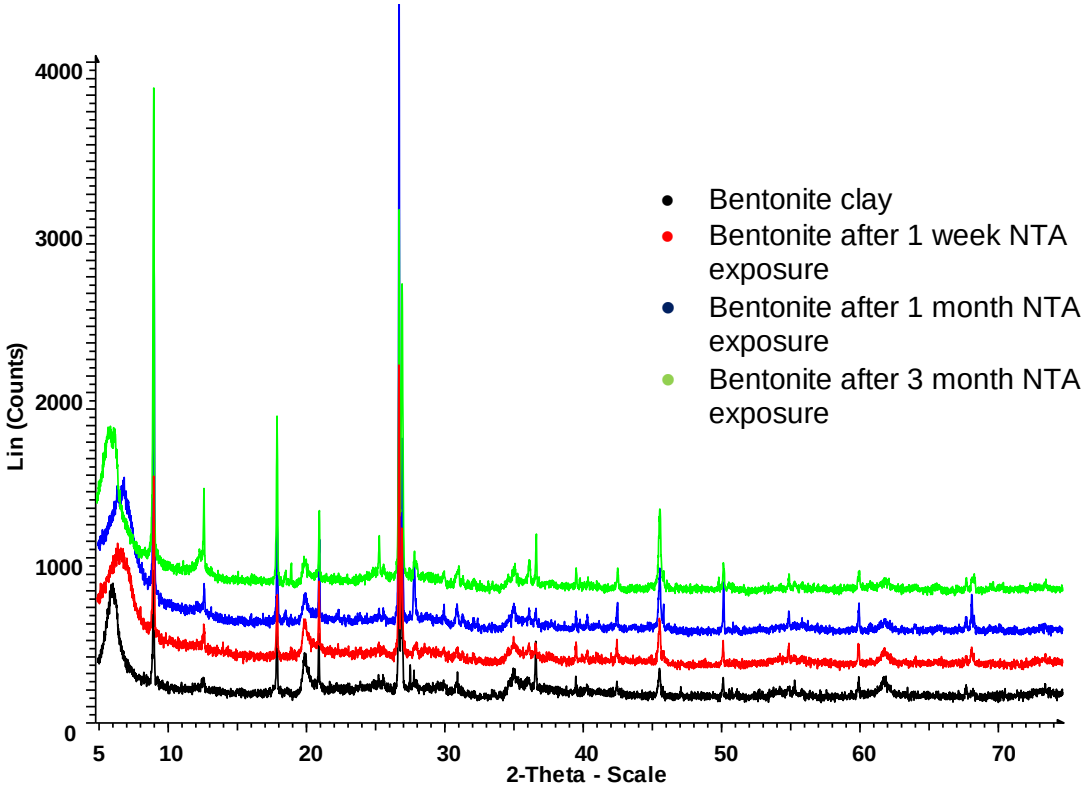

Figure 119. PXRD comparing NTA residence time and its effect on the structure of bentonite clay, using Cu K_{a1} radiation between 5 ° and 75 ° with a step size of 0.014 ° and a step time of 1.6 s

PXRD of EDTA Residence Time on Bentonite Clay

The XRD patterns for EDTA residence time appear to be identical and very close to the initial non-reacted bentonite clay even after three months residence time (Figure 120).

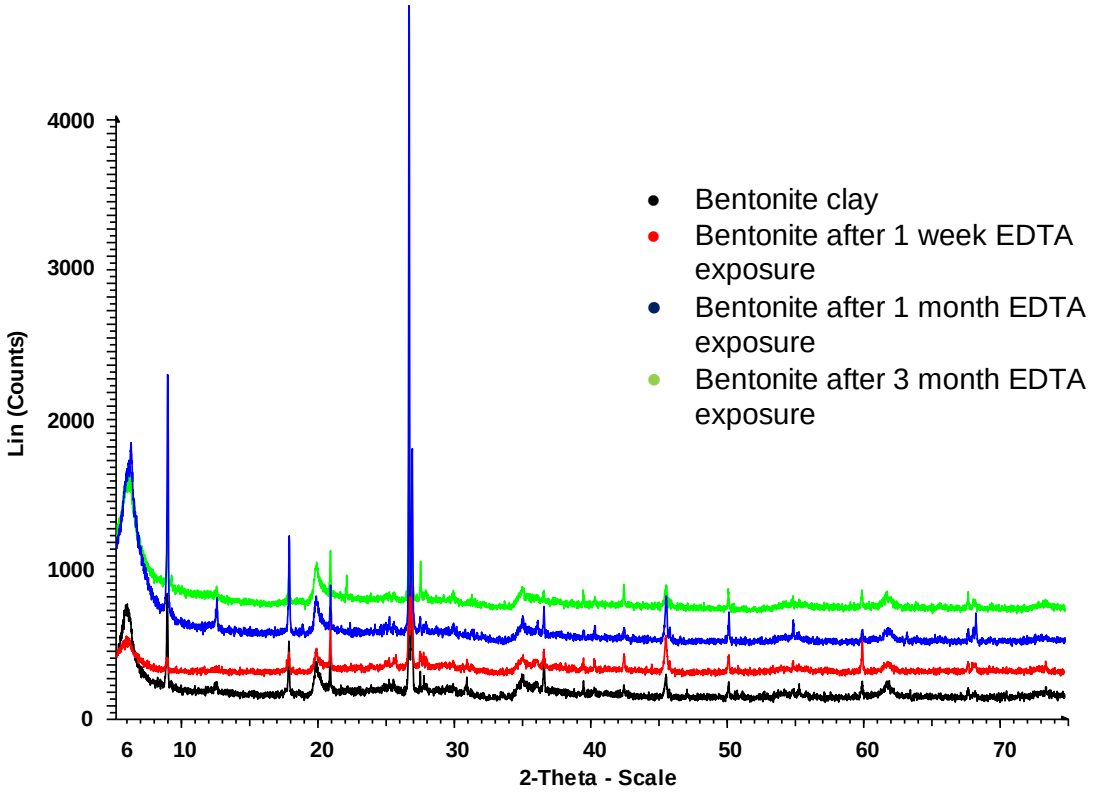

Figure 120. PXRD comparing EDTA residence time and its effect on the structure of bentonite clay, using Cu K_{a1} radiation between 5 ° and 75 ° with a step size of 0.014 ° and a step time of 1.6 s

3.9 Analysis of Leachates

The aqueous phases from the time dependent studies were analysed by ICP-OES to investigate if there were changes in the amount of cations being leached into solution over the three month residence period. Samples were prepared by acidifying with analytical grade HNO_3 before analysis. The results can be found in Table 33.

From these results it can be seen that, for a number of cations, the concentrations in the aqueous phase increases after the being in contact with organic ligands or deionised water for three months. Ca and Mg increased for bentonite in the presence of both picolinic acid and EDTA after three months, whilst an increase in Ca was observed for montmorillonite with NTA and picolinic acid. No significant increase in Mg concentration was observed for montmorillonite samples after three months. The silicon concentration increased after three months for all samples except deionised water and bentonite.

Significant quantities of iron were leached from montmorillonite in the presence of NTA and EDTA which increased after three months. There was no significant leaching of iron from montmorillonite in the presence of picolinic acid or from the bentonite samples.

Some cation concentrations appeared to decrease after three months, most notably the Na concentration with EDTA and bentonite and Ca with EDTA and montmorillonite.

Table 33. Comparison of one week and three month leachates in the presence of anthropogenic organic ligands

Sample	Contact Time	Cation Concentration / mg l^{-1}								
		Al	Ca	Fe	K	Mg	Mn	Na	Si	Zn
Montmorillonite + Deionised Water	1 Week	-	4.3	-	1.7	1.7	-	6.4	48.2	-
	3 Months	-	4.0	-	1.9	1.7	-	6.3	68.4	-
Montmorillonite + NTA	1 Week	27.3	1.8	53.8	1.1	<LOQ*	-		48.8	-
	3 Months	27.0	3.0	79.9	1.7	0.3	-		67.0	-
Montmorillonite + Picolinic Acid	1 Week	0.6	4.2	1.1	0.3	1.7	-	6.5	41.3	-
	3 Months	0.6	5.1	0.8	0.4	2.5	-	6.4	72.5	-
Montmorillonite + EDTA	1 Week	70.7	6.0	91.3	2.7	1.3	0.1		35.8	-
	3 Months	70.7	2.0	91.3	2.0	0.3	0.2		69.4	0.02
Bentonite + Deionised Water	1 Week	-		-	3.7	4.1	-	14.2	12.7	-
	3 Months	-	15.9	-	2.5	4.9	-	14.2	11.4	-
Bentonite + NTA	1 Week	-	439.4	-	3.3	33.5	0.1	325.0	15.3	<LOQ*
	3 Months	No Results Available								
Bentonite + Picolinic Acid	1 Week	-	106.1	0.1	9.6	37.9	0.6	19.1	12.3	-
	3 Months	-	146.4	-	6.3	52.5	2.1	18.2	15.6	0.04
Bentonite + EDTA	1 Week	5.4	373.2	11.5	13.2	28.8	2.8	423.7	14.4	0.1
	3 Months	-	503.3	15.7	7.8	41.0	7.7	383.7	17.0	0.1

*Limit of Quantification (LOQ) = 0.04 mg l^{-1} for Mg and 0.01 mg l^{-1} for Zn

3.10 Conclusions

The presence of anthropogenic organic ligands was found to affect the sorption of Cs and Sr to both montmorillonite and bentonite clays. It was found that EDTA had the greatest effect on Cs sorption to montmorillonite although this was only seen at high ligand concentration, 1 x 10^{-2} mol dm^{-3}. Sr sorption to montmorillonite was most affected by NTA at high ligand concentration, however picolinic acid was found to reduce the amount of sorption at lower ligand concentrations.

Sorption of Cs to bentonite was found not to be affected by the presence of anthropogenic organic ligands however, the sorption of Sr to bentonite was affected by all three organic ligands investigated with NTA having the greatest effect on sorption.

The absence of any real effect on Cs sorption to both clay minerals by the presence of anthropogenic organic ligands can be explained by their corresponding low stability complexes for Cs-Ligand complexes, Table 34. There are no data available for a Cs-Picolinic Acid complex. Sr stability complexes with NTA and EDTA are significantly higher than those for Cs explaining why the presence of these ligands increases the concentration of Sr in solution.

Table 34. Stability constants for picolinic acid, NTA and EDTA complexes with Cs and Sr[142]

Cation	Picolinic Acid		NTA		EDTA	
	Species	Log K	Species	Log K	Species	Log K
Cs^+			CsL^{2-}	0.84	CsL^{3-}	1.05
Sr^{2+}	SrL^+	1.8	SrL^-	6.3	SrL^{2-}	10.5
	SrL_2	3.0			$SrHL^-$	14.9

Compared to Cs, Sr appears to be more readily complexing with picolinic acid and is retained in the aqueous phase. This behaviour, however, is not witnessed with montmorillonite as the solid phase which could be due to the strong affinity that picolinic acid has for forming complexes with montmorillonite, as seen by TOC analysis. Due to the large amounts of picolinic acid sorbing to montmorillonite, there may be far more metal-ligand-surface complexes occurring so the amount of sorption to montmorillonite in the presence of picolinic acid will be higher than that to bentonite.

The effect of ligand residence time appeared to result in a decrease in sorption of Cs and Sr to both bentonite and montmorillonite with increasing residence time. Analysis

of the leachates showed an increase in silicon and iron leaching from montmorillonite, and an increase calcium, magnesium and silicon leaching from bentonite after three months. This aging of the clay minerals could lead to a reduction in available sorption sites for Cs and Sr resulting in the decrease in sorption that is witnessed after three months. Although there was an increase in the concentration of dissolved cations in solution after three months, PXRD of the clay minerals did not show any obvious differences between the aged and fresh clay samples.

Chapter 4: The Effect of Magnox Sludge on Cs and Sr Sorption to Montmorillonite and Bentonite

4.1 Introduction

The UK has a number of legacy fuel storage ponds and wet silos dating back to the earliest days of the nuclear industry. Fuel from reactors was shipped in water-filled transport flasks and stored in ponds at Sellafield. Some of the fuel remained in the ponds for several years and the Magnox cans corroded. Some of these facilities now contain large inventories of intermediate level sludge due to the corrosion of Magnox fuel elements. The main corrosion product of the Magnox fuel in these storage ponds is brucite ($Mg(OH)_2$) however, the long-term ingress of CO_2 into the pond environment may also facilitate the transformation of brucite to various Mg-hydroxycarbonate phases[75]. Brucite has low solubility, 9×10^{-4} g / 100 ml, making it relatively unreactive and it is less soluble than magnesium carbonate[143].

The presence of Magnox sludge in these storage ponds is problematic and there is a requirement to retrieve the wastes and decommission them due to the ponds nearing the end of their service life. The Magnox sludge has caused some unique issues for slurry management in the nuclear industry, such as:

- Magnox continues to corrode producing hydrogen. Some of this hydrogen is released harmlessly through ventilation and some is retained within the sludge.
- Due to the activity, heterogeneity and the restricted access to these wastes, characterisation is limited[144].

The following chapter investigates the effect that the presence of Magnox sludge in the storage ponds may have on sorption behaviour. The presence of competing ions in the storage ponds, in particular Mg^{2+}, as a result of dissolved magnesium from the corrosion of the Magnox fuel rods is a concern.

4.2 Effect of Magnox Simulant Sludge Equilibrated Water on Sorption of Cs and Sr to Montmorillonite and Bentonite

Simple reaction systems investigating the sorption of Cs or Sr to montmorillonite and bentonite have been studied in the previous chapter. However, these sorption results don't take into account the complexity of the storage ponds at Sellafield. The presence of large quantities of Magnox sludge in the ponds will result in a significant amount of magnesium ions being released into the pond liquor. The introduction of other cations can have consequences on the sorption behaviour studied by competing with other cations for the sorption sites.

There have been a number of investigations into the effect of competing ions on sorption to clay minerals. Possible cationic interferences on the sorption of strontium have previously been reported as:

$$K^+ > Na^+ > Ca^{2+} > Mg^{2+}$$ [145]

Liang found that K^+ and Na^+ may critically influence the sorption of Sr whereas Ca^{2+} and Mg^{2+} had less of an effect on the sorption of Sr.

4.2.1 Experimental Method

Solutions of equilibrated simulant Magnox sludge liquor were prepared by weighing out the corresponding amount of simulant Magnox sludge (dry weight equivalent) into two litre glass bottles, establishing final liquid to sludge ratios of 2000:1, 200:1 and 50:1, with two litres of deionised water. These solutions were then placed on an orbital shaker for one week at 100 rpm. After a week, each solution was filtered through a Whatman ashless 42 filter paper into clean two litre glass bottles.

Batch sorption experiments were carried out by placing 20 cm^3 of the required simulant Magnox sludge solution in 50 cm^3 centrifuge vials with 0.1 g of montmorillonite or bentonite. To these centrifuge vials, 200 µl of $CsNO_3$ or $Sr(NO_3)_2$ (concentrations ranging from 1×10^{-2} to 1×10^{-6} mol dm^{-3} establishing final cation concentrations of 1×10^{-4} to 1×10^{-8} mol dm^{-3}) and 100 µl of ^{137}Cs or ^{85}Sr were added. Samples were then thoroughly mixed with a whirlimixer and placed on an orbital shaker for one week at 100 rpm.

After 1 week, the samples were centrifuged at 6000 rpm for 20 minutes and the supernatant then decanted. 2 cm^3 of supernatant was filtered through a 0.45 µm

syringe filter and the gamma radiation counted with a Packard Cobra II Auto Gamma counter. pH of the remaining supernatant was recorded.

4.2.2 Results

Effect of Simulant Magnox Sludge on Cs Sorption to Montmorillonite

The effect of simulant Magnox sludge on Cs sorption to montmorillonite is shown below in Figure 121. At all simulant Magnox sludge concentrations investigated, there appears to be no effect on Cs sorption when compared with a sludge free system.

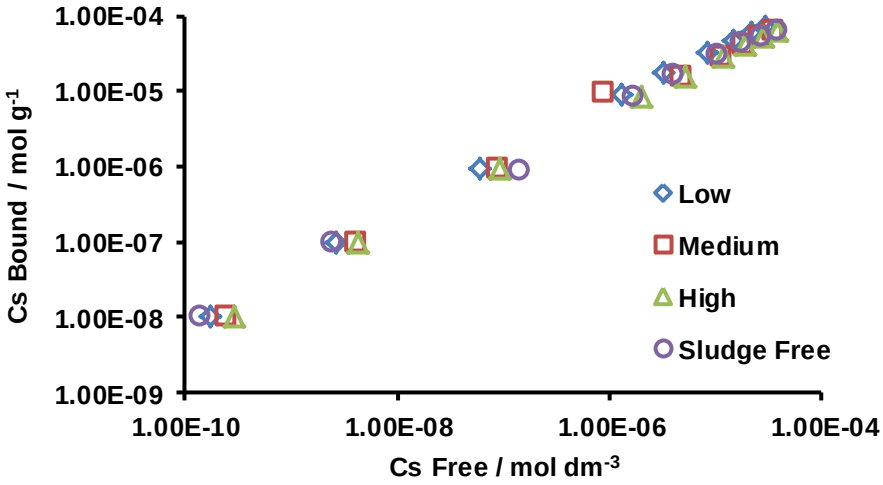

Figure 121. Log-Log plot showing the effect of simulant Magnox sludge on Cs sorption to montmorillonite. Experiments carried out with a solid:liquid ratio of 1:200, equilibrating *ca.* 7 days at room temperature. Three replicates per sample

Figure 122 illustrates the change in R_d for Cs sorption to montmorillonite for all simulant Magnox sludge concentrations investigated. There appears to be no difference in the trend across all Cs concentrations compared with a sludge free system, although the R_d values do decrease as the sludge concentration increases.

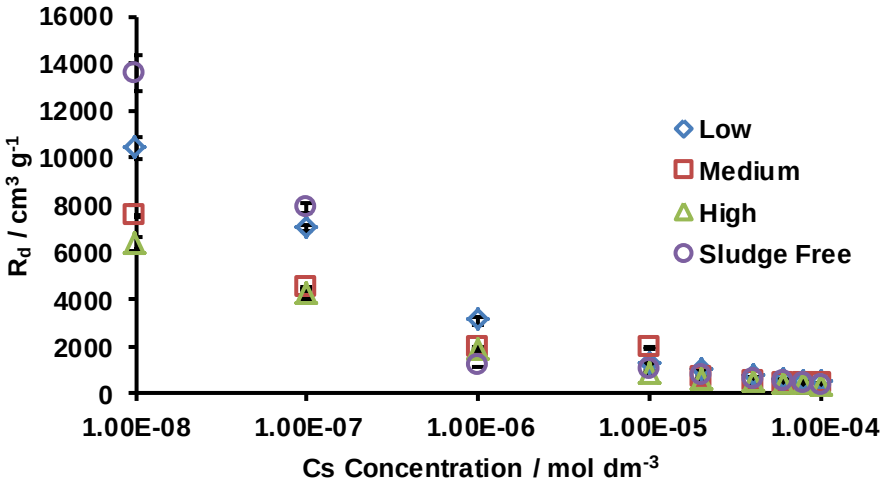

Figure 122. Effect of simulant sludge concentration on R_d for Cs sorption to montmorillonite. Experiments carried out with a solid:liquid ratio of 1:200, equilibrating *ca.* 7 days at room temperature. Three replicates per sample

Effect of Simulant Magnox Sludge on Sr Sorption to Montmorillonite

As the concentration of simulant Magnox sludge in solution increases, the amount of Sr sorption to montmorillonite decreases, as is illustrated in Figure 123. When the simulant sludge concentration is low, there only appears to be an effect on Sr sorption at low concentrations compared to the sludge free system. The highest sludge concentration affects sorption across the whole range of Sr concentrations investigated.

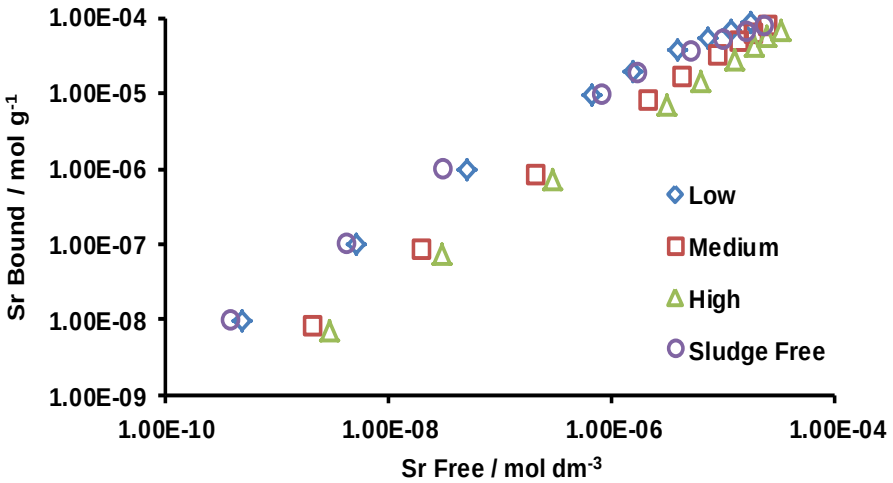

Figure 123. Log-Log plot showing the effect of simulant Magnox sludge on Sr sorption to montmorillonite. Experiments carried out with a solid:liquid ratio of 1:200, equilibrating *ca.* 7 days at room temperature. Three replicates per sample

Figure 124 illustrates the change in R_d for Sr sorption to montmorillonite for all simulant Magnox sludge concentrations investigated. There appears to be no difference in the trend for low simulant sludge and sludge free systems. The deviation from linearity observed when the simulant Magnox sludge concentration is medium or high occurs later than that observed for a sludge free system, deviation occurring above 6 x 10^{-5} mol dm^{-3} in comparison to 1 x 10^{-6} mol dm^{-3} for the sludge free system.

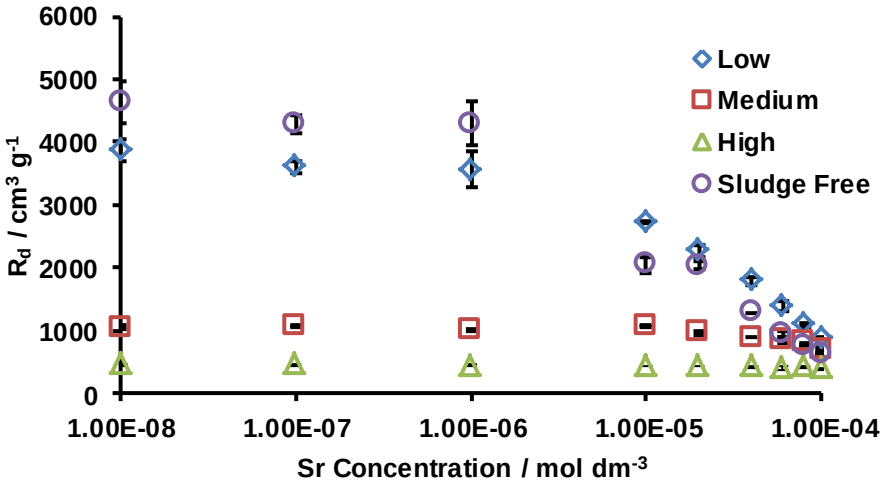

Figure 124. Effect of simulant sludge concentration on R_d for Sr sorption to montmorillonite. Experiments carried out with a solid:liquid ratio of 1:200, equilibrating *ca.* 7 days at room temperature. Three replicates per sample

Effect of Simulant Magnox Sludge on Cs Sorption to Bentonite

The presence of simulant Magnox sludge does not appear to alter the sorption of Cs to bentonite across all sludge concentrations investigated, as can be seen in Figure 125. As the dominant competing cation in solution is Mg^{2+}, the monovalent Cs^{+} ion may be competing for different sorption sites than the divalent Mg^{2+} cation.

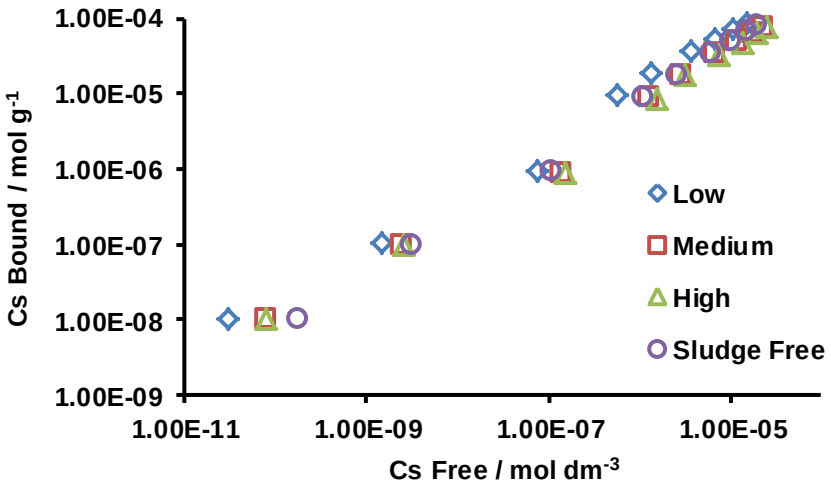

Figure 125. Log-Log plot showing the effect of simulant Magnox sludge on Cs sorption to bentonite. Experiments carried out with a solid:liquid ratio of 1:200, equilibrating *ca.* 7 days at room temperature. Three replicates per sample

Figure 126 illustrates the change in R_d for Cs sorption to bentonite for all simulant Magnox sludge concentrations investigated. There appears to be no difference in the trend across all concentration ranges when compared with a sludge free system, although the R_d values do decrease as the sludge concentration increases.

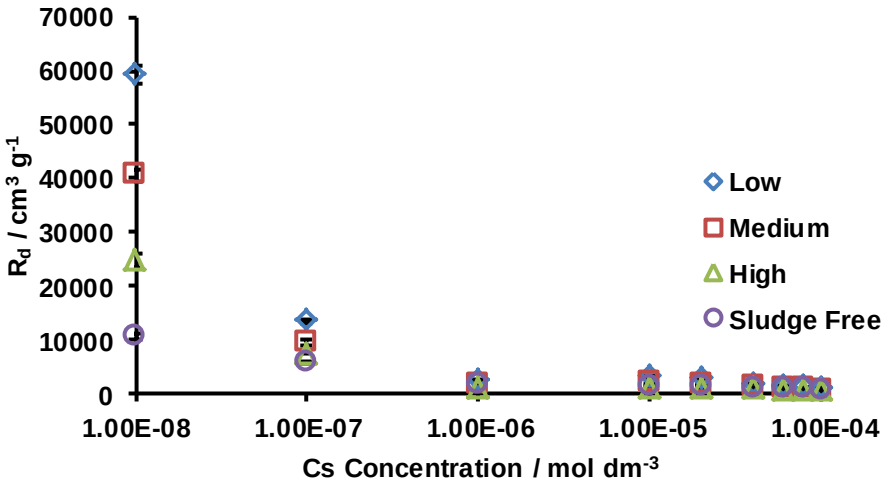

Figure 126. Effect of simulant sludge concentration on R_d for Cs sorption to bentonite. Experiments carried out with a solid:liquid ratio of 1:200, equilibrating *ca.* 7 days at room temperature. Three replicates per sample

Effect of Simulant Magnox Sludge on Sr Sorption to Bentonite

The sorption of Sr to bentonite decreases as the concentration of simulant Magnox in solution increases. The highest concentration of simulant Magnox sludge sees the

greatest decrease in strontium sorption, whilst it appears that the lowest sludge concentration sees a slight increase in strontium sorption to bentonite, Figure 127.

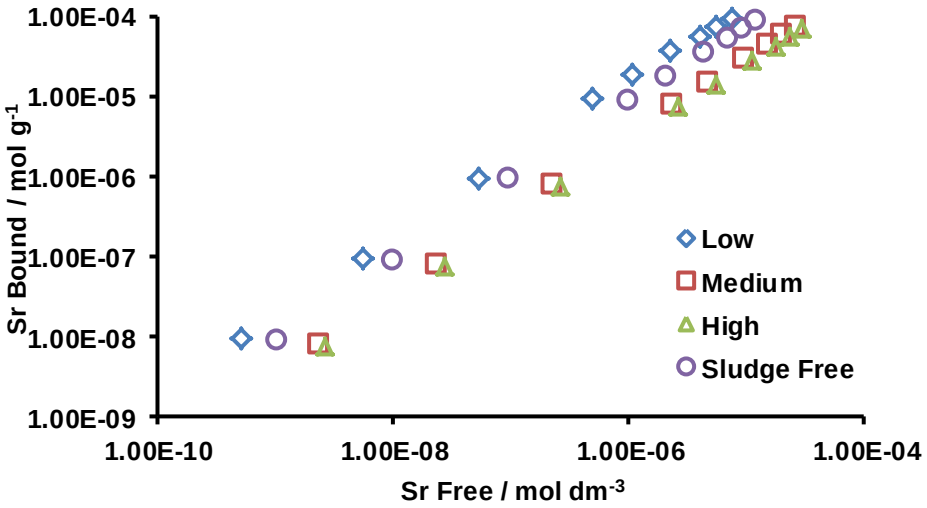

Figure 127. Log-Log plot showing the effect of simulant Magnox sludge on Sr sorption to bentonite. Experiments carried out with a solid:liquid ratio of 1:200, equilibrating *ca.* 7 days at room temperature. Three replicates per sample

Figure 128 illustrates the change in R_d for Sr sorption to bentonite for all simulant Magnox sludge concentrations investigated. There appears to be no difference in the trend for low simulant sludge and sludge free systems. The deviation from linearity observed when the simulant Magnox sludge concentration is medium or high occurs later than that observed for a sludge free system, deviation occurring above 4 x 10^{-5} mol dm^{-3} in comparison to 8 x 10^{-5} mol dm^{-3} for the sludge free system.

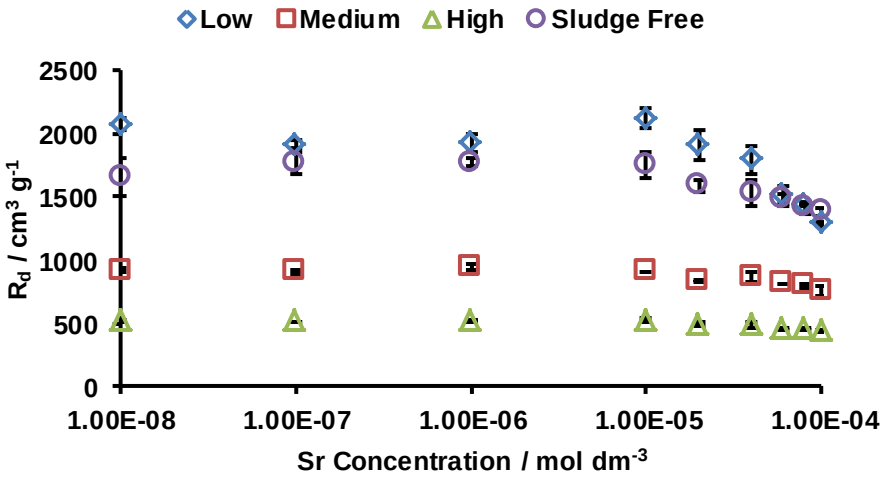

Figure 128. Effect of simulant sludge concentration on R_d for Sr sorption to bentonite. Experiments carried out with a solid:liquid ratio of 1:200, equilibrating *ca.* 7 days at room temperature. Three replicates per sample

4.3 Quaternary Systems: Effect of Simulant Magnox Sludge on the Sorption of Cs and Sr to Montmorillonite and Bentonite in the Presence of Anthropogenic Organic Ligands

The presence of Magnox sludge in the storage ponds results in a large release of competing ions, particularly Mg^{2+}, in to the pond liquor. The following experiments were devised to investigate whether the presence of these competing ions, coupled with the presence of anthropogenic organic ligands, further alters the sorption behaviour of the clay minerals studied. Using the results for the ternary systems obtained in chapter 3, a comparison can be made with the results obtained for quaternary systems, to see if the presence of the sludge results in an increase or decrease in sorption in the presence of anthropogenic ligands.

4.3.1 Experimental Method

Firstly, solutions of equilibrated simulant Magnox sludge liquor (2000:1, 200:1 and 50:1 L:S) and anthropogenic organic ligands (1, 1 x 10^{-2} and 1 x 10^{-4} mol dm^{-3}) were prepared. Batch sorption experiments were carried out by placing 20 cm^3 of the required simulant Magnox sludge solution in 50 cm^3 centrifuge vials with 0.1 g of montmorillonite or bentonite. To these centrifuge vials, 200 µl of organic ligand, 200 µl of $CsNO_3$ or $Sr(NO_3)_2$, 1 x 10^{-2} mol dm^{-3}, and 100 µl of ^{137}Cs or ^{85}Sr were added, establishing final ligand concentrations of 1 x 10^{-2} to 1 x 10^{-6} mol dm^{-3} and a final cation concentration of 1 x 10^{-4} mol dm^{-3}. Samples were then thoroughly mixed with a whirlimixer and placed on an orbital shaker for one week at 100 rpm.

After 1 week, the samples were centrifuged at 6000 rpm for 20 minutes and the supernatant then decanted. 2 cm^3 of supernatant was filtered through a 0.45 µm syringe filter and the gamma radiation counted with a Packard Cobra II Auto Gamma counter. pH of the remaining supernatant was recorded.

4.3.2 Results

Effect of Simulant Magnox Sludge on the Sorption of Cs to Montmorillonite and Bentonite in the Presence of Picolinic Acid

The effects of simulant Magnox sludge on the sorption of Cs to montmorillonite and bentonite in the presence of picolinic acid at different concentrations can be seen in Figure 129 - Figure 131. Figure 129, high picolinic acid concentration, shows that as

the sludge concentration increases, the sorption of Cs to both montmorillonite and bentonite decreases. The difference in the concentration of Cs bound to montmorillonite and bentonite, between low simulant sludge and high simulant sludge, was found to be 5.4 x 10^{-6} and 8 x 10^{-6} mol g^{-1} respectively, a decrease of 8% and 11%. Compared to the results obtained for the ternary system, i.e. clay mineral, cation and picolinic acid only, the sorption of Cs to montmorillonite increases with the presence of low and medium simulant sludge but no change is observed with the addition of high simulant Magnox sludge.

The influence of simulant sludge on Cs sorption to montmorillonite and bentonite in the presence of 1 x 10^{-4} mol dm^{-3} picolinic acid can be seen in Figure 130. Like with the results for a high picolinic acid concentration, as simulant sludge concentration increases, the sorption of Cs to bentonite decreases from 7.62 x 10^{-5} mol g^{-1} to 6.92 x 10^{-5} mol g^{-1}, a decrease of 9%. There is virtually no difference in the sorption of Cs to montmorillonite as the simulant sludge concentration increases, <2% which could be caused by normal experimental errors. When compared to the sludge free results, it appears that the amount of Cs sorption to montmorillonite actually increases in the presence of simulant sludge by 13%, from 5.95 x 10^{-5} to 6.72 x 10^{-5} mol g^{-1}. This is not seen for bentonite, where it appears that the addition of simulant sludge decreases the amount of Cs sorption occurring.

Figure 131 shows that the influence of Magnox sludge reduces the sorption of Cs to bentonite, with this reduction in sorption increasing as the sludge concentration increases. Compared to the sludge free result, it can be seen that the presence of Magnox sludge reduces the sorption of Cs across all sludge concentrations. Conversely, there appears to be a slight increase in Cs sorption to montmorillonite when Magnox sludge is introduced to the system. The greatest increase in sorption appears at the lowest sludge concentration, increasing from 6.24 x 10^{-5} mol g^{-1} for the sludge free system to 6.84 x 10^{-5} mol g^{-1}, an increase of 10%.

Figure 132 - Figure 134 compares the effect of picolinic acid on Cs sorption to bentonite and montmorillonite at different simulant Magnox sludge concentrations. When the simulant Magnox sludge concentration is high (Figure 132), sorption of Cs to bentonite appears to decrease with increasing picolinic acid concentration. There appears to be little effect on the sorption of Cs to montmorillonite under these conditions. A similar trend occurs for both low and medium simulant Magnox sludge concentrations, although at high picolinic acid concentration, there does appear to be a

slight increase in Cs sorption to montmorillonite. However, the error (standard deviation) for this sample would suggest that this is not the case and the sorption is not affected across the range of picolinic acid concentration.

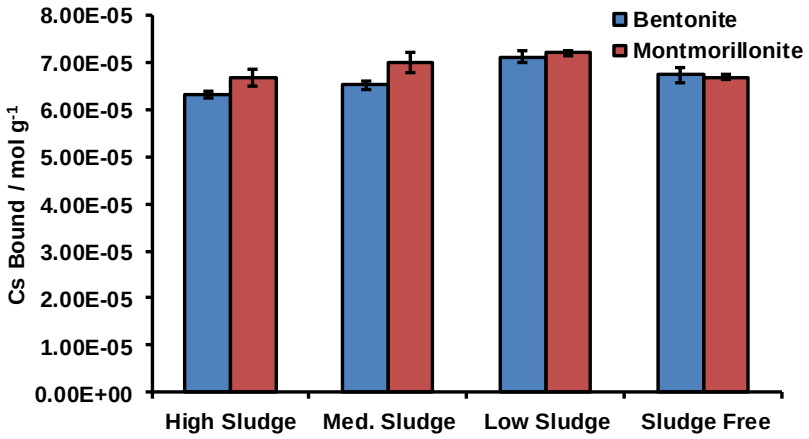

Figure 129. Effect of simulant Magnox sludge on the sorption of Cs to montmorillonite and bentonite in the presence of picolinic acid at a concentration of 1 x 10^{-2} mol dm^{-3}

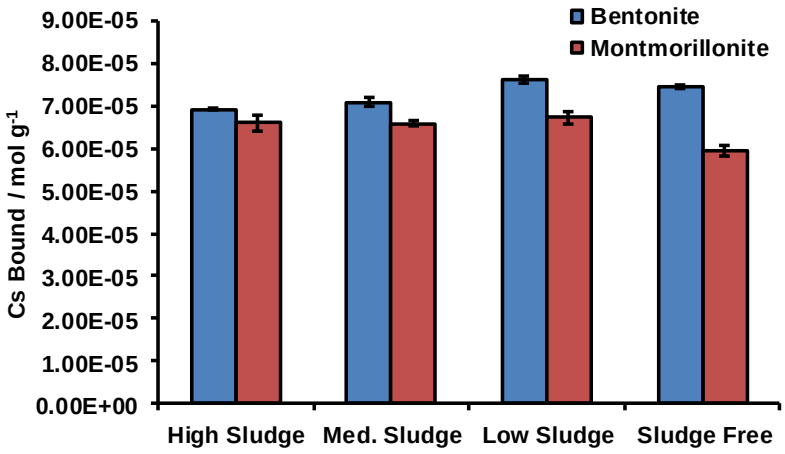

Figure 130. Effect of simulant Magnox sludge on the sorption of Cs to montmorillonite and bentonite in the presence of picolinic acid at a concentration of 1 x 10^{-4} mol dm^{-3}

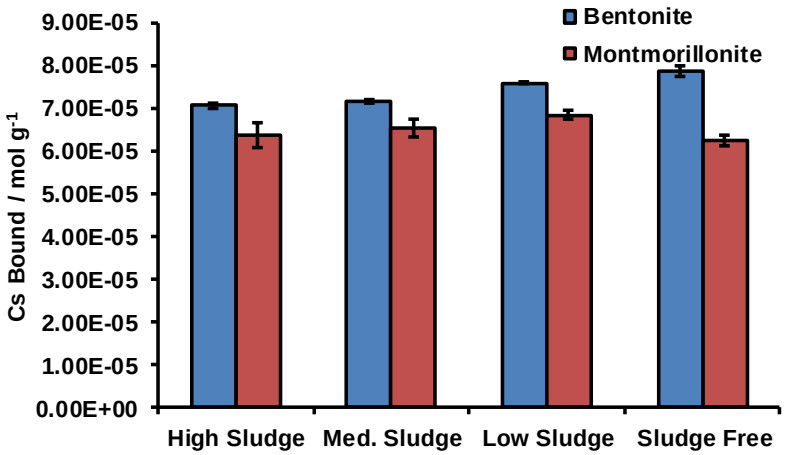

Figure 131. Effect of simulant Magnox sludge on the sorption of Cs to montmorillonite and bentonite in the presence of picolinic acid at a concentration of 1 x 10^{-6} mol dm^{-3}

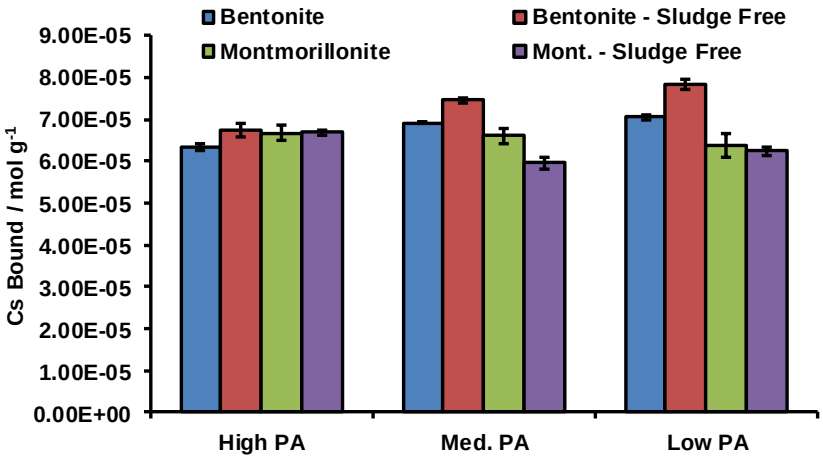

Figure 132. Effect of high simulant Magnox sludge concentration on the sorption of Cs to montmorillonite and bentonite in the presence of picolinic acid

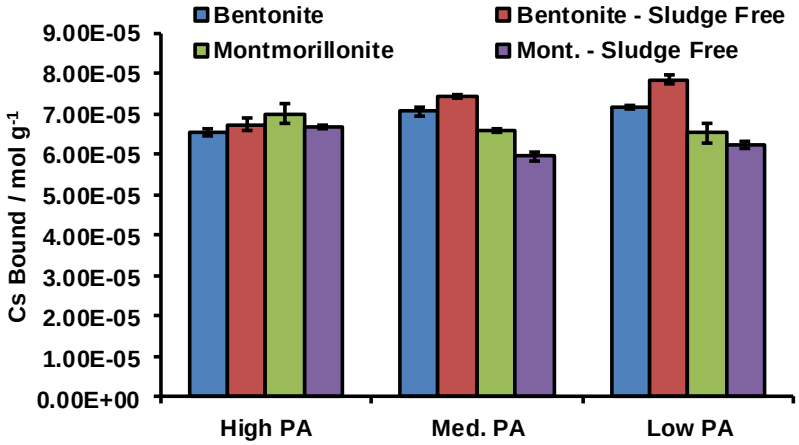

Figure 133. Effect of medium simulant Magnox sludge concentration on the sorption of Cs to montmorillonite and bentonite in the presence of picolinic acid

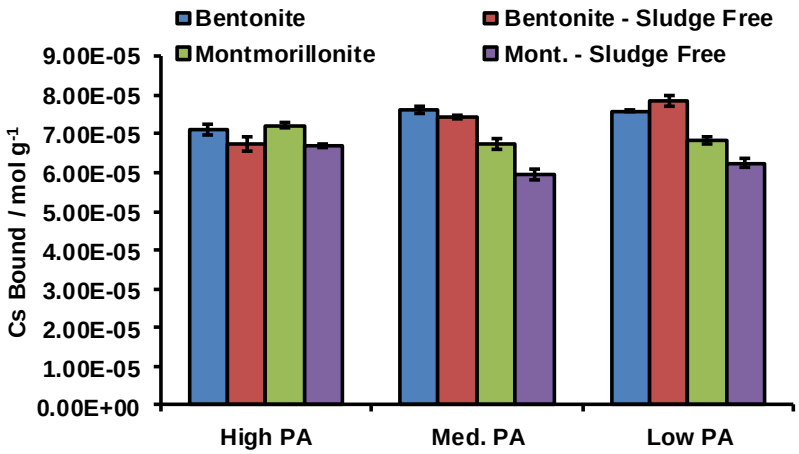

Figure 134. Effect of low simulant Magnox sludge concentration on the sorption of Cs to montmorillonite and bentonite in the presence of picolinic acid

Effect of Simulant Magnox Sludge on the Sorption of Sr to Montmorillonite and Bentonite in the Presence of Picolinic Acid

Figure 135 - Figure 137 show the effect of simulant Magnox sludge at different concentrations on the sorption of Sr to bentonite and montmorillonite in the presence of picolinic acid. At high picolinic acid concentration, Figure 135, the sorption of Sr to montmorillonite decreases with increasing sludge concentration, from 7 x 10^{-5} mol g^{-1} at low simulant sludge down to 4.32 x 10^{-5} mol g^{-1} at high simulant sludge, a decrease of 38%. Likewise, a decrease in Sr sorption to bentonite is seen as the concentration of Magnox sludge in solution increases. This decrease is not as great as that seen for montmorillonite, with a bound Sr concentration of 5.1 x 10^{-5} mol g^{-1} in the presence of low simulant sludge, decreasing to 4.47 x 10^{-5} mol g^{-1} at high simulant sludge concentration, an overall decrease of 12%. The presence of simulant Magnox sludge results in a decrease of Sr sorption to both montmorillonite and bentonite when compared to the corresponding sludge free systems. The decrease in sorption is roughly 50% between sludge free and high sludge results for montmorillonite and 33% for bentonite.

At a picolinic acid concentration of 1 x 10^{-4} mol dm^{-3}, the same trend seen for a high picolinic acid concentration is observed (Figure 136). Sorption decreases to both montmorillonite and bentonite with increasing Magnox sludge concentration. The presence of Magnox sludge in a system with 1 x 10^{-4} mol dm^{-3} picolinic acid and Sr, results in a decrease in sorption when compared to the sludge free results. The decrease in sorption is 49% between sludge free and high sludge results for montmorillonite, and 35% for bentonite.

At low picolinic acid concentration, Figure 137, sorption of Sr to both bentonite and montmorillonite decreases as the concentration of Magnox sludge increases. The amount of Sr sorption occurring to montmorillonite and bentonite, when there is Magnox sludge in the system, is less than what has been observed for a sludge free system. The difference between the sludge free system and a system with high Magnox sludge present was 50% with montmorillonite and 37% with bentonite.

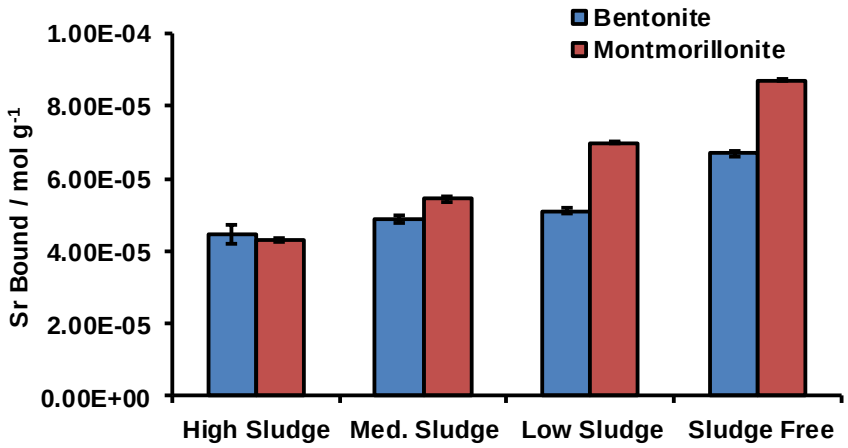

Figure 135. Effect of simulant Magnox sludge on the sorption of Sr to montmorillonite and bentonite in the presence of picolinic acid at a concentration of 1 x 10^{-2} mol dm^{-3}

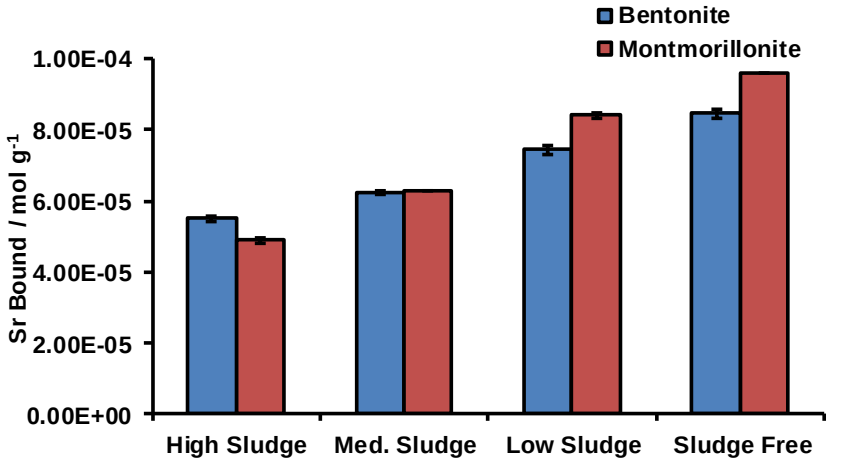

Figure 136. Effect of simulant Magnox sludge on the sorption of Sr to montmorillonite and bentonite in the presence of picolinic acid at a concentration of 1 x 10^{-4} mol dm^{-3}

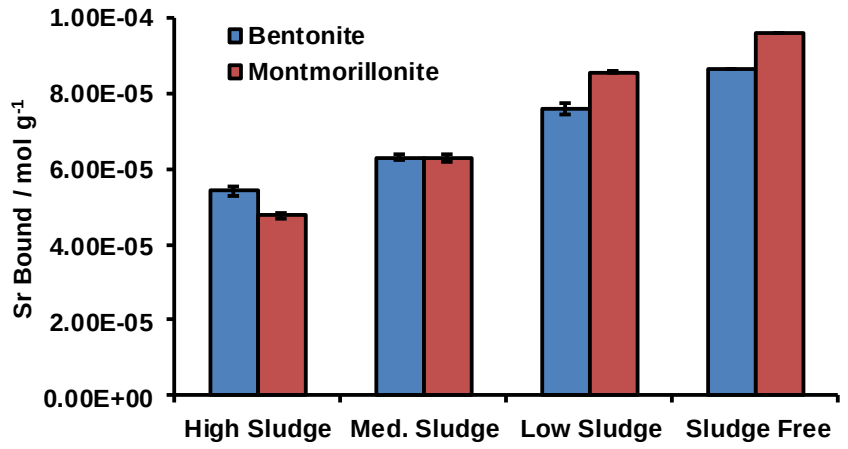

Figure 137. Effect of simulant Magnox sludge on the sorption of Sr to montmorillonite and bentonite in the presence of picolinic acid at a concentration of 1 x 10^{-6} mol dm^{-3}

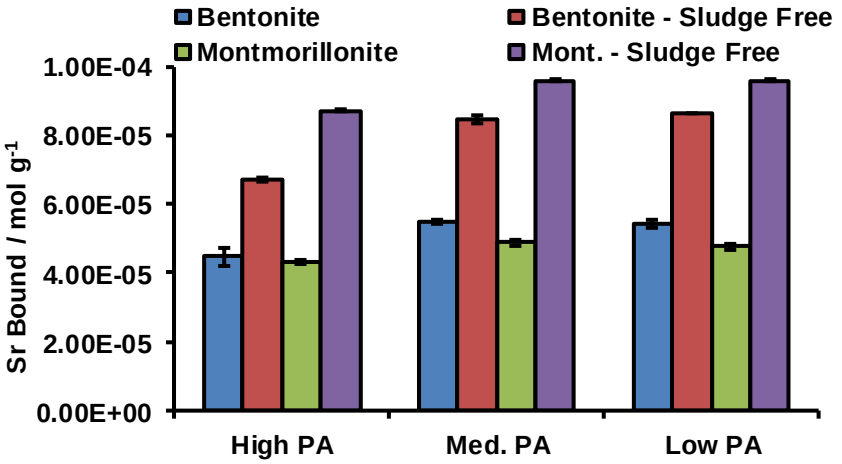

Figure 138. Effect of high simulant Magnox sludge concentration on the sorption of Sr to montmorillonite and bentonite in the presence of picolinic acid

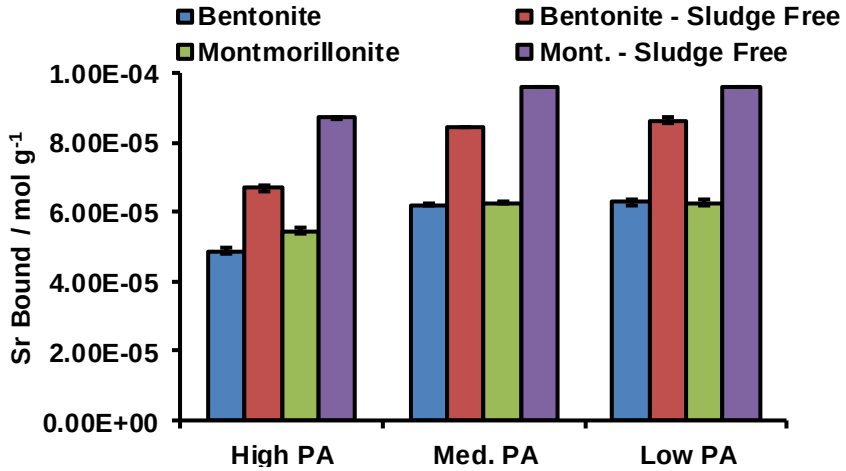

Figure 139. Effect of medium simulant Magnox sludge concentration on the sorption of Sr to montmorillonite and bentonite in the presence of picolinic acid

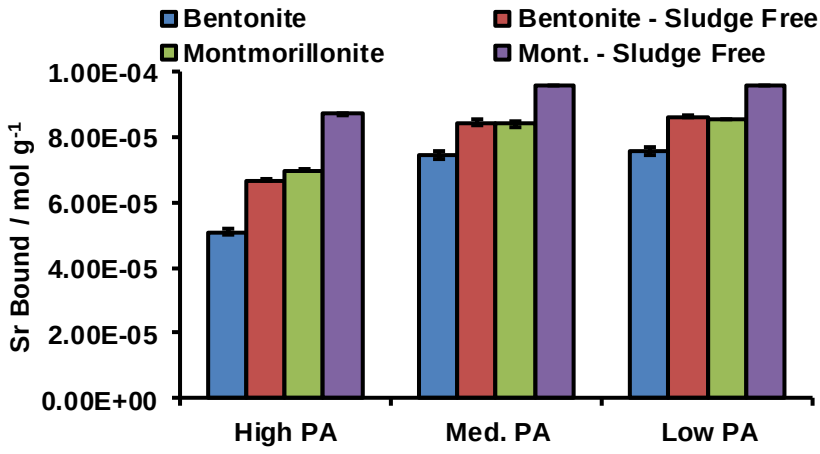

Figure 140. Effect of low simulant Magnox sludge concentration on the sorption of Sr to montmorillonite and bentonite in the presence of picolinic acid

Effect of Simulant Magnox Sludge on the Sorption of Cs to Montmorillonite and Bentonite in the Presence of NTA

Figure 141 - Figure 143 shows the effect that simulant Magnox sludge has on the sorption of Cs to montmorillonite and bentonite in the presence of NTA. From Figure 141 it can be seen that the presence of simulant Magnox sludge at all concentrations investigated had no effect on the Cs sorption to bentonite. Values obtained for a sludge free system and a system with a high sludge concentration were both found to be 8.55×10^{-5} mol g^{-1}. A slight decrease in the sorption of Cs to montmorillonite was observed when simulant sludge was present in the system. 7.77×10^{-5} mol g^{-1} of Cs was bound to montmorillonite in a ligand free system compared to 7.42×10^{-5} mol g^{-1} at a high Magnox sludge concentration, a decrease of 5%.

When the NTA concentration is 1×10^{-4} mol dm^{-3}, the presence of Magnox sludge causes a decrease in the sorption of Cs to montmorillonite, a decrease of 32%, significantly more than observed when the NTA concentration was 1×10^{-2} mol dm^{-3} (Figure 142). Sorption of Cs to bentonite also decreases with increasing Magnox sludge concentration with a NTA concentration of 1×10^{-4} mol dm^{-3}. The decrease in sorption was calculated to be 10%, not as significant as that observed for montmorillonite.

At the lowest NTA concentration, Figure 143, sorption of Cs to montmorillonite was affected in a similar way to that of a system with Magnox sludge and medium NTA concentration. A decrease in sorption of 30% was observed between the sludge free system and that with a high sludge concentration. Cs sorption to bentonite also decreased over this Magnox sludge concentration range, from 8.18×10^{-5} mol g^{-1} to 7.6×10^{-5} mol g^{-1}, a decrease of 7%.

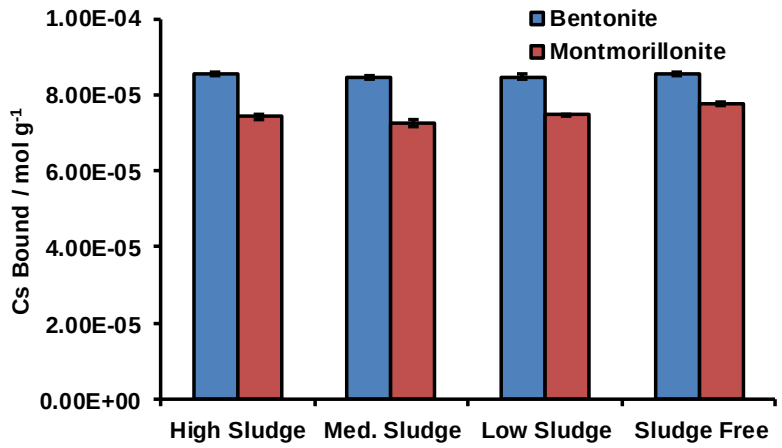

Figure 141. Effect of simulant Magnox sludge on the sorption of Cs to montmorillonite and bentonite in the presence of NTA at a concentration of 1 x 10^{-2} mol dm^{-3}

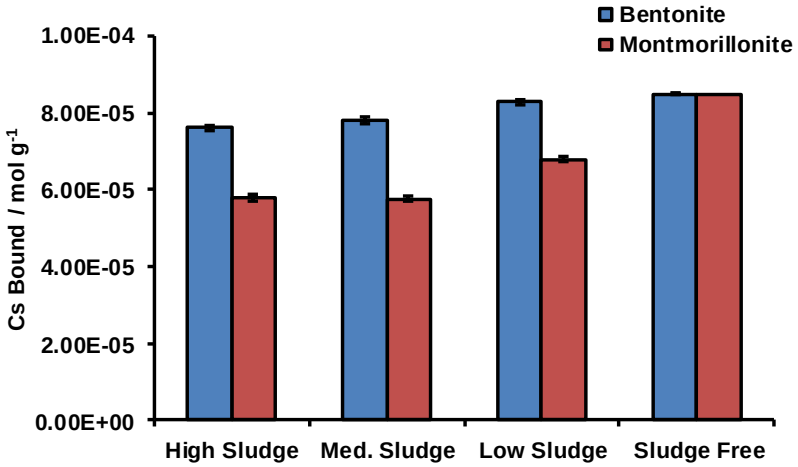

Figure 142. Effect of simulant Magnox sludge on the sorption of Cs to montmorillonite and bentonite in the presence of NTA at a concentration of 1 x 10^{-4} mol dm^{-3}

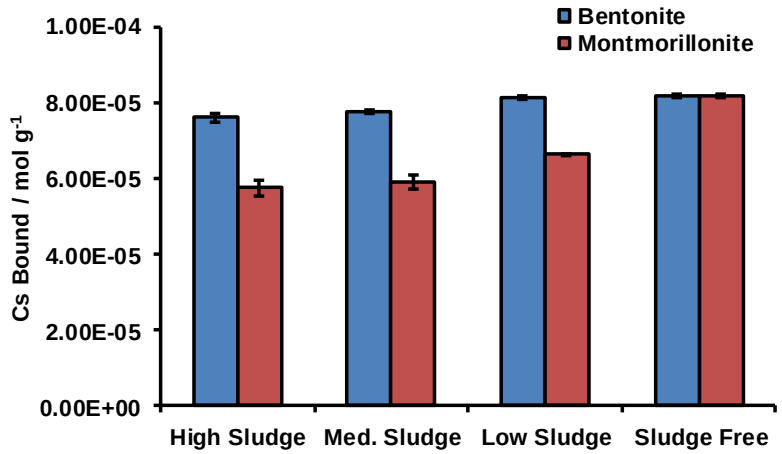

Figure 143. Effect of simulant Magnox sludge on the sorption of Cs to montmorillonite and bentonite in the presence of NTA at a concentration of 1 x 10^{-6} mol dm^{-3}

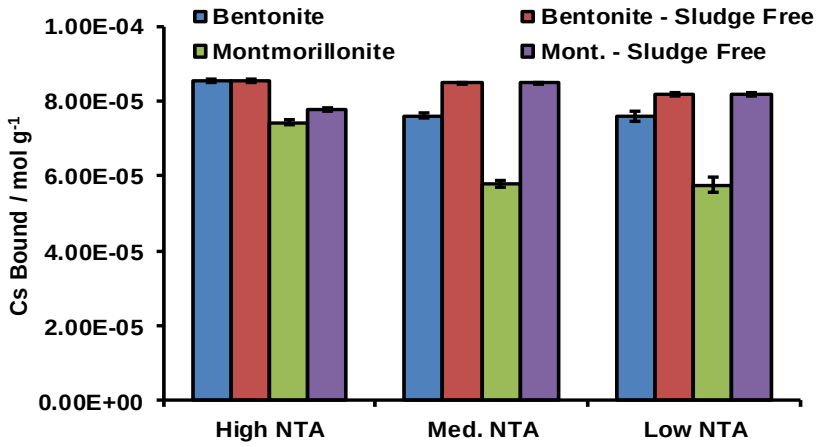

Figure 144. Effect of high simulant Magnox sludge concentration on the sorption of Cs to montmorillonite and bentonite in the presence of NTA

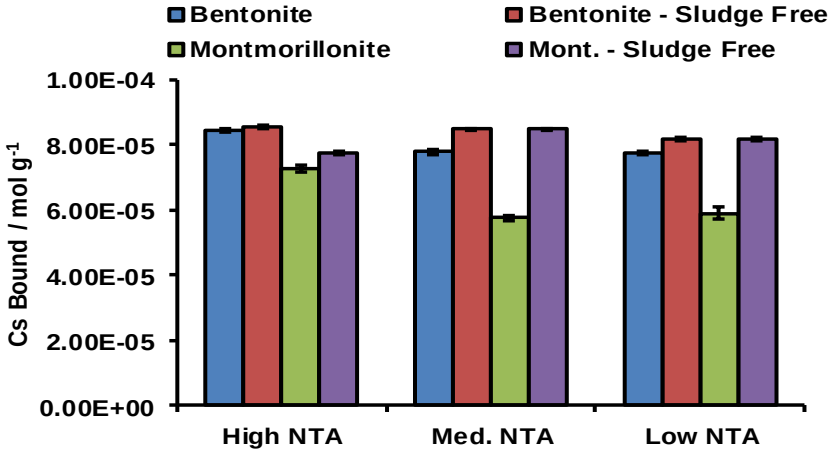

Figure 145. Effect of medium simulant Magnox sludge concentration on the sorption of Cs to montmorillonite and bentonite in the presence of NTA

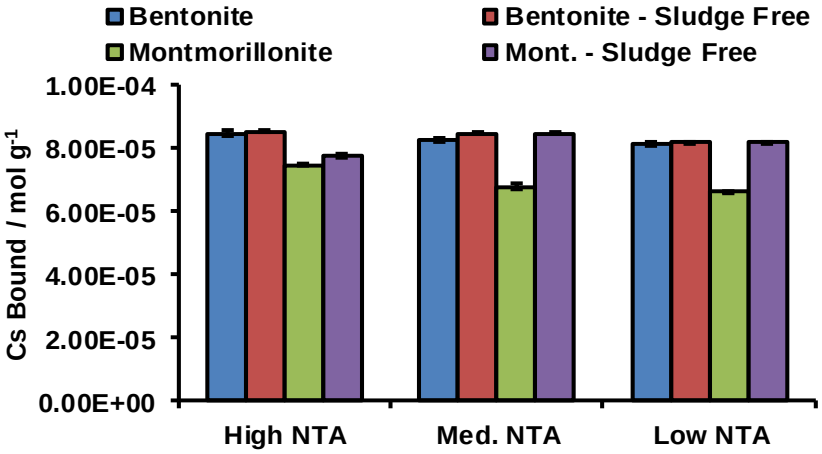

Figure 146. Effect of low simulant Magnox sludge concentration on the sorption of Cs to montmorillonite and bentonite in the presence of NTA

Effect of Simulant Magnox Sludge on the Sorption of Sr to Montmorillonite and Bentonite in the Presence of NTA

Figure 147 - Figure 149 show the effect of Magnox sludge on the sorption of Sr to bentonite and montmorillonite in the presence of NTA at varying concentrations. At high NTA concentration, Figure 147, the presence of Magnox sludge in the system does not appear to affect the sorption of Sr to bentonite across all sludge concentrations investigated. The amount of sorption occurring to bentonite in the sludge free system was calculated to be 1.55×10^{-5} mol g^{-1} compared to 1.5×10^{-5} mol g^{-1} at high Magnox sludge concentration. There appears to be a minor effect upon sorption of Sr to montmorillonite when Magnox sludge is added to the system, a decrease in sorption of approximately 16% is observed, a reduction in sorption from 1.43×10^{-5} mol g^{-1} to 1.2×10^{-5} mol g^{-1}.

From Figure 148 there is a clear correlation showing the effect of Magnox sludge on Sr sorption to both bentonite and montmorillonite at a NTA concentration of 1×10^{-4} mol dm^{-3}. As the concentration of sludge increases in the system, the amount of Sr sorption occurring decreases for both montmorillonite and bentonite by 33% and 23% respectively. Initially with sludge free and low sludge concentrations, there is a greater amount of Sr bound to montmorillonite than bentonite, 9.62×10^{-5} mol g^{-1} compared with 8.66×10^{-5} mol g^{-1}, as the sludge in the system increases there is less sorption of Sr to montmorillonite occurring than of that to bentonite. There is no observed change in sorption between sludge free and low sludge systems for both montmorillonite and bentonite.

A similar trend to that seen in Figure 148 is observed with a low NTA concentration in Figure 149. As the concentration of Magnox sludge in the solution increases, the sorption of Cs to both bentonite and montmorillonite decreases. A decrease in sorption of 14% is observed for Sr sorption to bentonite, and 31% for montmorillonite at high sludge concentration when compared to a sludge free system.

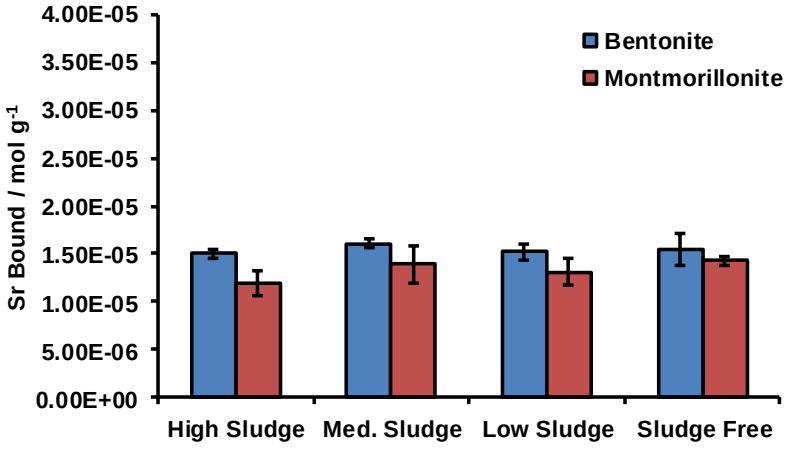

Figure 147. Effect of simulant Magnox sludge on the sorption of Sr to montmorillonite and bentonite in the presence of NTA at a concentration of 1 x 10^{-2} mol dm^{-3}

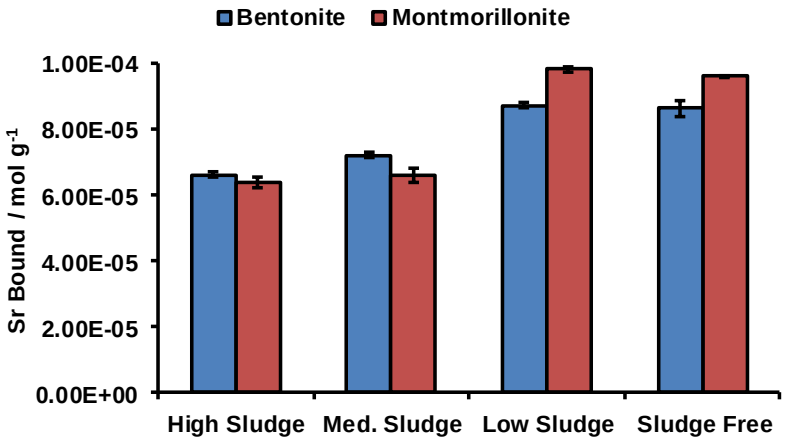

Figure 148. Effect of simulant Magnox sludge on the sorption of Sr to montmorillonite and bentonite in the presence of NTA at a concentration of 1 x 10^{-4} mol dm^{-3}

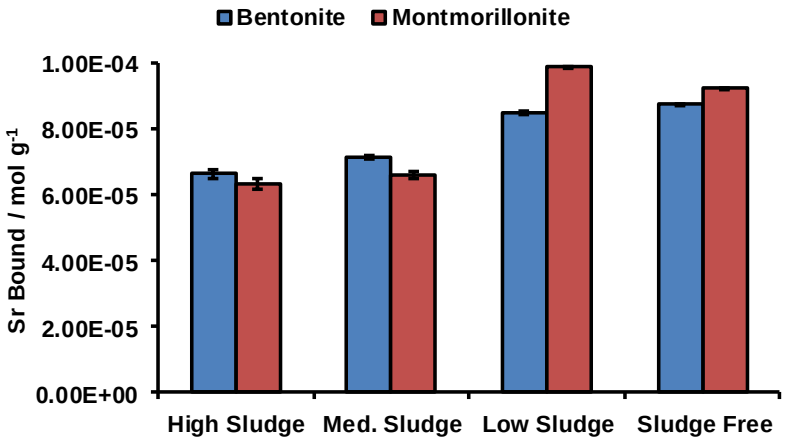

Figure 149. Effect of simulant Magnox sludge on the sorption of Sr to montmorillonite and bentonite in the presence of NTA at a concentration of 1 x 10^{-6} mol dm^{-3}

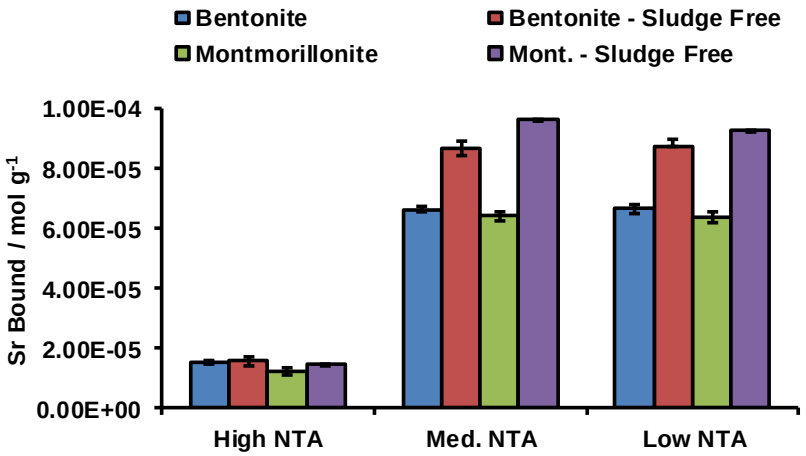

Figure 150. Effect of high simulant Magnox sludge concentration on the sorption of Sr to montmorillonite and bentonite in the presence of NTA

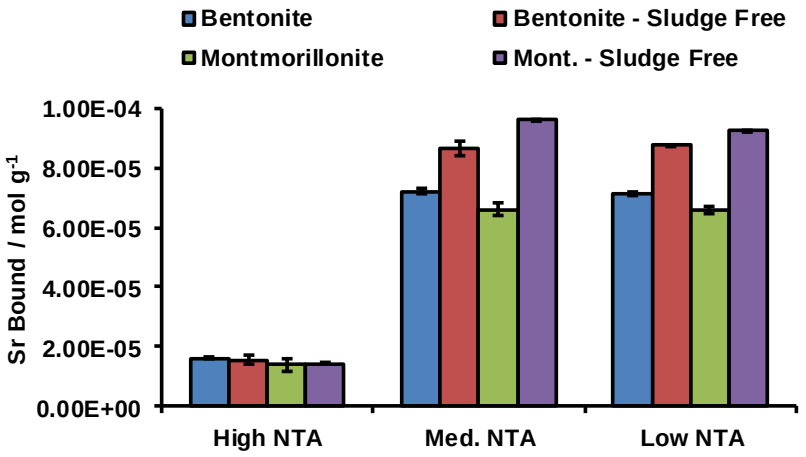

Figure 151. Effect of medium simulant Magnox sludge concentration on the sorption of Sr to montmorillonite and bentonite in the presence of NTA

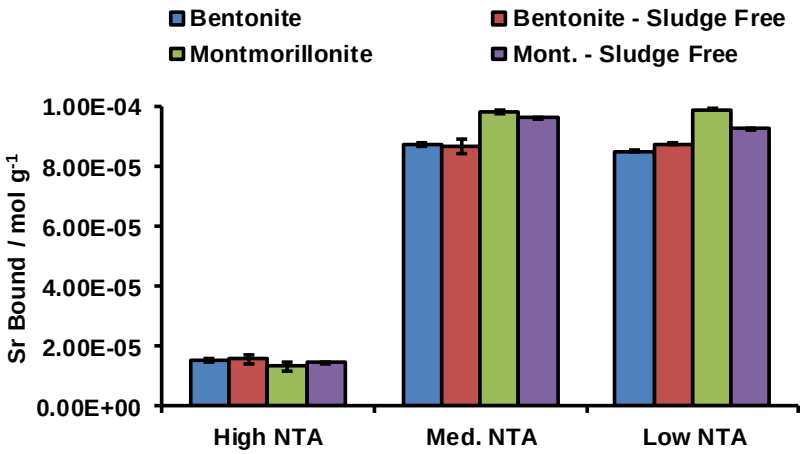

Figure 152. Effect of low simulant Magnox sludge concentration on the sorption of Sr to montmorillonite and bentonite in the presence of NTA

Effect of Simulant Magnox Sludge on the Sorption of Cs to Montmorillonite and Bentonite in the Presence of EDTA

Figure 153 - Figure 155 show the effect that Magnox sludge has on the sorption of Cs to montmorillonite and bentonite in the presence of EDTA with varying concentrations. From Figure 153 it can be seen that the presence of Magnox sludge results in an increase of Cs bound to both montmorillonite and bentonite, with an EDTA concentration of 1 x 10^{-2} mol dm^{-3}, when compared with the results obtained from a sludge free system. The increase in sorption observed for montmorillonite was calculated to be 11% at the highest sludge concentration investigated. This increase was observed across the range of Magnox sludge concentrations studied so it appears there is no further effect on sorption above a liquid:Magnox sludge ratio of 2000:1. The increase in sorption observed for Cs sorption to bentonite was calculated to be 7% and, like with montmorillonite, there was no further effect on sorption above a liquid:Magnox sludge ratio of 2000:1.

From Figure 154 it can be seen that with an EDTA concentration of 1 x 10^{-4} mol dm^{-3}, the presence of Magnox sludge results in a reduction of Cs sorption to both montmorillonite and bentonite as this sludge concentration increases. There is no apparent change in the bound concentration of Cs to montmorillonite from a sludge free system and a low sludge system however, as the sludge concentration increases, sorption decreases by 13%, from 6.78 x 10^{-5} mol g^{-1} to 5.89 x 10^{-5} mol g^{-1}. A decrease in Cs sorption to bentonite is also observed with increasing sludge concentration. The total decrease in Cs sorption was calculated to be 11%, from 7.98 x 10^{-5} mol g^{-1} for a sludge free system to 7.09 x 10^{-5} mol g^{-1} at highest sludge concentration.

At low EDTA concentration, Figure 155, there is a decrease in Cs sorption to montmorillonite and bentonite, however, this decrease in Cs sorption is less obvious than what was observed for an EDTA concentration of 1×10^{-4} mol dm^{-3}, 1% and 5% respectively.

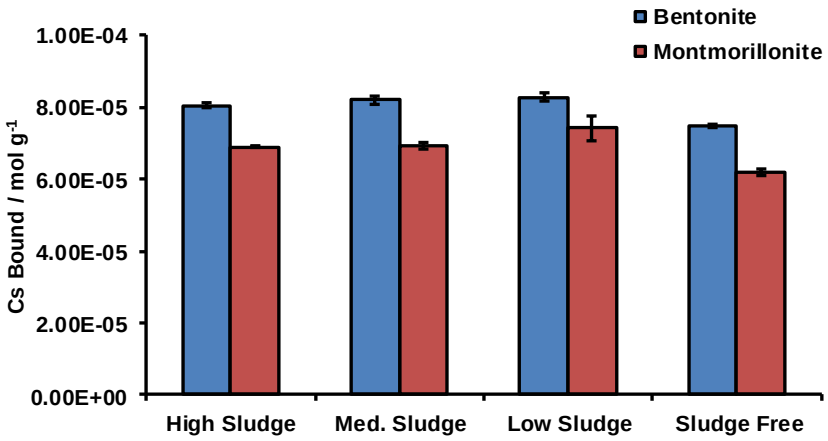

Figure 153. Effect of simulant Magnox sludge on the sorption of Cs to montmorillonite and bentonite in the presence of EDTA at a concentration of 1 x 10^{-2} mol dm^{-3}

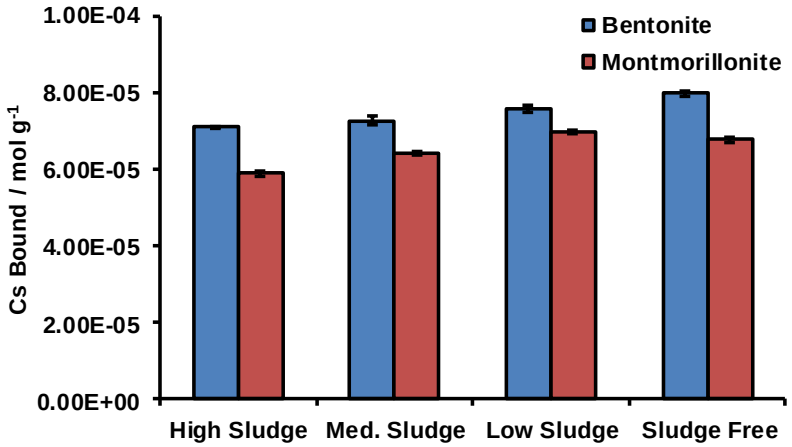

Figure 154. Effect of simulant Magnox sludge on the sorption of Cs to montmorillonite and bentonite in the presence of EDTA at a concentration of 1 x 10^{-4} mol dm^{-3}

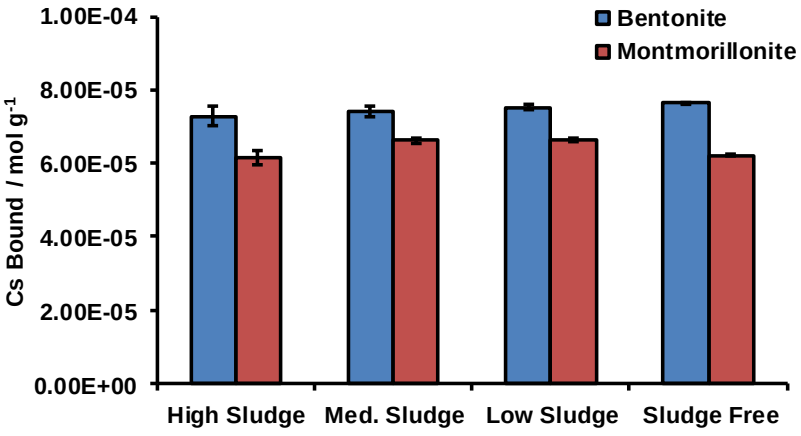

Figure 155. Effect of simulant Magnox sludge on the sorption of Cs to montmorillonite and bentonite in the presence of EDTA at a concentration of 1 x 10^{-6} mol dm^{-3}

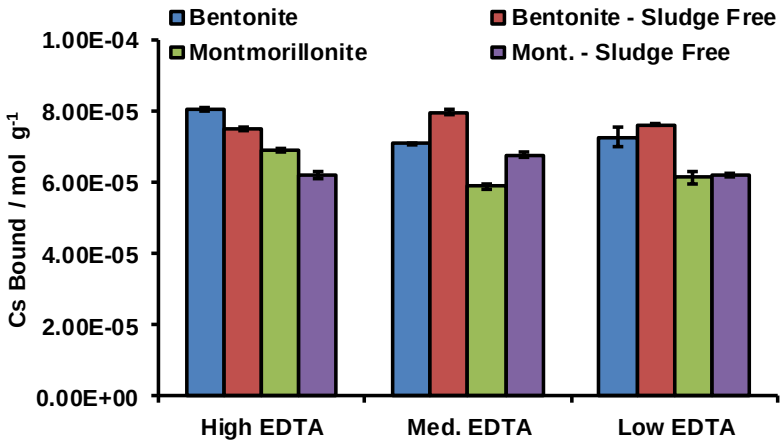

Figure 156. Effect of high simulant Magnox sludge concentration on the sorption of Cs to montmorillonite and bentonite in the presence of EDTA

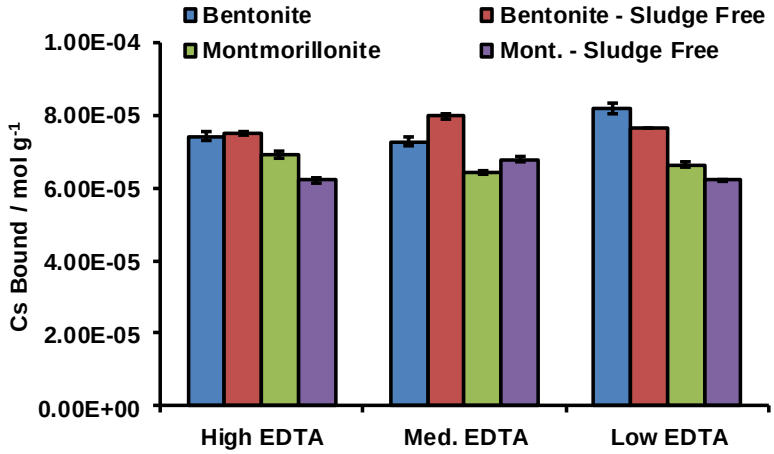

Figure 157. Effect of medium simulant Magnox sludge concentration on the sorption of Cs to montmorillonite and bentonite in the presence of EDTA

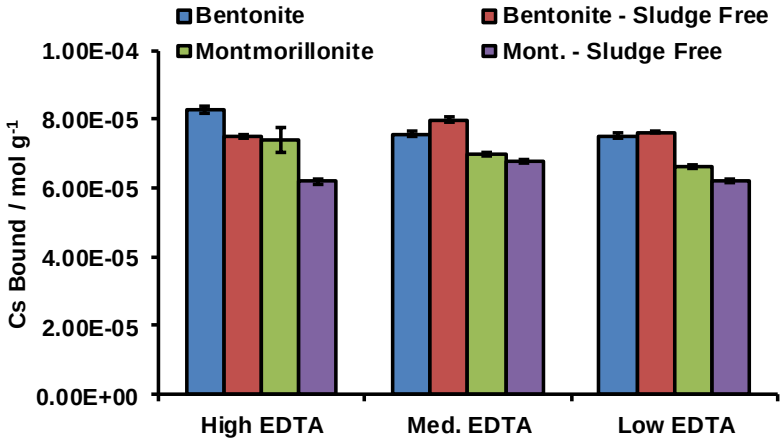

Figure 158. Effect of medium simulant Magnox sludge concentration on the sorption of Cs to montmorillonite and bentonite in the presence of EDTA

Effect of Simulant Magnox Sludge on the Sorption of Sr to Montmorillonite and Bentonite in the Presence of EDTA

Figure 159 - Figure 161 show the effect that Magnox sludge has on the sorption of Sr to bentonite and montmorillonite in the presence of at various EDTA concentrations. When the EDTA concentration is high, sorption of Sr to montmorillonite is significantly affected by the presence of Magnox simulant sludge, Figure 159. The decrease in Sr sorption observed was 79%, from a bound Sr concentration of 6.73 x 10^{-5} mol g^{-1} for a sludge free system to 7.58 x 10^{-6} mol g^{-1} at highest Magnox sludge concentration. A similar trend was observed for Sr sorption to bentonite at high EDTA concentration, although there was only a limited effect on sorption with low and medium sludge concentrations. Sr sorption to bentonite was found to be 6.38 x 10^{-5} mol g^{-1} for a sludge free system, compared to 5.7 x 10^{-5} mol g^{-1} for medium and low sludge concentrations, and 6.82 x 10^{-6} mol g^{-1} when the sludge concentration was at its highest, a decrease in Sr sorption of 79%.

With an EDTA concentration of 1 x 10^{-4} mol dm^{-3}, Figure 160, the effect of Magnox sludge on Sr sorption to montmorillonite is less dramatic across the Magnox sludge concentrations investigated. The decrease in sorption between a sludge free system and that with the highest concentration of Magnox sludge present was calculated to be 41%. For sorption of Sr to bentonite, the decrease in sorption was still significant at the highest Magnox sludge concentration, decreasing by 90% from 8.6 x 10^{-5} mol g^{-1} to 8.31 x 10^{-6} mol g^{-1}. There was no difference in the amount of bound Sr to bentonite at low and medium Magnox sludge concentrations, although sorption did decrease by 27% compared to the sludge free system.

From Figure 161 the effect of Magnox sludge on Sr sorption to montmorillonite and bentonite in the presence of 1 x 10^{-6} mol dm^{-3} of EDTA can be seen. Sorption of Sr to montmorillonite decreases with increasing Magnox sludge concentration, although at low Magnox sludge concentration, sorption does appear to increase slightly compared to the sludge free system, by 13%. The decrease in sorption at high sludge concentration, compared to the sludge free system, was calculated to be 26%. Sorption of Sr to bentonite also decreased across the Magnox sludge concentrations investigated. The concentration of bound Sr in a sludge free system was found to be 8.76 x 10^{-5} mol g^{-1}, which decreased to 5.54 x 10^{-6} mol g^{-1} in the presence of high Magnox sludge, a decrease of 94%.

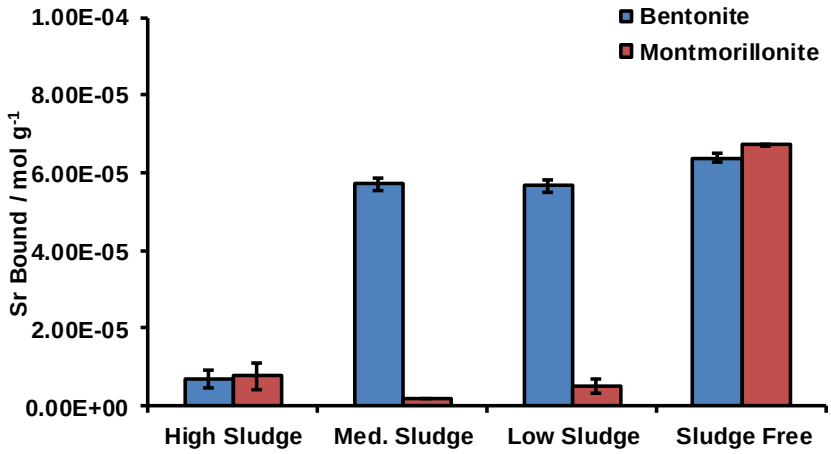

Figure 159. Effect of simulant Magnox sludge on the sorption of Sr to montmorillonite and bentonite in the presence of EDTA at a concentration of 1 x 10^{-2} mol dm^{-3}

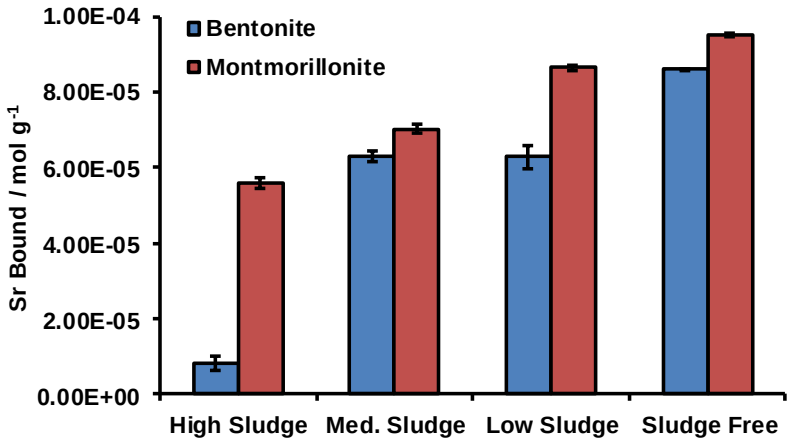

Figure 160. Effect of simulant Magnox sludge on the sorption of Sr to montmorillonite and bentonite in the presence of EDTA at a concentration of 1 x 10^{-4} mol dm^{-3}

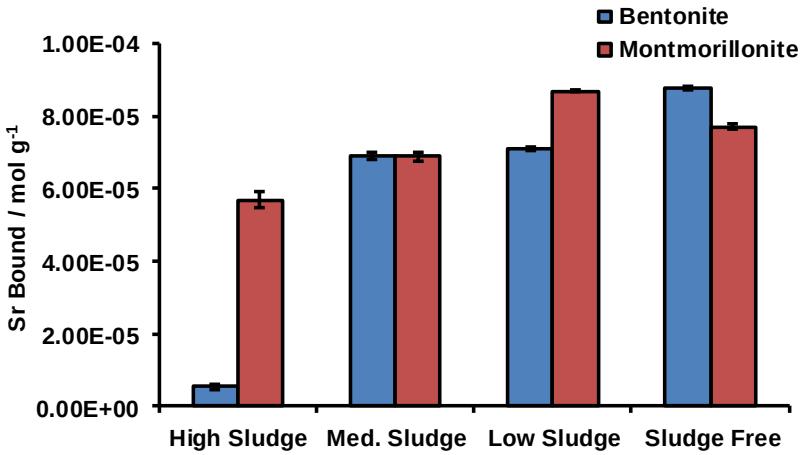

Figure 161. Effect of simulant Magnox sludge on the sorption of Sr to montmorillonite and bentonite in the presence of EDTA at a concentration of 1 x 10^{-6} mol dm^{-3}

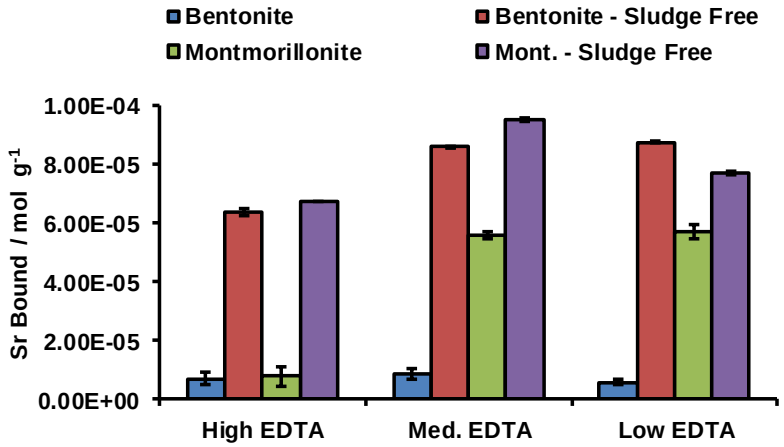

Figure 162. Effect of high simulant Magnox sludge concentration on the sorption of Sr to montmorillonite and bentonite in the presence of EDTA

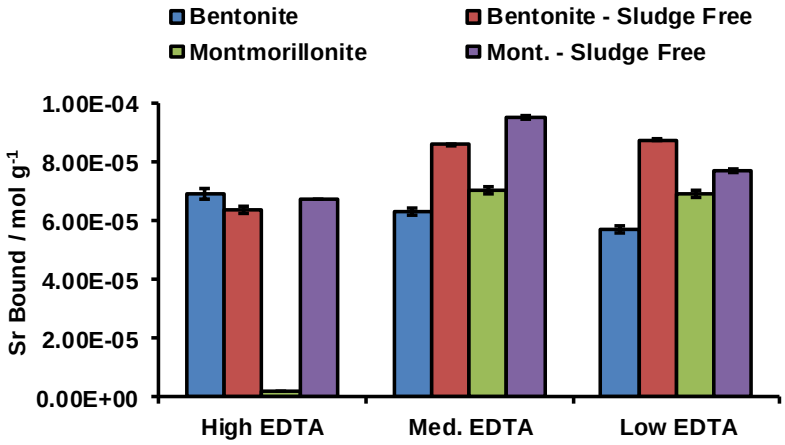

Figure 163. Effect of medium simulant Magnox sludge concentration on the sorption of Sr to montmorillonite and bentonite in the presence of EDTA

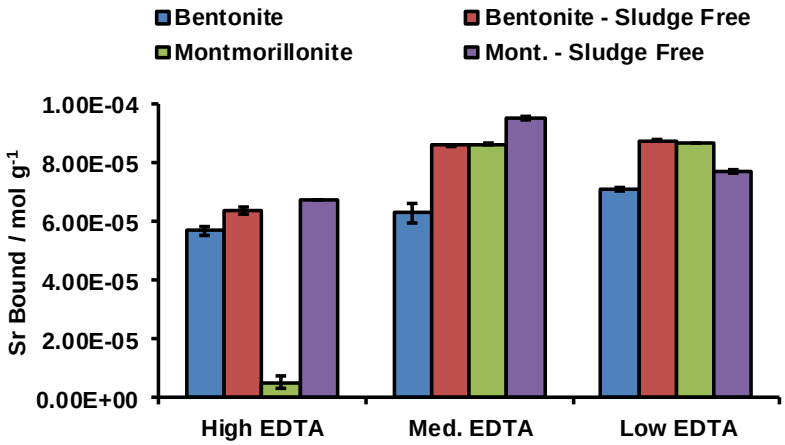

Figure 164. Effect of low simulant Magnox sludge concentration on the sorption of Sr to montmorillonite and bentonite in the presence of EDTA

4.4 Investigations into the Effect of Simulant Magnox Sludge on Cs and Sr Sorption Kinetics with Montmorillonite and Bentonite

The presence of competing ions from simulant Magnox sludge on sorption kinetics was studied. Two simulant sludge concentrations were chosen for the experiments, high and low, and results were compared to those obtained for a sludge free system.

4.4.1 Experimental Method

Solutions of 2000:1 and 50:1 equilibrated simulant Magnox sludge liquor were initially prepared. Batch sorption experiments were carried out by placing 20 cm^3 of the required simulant Magnox sludge solution in 50 cm^3 centrifuge vials with 0.1 g of montmorillonite or bentonite. To these centrifuge vials, 200 µl of $CsNO_3$ or $Sr(NO_3)_2$ (concentration of 1 x 10^{-2} mol dm^{-3} establishing a final cation concentration of 1 x 10^{-4} mol dm^{-3}) and 100 µl of ^{137}Cs or ^{85}Sr were added. Samples were then thoroughly mixed with a whirlimixer and placed on an orbital shaker for the required amount of time, ranging from 1 hour to 14 days, at 100 rpm.

After the required time, the samples were centrifuged at 6000 rpm for 20 minutes and the supernatant then decanted. 2 cm^3 of supernatant was filtered through a 0.45 µm syringe filter and the gamma radiation counted with a Packard Cobra II Auto Gamma counter. pH of the remaining supernatant was recorded.

4.4.2 Results

Kinetic Studies into the Sorption of Cs to Montmorillonite in the Presence of Simulant Magnox Sludge

The presence of simulant Magnox sludge does not appear to have an effect on the sorption kinetics for Cs and montmorillonite, although equilibrium appears to be slightly slower with high sludge concentration, as the value at 168 hours is still lower than that at 264, Figure 165.

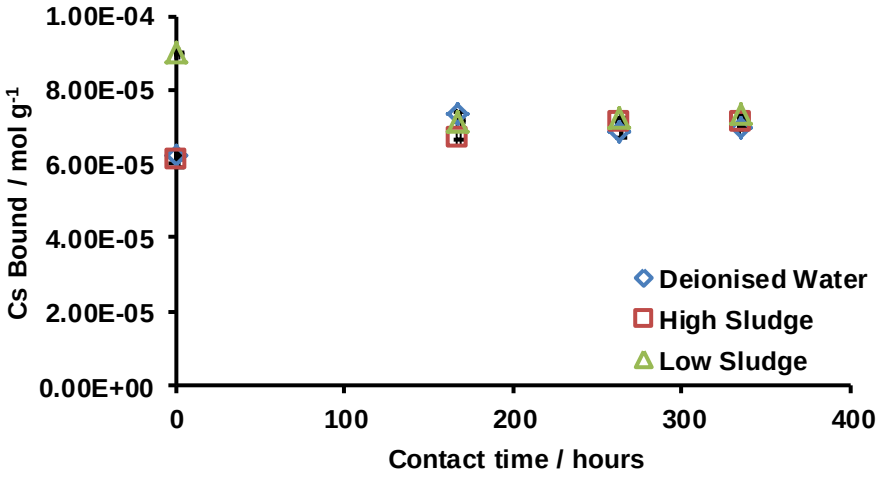

Figure 165. Kinetic studies into Cs (1 x 10^{-4} mol dm^{-3}) sorption to montmorillonite in the presence of simulant Magnox sludge. Experiments carried out with a solid:liquid ratio of 1:200, equilibrating *ca.* 7 days at room temperature. Three replicates per sample

Kinetic Studies into the Sorption of Sr to Montmorillonite in the Presence of Simulant Magnox Sludge

Kinetic investigations into strontium sorption to montmorillonite in the presence of simulant Magnox sludge shows that in the presence of a high sludge concentration, equilibrium appears to be slower than that of the instantaneous equilibrium of the other systems, Figure 166.

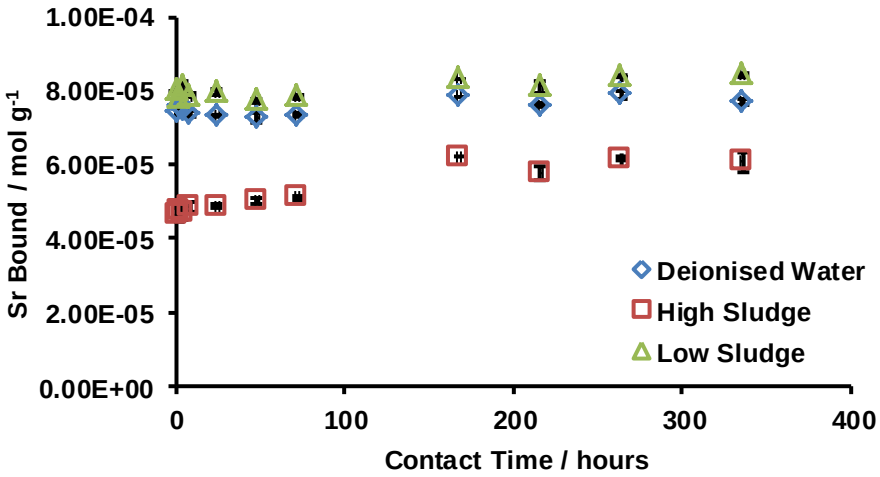

Figure 166. Kinetic studies into Sr (1 x 10^{-4} mol dm^{-3}) sorption to montmorillonite in the presence of simulant Magnox sludge. Experiments carried out with a solid:liquid ratio of 1:200, equilibrating *ca.* 7 days at room temperature. Three replicates per sample

Kinetic Studies into the Sorption of Cs to Bentonite in the Presence of Simulant Magnox Sludge

Kinetic investigations into Cs sorption to bentonite in the presence of simulant Magnox sludge showed that the presence of sludge resulted in instantaneous sorption of Cs whereas the process is slower in a sludge free system, Figure 167.

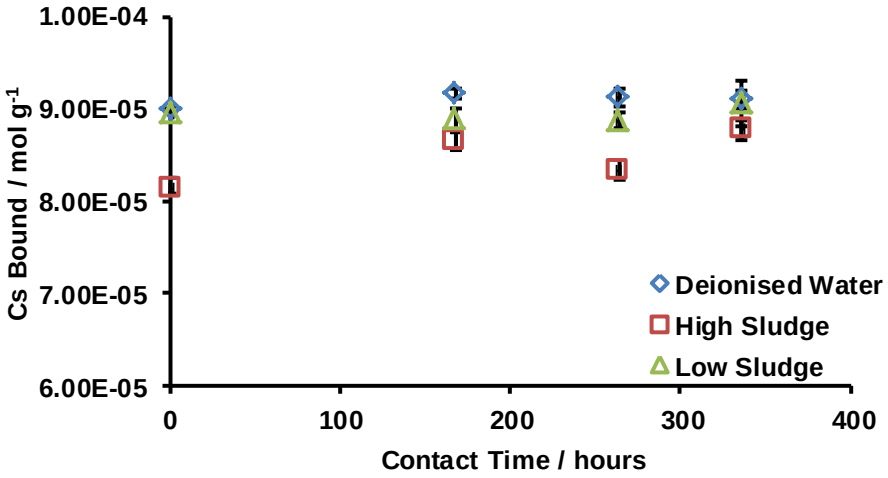

Figure 167. Kinetic studies into Cs (1×10^{-4} mol dm^{-3}) sorption to bentonite in the presence of simulant Magnox sludge. Experiments carried out with a solid:liquid ratio of 1:200, equilibrating *ca.* 7 days at room temperature. Three replicates per sample

Kinetic Studies into the Sorption of Sr to Bentonite in the Presence of Simulant Magnox Sludge

From the kinetic investigations into strontium sorption to bentonite in the presence of simulant Magnox sludge, it can be seen that there was no change in the time it took for sorption to reach equilibrium, with equilibrium being instantaneous for all systems investigated, Figure 168.

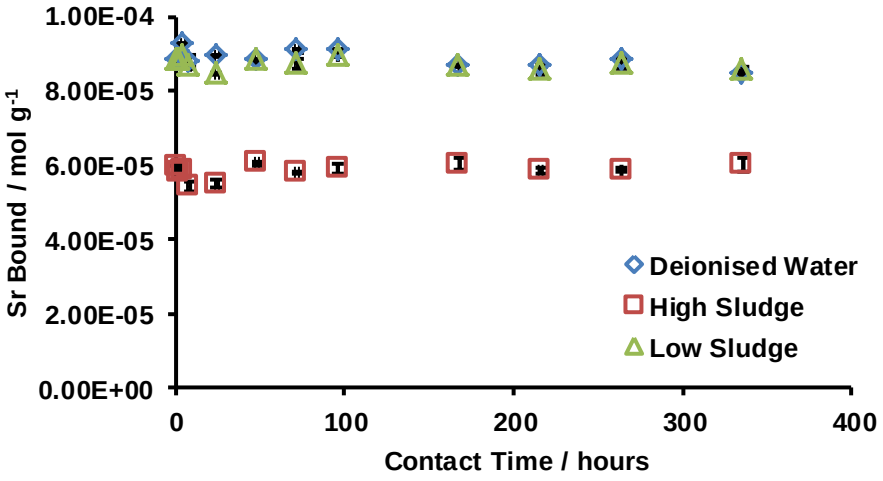

Figure 168. Kinetic studies into Sr (1 x 10^{-4} mol dm^{-3}) sorption to bentonite in the presence of simulant Magnox sludge. Experiments carried out with a solid:liquid ratio of 1:200, equilibrating *ca.* 7 days at room temperature. Three replicates per sample

4.5 Conclusions

The presence of simulant Magnox sludge was found to not have an effect on Cs sorption to montmorillonite or bentonite, but did cause the sorption of Sr to montmorillonite and bentonite to decrease at medium and high simulant sludge concentrations. The Mg present in the solutions from the simulant Magnox sludge is a divalent cation like Sr so will be directly competing for the same sorption sites, unlike the monovalent Cs cation. As the Mg concentration in solution increases, the Sr sorption decreases showing an exchange preference for Mg over Sr by the clay minerals.

The quaternary systems compared the effect of introducing simulant Magnox sludge equilibrated water into a system where anthropogenic ligands were present. The results were compared with the data collected in chapter 3. From the comparison of these results, the following is concluded:

Quaternary Systems Featuring Picolinic Acid and Simulant Magnox Sludge

- There is no effect on the sorption of Cs to montmorillonite.
- Sorption of Cs to bentonite slightly decreases.
- Sorption of Sr to montmorillonite and bentonite decreases.

Quaternary Systems Featuring NTA and Simulant Magnox Sludge

- There is little or no effect on Cs sorption to bentonite and montmorillonite when NTA concentration is high.
- As NTA concentration decreases, Cs sorption decreases with increases simulant sludge concentration.
- Sr sorption to montmorillonite and bentonite does not change at high NTA concentration.
- Sr sorption decreases with increasing simulant sludge concentration as the NTA concentration decreases.

Quaternary Systems Featuring EDTA and Simulant Magnox Sludge

- At high EDTA concentration, sorption of Cs to bentonite and montmorillonite slightly increases.
- Cs sorption appears to decrease, for both montmorillonite and bentonite, at medium EDTA concentrations but there is no change observed at low EDTA concentrations.

- Sr sorption decreases for both bentonite and montmorillonite across all EDTA concentration ranges studied.
- The most significant Sr sorption decrease observed occurs when EDTA concentration is high.

The sorption kinetics for Cs sorption to montmorillonite and bentonite showed that the presence of simulant Magnox sludge did not have any effect. Equilibrium does appear to take longer for Sr sorption to montmorillonite at high simulant sludge concentrations, though this effect is not significant. There is no real change observed in the sorption kinetics for Sr sorption to bentonite.

Chapter 5: Effect of Organic Hydrocarbons on Cs and Sr Sorption Behaviour to Montmorillonite and Bentonite

5.1 Introduction

Several environmental factors are widely considered to affect the mobility, bioavailability and biodegradability of synthetic organic compounds in the environment. Sorption of these synthetic organic compounds often exerts a significant influence on the fate of these compounds[146].

The sorption of an organic compound depends on many parameters including its physical and chemical properties and the nature of the adsorbent. One of the most important properties of organic compounds which influences their sorption is their solubility in water. If a clay mineral has metal cations in the exchange sites, its surface is hydrophilic and is often not a good adsorbent for poorly water-soluble organic species which cannot compete with highly polar water for adsorption on the clay mineral surface[147]. Adsorption of non-ionic compounds on montmorillonite can be enhanced by replacing the inorganic cations by larger cationic surfactants[148,149,150]. Chiou et al deduced that the more a non-ionic compound is soluble the less it will be adsorbed, suggesting that the uptake of neutral organic chemicals by soil is essentially a process of partitioning rather than physical adsorption[151].

A number of boreholes, primarily located down-hydraulic gradient from the Separation Area at Sellafield, have shown evidence for pollution of ground water by organic chemicals such as trichloroethene (TCE) and polyaromatic and petroleum hydrocarbons[1].

5.2 Hydrocarbons Investigated

5.2.1 Tricholroethene (TCE)

Chlorinated ethenes such as perchloroethene (PCE) and trichloroethene (TCE), are amongst the most frequent contaminants found in soil and ground water due to their extensive and widespread use as cleaning agents and metal degreasers[152] and as such are an Environmental Protection Agency (EPA) priority pollutant[153]. It is also an ingredient in adhesives, paint removers, rug-cleaning fluids, spot removers and pepper sprays[154]. In 2004, it was reported that chlorinated ethenes were by far the most common group of organic contaminants at sites prioritised for remediation in the US[155]. The molecular structure of TCE can be seen in Figure 169.

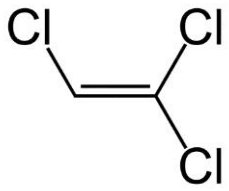

Figure 169. Structure of trichloroethene (TCE)

TCE is resistant to biodegradation in aerobic subsurface environments resulting in their persistence in polluted ground waters[156]. It is a volatile compound which causes irritation to the eyes and throat, can cause headaches, dizziness and difficulty with concentrating. Drinking water contaminated with small amounts of TCE may, over a length of time, cause liver and kidney damage, impaired immune system and is linked to possible birth defects. In animal studies, TCE has been linked to liver, kidney and lung cancers therefore it is regarded as being highly likely to be carcinogenic to humans[154].

Due to the abundance of TCE in the environment, a number of studies into the chemical behaviour and fate of TCE in the environment have been undertaken, primarily bioremediation techniques aimed at degrading TCE in ground water[157,158]. Tao et al. (1999) investigated the effect of montmorillonite on the photodecomposition of TCE at the air/soil interface[153]. In their study they found that the Ca-montmorillonite catalysed photodecomposition of TCE occurred over a period of days with dichloroacetic acid as the major photooxidation product found. They hypothesised that due to the layered silicate structure and cation exchange properties of montmorillonite

clays, the clays can have oxidising centres that initiate free radical processes and thus decomposition of TCE occurs.

Estes and Vilker (1989) discovered that inorganic minerals oxides – silica and montmorillonite – were able to absorb TCE in an aqueous environment. The suggested mechanism of sorption of TCE to montmorillonite was electron transfer however the exact mechanism of the reaction between TCE and the montmorillonite surface was unknown. The sorption to montmorillonite was found to be irreversible[159].

Another study carried out by Estes et al. (1988) noticed that a lack of equilibrium for TCE adsorption by montmorillonite clay could have been due to either:

- The clay surface is slowly changed during contact with the solution so that new sorption sites are continually being exposed.
- The overall process of TCE mass transfer to sorption sites and the sorption reaction is very slow[160].

5.2.2 Toluene

Toluene is a common solvent widely used in industry to dissolve paints, adhesives, rubber, lacquers and disinfectants. The major use of toluene is as a mixture added to gasoline to improve octane ratings. It is also used in the synthesis of trinitrotoluene (TNT) where it is nitrated with a mixture of sulfuric and nitric acid to produce mononitrotoluene (MNT). The MNT is separated and then renitrated to dinitrotoluene (DNT). This DNT is further nitrated to form TNT using an anhydrous mixture of nitric acid and fuming sulfuric acid. The molecular structure of toluene is shown in Figure 170.

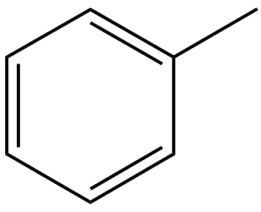

Figure 170. Structure of toluene

Toluene is a major component of wastewater from petroleum refineries[161] and thus there have been a number of investigations into toluene behaviour in the environment. Shih and Wu (2004) discovered that under dry clay conditions, toluene sorption to montmorillonite clays was higher than that on humid ones. They reported that under

dry conditions, montmorillonite clay provides more surfaces to toluene molecules than it does under wet conditions[162].

The sorption of toluene on montmorillonite has been reported to be irreversible and that sorption of this aromatic compound by smectite clays was a physical phenomenon[163]. The irreversibility found in Ca-montmorillonite was reported to result from the chemical bindings and the entrapment of toluene by the structural stereo-hindrance of nano- or micropores in montmorillonite[162].

As TNT was originally produced on the Sellafield site up until 1946, residual contamination derived from this period may be present in soils and drift. Due to extensive site redevelopment, any contamination from this period may have been diluted and widely dispersed.

5.2.3 Naphthalene

Naphthalene is one of a large number of non-ionic contaminants found in soils, surface sediments and ground water.

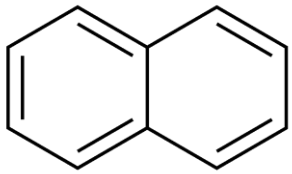

Figure 171. Structure of naphthalene

Magdaliniuk et al. (1995) investigated the sorption of naphthalene to purified Na-montmorillonite and found no significant difference between the control curve meaning that naphthalene was not adsorbed to montmorillonite clay. It was also reported that montmorillonite complex particles appear to interfere with the degradation of naphthalene as the montmorillonite particles are smaller than the bacteria used for biodegradation of naphthalene, essentially forming a ‘shield’ between the naphthalene and bacteria[146].

5.3 Time Dependent Studies – Investigations into the Effect of Hydrocarbon Contact Time on the Sorption of Cs and Sr to Montmorillonite and Bentonite

5.3.1 Introduction

The aim of the following experiments was to investigate the effect of hydrocarbon residence time on the sorption of Cs and Sr to montmorillonite and bentonite. It is believed that over a long period of time the presence of contaminants, such as toluene, TCE and naphthalene, may alter the surface of the clay minerals and thus have an impact on the sorption of cations to the clay minerals.

5.3.2 Experimental Method

20 cm^3 of trichloroethene (99+ %), toluene (99+ %) or naphthalene (approximately 2 x 10^{-4} mol dm^{-3}) was added to 0.1 g of montmorillonite or bentonite in 20 cm^3 glass vials. The samples were thoroughly mixed with a whirlimixer and then placed on an orbital shaker at 100 rpm for 1 week, 1 month or 3 months.

After the samples were left for the required period of time, the supernatant was decanted and the solid phase was left to dry in a fume cupboard. To each dried sample, 20 cm^3 of deionised water was added along with 200 µl of 1 x 10^{-2} mol dm^{-3} $CsNO_3$ or $Sr(NO_3)_2$ and 100 µl of ^{137}Cs or ^{85}Sr. These vials were thoroughly mixed once more with a whirlimixer, placed on an orbital shaker and then left for 1 week. Each sample was prepared in triplicate with a final activity of 3 kBq per vial.

After 1 week the supernatant was decanted and 2 cm^3 of supernatant was filtered through a 0.45 µm syringe filter ready for gamma counting. The gamma radiation was counted with a Packard Cobra II Auto Gamma counter.

5.3.3 Results

The Effect of Hydrocarbon Residence Time on Cs Sorption to Montmorillonite

The effect of TCE, toluene and naphthalene residence time on Cs sorption to montmorillonite can be seen in Figure 172. It appears that TCE has the greatest effect on Cs sorption with Cs sorption decreasing by 35 % after 3 months when compared to the 1 week results. Toluene and naphthalene do not appear to have a negative effect on Cs sorption to montmorillonite after 3 months residence time, although there does

appear to be a minor increase in sorption of Cs to montmorillonite for both naphthalene and toluene.

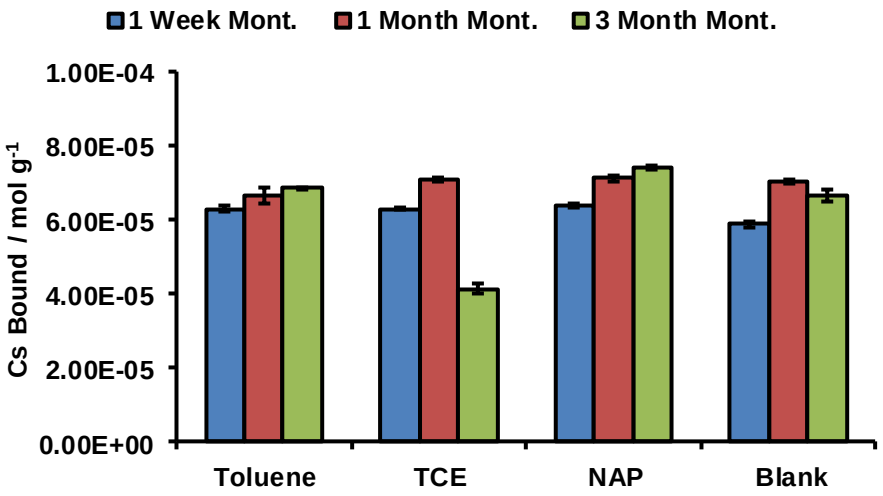

Figure 172. Effect of organic contaminants on the sorption of Cs (1×10^{-4} mol dm^{-3}) to montmorillonite. Experiments carried out with a solid:liquid ratio of 1:200, equilibrating *ca.* 7 days at room temperature. Three replicates per sample

The Effect of Hydrocarbon Residence Time on Sr Sorption to Montmorillonite

The effect of TCE, toluene and naphthalene residence time on Sr sorption to montmorillonite can be seen in Figure 173. Like with Cs sorption to montmorillonite, it appears that TCE has the greatest effect on the sorption of Sr with a decrease of 42 % observed after 3 months when compared to the 1 week results. There is no change in the behaviour of Sr sorption to montmorillonite after being exposed to toluene and naphthalene, when compared with the results obtained for deionised water only.

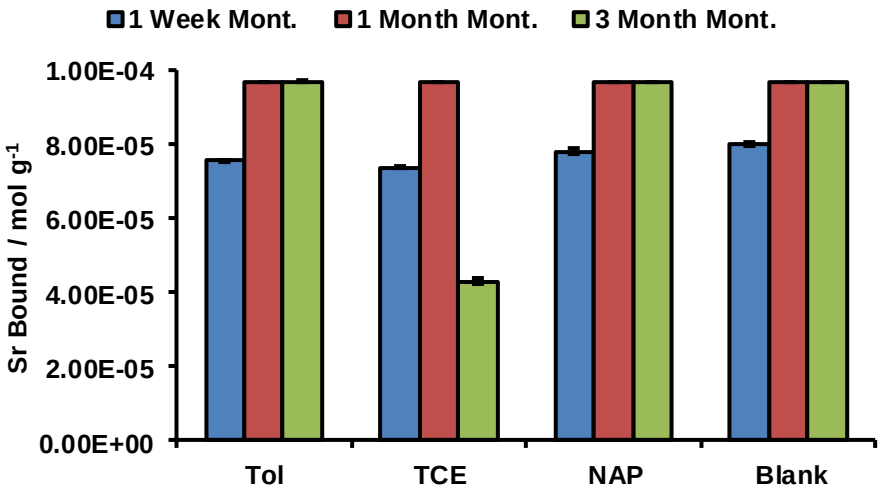

Figure 173. Effect of organic contaminants on the sorption of Sr (1×10^{-4} mol dm^{-3}) to montmorillonite. Experiments carried out with a solid:liquid ratio of 1:200, equilibrating *ca.* 7 days at room temperature. Three replicates per sample

The Effect of Hydrocarbon Residence Time on Cs Sorption to Bentonite

The effect of TCE, toluene and naphthalene residence time on Cs sorption to bentonite can be seen in Figure 174. Overall, there does not appear to be a significant effect on Cs sorption to bentonite after being in contact with TCE, toluene and naphthalene across all residence times investigated.

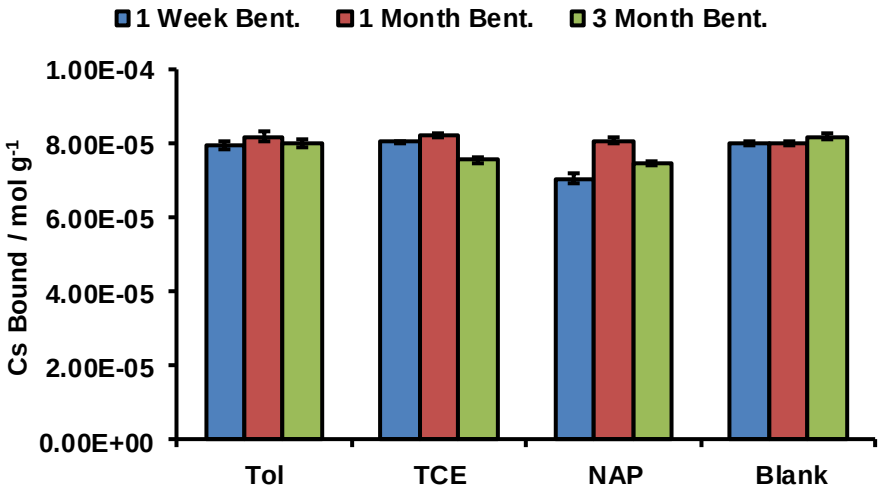

Figure 174. Effect of organic contaminants on the sorption of Cs (1×10^{-4} mol dm^{-3}) to bentonite. Experiments carried out with a solid:liquid ratio of 1:200, equilibrating *ca.* 7 days at room temperature. Three replicates per sample

The Effect of Hydrocarbon Residence Time on Sr Sorption to Bentonite

The effect of TCE, toluene and naphthalene residence time on Sr sorption to bentonite can be seen in Figure 175. Like with Cs sorption to bentonite, there does not appear to be a significant effect on Cs sorption to bentonite after being in contact with TCE, toluene and naphthalene across all residence times investigated.

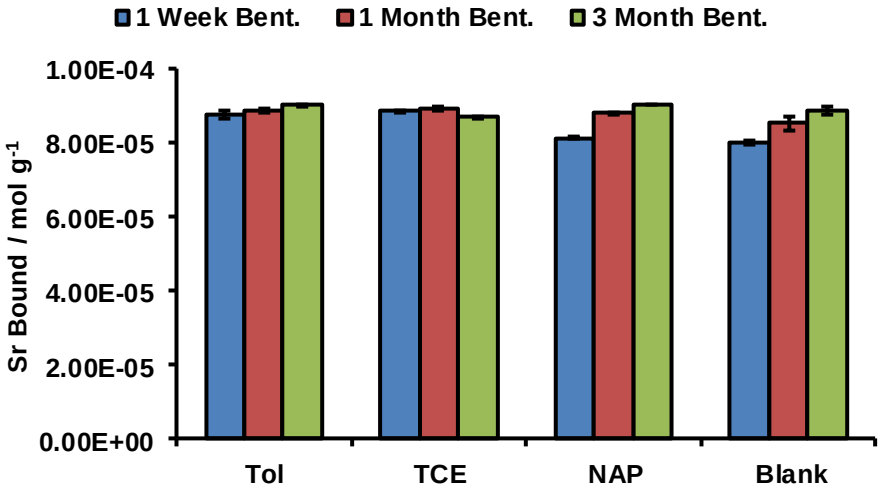

Figure 175. Effect of organic contaminants on the sorption of Sr (1×10^{-4} mol dm^{-3}) to bentonite. Experiments carried out with a solid:liquid ratio of 1:200, equilibrating *ca.* 7 days at room temperature. Three replicates per sample

5.4 PXRD of Hydrocarbon Contact Time on Montmorillonite and Bentonite

The evolution of the clay mineral structure and the formation of any secondary phases were monitored by Powder XRD.

5.4.1 Experimental Method

20 cm^3 of 1 x 10^{-2} mol dm^{-3} of TCE, toluene, naphthalene or deionised water was added to 1 g of clay mineral in a 20 cm^3 glass vial. Samples were thoroughly mixed with a whirlimixer and placed on an orbital shaker at 100 rpm for 1 week, 1 month or 3 months. After the required shaking time, the supernatant was decanted whilst the solid phases were air dried at room temperature in a fume cupboard ready for PXRD.

Samples were mounted in deep well Perspex holders and phase identification was performed using a continuous scan between the 2θ range of 5-75° with a step size of 0.014° over a period of 2 hours 20 minutes.

5.4.2 Results

PXRD of Toluene Residence Time on Montmorillonite Clay

The XRD patterns for toluene residence time appear to be identical with no apparent difference to the initial non-reacted montmorillonite clay even after three months residence time (Figure 176).

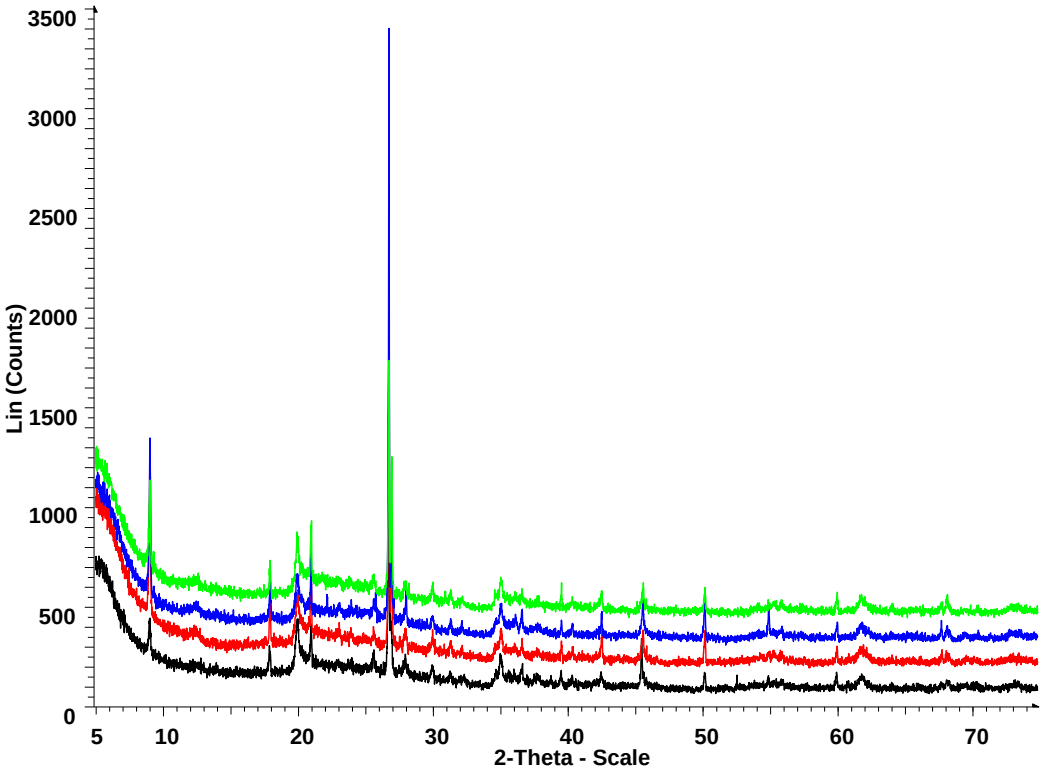

Figure 176. PXRD comparing toluene residence time and its effect on the structure of montmorillonite clay, using Cu K_{a1} radiation between 5 ° and 75 ° with a step size of 0.014 ° and a step time of 1.6 s

PXRD of TCE Residence Time on Montmorillonite Clay

The XRD patterns for TCE residence time appear to be identical with no apparent difference to the initial non-reacted montmorillonite clay even after three months residence time (Figure 177).

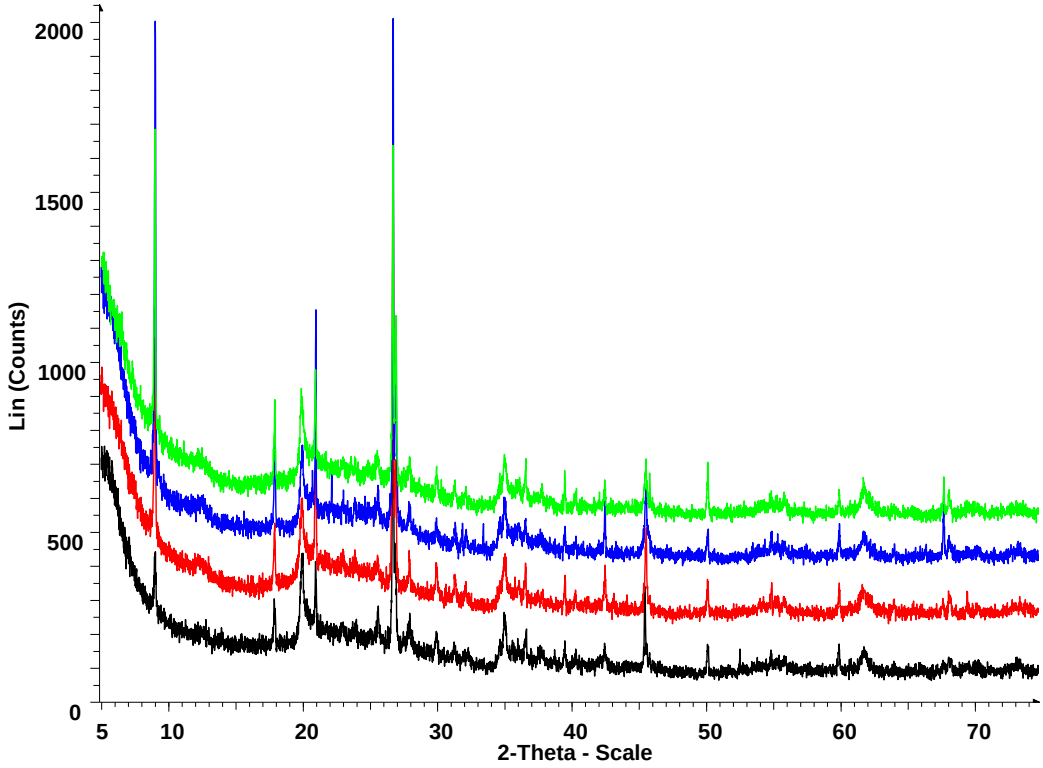

Figure 177. PXRD comparing TCE residence time and its effect on the structure of montmorillonite clay, using Cu K_{a1} radiation between 5 ° and 75 ° with a step size of 0.014 ° and a step time of 1.6 s

PXRD of Naphthalene Residence Time on Montmorillonite Clay

The XRD patterns for naphthalene residence time appear to be identical with no apparent difference to the initial non-reacted montmorillonite clay even after three months residence time (Figure 178).

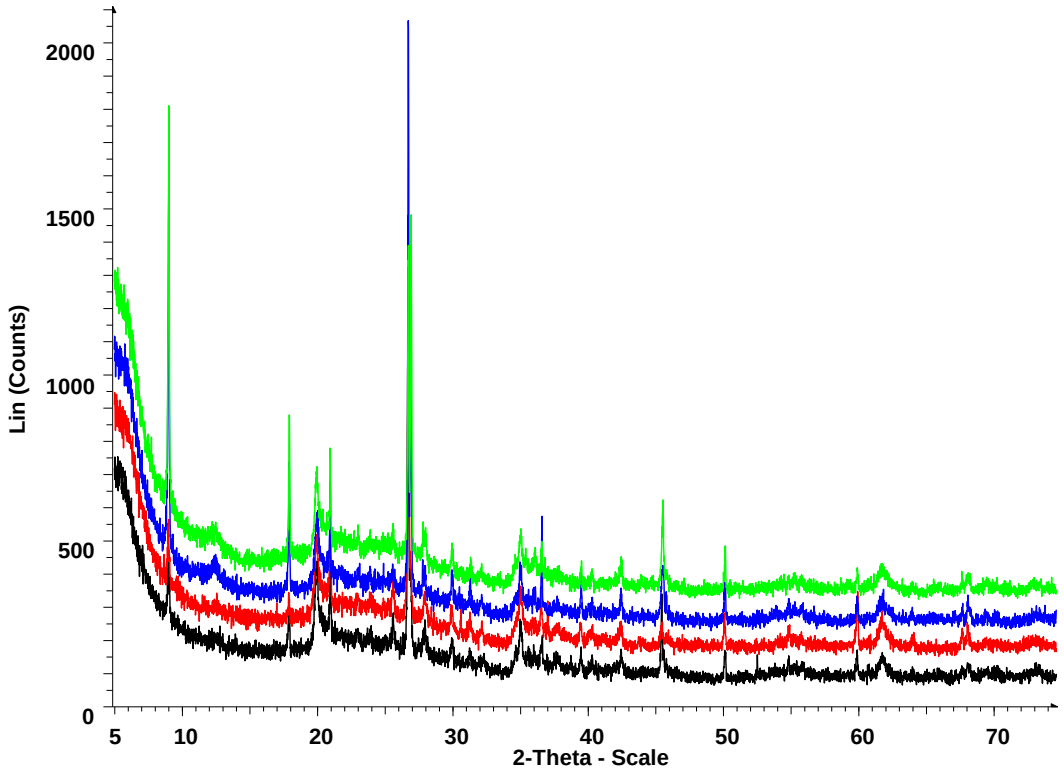

Figure 178. PXRD comparing naphthalene residence time and its effect on the structure of montmorillonite clay, using Cu K_{a1} radiation between 5 ° and 75 ° with a step size of 0.014 ° and a step time of 1.6 s

PXRD of Toluene Residence Time on Bentonite Clay

The XRD patterns for toluene residence time appear to be identical with no apparent difference to the initial non-reacted bentonite clay even after three months residence time (Figure 179).

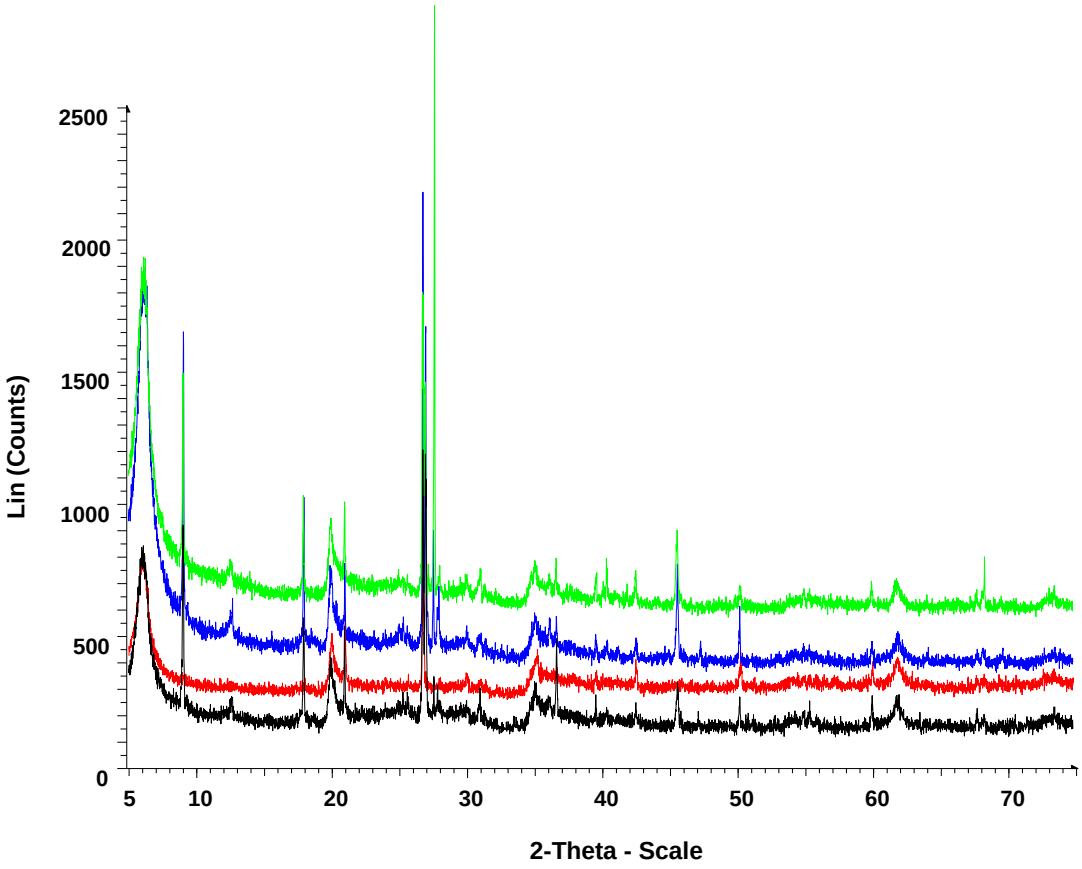

Figure 179. PXRD comparing toluene residence time and its effect on the structure of bentonite clay, using Cu K_{a1} radiation between 5 ° and 75 ° with a step size of 0.014 ° and a step time of 1.6 s

PXRD of TCE Residence Time on Bentonite Clay

The XRD patterns for TCE residence time appear to be identical with no apparent difference to the initial non-reacted bentonite clay even after three months residence time (Figure 180).

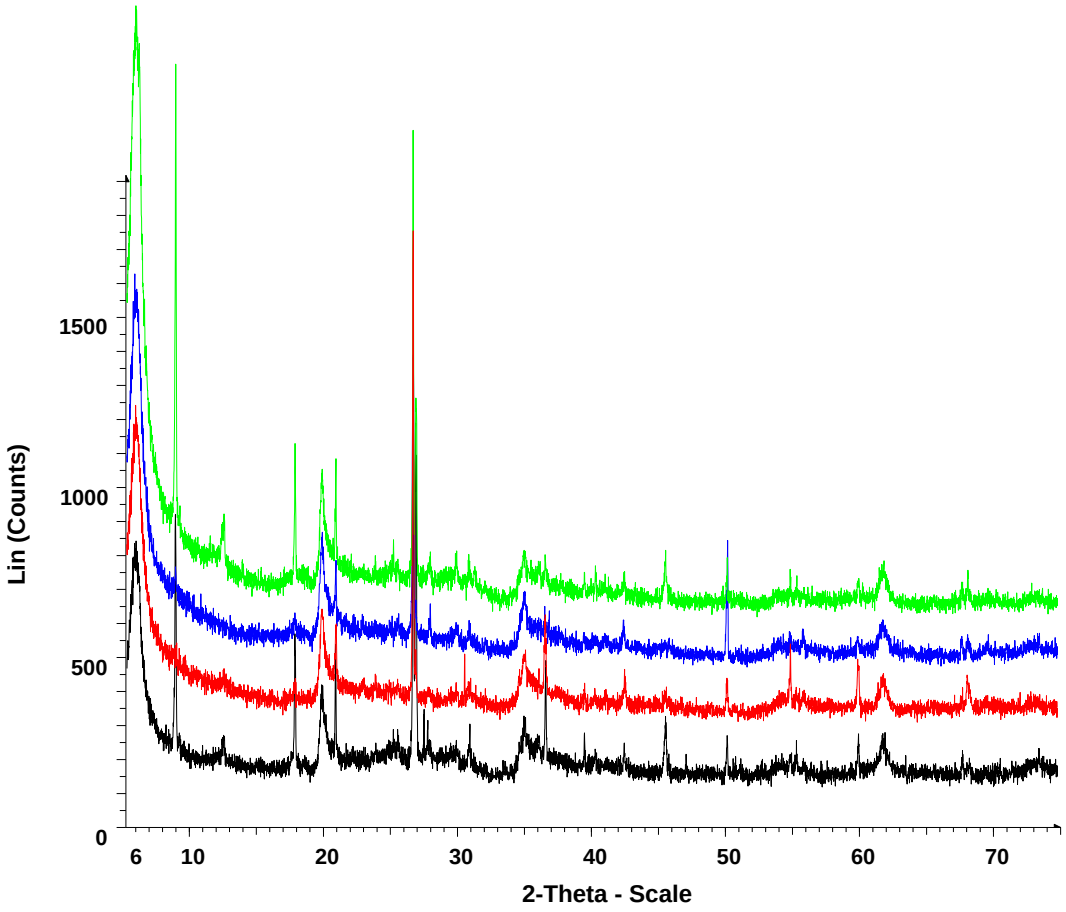

Figure 180. PXRD comparing TCE residence time and its effect on the structure of bentonite clay, using Cu K_{a1} radiation between 5 ° and 75 ° with a step size of 0.014 ° and a step time of 1.6 s

PXRD of Naphthalene Residence Time on Bentonite Clay

The XRD patterns for naphthalene residence time appear to be identical with no apparent difference to the initial non-reacted bentonite clay even after three months residence time (Figure 181).

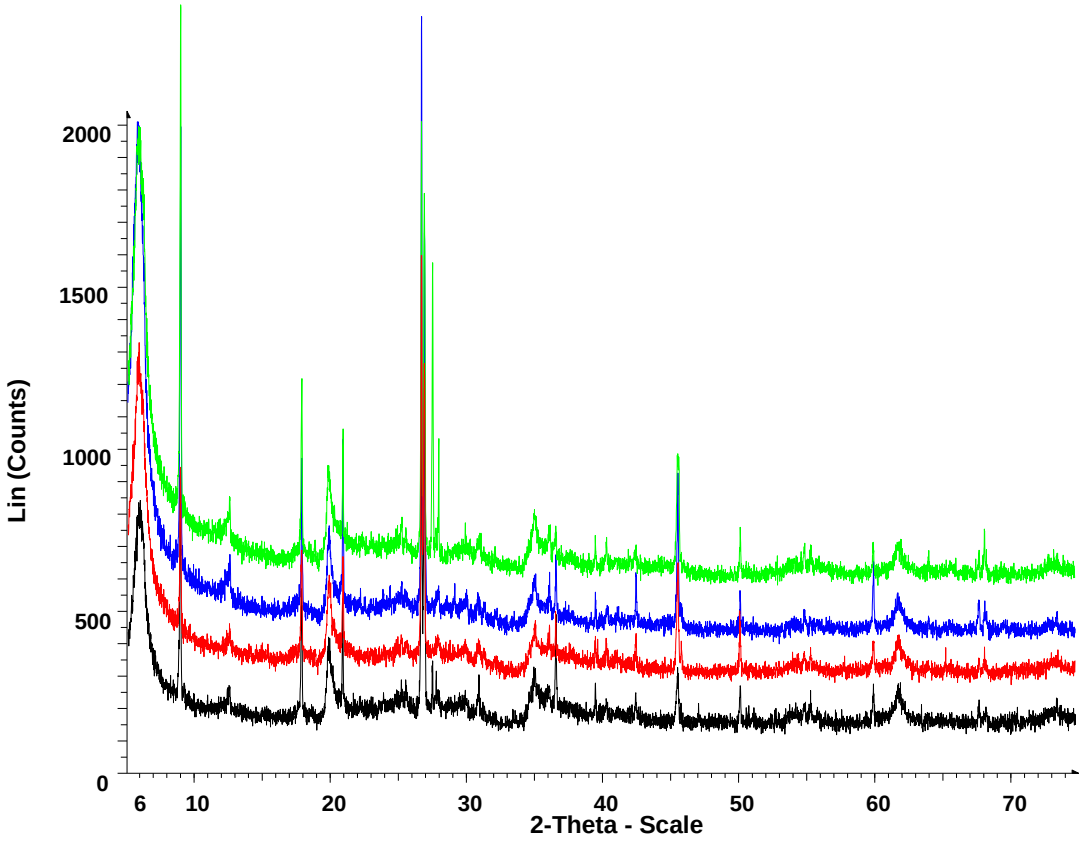

Figure 181. PXRD comparing naphthalene residence time and its effect on the structure of bentonite clay, using Cu K_{a1} radiation between 5 ° and 75 ° with a step size of 0.014 ° and a step time of 1.6 s

5.5 Conclusions

The sorption of Cs and Sr to bentonite and montmorillonite after the clay minerals had been exposed to hydrocarbons for up to 3 months was investigated and the following conclusions were found:

1. Cs Sorption to montmorillonite decreases after the montmorillonite had been in contact with TCE for 3 months. No other changes in Cs sorption to montmorillonite are observed.
2. Sr sorption to montmorillonite decreases after the montmorillonite had been in contact with TCE for 3 months. No other changes in Sr sorption to montmorillonite are observed.
3. There is no real change in Cs sorption to bentonite for all hydrocarbons investigated.
4. There is also no real change in Sr sorption to bentonite for all hydrocarbons investigated.
5. Powder XRD showed no obvious phase changes for all hydrocarbons investigated, including montmorillonite in contact with TCE for 3 months – the only sample to show a difference in sorption behaviour.

The TCE appears to be altering the surface of the montmorillonite after a residence time of 3 months as shown by the changing sorption behaviour. PXRD shows no apparent structural changes in the sample.

Chapter 6: Conclusions and Further Work

6.1 Conclusions and Further Work

This research project was supported by the Sellafield nuclear site where a number of known radioactive leaks to the ground, arising from historical nuclear wastes, are known to have occurred. The most significant of these leaks have occurred from the Magnox Silo, the Caesium Extraction Plant, the Magnox Reprocessing Pump House, the Sludge Storage Tanks, the Burial Pits and the Medium Active Evaporation and Thermal Denitration Plant. From on-site monitoring at Sellafield, long-lived, soluble fission products such as ^{137}Cs and ^{90}Sr have been found to be present in the groundwater and, as such, there is concern due to their potential to impact upon human health. Along with the radioactive contamination, there is expected to be other common components of spent nuclear fuel reprocessing, such as inorganic salts and solvents, along with industrial contaminants such as fuel, oils and organic compounds present in the storage ponds and groundwater.

The aim of this PhD project was to investigate the impact caused by contaminants predicted to be present in Magnox fuel storage ponds and groundwater at Sellafield, may have on the migration of Cs and Sr through the natural environment. Using montmorillonite and bentonite clays to mimic the immediate ground beneath the storage ponds, and organic compounds commonly used in industrial processes, batch sorption experiments were carried out in order to investigate any changes in the migration behaviour.

The first step was to understand the composition of the clay minerals used within this thesis, which required characterisation of the samples. Using elemental analysis followed by XRD, the montmorillonite K10 sample was found to have three dominant phases; quartz, muscovite magnesian and montmorillonite. The bentonite sample was found to have the same three phases characterised in the montmorillonite sample, along with a fourth phase characteristic of kaolinite. Both clays exhibited moderate swelling behaviour with swelling capacities of 21 cm^3 / 10 g for montmorillonite and 22 cm^3 / 10 g for bentonite, whilst the cation exchange capacity of bentonite was found to be almost three times as great as that of montmorillonite.

Initial sorption experiments found that both montmorillonite and bentonite displayed significant Freundlich behaviour for caesium and strontium sorption. Langmuir isotherms plotted for the same sorption data also showed strong correlation for all systems studied, however the sorption data was better modelled by the Freundlich equation than by the Langmuir equation. When data fits the Freundlich model better than the Langmuir model, it is supposed that the extra assumptions required for the

Langmuir model are not valid, i.e. the substrate is not homogeneous with respect to the bonding energy of sites and that desorption does takes place. From analysis of the Freundlich isotherms, all values of n were found to be > 1 meaning the sorption of Cs and Sr to montmorillonite and bentonite clays is deemed favourable. The Langmuir model predicted maximum sorption capacities of 8.42×10^{-5} mol g^{-1} and 8.69×10^{-5} mol g^{-1} for Cs and Sr sorption to montmorillonite, and 1.49×10^{-4} mol g^{-1} and 3.96×10^{-4} mol g^{-1} for Cs and Sr sorption to bentonite.

With regard to sorption kinetics, the equilibration of Cs and Sr in a binary system with bentonite, and Sr with montmorillonite was found to be instantaneous, whereas Cs equilibration with montmorillonite was slower. Ternary kinetic experiments showed that there was no change in the equilibration time when anthropogenic organic ligands were added to the system for both Cs and Sr sorption to montmorillonite and bentonite. As with the introduction of anthropogenic organic ligands, no significant changes were observed in the sorption kinetics for ternary systems containing simulant Magnox sludge across all simulant Magnox sludge concentration ranges investigated.

Investigations into how the pH of a system affected the sorption of Cs or Sr showed some interesting variations. The sorption of Cs to both montmorillonite and bentonite increased with increasing pH. This trend was also observed with Sr sorption to bentonite, but Sr sorption to montmorillonite was found to be independent of pH. This suggests that strontium is only involved in exchange reactions with the montmorillonite clay. Investigations into how the pH influences the sorption of Cs and Sr in ternary systems containing anthropogenic organic ligands produced some further interesting results. In ternary systems with Sr and montmorillonite, the presence of picolinic acid had no effect on the sorption of Sr when compared with results obtained from a simple binary system, conversely, when EDTA or NTA are present, the amount of Sr sorption to montmorillonite decreases with increasing pH. This is consistent with anionic adsorption behaviour where Sr ternary complexes are strongest at low pH and decrease as the pH increases. This behaviour was different to that observed for ternary systems with Sr sorption to bentonite. The degree of Sr sorption when NTA or EDTA was present in the system was independent of pH with no change in sorption observed as pH increased. Ternary systems with bentonite, Sr and picolinic acid followed the same trend as the simple binary system; sorption increased with increasing pH. The sorption of Cs to montmorillonite or bentonite in ternary systems showed no significant changes when compared with the data from the binary experiments.

From investigations into the impact of anthropogenic organic ligands on metal ion sorption, the organic ligands were found to reduce the amount of Sr sorption occurring to both montmorillonite and bentonite, but only when the concentration of the organic ligand in the system was high (1×10^{-2} mol dm^{-3}). NTA appeared to have the greatest effect on the amount of Sr sorption occurring with both montmorillonite and bentonite. Cs sorption to bentonite and montmorillonite did not appear to be affected by the presence of anthropogenic organic ligands at all ligand concentrations investigated. The absence of any real effect on Cs sorption to both clay minerals can be explained by their corresponding low stability constants. The low stability constants for Cs-ligand complexes suggests sorption of the metal ion to the clay mineral is favoured over the formation of complexes with the ligand.

After investigating the effects that anthropogenic organic ligands had on the sorption of Cs and Sr in Chapter 3, simulant Magnox sludge was introduced to the system in order to investigate how sludge, present in the Magnox storage ponds at Sellafield, influenced Cs and Sr sorption behaviour. Results from ternary investigations showed that Cs sorption to both montmorillonite and bentonite was independent of simulant Magnox sludge across all sludge concentrations investigated. Unlike Cs sorption, Sr sorption to montmorillonite and bentonite was found to be influenced by the presence of simulant Magnox sludge at high (50:1 deionised water:sludge) and medium (200:1 deionised water:sludge) simulant sludge concentrations. No change in Sr sorption was observed at low (2000:1 deionised water:sludge) sludge concentrations.

Quaternary systems involving bentonite or montmorillonite, Cs or Sr, anthropogenic organic ligands and simulant Magnox sludge were undertaken in order to see if the sorption behaviour that was previously reported in Chapter 3, changed with the presence of the simulant sludge. From batch sorption experiments, it was found that simulant Magnox sludge had a greater impact on reducing Sr sorption to both bentonite and montmorillonite for the quaternary systems compared to Cs. Results showed that Sr sorption decreased across all quaternary systems, most significantly when EDTA was present, whereas ternary investigations had found the presence of NTA to have the greatest influence on Sr sorption behaviour. Cs does not appear to be affected by the presence of simulant Magnox sludge in the quaternary systems when compared with the ternary system results. It is expected that the presence of divalent Mg ions in solution from the simulant Magnox sludge are directly competing with the divalent Sr ions. Cs is unaffected by the presence of divalent Mg cations as it is a monovalent cation.

It has been suggested that increasing the residence time of metals reduced desorption from soils and their potential bioavailability. Over long periods of time, a continuous decrease in dissolution rates of smectite minerals has been observed in a number of reports, which decreases the percentage of available reactive edge sites. At Sellafield, there have been periods of extended storage times where the spent nuclear fuel has been stored in Magnox ponds leading to a number of radioactive contamination issues. Investigations into the effect of anthropogenic organic ligand residence time were carried out and appeared to show that the sorption of Cs and Sr to montmorillonite and bentonite, decreased with increasing residence time. ICP-OES analysis of leachates showed an increase in metal ions in solution after three months, in particular silicon. It appears that the aging of montmorillonite and bentonite over a period of three months resulted in a decrease in available sorption sites for both clays. PXRD was used to analyse the clays in order to determine if any phase changes occurred over three months but the diffraction patterns appeared to be negative. The changes observed in sorption behaviour would appear to be due to surface alterations and not phase changes. Unfortunately PXRD is a good technique for phase identification but is not sensitive enough for surface analysis. In future a good surface analysis technique, such as Secondary Ion Mass Spectrometry (SIMS), should be used as this would hopefully show any changes in the clay morphology that PXRD was unable to do.

From the research presented and discussed in this thesis, it has been shown that the presence of both anthropogenic organic ligands and simulant Magnox sludge reduces the amount of metal ion sorption to montmorillonite and bentonite. The results show that there does not appear to be a difference in the sorption behaviour between montmorillonite and bentonite. As bentonite is essentially 75 % montmorillonite with the remaining 25 % consisting of impurities arising from cation exchange, and with no observable differences between the two clay minerals, it can be assumed that the results presented in this thesis are effects associated with the montmorillonite fraction. Bentonite clays are commonly used throughout the nuclear industry but the clays vary significantly in composition from region to region. This thesis has shown that it is the montmorillonite fraction which dictates the sorption behaviour of Cs and Sr under a number of conditions and as such, these results may have a wider industrial use. In future, to try and understand the sorption processes occurring in the batch sorption experiments carried out in this thesis, speciation and sorption modelling should be undertaken. Modelling will provide an understanding of the species present in the sorption systems and will enable us to predict future sorption behaviour under a number of different conditions, mimicking the conditions found across nuclear sites.

References

1. Hunter, J. *SCLS Phase 1-Conceptual model of contamination below ground at Sellafield*. 1–47 (2004). at <http://scholar.google.com/scholar?hl=en&btnG=Search&q=intitle:SCLS+Phase+1+–+Conceptual+Model+of+Contamination+Below+Ground+at+Sellafield#0>

2. Choppin, G. R., Liljenzin, J. O. & Rydberg, J. *Radiochemistry and Nuclear Chemistry*. (Butterworth-Heinemann, 2002).

3. Nero, A. V. *A Guidebook to Nuclear Reactors*. (University of California Press, 1979). at <http://books.google.co.uk/books?id=O0YB-T9usjIC>

4. Wiles, D. *The chemistry of nuclear fuel waste disposal*. (2002). at <http://books.google.com/books?hl=en&lr=&id=wnlk7g3QUrIC&oi=fnd&pg=PR3&dq=The+Chemistry+of+Nuclear+Fuel+Waste+Disposal&ots=Ls_FvzrADP&sig=SlUr7AnM6OMKdT22xyf2agBzdnE>

5. Wilson, P. D. *The Nuclear Fuel Cycle: From Ore to Wastes*. (Oxford University Press, 1996).

6. Rudling, P., Strasser, A., Garzarolli, F. & van Swam, L. Welding of Zirconium Alloys. *IZNA7 Spec. Top. Rep. Weld. Zircon. Alloy.* (2007).

7. Power Generation. at <http://www.physics.ohio-state.edu/~wilkins/energy/Resources/Lectures/nucplant-land.html>

8. Nuclear Power Plants. at <http://www.solcomhouse.com/nuclearpowerplants.htm>

9. File:Magnox reactor schematic.png. at <http://commons.wikimedia.org/wiki/File:Magnox_reactor_schematic.png>

10. Magnox Reprocessing. at <http://www.sellafieldsites.com/solution/spent-fuel-management/magnox-reprocessing/>

11. Keshmiri, A. Three-dimensional simulation of a simplified advanced gas-cooled reactor fuel element. *Nucl. Eng. Des.* **241,** 4122–4135 (2011).

12. File:AGR reactor schematic.png. at <http://commons.wikimedia.org/wiki/File:AGR_reactor_schematic.png>

13. Bayliss, C. & Langley, K. *Nuclear Decommissioning, Waste Management, and Environmental Site Remediation*. (Elsevier Science, 2003). at <http://books.google.co.uk/books?id=j2ehiQgVgY4C>

14. Ojovan, I. & Lee, W. E. *An Introduction to Nuclear Waste Immobilisation*. (Elsevier Science, 2010). at <http://books.google.co.uk/books?id=vQkQnmo_bE0C>

15. Multi-Barrier System for Disposal. at <http://www.sck.be/var/plain_site/storage/images/media/images/ehs_disposal/multibarrier_system_for_disposal/21170-8-eng-GB/multibarrier_system_for_disposal.jpg>

16. Engineered Barrier Systems (EBS): Design Requirements and Constraints. in (NEA, 2004). at <http://www.oecd-nea.org/rwm/reports/2004/nea4548-ebs.pdf>

17. Chapman, N. A., McKinley, I. G. & Hill, M. D. *The geological disposal of nuclear waste*. (J. Wiley, 1987). at <http://books.google.co.uk/books?id=3QdSAAAAMAAJ>

18. Hands, B. J. UK (BNFL) practices on wet fuel storage at Sellafield. in *IMechE Conf. Trans.* **7,** 151–160 (MECHANICAL ENGINEERING PUBLICATIONS, 1996).

19. Berkhout, F. *Radioactive Waste: Politics and Technology*. (Routledge, Chapman & Hall, Incorporated, 1991). at <http://books.google.co.uk/books?id=zl3QmAEACAAJ>

20. Institution of Mechanical Engineers (Great Britain). Nuclear Energy Committee. *Storage in Nuclear Fuel Cycle - IMechE Conference*. (Wiley, 1996). at <http://books.google.co.uk/books?id=wqWFQgAACAAJ>

21. Ma, B., Oh, S., Shin, W. S. & Choi, S.-J. Removal of Co2+, Sr2+ and Cs+ from aqueous solution by phosphate-modified montmorillonite (PMM). *Desalination* **276,** 336–346 (2011).

22. Francis, A. C. & Griffiths, C. J. *The Characterisation of B30 Pond Sludge (1988 Samples) at AEE Winfrith*. 1–21 (1989).

23. Pöyry Energy Limited. *The 2007 UK Radioactive Waste Inventory*. 1–132 (2008).

24. AC03611317, A. Safe enclosure of nuclear facilities during deferred dismantling. *IAEA Saf. Rep.* **26,** (2002).

25. Waggoner, M. A. Radioactive Decay of Cs137. *Phys. Rev.* **82,** 906–909 (1951).

26. KASE, T., KONASHI, K., TAKAHASHI, H. & HIRAO, Y. Transmutation of Cesium-137 Using Proton Accelerator. *J. Nucl. Sci. Technol.* **30,** 911–918 (1993).

27. Argonne National Laboratory. Strontium. 1–2 (2005).

28. Woods, M. J., Baker, M. I., Tyler, D. K. & Chari, K. Comparison of strontium-89 solution sources in UK hospitals, 2003. *Appl. Radiat. Isot.* **64,** 1375–9 (2006).

29. Blake, G. M. *et al.* Strontium-89 therapy: measurement of absorbed dose to skeletal metastases. *J. Nucl. Med.* **29,** 549–57 (1988).

30. Emmerich, W. & Kurbatov, J. Disintegration of the Ground-State Sr85 and Metastable Energy Level of 514 Kev in Rb85. *Phys. Rev.* **85,** 149–150 (1952).

31. Sunyar, A. *et al.* Decay of Sr85 and Sr85m. *Phys. Rev.* **86,** 1023–1027 (1952).

32. Sattler, A. Decay of Sr85. *Phys. Rev.* **127,** 854–859 (1962).

33. Luckham, P. & Rossi, S. The colloidal and rheological properties of bentonite suspensions. *Adv. Colloid Interface Sci.* **82,** 43–92 (1999).

34. Hollenbach, M., Grohs, J. & Mamich, S. Determination of technetium-99, thorium-230 and uranium-234 in soils by inductively coupled plasma mass spectrometry using flow injection preconcentration. *J. Anal. At. …* **9,** (1994).

35. Cresser, M., Killham, K. & Edwards, A. *Soil Chemistry and Its Applications*. (Cambridge University Press, 1993). at <http://books.google.co.uk/books?id=eIzu0nrouPwC>

36. Chain silicates. *Britannica* at <http://media-2.web.britannica.com/eb-media/55/2655-004-8A9554CC.gif>

37. Worrall, W. E. *Clays and Ceramic Raw Materials*. (Springer, 1986).

38. Sparks, D. L. *Environmental Soil Chemistry*. (Acad. Press, 2003). at <http://books.google.co.uk/books?id=_8E2hU5m5cMC>

39. Inglethorpe, S., Morgan, D. & Highley, D. *Industrial Minerals laboratory manual: bentonite*. (1993). at <http://scholar.google.com/scholar?hl=en&btnG=Search&q=intitle:Industrial+Minerals+Laboratory+Manual+Bentonite#0>

40. Odom, I. Smectite clay minerals: properties and uses. *… Trans. R. Soc. …* **311,** 391–409 (1984).

41. Brindley, G. W. & Brown, G. *Crystal Structures of Clay Minerals and Their X-ray Identification*. (Mineralogical Society, 1980). at <http://books.google.com.au/books?id=KhAJAQAAIAAJ>

42. Damour, A. & Salvetat, D. Analyses sur un hydrosilicate d′alumine trouvé à Montmorillon. *Ann. Chim. Phys.* **3,** 376–383 (1847).

43. Ross, C. S. & Hendricks, S. B. *Minerals of the montmorillonite group: their origin and relation to soils and clays*. (U. S. Govt. Print. Off., 1943). at <http://books.google.co.uk/books?id=rPY9AAAAYAAJ>

44. Ijagbemi, C. O., Baek, M.-H. & Kim, D.-S. Montmorillonite surface properties and sorption characteristics for heavy metal removal from aqueous solutions. *J. Hazard. Mater.* **166,** 538–46 (2009).

45. Carroll, D. Ion exchange in clays and other minerals. *Geol. Soc. Am. Bull.* **70,** 749–779 (1959).

46. Yener, N., Biçer, C., Önal, M. & Sarıkaya, Y. Simultaneous determination of cation exchange capacity and surface area of acid activated bentonite powders by methylene blue sorption. *Appl. Surf. Sci.* **258,** 2534–2539 (2012).

47. Nagy, N. & Kónya, J. Acid–base properties of bentonite rocks with different origins. *J. Colloid Interface Sci.* **295,** 173–80 (2006).

48. Baik, M. & Lee, S. Colloidal stability of bentonite clay considering surface charge properties as a function of pH and ionic strength. *J. Ind. Eng. Chem.* **16,** 837–841 (2010).

49. Hosterman, J. *Bentonite and fullers earth resources of the United States*. (1985). at <http://agris.fao.org/agris-search/search/display.do?f=2013/US/US2013071560007156.xml;US20130071560626>

50. OO, J. & MESUBI, M. Beneficiation and characterisation of a bentonite from north-easter Nigeria. *J. North …* **124,** 154–158 (2008).

51. Bradbury, M. & Baeyens, B. *Laboratory for Waste Management Near Field Sorption Data Bases for Compacted MX-80 Bentonite for Performance Assessment of a High-Level Radioactive Waste Repository in Opalinus Clay Host Rock*. (2003).

52. Khan, S. A., Riaz-ur-Rehman & Khan, M. A. Sorption of strontium on bentonite. *Waste Manag.* **15,** 641–650 (1995).

53. Do, D. D. *Adsorption Analysis: Equilibria and Kinetics*. (Imperial College Press, 1998). at <http://books.google.co.uk/books?id=8xFlXq6Xf2oC>

54. Segalini, J., Iwama, E., Taberna, P.-L., Gogotsi, Y. & Simon, P. Steric effects in adsorption of ions from mixed electrolytes into microporous carbon. *Electrochem. commun.* **15,** 63–65 (2012).

55. Schnoor, J. L. *Environmental modeling: fate and transport of pollutants in water, air, and soil*. (J. Wiley, 1996). at <http://books.google.co.uk/books?id=RlbxAAAAMAAJ>

56. Limousin, G. *et al.* Sorption isotherms: A review on physical bases, modeling and measurement. *Appl. Geochemistry* **22,** 249–275 (2007).

57. Campbell, L. & Davies, B. Soil sorption of caesium modelled by the Langmuir and Freundlich isotherm equations. *Appl. geochemistry* **10,** 715–723 (1995).

58. McKay, G. *Use of Adsorbents for the Removal of Pollutants from Wastewater K Parameters*. (CRC PressINC, 1996). at <http://books.google.co.uk/books?id=ep5bLsOs4IwC>

59. Dada, A., Olalekan, A., Olatunya, A. & DADA, O. Langmuir, Freundlich, Temkin and Dubinin–Radushkevich Isotherms Studies of Equilibrium Sorption of Zn 2 Unto Phosphoric Acid Modified Rice Husk. *iosrjournals.org* **3,** 38–45 (2012).

60. Langmuir, I. The adsorption of gases on plane surfaces of glass, mica and platinum. *J. Am. Chem. Soc.* **40,** 1361–1403 (1918).

61. Grim, R. E. Properties of Clay: Part 6. Special Features of Sediments. *SP 10 Recent Mar. Sediments* 466–495 (1939).

62. Hayati-Ashtiani, M. Characterization and Surface Properties of Bentonites in the Separation Process of Iron(III). *Part. Sci. Technol.* **31,** 419–425 (2013).

63. Foster, M. Geochemical studies of clay minerals: II. Relation between ionic substitution and swelling in montmorillonites. *Am. Mineral.* (1953). at <http://scholar.google.com/scholar?hl=en&btnG=Search&q=intitle:Geochemical+studies+of+clay+minerals:+II+-+Relation+between+ionic+substitution+and+swelling+in+montmorillonites#0>

64. Alther, G. The effect of the exchangeable cations on the physico-chemical properties of Wyoming bentonites. *Appl. Clay Sci.* **1,** (1986).

65. Dean, J. R. *Practical Inductively Coupled Plasma Spectroscopy*. (Wiley, 2005). at <http://books.google.co.uk/books?id=ePHnX1Hets4C>

66. Chen, M. & Ma, L. Comparison of three aqua regia digestion methods for twenty Florida soils. *Soil Sci. Soc. Am. J.* 491–499 (2001). at <https://dl.sciencesocieties.org/publications/sssaj/abstracts/65/2/491>

67. Smart, L. & Moore, E. *Solid State Chemistry: An Introduction*. (Stanley Thornes, 1995). at <http://books.google.co.uk/books?id=HGuPQzrh9gUC>

68. West, A. R. *Solid State Chemistry and Its Applications*. (Wiley, 1985). at <http://books.google.co.uk/books?id=-EKCm5UQaqEC>

69. X-ray Crystallography. at <http://www.geology.wisc.edu/courses/g360/xray992.html>

70. Ulery, A. L., Drees, L. R. & America, S. S. S. of. *Methods of Soil Analysis: Mineralogical methods. Part 5*. (Soil Science Society of America, 2008). at <http://books.google.co.uk/books?id=Lqh6mYoKjdQC>

71. Young, R. A. *The Rietveld Method*. (Oxford University Press, 1995). at <http://books.google.co.uk/books?id=z_53QIzn69wC>

72. Ong, J. L., Farley, D. W. & Norling, B. K. Quantification of leucite concentration using X-ray diffraction. *Dent. Mater.* **16,** 20–5 (2000).

73. Hurst, V., Schroeder, P. & Styron, R. Accurate quantification of quartz and other phases by powder X-ray diffractometry. *Anal. Chim. Acta* **337,** 233–252 (1997).

74. Parry, S., Livens, F. & O'Brien, L. Corroded Magnox Sludge and Plutonium Waste Cementation. *Geochim. Cosmochim. Acta* **71,** Supplement 758 (2007).

75. Gregson, C. R., Goddard, D. T., Sarsfield, M. J. & Taylor, R. J. Combined electron microscopy and vibrational spectroscopy study of corroded Magnox sludge from a legacy spent nuclear fuel storage pond. *J. Nucl. Mater.* **412,** 145–156 (2011).

76. Hawkes, P. W. *Electron optics and electron microscopy*. 244 (Taylor and Francis, 1972). at <http://books.google.co.uk/books/about/Electron_optics_and_electron_microscopy.html?id=AirKWG9ltHoC&pgis=1>

77. Wittke, J. H. SEM Microprobe. at <http://www4.nau.edu/microanalysis/microprobe-sem/instrumentation.html>

78. Swapp, S. Scanning Electron Microscopy (SEM). at <http://serc.carleton.edu/research_education/geochemsheets/techniques/SEM.html>

79. Wilson, M. J. *Clay Mineralogy: Spectroscopic and Chemical Determinative Methods*. (Chapman & Hall, 1994). at <http://books.google.co.uk/books?id=-EVKpdzHQq8C>

80. Tunç, S. & Duman, O. The effect of different molecular weight of poly(ethylene glycol) on the electrokinetic and rheological properties of Na-bentonite suspensions. *Colloids Surfaces A Physicochem. Eng. Asp.* **317,** 93–99 (2008).

81. Navratilova, Z. & Wojtowicz, P. Sorption of alkylammonium cations on montmorillonite. *Acta Geodyn. …* **4,** 59–65 (2007).

82. Gates, W. P. A method of improving hydraulic performance of clay. (2010).

83. Russell, J. & Fraser, A. IR spectroscopic evidence for interaction between hydronium ions and lattice OH groups in montmorillonite. *Clays Clay Miner.* (1971). at <http://clays.org/journal/archive/volume 19/19-1-55.pdf>

84. Brindley, G. W. & Kao, C.-C. Structural and IR relations among brucite-like divalent metal hydroxides. *Phys. Chem. Miner.* **10,** 187–191 (1984).

85. Zhang, Z. *et al.* Temperature- and pH-dependent morphology and FT-IR analysis of magnesium carbonate hydrates. *J. Phys. Chem. B* **110,** 12969–73 (2006).

86. Harward, M. & Brindley, G. Swelling properties of synthetic smectites in relation to lattice substitutions. *Clays Clay Miner.* 209–222 (1965). at <http://www.clays.org/journal/archive/volume 13/13-1-209.pdf>

87. Kawamura, K., Ichikawa, Y. & Nakano, M. Swelling properties of smectite up to 90° C: In situ X-ray diffraction experiments and molecular dynamic simulations. *Eng. …* **54,** 75–79 (1999).

88. Komine, H. & Ogata, N. Predicting swelling characteristics of bentonites. *J. Geotech. geoenvironmental Eng.* **130,** 818–829 (2004).

89. Kaufhold, S. & Dohrmann, R. The variable charge of dioctahedral smectites. *J. Colloid Interface Sci.* **390,** 225–33 (2013).

90. Aran, D., Maul, A. & Masfaraud, J.-F. A spectrophotometric measurement of soil cation exchange capacity based on cobaltihexamine chloride absorbance. *Comptes Rendus Geosci.* **340,** 865–871 (2008).

91. Adeleye, S., Rautiu, R., White, D. & Clay, P. Clay minerals as sorbents for nuclear reactor activation products. *J. Mater. Sci.* **30,** 583–586 (1995).

92. Helling, C. S., Chesters, G. & Corey, R. B. Contribution of Organic Matter and Clay to Soil Cation-Exchange Capacity as Affected by the pH of the Saturating Solution1. *Soil Sci. Soc. Am. J.* **28,** 517–520 (1964).

93. Faust, G. T. & Murata, K. J. Stevensite, redefined as a member of the montmorillonite group. *Am. Mineral.* **38,** 973–987 (1953).

94. Bhattacharyya, K. G. & Gupta, S. Sen. Adsorption of a few heavy metals on natural and modified kaolinite and montmorillonite: a review. *Adv. Colloid Interface Sci.* **140,** 114–31 (2008).

95. Galamboš, M. *et al.* Cesium sorption on bentonites and montmorillonite K10. *J. Radioanal. Nucl. Chem.* **284,** 55–64 (2010).

96. Sawhiney, B. Selective sorption and fixation of cations by clay minerals: a review. *Clays Clay Miner.* **20,** 93–100 (1972).

97. Shainberg, I. & Kemper, W. D. Hydration Status of Adsorbed Cations. *Soil Sci. Soc. Am. J.* **30,** 707 (1966).

98. Sawhney, B. L. Sorption and Fixation of Microquantities of Cesium by Clay Minerals: Effect of Saturating Cations1. *Soil Sci. Soc. Am. J.* **28,** 183 (1964).

99. Alkan, M. & Doğan, M. Adsorption of Copper(II) onto Perlite. *J. Colloid Interface Sci.* **243,** 280–291 (2001).

100. Bohn, H. L., McNeal, B. L. & O'Connor, G. A. *Soil chemistry*. 341 (Wiley, 1985). at <http://books.google.co.uk/books/about/Soil_chemistry.html?id=VXNRAAAAMAAJ&pgis=1>

101. Liu, D., Hsu, C. & Chuang, C. Ion-exchange and sorption kinetics of cesium and strontium in soils. *Appl. Radiat. Isot.* **46,** 839–846 (1995).

102. Khan, S. A. & Khan, M. A. Sorption of cesium on bentonite. *Waste Manag.* **14,** 629–642 (1994).

103. Tertre, E., Berger, G., Castet, S., Loubet, M. & Giffaut, E. Experimental sorption of Ni2+, Cs+ and Ln3+ onto a montmorillonite up to 150°C. *Geochim. Cosmochim. Acta* **69,** 4937–4948 (2005).

104. Baeyens, B. & Bradbury, M. H. A mechanistic description of Ni and Zn sorption on Na-montmorillonite Part I: Titration and sorption measurements. *J. Contam. Hydrol.* **27,** 199–222 (1997).

105. Gutierrez, M. & Fuentes, H. R. A mechanistic modeling of montmorillonite contamination by cesium sorption. *Appl. Clay Sci.* **11,** 11–24 (1996).

106. Wang, X., Chen, Y. & Wu, Y. Sorption and desorption of radiostrontium on powdered bentonite: Effect of pH and fulvic acid. *J. Radioanal. Nucl. Chem.* **261,** 497–500 (2004).

107. Chen, C.-C. & Hayes, K. F. X-ray absorption spectroscopy investigation of aqueous Co(II) and Sr(II) sorption at clay–water interfaces. *Geochim. Cosmochim. Acta* **63,** 3205–3215 (1999).

108. Jenne, E. *Adsorption of Metals by Geomedia: Variables, Mechanisms, and Model Applications*. (Elsevier Science, 1998). at <http://books.google.co.uk/books?id=8X2BAljgaHIC>

109. Bostick, B. C., Vairavamurthy, M. A., Karthikeyan, K. G. & Chorover, J. Cesium adsorption on clay minerals: an EXAFS spectroscopic investigation. *Environ. Sci. Technol.* **36,** 2670–6 (2002).

110. Coughlin, B. R. & Stone, A. T. Nonreversible adsorption of divalent metal ions (MnII, CoII, NiII, CuII, and PbII) onto goethite: effects of acidification, FeII addition, and picolinic acid addition. *Environ. Sci. Technol.* **29,** 2445–2455 (1995).

111. McBride, M. Influence of glycine on Cu2+ adsorption by microcrystalline gibbsite and boehmite. *Clays Clay Min.* **33,** 397–402 (1985).

112. Reinoso-Maset, E., Worsfold, P. J. & Keith-Roach, M. J. The effect of EDTA, NTA and picolinic acid on Th(IV) mobility in a ternary system with natural sand. *Environ. Pollut.* **162,** 399–405 (2012).

113. Killey, R. W., McHugh, J. O., Champ, D. R., Cooper, E. L. & Young, J. L. Subsurface cobalt-60 migration from a low-level waste disposal site. *Environ. Sci. Technol.* **18,** 148–57 (1984).

114. Cleveland, J. & Rees, T. Characterization of plutonium in Maxey Flats radioactive trench leachates. *Science (80-.).* (1981). at <http://www.sciencemag.org/content/212/4502/1506.short>

115. Bourg, A. & Schindler, P. W. Effect of ethylenediaminetetraacetic acid on the adsorption of copper (II) at amorphous silica. *Inorg. Nucl. Chem. Lett.* **15,** 225–229 (1979).

116. Elliott, H. a. & Huang, C. P. The effect of complex formation on the adsorption characteristics of heavy metals. *Environ. Int.* **2,** 145–155 (1979).

117. Nowack, B., Xue, H. & Sigg, L. Influence of Natural and Anthropogenic Ligands on Metal Transport during Infiltration of River Water to Groundwater. *Environ. Sci. Technol.* **31,** 866–872 (1997).

118. Sellers, R. M. The radiation chemistry of nuclear reactor decontaminating reagents. *Radiat. Phys. Chem.* **21,** 295–305 (1983).

119. Delegard, C. H., Barney, G. S. & Gallagher, S. A. in *Geochemical Behav. Disposed Radioact. Waste* **246,** 95–112 (American Chemical Society, 1984).

120. Maset, E. R. *et al.* Effect of organic co-contaminants on technetium and rhenium speciation and solubility under reducing conditions. *Environ. Sci. Technol.* **40,** 5472–7 (2006).

121. Keith-Roach, M. J. The speciation, stability, solubility and biodegradation of organic co-contaminant radionuclide complexes: a review. *Sci. Total Environ.* **396,** 1–11 (2008).

122. Novak, J., Jayachandran, K., Moorman, T. & Webber, J. Sorption and binding of organic compounds in soils and their relation to bioavailability. *Bioremediation …* 13–32 (1995). at <https://dl.sciencesocieties.org/publications/books/abstracts/sssaspecialpubl/bioremediation/13>

123. Tan, K. H. *Principles of Soil Chemistry, Fourth Edition*. (Taylor & Francis, 2011). at <http://books.google.co.uk/books?id=Z_oFtRMUCeAC>

124. Bucheli-Witschel, M. & Egli, T. Environmental fate and microbial degradation of aminopolycarboxylic acids. *FEMS Microbiol. Rev.* **25,** 69–106 (2001).

125. Nowack, B., Kari, F. & Krüger, H. The remobilization of metals from iron oxides and sediments by metal-EDTA complexes. *Water. Air. Soil Pollut.* 243–257 (2001). at <http://link.springer.com/article/10.1023/A:1005296312509>

126. Serne, R., Felmy, A. & Cantrell, K. *Characterization of Radionuclide-Chelating Agent Complexes Found in Low-Level Radioactive Decontamination Waste*. *Off. Nucl. Regul. Res.* (1996). at <http://www.iaea.org/inis/collection/nclcollectionstore/_public/27/063/27063466.pdf>

127. March, R. *et al.* Synthesis, characterisation and magnetic properties of cobalt(II) complexes with picolinic acid derivatives: the crystal and molecular structures of [Co(MeC5H3NCOO)2(H2O)2] and [CoCl2(C5H4NCOOPri)2]. *Inorganica Chim. Acta* **353,** 129–138 (2003).

128. Rufus, A., Sathyaseelan, V., Velmurugan, S. & Narasimhan, S. NTA-based formulation for the chemical decontamination of nuclear power plants. *Nucl. Energy* **43,** 47–53 (2004).

129. Elliott, H. A. & Brown, G. A. Comparative evaluation of NTA and EDTA for extractive decontamination of Pb-polluted soils. *Water. Air. Soil Pollut.* **45,** (1989).

130. Sunda, W. G., Engel, D. W. & Thuotte, R. M. Effect of chemical speciation on toxicity of cadmium to grass shrimp, Palaemonetes pugio: importance of free cadmium ion. *Environ. Sci. Technol.* **12,** 409–413 (1978).

131. Pope, C. G., Matijević, E. & Patel, R. C. Adsorption of nicotinic, picolinic, and dipicolinic acids on monodispersed sols of α-Fe2O3 and Cr(OH)3. *J. Colloid Interface Sci.* **80,** 74–83 (1981).

132. Nicholls, P. H. & Evans, A. A. Sorption of ionisable organic compounds by field soils. Part 1: Acids. *Pestic. Sci.* **33,** 319–330 (1991).

133. Nicholls, P. H. & Evans, A. A. Sorption of Ionisable organic compounds by field soils. Part 2: Cations, bases and zwitterions. *Pestic. Sci.* **33,** 331–345 (1991).

134. Swanson, J. L. *Organic complexant-enhanced mobility of toxic elements in low-level wastes*. (Pacific Northwest Lab., Richland, WA (USA), 1984).

135. Nowack, B. & Sigg, L. Adsorption of EDTA and Metal-EDTA Complexes onto Goethite. *J. Colloid Interface Sci.* **177,** 106–121 (1996).

136. Serne, R., Cantrell, C. & Lindenmeier, C. *Radionuclide-Chelating Agent Complexes in Low-Level Radioactive Decontamination Waste; Stability, Adsorption and Transport Potential*. (2002). at <http://www.osti.gov/bridge/product.biblio.jsp?osti_id=975006>

137. Reinoso-Maset, E. Aqueous and solid phase interactions of radionuclides with organic complexing agents. (2010). at <http://lib-srvr9.lib.plymouth.ac.uk:8080/handle/10026.1/300>

138. Ford, R. G., Scheinost, A. C., Scheckel, K. G. & Sparks, D. L. The Link between Clay Mineral Weathering and the Stabilization of Ni Surface Precipitates. *Environ. Sci. Technol.* **33,** 3140–3144 (1999).

139. Bickmore, B., Bosbach, D., Hochella Jr., M., Charlet, L. & Rufe, E. In situ atomic force microscopy study of hectorite and nontronite dissolution: Implications for phyllosilicate edge surface structures and dissolution mechanisms. *Am. …* **86,** 411–423 (2001).

140. Golubev, S. V., Bauer, A. & Pokrovsky, O. S. Effect of pH and organic ligands on the kinetics of smectite dissolution at 25°C. *Geochim. Cosmochim. Acta* **70,** 4436–4451 (2006).

141. Oueslati, W., Benrhaiem, H., Lanson, B. & Benhajamara, a. Selectivity of Na–montmorillonite in relation with the concentration of bivalent cation (Cu2+, Ca2+, Ni2+) by quantitative analysis of XRD patterns. *Appl. Clay Sci.* **43,** 224–227 (2009).

142. Stumm, W. & Morgan, J. J. *Aquatic chemistry: chemical equilibria and rates in natural waters*. (Wiley, 1996). at <http://books.google.co.uk/books?id=xvZOAAAAMAAJ>

143. Collier, N. C. & Milestone, N. B. The encapsulation of Mg(OH)2 sludge in composite cement. *Cem. Concr. Res.* **40,** 452–459 (2010).

144. Hastings, J. J., Rhodes, D., Fellerman, a. S., Mckendrick, D. & Dixon, C. New approaches for sludge management in the nuclear industry. *Powder Technol.* **174,** 18–24 (2007).

145. Liang, T. The influence of cation concentration on the sorption of strontium on mordenite. *Appl. Radiat. Isot.* **51,** 6–11 (1999).

146. Magdaliniuk, S. *et al.* Biodegradation of naphthalene in montmorillonite/polyacryamide suspensions. *Water Sci. Technol.* **31,** 85–94 (1995).

147. Ogawa, M., Shirai, H., Kuroda, K. & Kato, C. Solid-state intercalation of naphthalene and anthracene into alkylammonium-montmorillonites. *Clays Clay Miner.* **40,** 485–490 (1992).

148. Boyd, S., Lee, J. & Mortland, M. Attenuating organic contaminant mobility by soil modification. *Nature* **333,** 345–347 (1988).

149. Tsay, S.-Y., Chen, B.-K. & Chen, C.-P. Synthesis and properties of polyimide (containing naphthalene) nanocomposites with organo-modified montmorillonites. *J. Appl. Polym. Sci.* **99,** 2966–2972 (2006).

150. Changchaivong, S. & Khaodhiar, S. Adsorption of naphthalene and phenanthrene on dodecylpyridinium-modified bentonite. *Appl. Clay Sci.* **43,** 317–321 (2009).

151. Chiou, C., Peters, L. & Freed, V. A physical concept of soil-water equilibria for nonionic organic compounds. *Science (80-.).* **206,** 831–832 (1979).

152. Stroo, H. F. H. *et al.* Remediating chlorinated solvent source zones. *Environ. Sci. Technol.* **37,** 224A–230A (2003).

153. Tao, T., Yang, J. J. & Maciel, G. E. Photoinduced Decomposition of Trichloroethylene on Soil Components. *Environ. Sci. Technol.* **33,** 74–80 (1999).

154. *Trichloroethylene (TCE)*. 1–13 (2007). at <http://www.epa.gov/teach/chem_summ/TCE_summary.pdf>

155. Lemming, G. *et al.* Environmental impacts of remediation of a trichloroethene-contaminated site: life cycle assessment of remediation alternatives. *Environ. Sci. Technol.* **44,** 9163–9 (2010).

156. Wilson, J. & Wilson, B. Biotransformation of trichloroethylene in soil. *Appl. Environ. Microbiol.* **49,** 242–243 (1985).

157. McCarty, P. L. *et al.* Full-Scale Evaluation of In Situ Cometabolic Degradation of Trichloroethylene in Groundwater through Toluene Injection. *Environ. Sci. Technol.* **32,** 88–100 (1998).

158. Sutfin, J. A. & Ramey, D. In situ biological treatment of TCE-impacted soil and groundwater: Demonstration results. *Environ. Prog.* **16,** 287–296 (1997).

159. Estes, T. J. & Vilker, V. L. Selective adsorption of low-molecular-weight halocarbons from water by montmorillonite and silica. *J. Colloid Interface Sci.* **133,** 166–175 (1989).

160. Estes, T. J. T., Shah, R. R. V. & Vilker, V. L. V. Adsorption of low molecular weight halocarbons by montmorillonite. *Environ. Sci. Technol.* **22,** 377–381 (1988).

161. Koh, S.-M. & Dixon, J. B. Preparation and application of organo-minerals as sorbents of phenol, benzene and toluene. *Appl. Clay Sci.* **18,** 111–122 (2001).

162. Shih, Y.-H. & Wu, S.-C. Kinetics of toluene sorption and desorption in Ca- and Cu-montmorillonites investigated with Fourier transform infrared spectroscopy under two different levels of humidity. *Environ. Toxicol. Chem.* **23,** 2061–7 (2004).

163. Morrissey, F. a & Grismer, M. E. Kinetics of volatile organic compound sorption/desorption on clay minerals. *J. Contam. Hydrol.* **36,** 291–312 (1999).

Appendices

Appendix – Chapter 2: Particle Size Characterisation of Simulant Magnox Sludge

Sieve Aperture Size / μm	Mass of Sieve / g	Mass of Sieve With Sludge / g	Mass of dry sludge / g	Composition / %
1400	447.74	4523.68	4.94	14.70
1000	378.44	380.87	2.43	7.23
790	443.22	444.64	1.42	4.23
500	388.87	393.66	4.79	14.26
355	367.61	373.16	5.55	16.52
250	365.28	369.36	4.08	12.14
212	305.19	307.34	2.15	6.40
180	360.76	362.01	1.25	3.72
Base	238.99	245.98	6.99	20.80

Appendix – Chapter 2: ICP-OES Calibration Curves

Aluminium

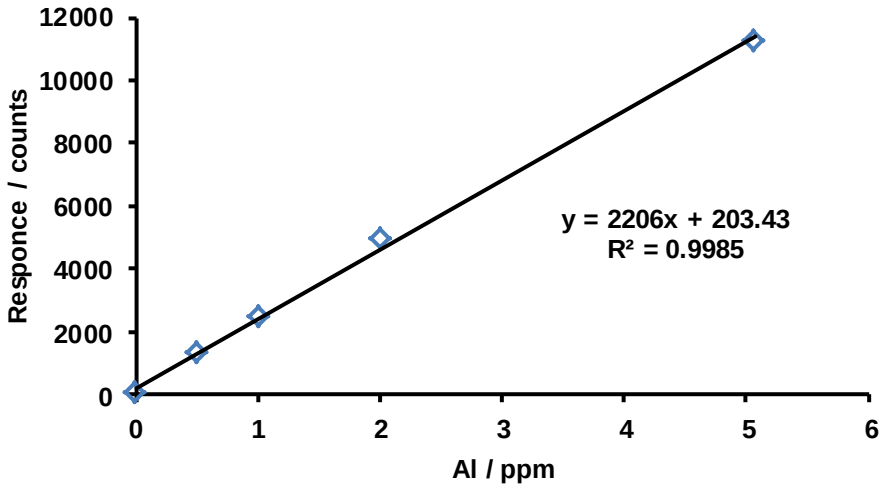

Calcium

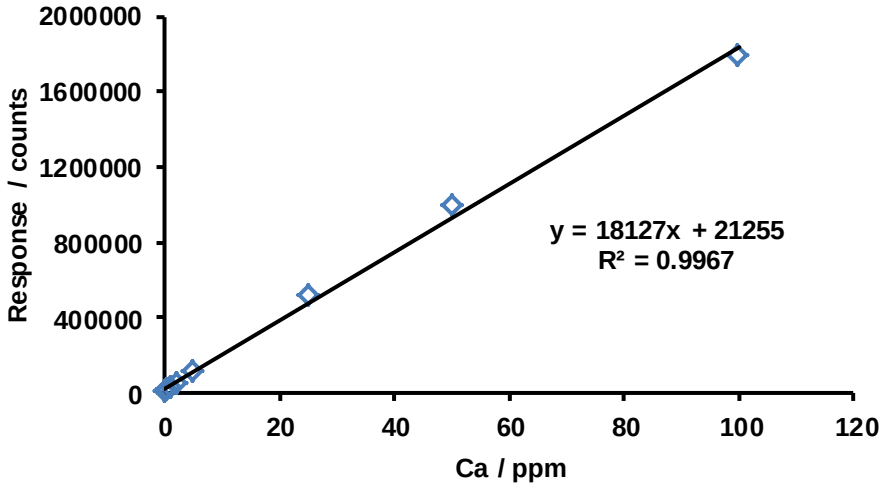

Iron

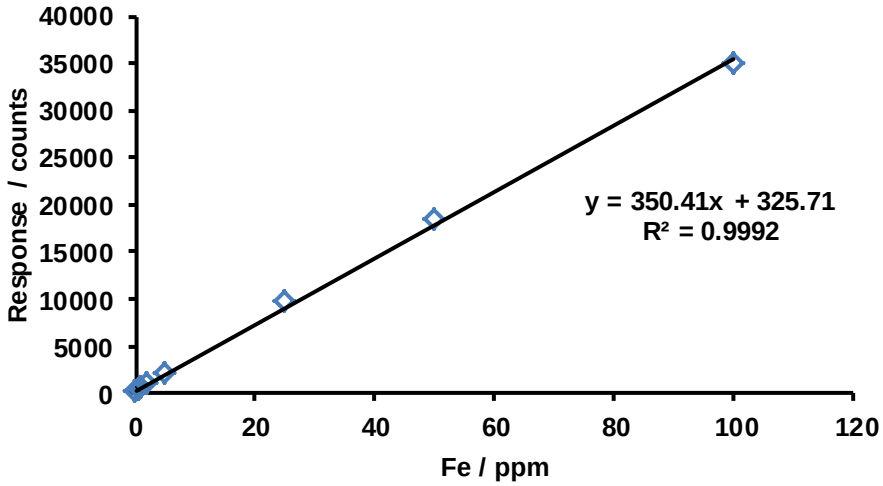

Potassium

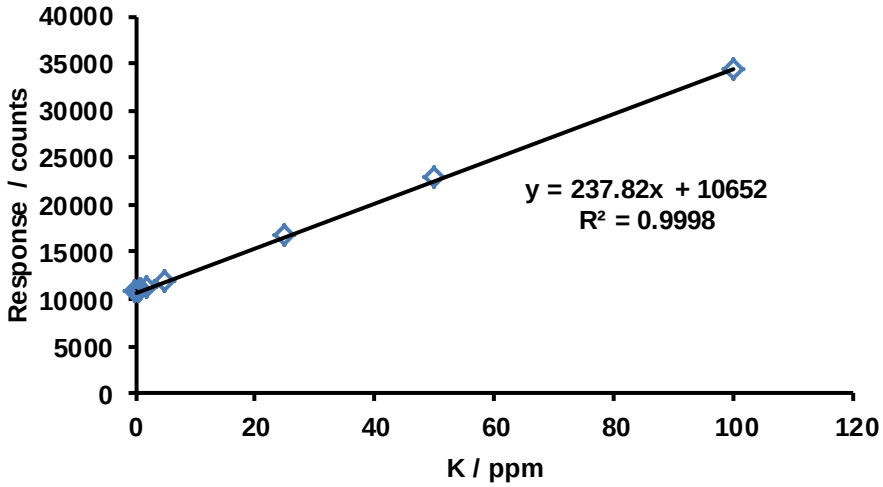

Magnesium

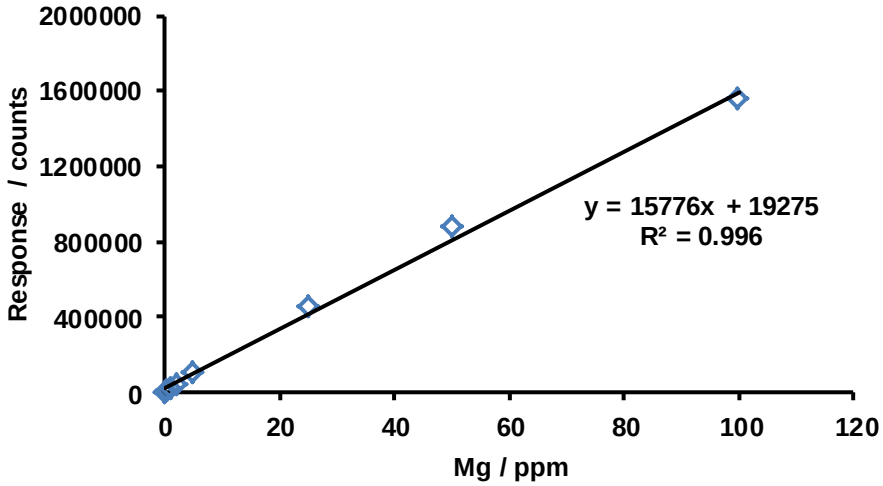

Manganese

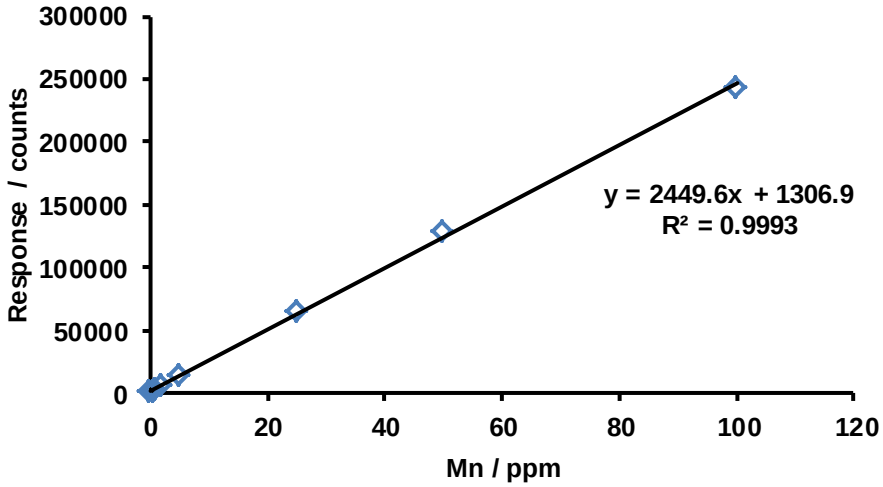

Sodium

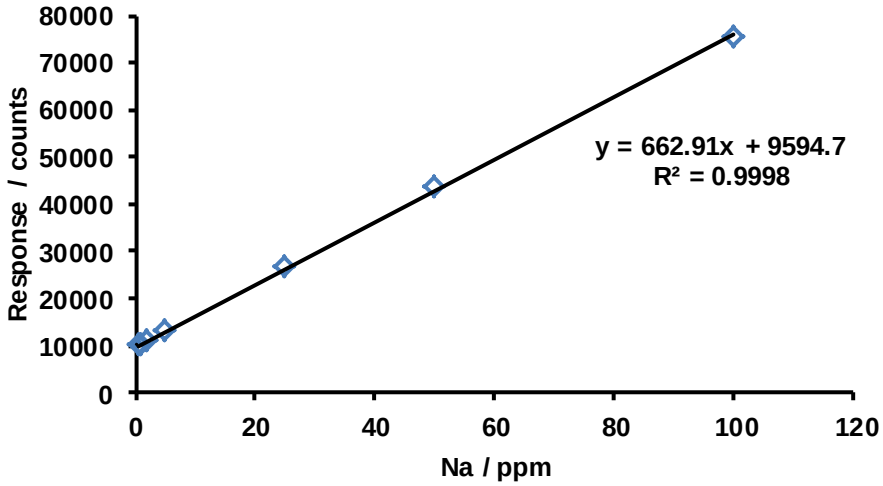

Silicon

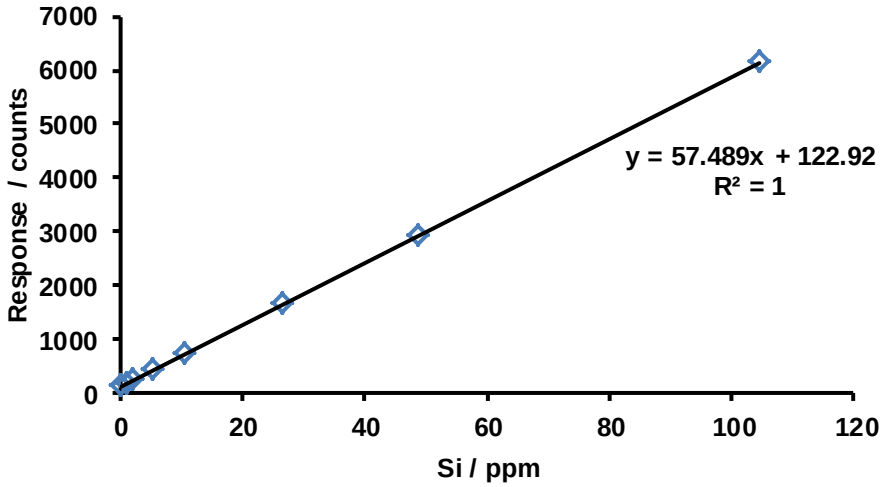

Zinc